

**NUMERICAL DETERMINATION OF FORCES
ACTING ON MATERIAL INTERFACES:
AN APPLICATION TO RAFTING IN
Ni-SUPERALLOYS**

by

Simona Socrate

**Laurea in Nuclear Engineering
University of Rome
(Rome, Italy, 1984)**

**Submitted in partial fulfillment of the
requirements for the degree of Master of Science in
Mechanical Engineering**

at the

**Massachusetts Institute of Technology
August, 1990**

© Massachusetts Institute of Technology

Signature of Author _____

**Department of Mechanical Engineering
August, 1990**

Certified by _____

**David M. Parks
Associate Professor of Mechanical Engineering
Thesis Supervisor**

Accepted by _____

**Ain A. Sonin, Chairman
Departmental Committee on Graduate Studies**

**MASSACHUSETTS INSTITUTE
OF TECHNOLOGY**

APR 26 1991

LIBRARIES

ARCHIVES

**NUMERICAL DETERMINATION OF FORCES
ACTING ON MATERIAL INTERFACES:
AN APPLICATION TO RAFTING IN
Ni-SUPERALLOYS**

by
Simona Socrate

Submitted to the Department of Mechanical Engineering
on August 10, 1990 in partial fulfillment of the requirements
for the Degree of Master of Science in Mechanical Engineering

ABSTRACT

Numerical techniques have been developed to evaluate local driving forces acting on material interfaces. Since migrations of the interfaces are associated with modifications of the microstructure, these methods can be applied to predict and model morphological evolution in multi-phase materials. Here this methodology has been applied to the study of an evolution of the morphology of γ' precipitates in Ni-superalloys, which has been termed *rafting*.

It is shown how predictions of the model agree with available experimental data, and a comprehensive treatment of the rafting phenomenon is proposed.

Thesis Supervisor: Dr. David M. Parks
Title: Associate Professor of Mechanical Engineering

ACKNOWLEDGEMENTS

I would like to express my sincerest gratitude to Professor David M. Parks for his guidance and support during this project. Not only his uncommon knowledge and understanding have always been offered when needed, but, most important, his generosity and friendship have been an invaluable help through any difficult situation.

I also extend my thanks to Professors Ali Argon, Rohan Abeyaratne and Mary Boyce for their help through numerous discussions.

Thanks to my office mates, and to all the Mechanics of Materials research group, for creating a nice working environment, for being always willing to lend a hand, for keeping together our computer facility and for watering my plants when I forget to.

A special thank to Mary Toscano, without whom this manuscript wouldn't exist. She is nice, patient and amazingly efficient: three qualities that rarely coexist in one person.

I would also like to thank Leslie Regan and Joan Kravit for having always been extremely friendly and helpful.

I think I should also thank Dr. R. G. S. P. Stringfellow. Thank you Richy for having been always at my side, for your *paramount* help and support and for having made my life worth living.

Finally, I would like to thank my mother and sister. I will have to do this in Italian since my mother is still at her third English lesson and my sister has just got a "C" in her latest English exam.

Grazie mamma e Carla per avermi sempre aiutato e incoraggiato anche quando le mie scelte hanno portato dolore e sacrifici. Siete sempre nel mio cuore e questo Master é per voi (e per papa se mi può vedere in qualche modo).

This work was supported by the Ida Green Fellowship and by the M.I.T. Center for Material Science and Engineering under National Science Foundation Grant No. DMR-87-19217.

TABLE OF CONTENTS

	Page
ABSTRACT	2
ACKNOWLEDGEMENTS	3
TABLE OF CONTENTS	4
LIST OF FIGURES	6
INTRODUCTION	10
1. RAFTING IN $\gamma - \gamma'$ Ni SUPERALLOYS	12
1.1 Introduction	12
1.2 Experimental Observations	17
1.3 Energy Approaches	22
1.4 Historical Review of Rafting Models	25
2. THE FORCE ON A MATERIAL INTERFACE	30
2.1 Introduction	30
2.2 The Energy Momentum Tensor in Continuum Mechanics	33
2.3 An Expression for the Force on an Interface	36
3. NUMERICAL METHODS	42
3.1 Introduction	42
3.2 A Direct Approach: The Computer Program POSTABQ	43
3.3 A Domain Integral Approach:	
The Computer Program DOMAIN	46
3.3.1 Historical perspective	46
3.3.2 Derivation of a domain integral expression	
for the energy perturbation	47
3.3.3 Finite element implementation	50
4. ANALYSIS OF RAFTING	59
4.1 Introduction	59
4.2 Test Case: A Cylindrical Inclusion in an Infinite Matrix	60
4.3 Problem Description	73
4.4 Elastic Analysis	80
4.5 Analysis of the Stress-annealing Transients	93
4.6 Discussion	139
5. CONCLUSIONS	149
5.1 Summary of Results	149
5.2 Suggestions for Future Study	150

TABLE OF CONTENTS

	Page
REFERENCES	151
APPENDIX I: The Computer Program POSTABQ	154
APPENDIX II: The Computer Program DOMAIN	218
APPENDIX III: The Computer Program GOODIER	264
APPENDIX IV: ABAQUS Input File for the Test Case: a Cylindrical Inclusion in an Infinite Matrix	267
APPENDIX V: Typical ABAQUS Input File for the Elastic Analysis of a $\gamma - \gamma'$ Unit Cell	275
APPENDIX VI: Typical ABAQUS Input File for the Analysis of a Stress-Annealing Transient for a $\gamma - \gamma'$ Unit Cell	280

LIST OF FIGURES

No.	Page
1.1 Typical microstructure of the fully heat treated single crystal [30]	13
1.2 Lattice misfit and its effect on the internal stress state	14
1.3 Directional coarsening of γ' precipitates [15]	16
1.4 Effect of the initial microstructure on the coarsening process [24]	19
1.5 Energy approaches	24
1.6 A schematic summarizing the effects of stress orientation on the stress annealed shape of the γ' precipitates [13]	26
1.7 Correspondence between the model problem and the actual morphology	27
1.8 Map giving the conditions which lead to the lowest total elastic energy for spheres (S) , plates normal to the stress axis (N) and needles parallel to the stress axis (P). [11]	29
2.1 Interface configuration	32
2.2 Variation in energy associated with a migration of the interface	37
2.3 τ_n as a driving force for shape evolution.	40
2.4 Schematic plot of the force along the interface for 2-D models	41
3.1 Finite element model of a boundary value problem	45
3.2 Definition of the domain of integration	48
3.3 Finite element discretization of the interface	51
3.4 Finite element discretization of the domain of integration	55
3.5 Perturbation patterns	56
3.6 Test for the accuracy of the numerical solution	58
4.1 Cylindrical inclusion in an infinite matrix	63
4.2 Relation between the profile of τ_n along the interface and the tendency toward morphological evolution	64
4.3 Parametric study of τ_n profile for: $\delta = 0.1\%$; $E_m = 100$ GPa; $0.4 \leq E_p/E_m \leq 2.0$	65
4.4 Parametric study of τ_n profile for: $\delta = 0.1\%$; $E_m = 100$ GPa; $0.1 \leq E_p/E_m \leq 10.0$	66
4.5 Evolution map for an isotropic cylindrical inclusion in an infinite matrix	67
4.6 Parametric study of τ_n profile for: $\delta = -0.1\%$; $E_m = 100$ GPa; $0.4 \leq E_p/E_m \leq 2.0$	68

4.7 Parametric study of $\tau_{\mathbf{n}}$ profile for: $\delta = 0.3\%$; $E_m = 100$ GPa; $0.4 \leq E_p/E_m \leq 2.0$	69
4.8 Schematic description of the cylindrical inclusion problem modeled, with the boundary conditions indicated ($r^\Omega/L_\infty = 1/20$)	70
4.9 Finite element mesh for the cylindrical inclusion problem modeled. In this figure the bottom mesh (“near-particle” region) fits into the indicated area of the top mesh (“nominal far-field” region)	71
4.10 Comparison of analytical and numerical results (for $E_m = 200$ GPa; $E_p/E_m = 0.5$; $\sigma_\infty = 1000$ MPa; $\delta = -0.1\%$)	72
4.11 Finite element discretization of the unit cell	74
4.12 Comparison of $\tau_{\mathbf{n}}$ profiles obtained with different choices of mesh and/or numerical method	75
4.13 $\tau_{\mathbf{n}}$ profile for the elastic analysis of case 1 (MNMT)	82
4.14 $\tau_{\mathbf{n}}$ profile for the elastic analysis of case 2 (MNMC)	83
4.15 $\tau_{\mathbf{n}}$ profile for the elastic analysis of case 3 (TCT)	84
4.16 $\tau_{\mathbf{n}}$ profile for the elastic analysis of case 4 (TCC)	85
4.17 $\tau_{\mathbf{n}}$ profile for the elastic analysis of case 5 (PLT)	86
4.18 $\tau_{\mathbf{n}}$ profile for the elastic analysis of case 6 (PHT)	87
4.19 $\tau_{\mathbf{n}}$ profile for the elastic analysis of case 7 (MNMT _{INV})	88
4.20 $\tau_{\mathbf{n}}$ profile for the elastic analysis of case 8 (MNMT _{NMS})	89
4.21 $\tau_{\mathbf{n}}$ profile for the elastic analysis of case 9 (TCT _{PMS})	90
4.22 $\tau_{\mathbf{n}}$ profile for the elastic analysis of case 10 (TCC _{PMS})	91
4.23 $\tau_{\mathbf{n}}$ profile for the elastic analysis of case 11 (PLT _{ISO})	92
4.24 Contours of σ_{11} due to misfit only ($\delta = +.56\%$) for the alloy tested by Miyazaki, Nakamura and Mori [16]	97
4.25 Contours of σ_{22} due to misfit only ($\delta = +.56\%$) for the alloy tested by Miyazaki, Nakamura and Mori [16]	98
4.26 Contours of σ_{21} due to misfit only ($\delta = +.56\%$) for the alloy tested by Miyazaki, Nakamura and Mori [16]	99
4.27 Contours of σ_{11} due to misfit only ($\delta = -0.38\%$) for the alloy tested by Pollock [25]	100
4.28 Contours of σ_{22} due to misfit only ($\delta = -0.38\%$) for the alloy tested by Pollock [25]	101
4.29 Contours of σ_{12} due to misfit only ($\delta = -0.38\%$) for the alloy tested by Pollock [25]	102

4.30 Schematic representation of the evolution of the stress and strain fields in the primary stage of the creep transient	103
4.31 Contours of ϵ_{eq}^{creep} for the transient analyzed in case 1 (MNMT) at creep time $t = 0.011$ sec.	104
4.32 Contours of ϵ_{eq}^{creep} for the transient analyzed in case 1 (MNMT) at creep time $t = 4.46$ sec.	105
4.33 Contours of ϵ_{eq}^{creep} for the transient analyzed in case 1 (MNMT) at creep time $t = 63.47$ sec.	106
4.34 Contours of ϵ_{eq}^{creep} for the transient analyzed in case 1 (MNMT) at creep time $t = 50,000$ sec.	107
4.35 Contours of ϵ_{eq}^{creep} for the transient analyzed in case 2 (MNMC) at creep time $t = 0.011$ sec.	108
4.36 Contours of ϵ_{eq}^{creep} for the transient analyzed in case 2 (MNMC) at creep time $t = 3.86$ sec.	109
4.37 Contours of ϵ_{eq}^{creep} for the transient analyzed in case 2 (MNMC) at creep time $t = 252$ sec.	110
4.38 Contours of ϵ_{eq}^{creep} for the transient analyzed in case 2 (MNMC) at creep time $t = 50,000$ sec.	111
4.39 Contours of σ_{11} at the end of the analyzed transient for case 1 (MNMT)	112
4.40 Contours of σ_{22} at the end of the analyzed transient for case 1 (MNMT)	113
4.41 Contours of σ_{11} at the end of the analyzed transient for case 3 (TCT)	114
4.42 Contours of σ_{22} at the end of the analyzed transient for case 3 (TCT)	115
4.43 Contours of σ_{11} at the end of the analyzed transient for case 5 (PLT)	116
4.44 Contours of σ_{22} at the end of the analyzed transient for case 5 (PLT)	117
4.45 Contours of σ_{11} at the end of the analyzed transient for case 6 (PHT)	118
4.46 Contours of σ_{22} at the end of the analyzed transient for case 6 (PHT)	119
4.47 Contours of σ_{11} at the end of the analyzed transient for case 9 (TCT _{PMS})	120
4.48 Contours of σ_{22} at the end of the analyzed transient for case 9 (TCT _{PMS})	121
4.49 Contours of σ_{11} at the end of the analyzed transient for case 2 (MNMC)	122
4.50 Contours of σ_{22} at the end of the analyzed transient for case 2 (MNMC)	123

4.51 Contours of σ_{11} at the end of the analyzed transient for case 4 (TCC)	124
4.52 Contours of σ_{22} at the end of the analyzed transient for case 4 (TCC)	125
4.53 Contours of σ_{11} at the end of the analyzed transient for case 10 (TCC _{PMS})	126
4.54 Contours of σ_{22} at the end of the analyzed transient for case 10 (TCC _{PMS})	127
4.55 Evolution of the τ_n profile during the stress-annealing transient for case 1 (MNMT)	128
4.56 Evolution of the τ_n profile during the stress-annealing transient for case 2 (MNMC)	129
4.57 Evolution of the τ_n profile during the stress-annealing transient for case 3 (TCT)	130
4.58 Evolution of the τ_n profile during the stress-annealing transient for case 4 (TCC)	131
4.59 Evolution of the τ_n profile during the stress-annealing transient for case 5 (PLT)	132
4.60 Evolution of the τ_n profile during the stress-annealing transient for case 6 (PHT)	133
4.61 Evolution of the τ_n profile during the stress-annealing transient for case 7 (MNMT _{INV})	134
4.62 Evolution of the τ_n profile during the stress-annealing transient for case 8 (MNMT _{NMS})	135
4.63 Evolution of the τ_n profile during the stress-annealing transient for case 9 (TCT _{PMS})	136
4.64 Evolution of the τ_n profile during the stress-annealing transient for case 10 (TCC _{PMS})	137
4.65 Evolution of the τ_n profile during the stress-annealing transient for case 11 (PLT _{ISO})	138
4.66 A typical creep curve with corresponding micrographs which show the development of directional coarsening [22]	144
4.67 Creep curve and corresponding changes in microstructure [23]	145
4.68 A schematic diagram showing the τ_n levels at the end of the primary stage of the creep transient	146
4.69 Evolution of $\Delta\tau_n/\sigma\delta$ for the analyzed creep transients	147
4.70 Comparison of “Type P” and “Type N” evolution curves for $\Delta\tau_n/\sigma\delta$	148

INTRODUCTION

The mechanical and physical properties of any material depend critically on two parameters. The first is its *constitution*: the overall composition, the number of phases and their relative volume fractions and compositions. The second is its *microstructure*: the shape, size and distribution of each phase.

The application of external loads to a multi-phase crystalline solid can significantly alter its microstructure.

Limiting our attention to the most common case of a two-phase (matrix/precipitate) alloy, an external stress can modify the morphology of the precipitates, influence the precipitate coarsening kinetics and alter the relative stability of the two phases.

The influence of the applied loading conditions on the morphology and stability of the microstructure depends on the material parameters of the precipitate and of the matrix, and on the magnitude and nature of the applied loads.

Since many of the properties of the alloy are determined by its microstructure, it is of technological relevance to be able to predict microstructural development. The microstructure evolution of the precipitate phase can be understood on the basis of simple energy arguments. When the morphology of the microstructure evolves, it is because there is a *driving force* for the change: the system is trying to lower its total energy by modifying its configuration.

Obviously, the mere presence of a driving force does not guarantee that a change will occur: the kinetics of the process will dictate the pace at which the structural change will eventually take place. Nevertheless, quantifying the driving force for the morphological evolution is still the essential first step toward a complete modeling of the phenomenon.

In analyzing the evolution of the crystal microstructure, we can focus our attention on the migration of the interfaces between different phases: an evolution of the microstructure corresponds to a migration of the interfaces. Thus we can think of the driving forces for microstructure development as forces acting on the interfaces and driving their migration.

The objective of this research has been to develop numerical techniques for the determination of the forces acting on material interfaces, and to apply these techniques to the analysis of morphological evolution in $\gamma - \gamma'$ Nickel superalloys.

We will first describe, in chapter 1, the phenomenon that we intend to analyze: an evolution of the morphology of γ' precipitates in Ni-superalloys, which has been termed *rafting*. We will present a brief historical review of the experimental observations and discuss the models which have been proposed in the literature.

In chapter 2 we will define, in a more rigorous context, the notion of *force on a material interface*, and in chapter 3 we will introduce numerical techniques to evaluate it.

In chapter 4 we will apply these techniques to the analysis of rafting in $\gamma - \gamma'$ Ni-superalloys; we will compare the predictions of our model with available experimental data and present a general discussion of the rafting process.

Finally, in chapter 5, we will draw the conclusions of this research and discuss some suggestions for future studies.

CHAPTER 1

RAFTING IN $\gamma - \gamma'$ Ni-SUPERALLOYS

1.1 Introduction

Nickel-base superalloy single crystals are a class of two-phase precipitation-strengthened materials.

The microstructure consists of an fcc nickel solid solution matrix, γ , with Ni_3Al precipitates, γ' . The precipitate phase, an fcc intermetallic compound, is ordered and coherent with the matrix and can constitute up to 70 percent of the volume of the crystal. After complete aging the precipitates are distributed in the γ matrix as a stable periodic array of $\langle 100 \rangle$ aligned cuboids of fairly uniform size, usually in the range of 0.2 - 0.5 μm in diameter (Figure 1.1)

Typically, a lattice parameter mismatch, δ , exists between the γ and γ' phases:

$$\delta = \frac{a_{\gamma'} - a_{\gamma}}{a_{\gamma}}, \quad (1.1)$$

where $a_{\gamma'}$ and a_{γ} are the lattice parameters of the two phases.

In most commercial alloys the magnitude of the misfit is minimal ($|\delta|$ less than 0.5%); nevertheless, since the matrix-precipitate interface is coherent, the lattice misfit introduces a significant internal stress in the crystal (Figure 1.2).

The $\gamma - \gamma'$ misfit, which is temperature-dependent due to the differing coefficients of thermal expansion in the two phases, has remarkable effects on the evolution of the morphology of the γ' precipitates.

Nathan [1] observed that, during the aging treatment, the morphology change, from spherical to cuboid, occurs at smaller sizes of the precipitates for higher levels of misfit.

But the most dramatic effect of the magnitude and sense of the misfit has been recognized in a phenomenon, called *rafting*, which has been observed by various researchers during stress-annealing experiments or during creep tests at elevated temperatures.

At high temperatures – above 900°C for most commercial alloys – the γ' cuboidal precipitates become unstable. The cubic γ' particles link together to form rods and/or plates (rafts).

When the crystal is annealed in the absence of an applied stress, the new lamellar structure is randomly oriented along the three $\langle 100 \rangle$ cube directions, without showing a preferential orientation (Figure 1.3(a)).

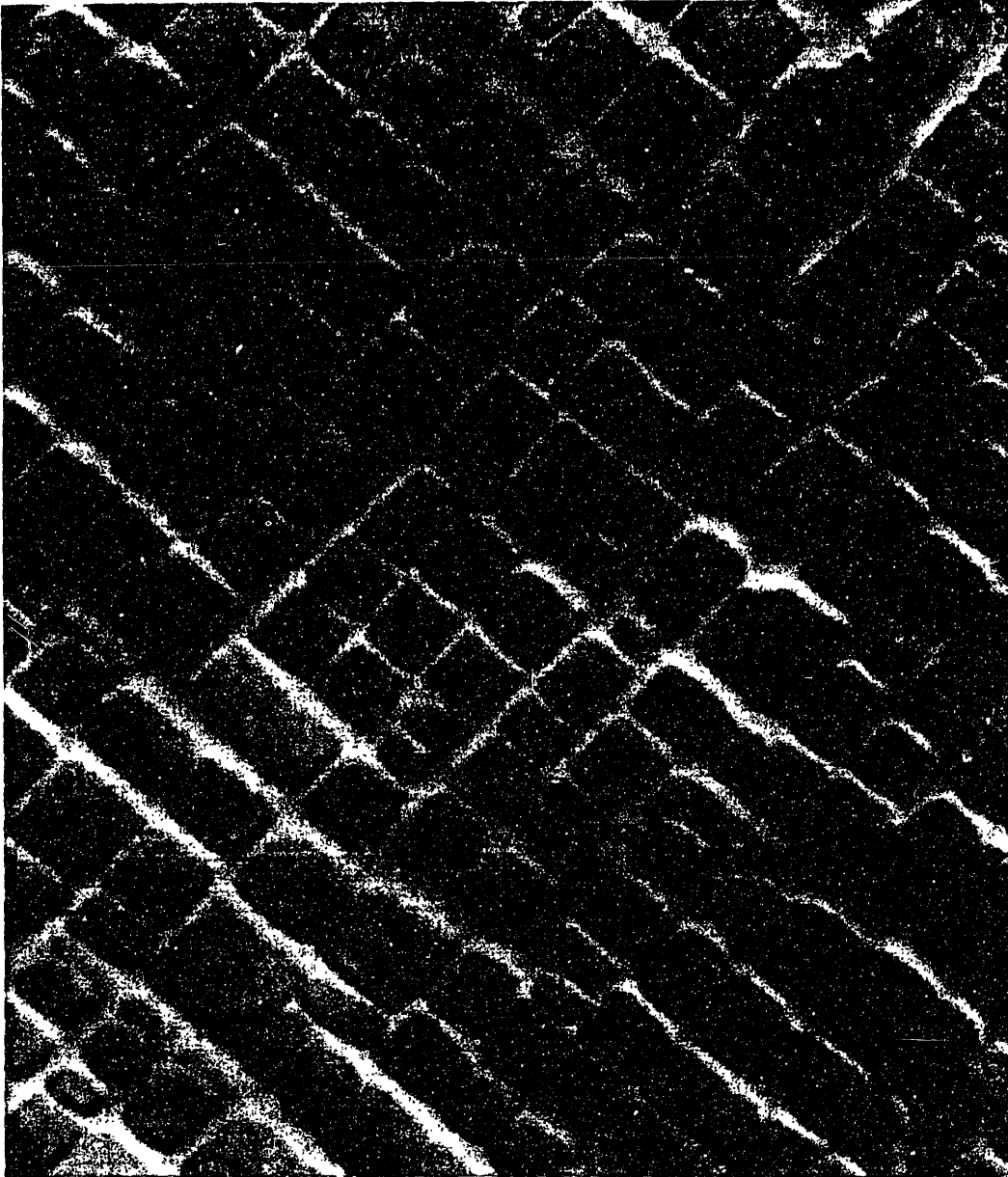


Figure 1.1 Typical microstructure of the fully heat treated single crystal [30].

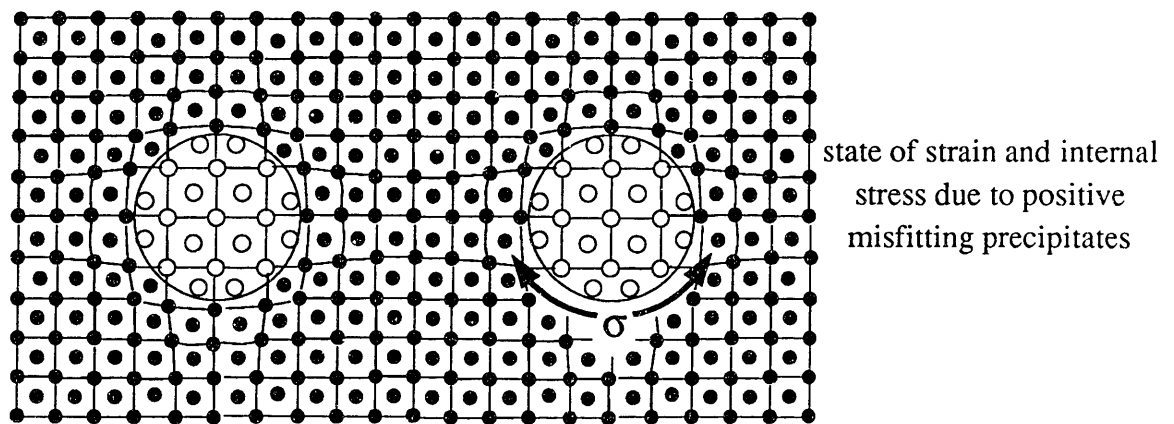
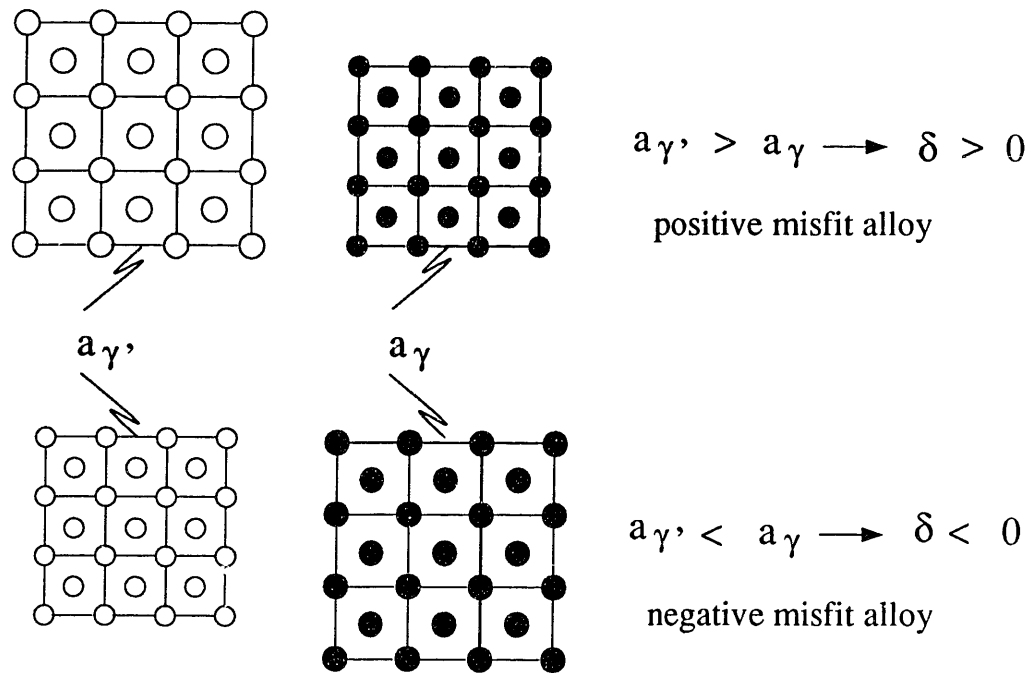


Figure 1.2 Lattice misfit and its effect on the internal stress state.

When a tensile or compressive stress is applied along the $\langle 001 \rangle$ direction, the morphological evolution of the precipitates exhibits a marked *directionality*. Two different types of behavior for the coarsening of the precipitates have been observed:

- Type P (Parallel): the cuboids coarsen preferentially along the direction of the applied stress: the precipitates assume the form of plates which lie parallel to the stress direction. In alloys with small volume fraction of γ' , strings of γ' cubes can coarsen along the $\langle 001 \rangle$ direction and form rods (Figure 1.3(b)).
- Type N (Normal): the cuboids coarsen preferentially along the directions normal to the applied stress: the precipitates assume the form of broad flat plates with their faces *normal* to the stressed $\langle 001 \rangle$ direction (Figure 1.3(c))

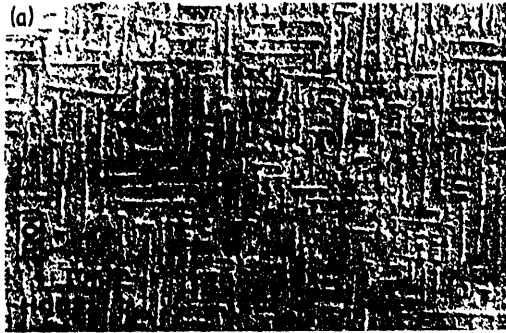
Several rafting observations have been reported over the last two decades [2-9,12,13,15-25]. According to these observations, different materials can coarsen in opposite directions under the same loading conditions.

The lattice misfit was soon recognized as a key parameter controlling the rafting behavior of the alloys.

Since the morphology of the precipitates strongly affects the mechanical properties of the alloy, several studies have been carried out in order to model, predict and control the γ' morphology evolution.

In the following paragraphs, we give a brief survey of rafting observations, identify possible approaches to analyze the phenomenon, and discuss the models proposed in the literature.

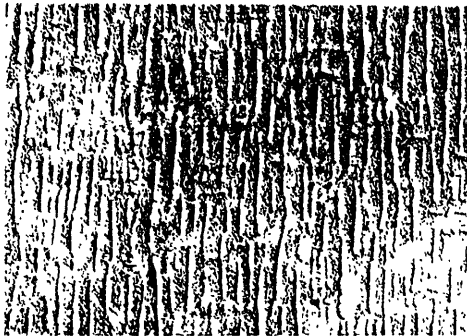
(1) Rafted structure after annealing in absence of an applied stress.



(a) Isotropic Behavior

(2) Rafted structure after stress annealing (the direction of stress is vertical in the figure)

(b) "Type P" Behavior



(c) "Type N" Behavior

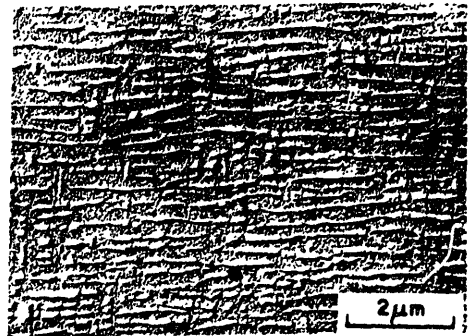


Figure 1.3 Directional coarsening of γ' precipitates [15].

1.2 Experimental Observations

Directional coarsening of the γ' precipitates was first observed in commercial Ni-superalloys after prolonged creep exposure [2-9].

These instabilities of the γ' phase were viewed initially with some concern since it was observed that they were generally associated with a reduction in the creep resistance of the alloy [5,9,10,11]. This led to a number of theoretical and experimental studies, toward a better understanding of the rafting phenomenon [12-15]. These studies, which will be discussed in greater detail in paragraph 1.4, identified some of the major factors related to the stress coarsening behavior, and suggested that rafting of the γ' precipitates could be essentially eliminated by reducing the $\gamma - \gamma'$ lattice misfit through careful alloy design.

In the early '80s, Pearson, Kear and Lemkey [18,19] presented an innovative study where they demonstrated that directional coarsening significantly *enhanced* the high temperature creep properties of an experimental alloy with an unusually high negative value of the misfit ($\delta = -0.78\%$).

These results brought about a wave of renewed attention for the rafting phenomenon. A number of investigations were undertaken concerning the actual development, under different testing conditions, of the γ' rafts and their influence on the creep properties of the crystal [16-25]. The creep loads were generally applied along the $\langle 001 \rangle$ crystal direction. While in most studies only tensile loads were considered, in some experiments the effect of compressive loads was also investigated.

Here we will briefly review some of the results of these observations, together with the models proposed to explain the observed variation in creep resistance.

1. The rafts begin to form early in primary creep [17-24,27]. The time needed to attain a fully-developed lamellar structure appears to be influenced by:
 - (a) the test temperature: the rate of directional coarsening increases when the test temperature is raised [24];
 - (b) the applied load : upon increasing the magnitude of the applied load a hastening of the rafting process is observed [24];
 - (c) the lattice misfit: under the same conditions of applied load and test temperature, alloys with larger magnitude of misfit exhibit a higher rate of directional coarsening [27];
 - (d) the initial microstructure: a fine microstructure with closely-spaced, small-sized γ' precipitates considerably hastens the development of rafts [22].
2. The rafted configuration is very stable [18,20,22,24]. The average thickness of the rafts is initially very close to the original γ' particle size [17-25]. As the creep

transient progresses, contradictory observations have been reported concerning the evolution of raft thickness and interlamellar spacing.

Some researchers [22,24,25] report that the thickness of the rafts remains constant up to the onset of tertiary creep and the interlamellar spacing also shows a similar behavior, while other research groups [18,20,23] have observed a gradual thickening of the rafted lamellae during steady state creep.

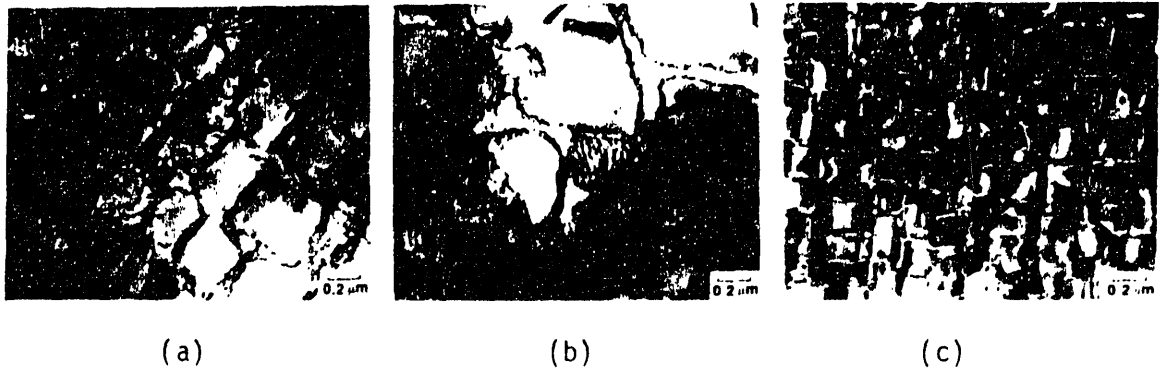
Differences in the alloy composition could be responsible for these discrepancies: alloys with higher levels of refractory elements are characterized by reduced diffusion rates so that, for these alloys, the thickening of the lamellae might be hindered [24].

In tertiary creep the rafts become irregularly shaped, lose their perfect alignment and coarsen considerably prior to failure.

3. The initial microstructure prior to testing can drastically affect the resulting rafted morphology [18, 19, 21, 22]. An ordered, perfectly-aligned structure of γ' cuboids promotes a rapid formation of more perfect platelets with a high aspect ratio. Since the initial thickness of the rafts basically coincides with the original dimension of the γ' cuboids, a finer initial microstructure will produce a finer rafted structure. In contrast, if the initial structure is overaged, and is characterized by irregularly-shaped γ' particles, the raft morphology will appear very irregular as well, with a very low average aspect ratio (Fig. 1.4).
4. A characteristic feature of the stress-coarsened structure is the presence of networks of dislocations at the $\gamma - \gamma'$ interfaces [17, 18, 19, 21, 23, 25]. These dislocations are true misfit dislocations since their Burgers' vectors are appropriate for relaxing the internal stress due to the misfit. Merging interfaces of coarsening cuboids are usually deprived of dislocations [23, 25].
5. Under *low stress*, at high temperatures, the operative creep mechanism involves dislocation motion primarily in the γ -matrix with the mobile dislocations circumventing the γ' particles which remain virtually dislocation-free [18, 19, 21, 22, 25]. Thus, γ' -rafts with a high aspect ratio provide an ideal structure for creep resistance because circumvention of the γ' phase is eliminated. Significant creep can occur only by insertion of dislocations through the ordered intermetallic γ' phase, resulting in dramatically improved creep resistance [18, 19, 22]. Furthermore, the misfit dislocation networks at the $\gamma - \gamma'$ interfaces act as obstacles to the penetration of the dislocations inside the precipitates.

Under *high stresses*, at high temperatures, γ' particle shearing tends to become the prevailing creep mode [18, 19]. For these loading conditions, a directionally-coarsened structure may not be beneficial since one set of $\gamma - \gamma'$ interfaces is essentially eliminated [24].

(1) Morphology of the precipitates prior to creep test



(2) Rafted structure after 50 hours of creep testing

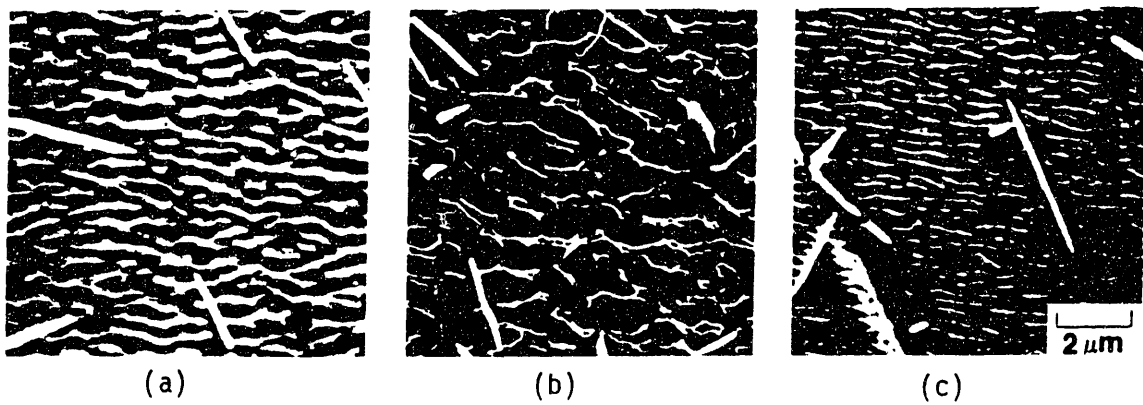


Figure 1.4 Effect of the initial microstructure on the coarsening process [24].

We can thus think of two possible explanations for the earlier observations [5, 9, 10, 11] in which rafted crystals did not exhibit an improvement in their creep resistance. First, in some studies the yield behavior of the alloy was investigated [11] so that the tests were conducted at stress levels well inside the range in which γ' particle shearing is the predominant mechanism of creep. Second, for the tests conducted in the low stress regimes, the overaged, irregular and coarser microstructure of the γ' rafts in these early alloys was easily circumvented by the dislocations in the γ phase [22].

Finally, a number of observations concerning the direction of coarsening of the γ' precipitates under tensile and compressive creep loads applied along the $\langle 001 \rangle$ crystal direction are schematically summarized in Table 1.1.

Here, assuming that the direction of the $\langle 001 \rangle$ applied load is as shown, we graphically identify a “type N” behavior with a horizontal rectangle and a “type P” behavior with a vertical rectangle.

The sign of the misfit of the alloy is also indicated. Note that in three cases (a, c, f), two different signs of the misfit are given. For these cases, the first sign corresponds to the value given by the authors in the referenced paper, while the second sign corresponds to the actual sign of the misfit for the alloy at test temperature. In particular, for the three cases:

- (a) Tien and Copley [12, 13] state the value of the misfit of their alloy, Udimet-700, as +0.02%, as measured by Oblack and Kear [16] at room temperature. This value should be therefore corrected to obtain the value of the misfit at test temperature.

In several studies [23, 27, 28], the expansion coefficients of the γ' phase have been found to be lower than those of the γ phase; this is consistent with the long-range ordered structure of γ' [29]. According to the data of Grose and Ansell [28], we can infer that the value of the misfit of Udimet-700 at the test temperature of 954°C is of the order of -0.3%.

- (c) The value of the misfit given by Caron and Khan in [21] (+0.14%) has also been measured at room temperature. Fredholm and Strudel have subsequently determined that the actual value of the misfit at test temperature is -0.33% [23].
- (f) In [17] Carry and Strudel give a negative value for the misfit (- 0.4%). This value has been corrected in a subsequent study [23] where the actual value of the misfit has been found to be + 0.38%. The erroneous value reported in [17] was probably due to an incorrect Burgers' vector sign convention.

Since the sign of the misfit at test temperature plays a fundamental role in the rafting behavior of the alloys, these misleading indications in the literature have brought about a substantial confusion both in the interpretation of the experimental results and in the modeling of the rafting phenomenon.

Researchers	References	Year	Misfit sign in paper/actual	Tension	Compression
(a) Tien and Copley	12, 13	1971	+ / -		
(b) Miyazaki, Nakamura, Mori	15	1979	+		
(c) Carry and Strudel	16, 17	1979	- / +		
(d) Pearson, Lemkey, Kear	18, 19	1980	-		
(e) Nathal and Ebert	20	1983	-		
(f) Caron and Khan	21	1983	+ / -		
(g) Mackay and Ebert	22	1984	-		
(h) Fredholm and Strudel	23	1984	-		
(i) Mackay and Ebert	24	1985	-		
(j) Pollock	25	1989	-		
(k) Pollock	25	1989	+		

Table 1.1 Rafting Observations

1.3 Energy Approaches

The rafting phenomenon is an interesting example of how an externally applied loading condition can influence the morphology evolution of the microstructure in a multi-phase material.

The most puzzling point in this phenomenon is the marked directionality of the coarsening process in presence of an applied stress. We can ask ourselves two basic questions:

What are the parameters that affect the direction of rafting?

How can we predict, knowing the value of these parameters, the rafting behavior of the material?

The evolution of precipitate morphology can be qualitatively understood by using an energy analysis. Rafting is a spontaneous evolution of the microstructure; thus we can conclude that it must be associated with a decrease in the energy level of the system.

If we consider the original cuboidal morphology and the final rafted configuration, the variation in energy, ΔE^T , associated with this variation in the microstructure, can be roughly broken down into three terms:

$$\Delta E^T = \Delta E_{chem} + \Delta E_{int} + \Delta E_{EL}^T. \quad (1.2)$$

Here, the first two terms, ΔE_{chem} and ΔE_{int} , account for, respectively, the variation in chemical energy and interfacial energy. They are most certainly important terms that play a fundamental role in the coarsening process, but they “cannot discern among the three $\langle 100 \rangle$ crystal directions”. In other words, the value of these two terms will be the same for all the rafted configurations shown in Fig. 1.3: they are, giving to the word a broader meaning, *isotropic* terms and cannot account for the directionality of coarsening under stress annealing. Thus the key to the problem must lie in the third term, ΔE_{EL}^T : the variation of the total elastic energy of the system.

Since this is the *only* term which is sensitive to the direction of the applied stress, we can infer that the directionality of rafting is controlled by a tendency to decrease the total elastic energy E_{EL}^T which is given by the sum of the elastic energy of the crystal plus the potential energy of the loading system.

If we express the total energy of the crystal as a function of the precipitate morphology, the misfit, the applied stress, σ_∞ , and all the other parameters that characterize the system:

$$E^T = \hat{E}^T(\gamma'_{-morphology}, \delta, \sigma_\infty \dots), \quad (1.3)$$

then we can think of two possible approaches to predict the morphology evolution of the precipitates (Fig. 1.5).

A first approach can be termed an *energy minimization* approach: we calculate the finite energy levels for different morphologies of the precipitates relative to some reference state such as a homogeneous Ni-Al solid solution crystal. We then compare the energy levels of the different morphologies under a certain loading condition and infer that the system will evolve toward the morphology that corresponds to the lowest value of the total energy.

An alternative approach can be termed an *energy perturbation* approach: we consider the actual initial configuration with γ' cuboids, and investigate the effect of a perturbation of the morphology of the precipitates on the total energy. We can thus determine the driving force:

$$f = \frac{-\delta E^T}{\delta \gamma'_{\text{morphology}}} \quad (1.4)$$

which is acting on the system, and infer the most likely direction for morphology evolution.

Note that, in both approaches, we implicitly assume that there exists a mechanism, characterized by suitable kinetics, to accomplish the morphology evolution.

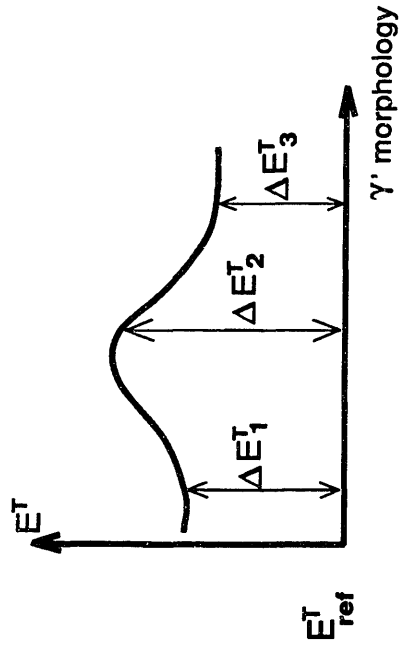
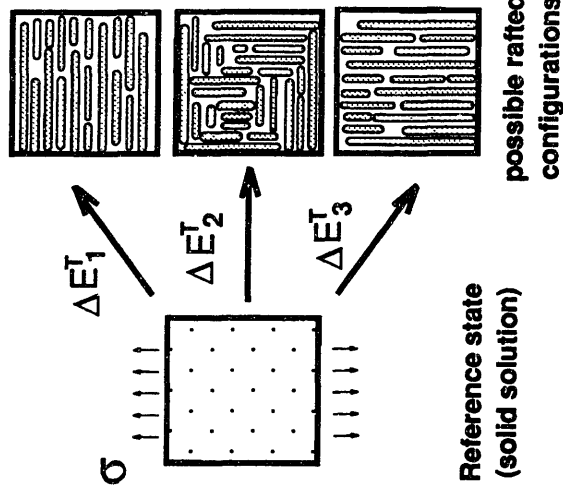
If we compare the two approaches on a schematic “total energy vs. γ' -morphology” graph (Fig. 1.5), the first approach corresponds to the determination of the minimum of the curve, while the second approach corresponds to the determination of the slope of the curve for the initial morphology.

The first approach seems to be more suitable to study displacive transformations, where the microstructure instantaneously switches to the lowest energy configuration, while the second approach appears to be more easily incorporated in a kinetic model to study diffusive transformations, where the morphology evolution is controlled by the instantaneous value of the driving force as well as by the kinetics of the diffusion process.

Historically, in the study of rafting, the energy minimization approach has been more widely used, as we will briefly discuss in the next paragraph.

In our study we will instead follow an energy perturbation approach.

a) Energy minimization approach



b) Energy perturbation approach

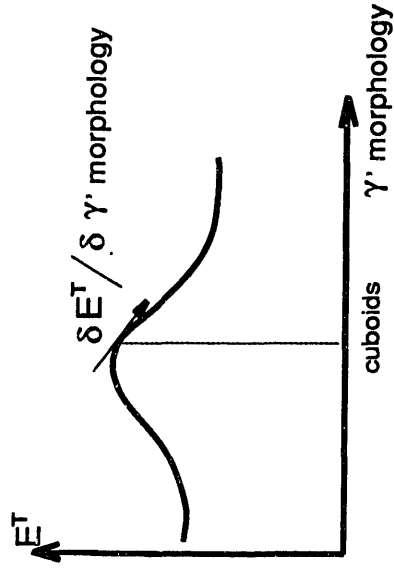
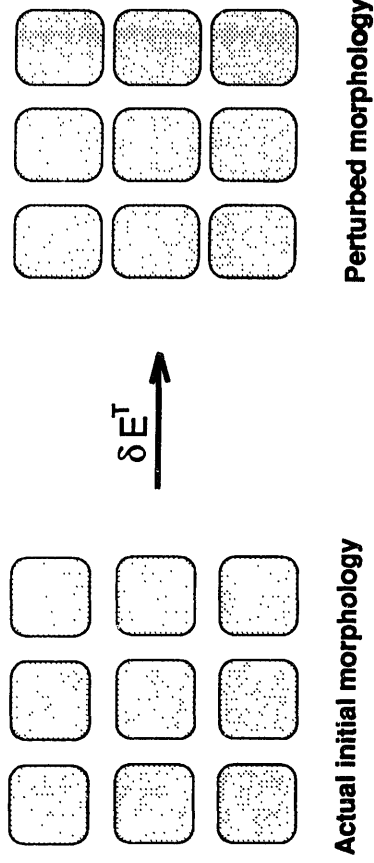


Figure 1.5 Energy approaches .

1.4 Historical Review of Rafting Models

The first attempt to explain the rafting behavior through energy considerations is due to Tien and Copley [13]. They observed the structure of the γ' precipitates in Udimet-700 and found that the sense and crystallographic orientation of the external stress influenced the final rafted morphology of the γ' precipitates. Their observations are graphically summarized in Fig. 1.6. The dotted cubes show the initial orientation of the γ' cuboids with respect to the direction of stress (vertical in the figure). The shapes bounded by solid lines represent the aligned plates, parallelepipeds and cuboids that result from stress annealing.

In the discussion of their observation, Tien and Copley gave only a qualitative theoretical analysis and could not draw quantitative conclusions regarding the influence of elastic energy on the final particle shape.

A significant step in the understanding of the rafting phenomenon is due to Pineau [14]. Since the evaluation of the total energy for the actual $\gamma - \gamma'$ microstructure is extremely arduous, the calculations are drastically simplified by considering a parallel model problem in which a single, ellipsoidal inclusion, representing the γ' phase, is embedded in an infinite γ -matrix. The fundamental idea behind this approach is that there would exist a direct correspondence between the actual problem and the model problem so that the results of the model problem could be directly extrapolated to the real microstructure (Fig. 1.7). In other words, if for the model problem an ellipsoid prolate in the direction of the applied stress minimizes the energy, then a "type P" behavior is inferred for the actual microstructure, while if an oblate ellipsoid minimizes the energy, a "Type N" behavior is inferred.

Pineau systematically applies Eshelby's theory and calculates the energy of a solid containing misfitting coherent precipitates of various shapes subjected to applied stresses. Three shapes are considered: spheres, plates perpendicular to the stress axis and needles aligned with the stress axis. Matrix and precipitates are assumed to be elastically isotropic.

Based on these calculations, the most stable shapes (corresponding to the lowest elastic energy), have been determined, and the final results are presented in the graphical form shown in Fig. 1.8.

According to this map, the major factors which affect stress coarsening behavior are the direction and the value of the applied stress, normalized by the elastic modulus of the matrix, the ratio between the elastic moduli of the two phases, and the $\gamma - \gamma'$ misfit. The derivations of Pineau have been generally accepted, for a certain time, as the most satisfactory treatment of the rafting process.

Unfortunately, as noted by Fredholm and Strudel [23], the model considered by Pineau leads to predictions that agree with the experimental observations summarized in Table 1.1, only if it is assumed that the γ' particles are stiffer than the matrix for all the tested alloys. But for at least two cases [13, 15], we have positive evidence

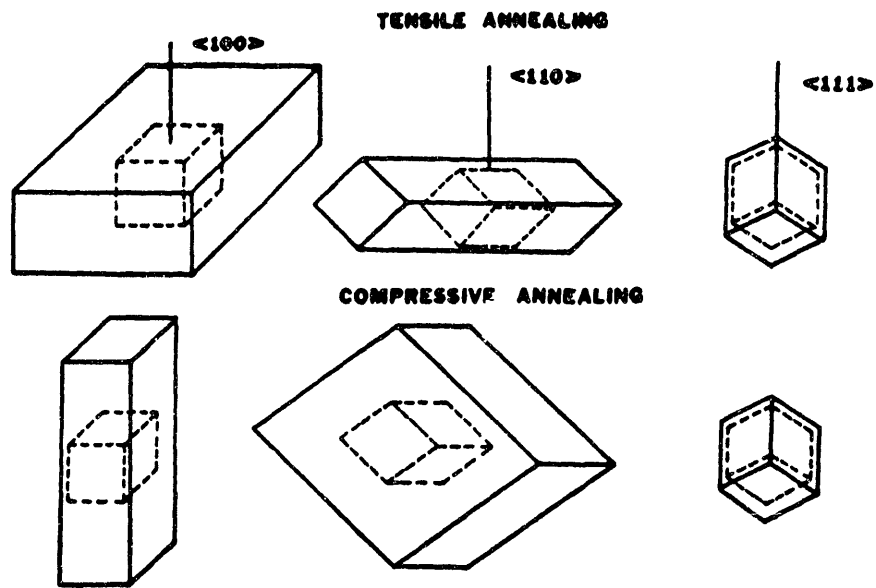


Figure. 1.6 A schematic summarizing the effects of stress orientation on the stress annealed shape of the γ' precipitates [13].

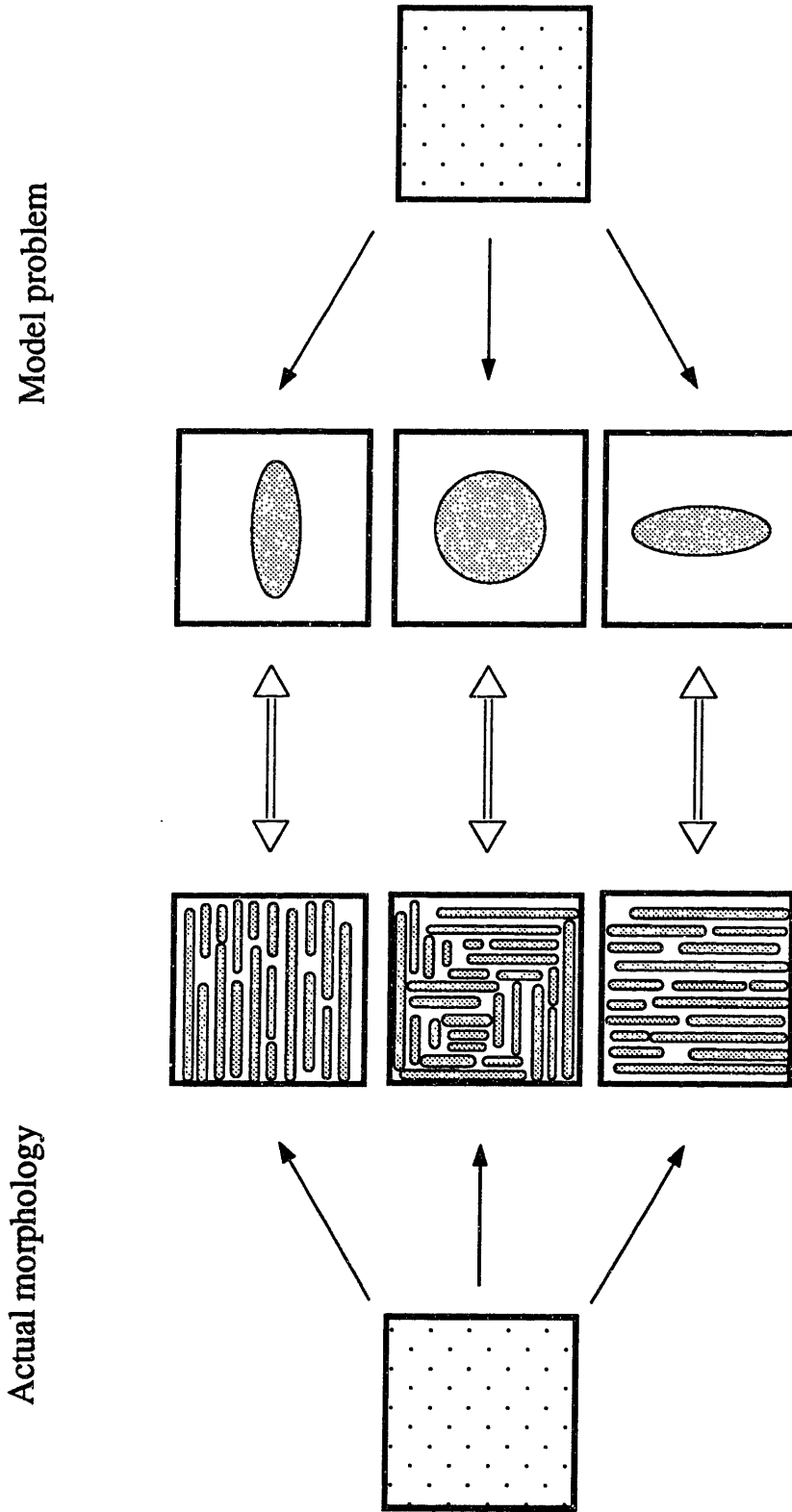


Figure 1.7 Correspondence between the model problem and the actual morphology.

that the precipitate phase is actually softer than the matrix so that Pineau's map predictions do not agree with the experimental data.

In order to obtain results more consistent with the experimental observations, subsequent studies have tried to reduce the number of simplifications in the Pineau model.

The Eshelby equivalent inclusion approach can be successfully applied to the study of ellipsoidal inclusions in anisotropic media, and models based on anisotropic elasticity have been derived in a number of studies [15, 31, 35].

The complexity of the problem increases by an order of magnitude when a cuboidal shape for the precipitate is considered. Faivre [33] has treated the problem of a single cuboidal inclusion for isotropic media and Chang [35] introduced a method based upon Green's function techniques to study single cuboidal precipitates in anisotropic media.

Regarding the actual periodic structure of the $\gamma - \gamma'$ morphology, and the effect of interaction energy between particles, Johnson [34] has considered the problem of two spherical inhomogeneities under the influence of an applied stress and studied the coarsening kinetics of the two particles; Jankowski, Wingo and Tsakalakos [32] have modeled the periodicity of the microstructure by using a space and time-dependent Fourier series; finally, Chang [35] has attempted, with partial success, to apply the Mura trigonometric series method and the finite element method to treat arrays of inclusions.

Still, no comprehensive model is available that accounts for the actual structure of the crystal and gives predictions which explain all the experimental results.

The reasons for this failure lie not only in the inherent limitations of the Eshelby inclusion approach: even a perfect elastic model of the real microstructure would not yield correct predictions for the rafting behavior.

The essential common flaw for all the model proposed in the literature is that the *inelastic* response of the γ -matrix, due to dislocation motion, is always *neglected* in the evaluation of the stress and strain fields. As mentioned in paragraph 1.2, a network of misfit dislocations is always observed at the $\gamma - \gamma'$ interfaces during rafting. The presence of these dislocations suggest that a localized "creep process" is relieving the $\gamma - \gamma'$ misfit, altering the state of stress in the crystal. As will be shown in Chapter 4, only a model that takes into account this effect can successfully account for the rafting behavior of Ni-superalloys.

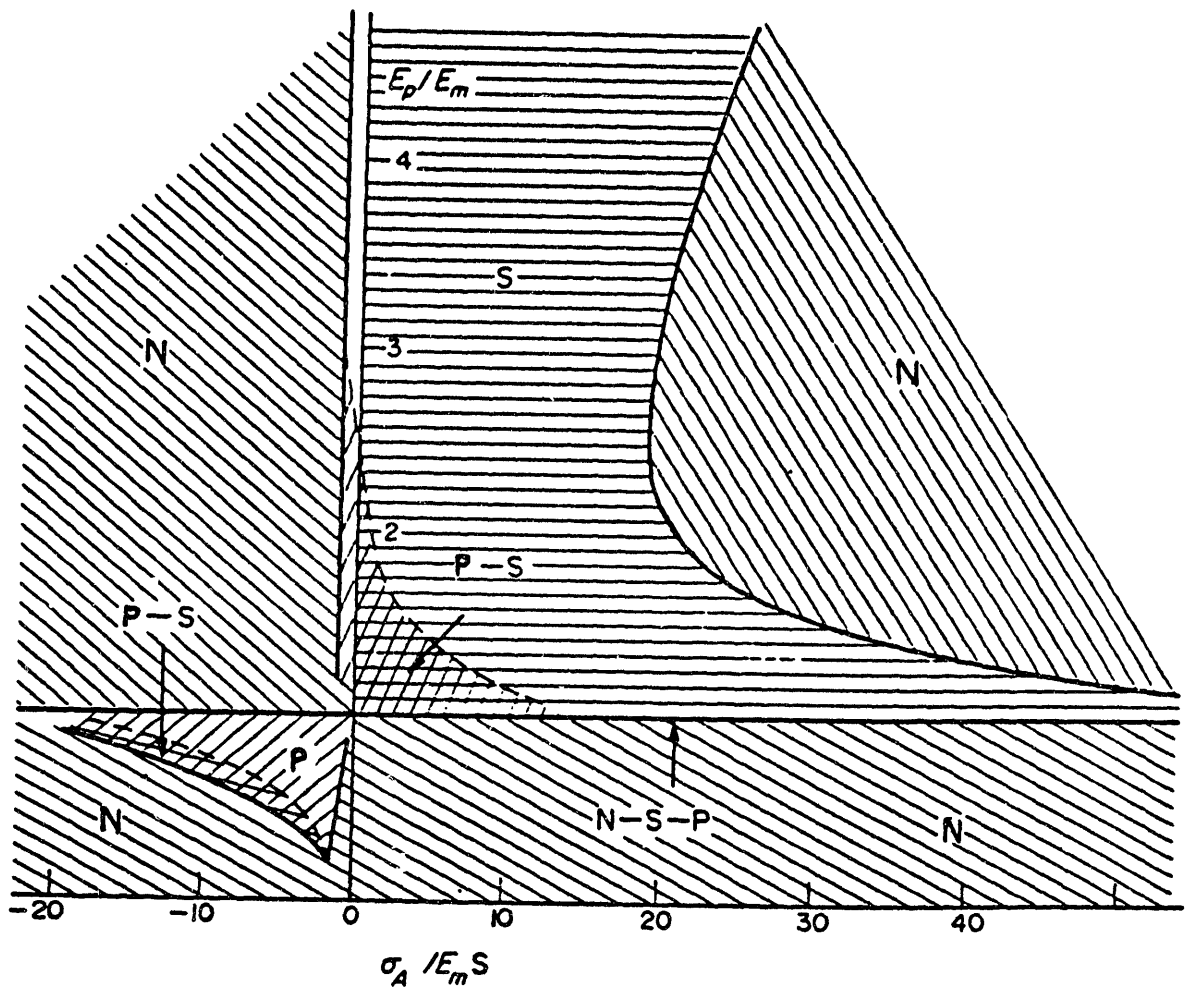


Figure. 1.8 Map giving the conditions which lead to the lowest total elastic energy for spheres (S), plates normal to the stress axis (N) and needles parallel to the stress axis (P). E_p/E_m is the ratio of the Young's modulus of the precipitate and that of the matrix, σ_A is the applied stress and δ the misfit between the precipitates and the matrix. The domains where two or three shapes are indicated for the particles are those where the difference in the corresponding elastic energies is less than $0.1 E_m \delta^2$. [11]

CHAPTER 2

THE FORCE ON A MATERIAL INTERFACE

2.1 Introduction

Consider a generic system whose configuration can be identified by a suitable number of parameters $\beta_1, \beta_2 \dots \beta_n$. We can express the *total energy* of the system, E^T , as a function of these parameters:

$$E^T = \hat{E}^T(\beta_1, \beta_2, \dots \beta_i, \dots \beta_n). \quad (2.1)$$

Following the terminology of analytical mechanics and thermodynamics, we can introduce the notion of *generalized force conjugate to the i^{th} parameter, f_i* , defined as

$$f_i = -\frac{\partial E^T}{\partial \beta_i}. \quad (2.2)$$

Thus f_i , which we may regard as the force *acting* on β_i , is the rate of decrease of the total energy with respect to the parameter β_i .

It is important to note that, in this definition, E^T is the *total energy*, i.e., the energy of the system we are studying plus the energy of the environment with which it interacts.

We will now restrict our attention to solid bodies with prescribed boundary conditions.

We can expect, in the material of the body, departures from uniformity on various scales which we may call *imperfections*. Examples on a microscopic scale are dislocations, foreign atoms, vacant lattice points and grain boundaries. On a macroscopic scale, there might be inclusions of one phase in another, cavities and cracks.

If the boundary conditions are held constant, the total energy of the system (the energy of the body plus the potential energy of the loading device) is a function of the set of parameters necessary to specify the configuration of the imperfections.

Thus, following the general derivation, we can define the force on a gliding dislocation, on an extending crack, or on a growing cavity.

For the particular case of inclusions and precipitates of one phase in another, such as martensitic plates in ferrite or γ' precipitates in a γ matrix in Ni-superalloys, if the two phases are uniform within themselves, we can consider the *interface itself to be the imperfection*.

If \mathcal{C}^* is a reference configuration for the interface, we can characterize any other configuration, \mathcal{C} , in terms of the normal displacement of the interface, ξ_n , with respect to \mathcal{C}^* (Fig. 2.1).

Thus the energy level E^T is determined by the parameter, $\xi_{\mathbf{n}}$, which is a function of the position \vec{x} along the interface:

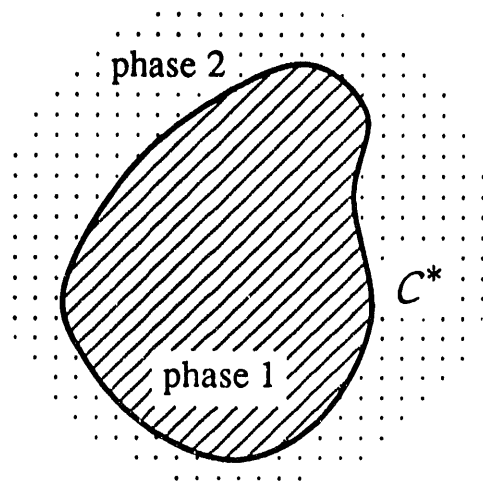
$$E^T = \hat{E}^T(\xi_{\mathbf{n}}(\vec{x})) \quad (2.3)$$

It is then straightforward to define a normal force acting on the interface, $\tau_{\mathbf{n}}$, which is work-conjugate to $\xi_{\mathbf{n}}$, as:

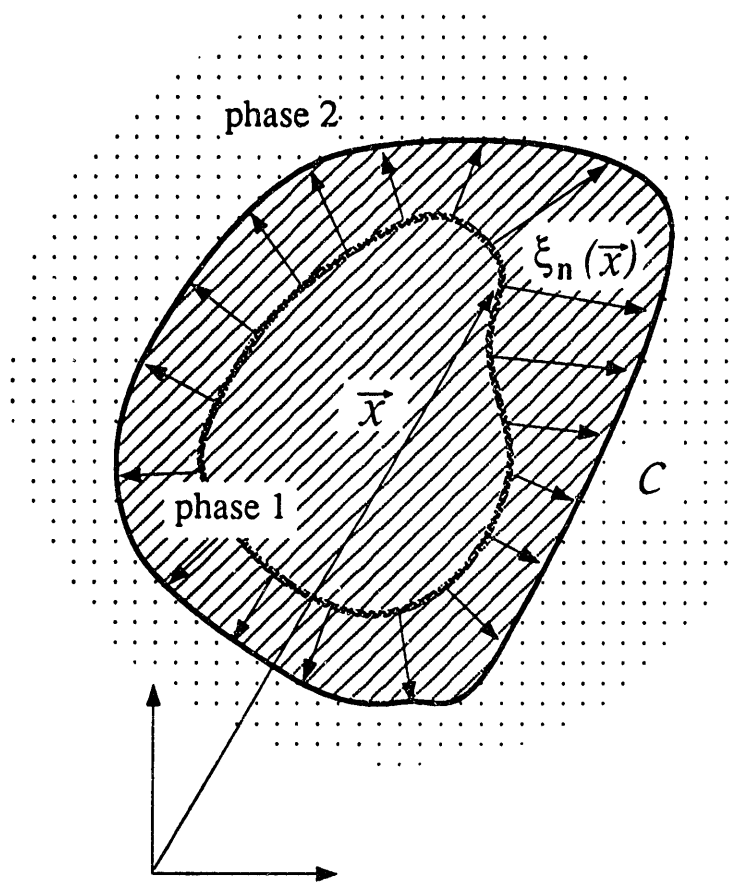
$$\tau_{\mathbf{n}}(\vec{x}) = \frac{-\partial E^T}{\partial \xi_{\mathbf{n}}(\vec{x})}. \quad (2.4)$$

It is possible to express this generalized force, $\tau_{\mathbf{n}}$, in an extremely convenient form using a quantity whose interesting features were first recognized by Eshelby [36], and which is therefore known as *Eshelby's Energy Momentum Tensor* (EMT).

In the following paragraphs, which closely follow the derivation presented by Eshelby in [37], we will first describe the mathematical process which generates the EMT, then we will discuss some physical interpretations and derive an expression for the force on a material interface.



Reference configuration C^*
 $E^T = E_0^T = E^T(\xi_n = 0)$



Current configuration C
 $E^T = \hat{E}^T(\xi_n(\bar{x}))$

Figure 2.1 Interface configuration.

2.2 The Energy Momentum Tensor in Continuum Mechanics

We will derive an expression for the EMT in the framework of finite deformation theory with a hyperelastic stress-strain relation.

Rectangular Cartesian coordinates X_i are used to label the position of material particles in the initial state.

If u_i is the displacement field, the final position of the particle, in the same coordinate system, will be x_i so that

$$u_i = x_i - X_i. \quad (2.5)$$

As a stress measure, we use the nominal Piola Kirchhoff stress, p_{ij} , so that, if W is the Lagrangian strain energy density,

$$p_{ij} = \frac{\partial W}{\partial u_{i,j}}. \quad (2.6)$$

The equilibrium condition is

$$\frac{\partial p_{ij}}{\partial X_j} + \rho b_i = 0_i, \quad (2.7)$$

where b_i are the body forces per unit mass (which will include the D'Alembert inertial force in dynamic problems), and ρ is the mass density referred to the initial volume.

We will consider the general case in which the strain energy density, W , depends on the gradient of the displacement field $u_{i,j}$ and also *explicitly* on the X_m :

$$W = \hat{W}(u_{i,j}; X_m). \quad (2.8)$$

This explicit dependency on X_m allows us to consider material inhomogeneities (regions with varying elastic constants) as well as states of internal stress characterized by the presence of *eigenstrains* $\epsilon_{ij}^T(X_m)$.

Here, with the term eigenstrains we indicate all such nonelastic strains as those associated with thermal expansion, phase transformation, creep, plastic flow, and lattice misfit [38].

For the elastic calculations of the force on a material interface, we will consider these strain fields as “frozen” in the material, i.e., the eigenstrain field will depend *only* on the location X_m .

Under these conditions it is perfectly equivalent to regard ϵ_{ij}^T as an extra field variable or to absorb the ϵ_{ij}^T -dependence of W into its explicit dependence on X_m .

If we substitute Eq. (2.6) in (2.7), we obtain an alternative form of the equilibrium equations

$$\frac{\partial}{\partial X_j} \frac{\partial W}{\partial u_{i,j}} = -\rho b_i. \quad (2.9)$$

At this point we need to distinguish the gradient of W , $\partial W/\partial X_i$, defined by

$$W(\vec{X} + d\vec{X}) = W(\vec{X}) + \frac{\partial W}{\partial X_i} dX_i + o(dX_i)^2, \quad (2.10)$$

from the explicit partial derivative of W with respect to X_i ,

$$\left(\frac{\partial W}{\partial X_i} \right)_{\text{exp}} = \frac{\partial W(u_{i,j}; X_m)}{\partial X_i} \Bigg|_{\substack{u_{i,j} = \text{const.} \\ X_m = \text{const. } m \neq i}}. \quad (2.11)$$

The gradient of W is thus given by

$$\frac{\partial W}{\partial X_k} = \frac{\partial W}{\partial u_{i,j}} \frac{\partial u_{i,j}}{\partial X_k} + \left(\frac{\partial W}{\partial X_k} \right)_{\text{exp}}. \quad (2.12)$$

Noting that $u_{i,jk} = u_{i,kj}$ and using the rule for differentiating a product, we obtain

$$\frac{\partial W}{\partial X_k} = \frac{\partial}{\partial X_j} \left(\frac{\partial W}{\partial u_{i,j}} u_{i,k} \right) - \frac{\partial}{\partial X_j} \left(\frac{\partial W}{\partial u_{i,j}} \right) u_{i,k} + \left(\frac{\partial W}{\partial X_k} \right)_{\text{exp}}. \quad (2.13)$$

Substituting (2.9) and (2.6) in (2.13), we have

$$\frac{\partial}{\partial X_j} (W \delta_{jk} - p_{ij} u_{i,k}) = \left(\frac{\partial W}{\partial X_k} \right)_{\text{exp}} + \rho b_i u_{i,k}. \quad (2.14)$$

We can now introduce the Energy Momentum Tensor, P , whose components are given by

$$P_{kj} = W \delta_{kj} - p_{ij} u_{i,k}, \quad (2.15)$$

so that eq. (2.14) reads

$$\frac{\partial P_{kj}}{\partial X_j} = \left(\frac{\partial W}{\partial X_k} \right)_{\text{exp}} + \rho b_i u_{i,k}. \quad (2.16)$$

Thus the divergence of P vanishes wherever W does not explicitly depend on X_m and there are no body forces.

Note how, for a more concise notation, here we have incorporated the ϵ_{ij}^T -dependence of W into its dependence on X_m ; if we regard ϵ_{ij}^T as an extra field variable, then

$$W = \hat{W}(u_{i,j}; \epsilon_{ij}^T(X_m); X_m). \quad (2.17)$$

We can expand $\left(\frac{\partial W}{\partial X_k} \right)_{\text{exp}}$ into two contributions:

$$\left(\frac{\partial W}{\partial X_k} \right)_{\text{exp}} = \left(\frac{\partial W}{\partial X_k} \right)_{\text{inhom}} + \frac{\partial W}{\partial \epsilon_{mn}^T} \frac{\partial \epsilon_{mn}^T}{\partial X_k}, \quad (2.18)$$

where the first term accounts for material inhomogeneities as well as, in a more general context, for any effect due to space gradients of elastic constants (e.g., temperature dependence of elastic constants associated with a temperature gradient).

An interesting interpretation of the physical meaning of P can be derived if we consider an elastic body subject only to surface loading (with no body forces), containing a certain number of imperfections I_1, I_2, \dots, I_n . These imperfections might be inhomogeneities, inclusions with an eigenstrain, point defects, etc. We assume that, apart from these imperfections, the remaining material is “good” elastic material where

$$\left(\frac{\partial W}{\partial X_k}\right)_{\text{exp}} = 0_k. \quad (2.19)$$

If the generic defect I suffers a small translation $\delta\vec{\xi}$, there will be a variation in the total energy of the system

$$\delta E^T = -\delta\xi_k f_k, \quad (2.20)$$

where \vec{f} is the generalized force acting on I .

It can be proved [37] that the components of \vec{f} are given by:

$$f_k = \int_S P_{kj} dS_j, \quad (2.21)$$

where S is any surface surrounding I and isolating it from all the other imperfections, and $d\vec{S} = dS\vec{n}$ is the oriented surface element with \vec{n} being the unit *outward* normal to the surface. Note that S can be chosen arbitrarily, without altering \vec{f} , only as long as it remains in “good” material where (2.19) holds.

2.3 An Expression for the Force on an Interface

We are now concerned with the special case where the imperfection is represented by the interface between an *inclusion*, Ω , and an otherwise homogeneous medium which we will call the *matrix*, D (Fig. 2.2). We limit our attention to coherent interfaces, for which the displacement field \vec{u} is continuous at the interface. The inclusion may have elastic constants differing from those of the matrix, and the body may be subjected to an eigenstrain field, ϵ_{ij}^T , which might be discontinuous across the interface.

We will derive an expression for the generalized normal force acting on the interface as a result both of the internal state of stress, due to the ϵ_{ij}^T -field, and of the externally applied loads. This quantity will be a measure of the force driving the migration of the interface.

Consider a reference configuration for the interface, S^* , and an infinitesimal migration to a current configuration S (Fig. 2.2). The migration can be specified by a small vector $\delta\vec{\xi}$ at each point of S^* .

We want to evaluate the change in the total energy of the system, δE^T , as a result of the migration $S^* \rightarrow S$. We can obtain our result with the help of a sequence of imaginary steps which simulate the migration.

We start with the interface in the S^* configuration, a displacement field \vec{u}^* in the body (\vec{u}^{*D} in the matrix, $\vec{u}^{*\Omega}$ in the inclusion), and we want to end up with the interface in the S configuration and a displacement field \vec{u} in the body (\vec{u}^D in the matrix, \vec{u}^Ω in the inclusion).

Step 1. We cut out and remove the “ D -material” which lies in the region between S^* and S , and apply suitable surface tractions to the “hole” to prevent relaxation.

The variation in energy for step 1 is

$$\delta E_{(1)}^T = - \int \delta \xi_j W^D dS_j, \quad (2.22)$$

where $d\vec{S} = dS\vec{n}$, with \vec{n} being the unit outward normal to the interface (from Ω to D : see Fig. 2.2), and W^D is the elastic energy of the “ D -material” that we are removing.

The displacement on the boundary, S , of D is now $u_i^{*D} + \delta \xi_k u_{i,k}^{*D}$ and the traction is $p_{ij}^D(-dS_j) + o(d\xi_j)$.

Step 2. We bring the displacement field at the boundary of D to its final value \vec{u}^D . The variation in energy is:

$$\delta E_{(2)}^T = - \int [u_i^D - (u_i^{*D} + \delta \xi_k u_{i,k}^{*D})] p_{ij}^D dS_j. \quad (2.23)$$

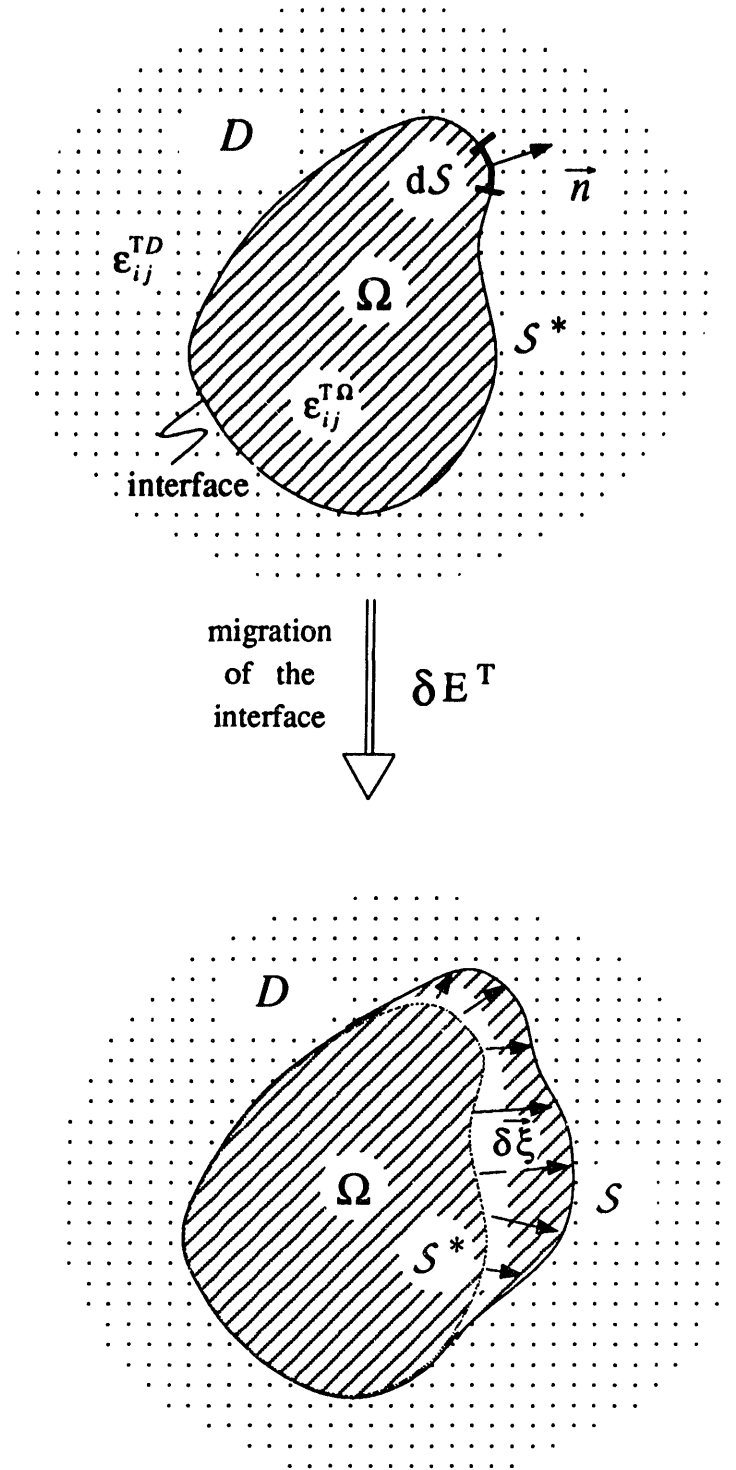


Figure 2.2 Variation in energy associated with a migration of the interface .

Step 3. We allow the material that we have removed to transform from “ D -material” to “ Ω -material” and we put it back in place.

The variation in energy is then

$$\delta E_{(3)}^T = \int \delta \xi_j W^\Omega dS_j. \quad (2.24)$$

The displacement on the boundary S of Ω is now $u_i^{*\Omega} + \delta \xi_k u_{i,k}^{*\Omega}$ and the traction is $p_{ij}^\Omega dS_j + o(d\xi_j)$.

Step 4. We alter the displacement of the boundary of Ω to its final value, \vec{u}^Ω , with a variation in energy:

$$\delta E_{(4)}^T = \int [u_i^\Omega - (u_i^{*\Omega} + \delta \xi_k u_{i,k}^{*\Omega}) p_{ij}^\Omega dS_j]. \quad (2.25)$$

Note that if the transformation from “ D -material” to “ Ω -material” brings about a variation in chemical energy, we should also include a term

$$\delta E_{chem}^T = \int \delta \xi_j (W_o^\Omega - W_o^D) dS_j, \quad (2.26)$$

where $(W_o^\Omega - W_o^D)$ is the work required to transform a unit volume of unstressed D into an equal mass of unstressed Ω .

Furthermore, if a surface energy γ_{int} is associated with the interface, the displacement of the boundary brings about a variation in energy:

$$\delta E_{int}^T = \int \delta \xi_j \gamma_{int} K dS_j, \quad (2.27)$$

with $K = 1/R_1 + 1/R_2$, where R_1, R_2 are the local principal radii of curvature of the surface.

As previously mentioned (paragraph 1.3), in order to give an explanation for the directionality of rafting we can actually restrict our attention to the variation of the total elastic energy $\delta E_{EL}^T (= \delta E_{(1)}^T + \delta E_{(2)}^T + \delta E_{(3)}^T + \delta E_{(4)}^T)$ so that we will neglect the chemical and interface energy terms in the following derivation. Thus, the expression for the force acting on the interface $\tau_{\mathbf{n}}$, that we will derive in the following section, actually gives only the “elastic contribution” to the force on the interface.

Chemical and interface energy terms should, however, be included in more general applications.

Since \vec{u} is continuous across the interface, we have $u_i^D = u_i^\Omega$ and $u_i^{*D} = u_i^{*\Omega}$ for each element dS_j . Also, the traction vector $p_{ij} dS_j$ is continuous at the interface, so that on adding the four contributions (2.22, 2.23, 2.24, 2.25), we obtain the total variation:

$$\delta E_{EL}^T = - \int_{S^*} \delta \xi_k \{ (W^D \delta_{kj} - p_{ij} u_{i,k}^D) - (W^\Omega \delta_{kj} - p_{ij} u_{i,k}^\Omega) \} dS_j, \quad (2.28)$$

and, using the definition (2.15),

$$\delta E_{EL}^T = - \int_{S^*} \delta \xi_k \{ P_{kj}^D - P_{kj}^\Omega \} dS_j. \quad (2.29)$$

It is natural to choose the direction of $\delta \vec{\xi}$ normal to the interface: $\delta \vec{\xi} = \delta \xi_n \vec{n}$. If we use the notation $[A]$ to denote the discontinuity of the generic quantity A across the interface, we can recast Eq. (2.29) in the form

$$\delta E_{EL}^T = - \int_S \delta \xi_n (n_k [P_{kj}] n_j) dS. \quad (2.30)$$

If we compare Eq. (2.30) and Eq. (2.4) we can easily see that Eq. (2.30) is equivalent to the statement that there is an effective normal force per unit area of the interface of magnitude

$$\tau_n = n_k [P_{kj}] n_j, \quad (2.31(a))$$

or, if we substitute expression (2.15) for P ,

$$\tau_n = [W] - t_i \left[\frac{\partial u_i}{\partial n} \right], \quad (2.31(b))$$

where $t_i = p_{ij} n_j$ are the components of the traction vector \vec{t} at the interface and $\partial/\partial n$ denotes spatial differentiation along the normal direction.

Note how, throughout our derivation of τ_n , we have never needed to invoke condition (2.19). This means that expressions (2.31) for τ_n hold also in the presence of eigenstrains ϵ_{ij}^T and body forces b_i . In fact, we will actually use these expressions to evaluate the elastic driving force for morphology evolution of γ' precipitates in Ni-superalloys.

We will first perform our calculations for merely elastic fields in which the only eigenstrain is due to the $\gamma - \gamma'$ lattice misfit, then we will follow the evolution of the force on the interface during a stress-annealing transient where creep strains set in, so that the eigenstrain field will be the superposition of the initial misfit field and of the creep field.

Before concluding this paragraph, it is perhaps appropriate to emphasize that τ_n is an extremely convenient measure of the elastic driving force for the evolution of the inclusion shape.

A positive value of τ_n (Fig. 2.3) means that the total elastic energy will be reduced if the interface migrates outward, thus indicating a tendency for the inclusion to grow. Conversely, a negative value of τ_n indicates a tendency for the interface to reduce its volume.

We can construct graphs of the distribution of τ_n over the interface; in particular, if we limit ourselves to 2D-problems, we can plot the value of τ_n as a function of the arclength along the interface (Fig. 2.4).

We will introduce numerical methods to calculate τ_n in Chapter 3, and in Chapter 4 we will apply these methods to the analysis of rafting in $\gamma - \gamma'$ superalloys.

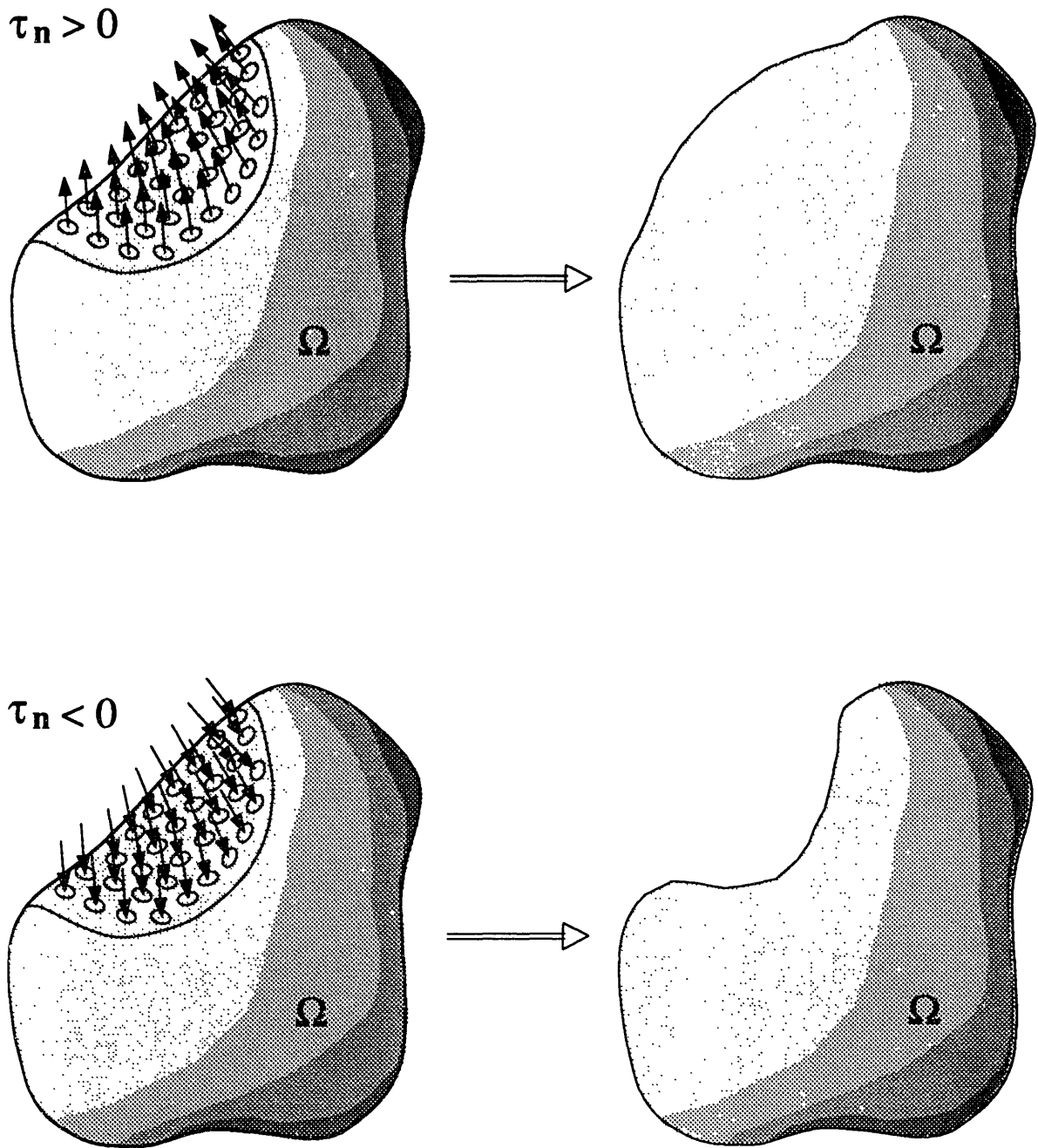


Figure 2.3 τ_n as a driving force for shape evolution.

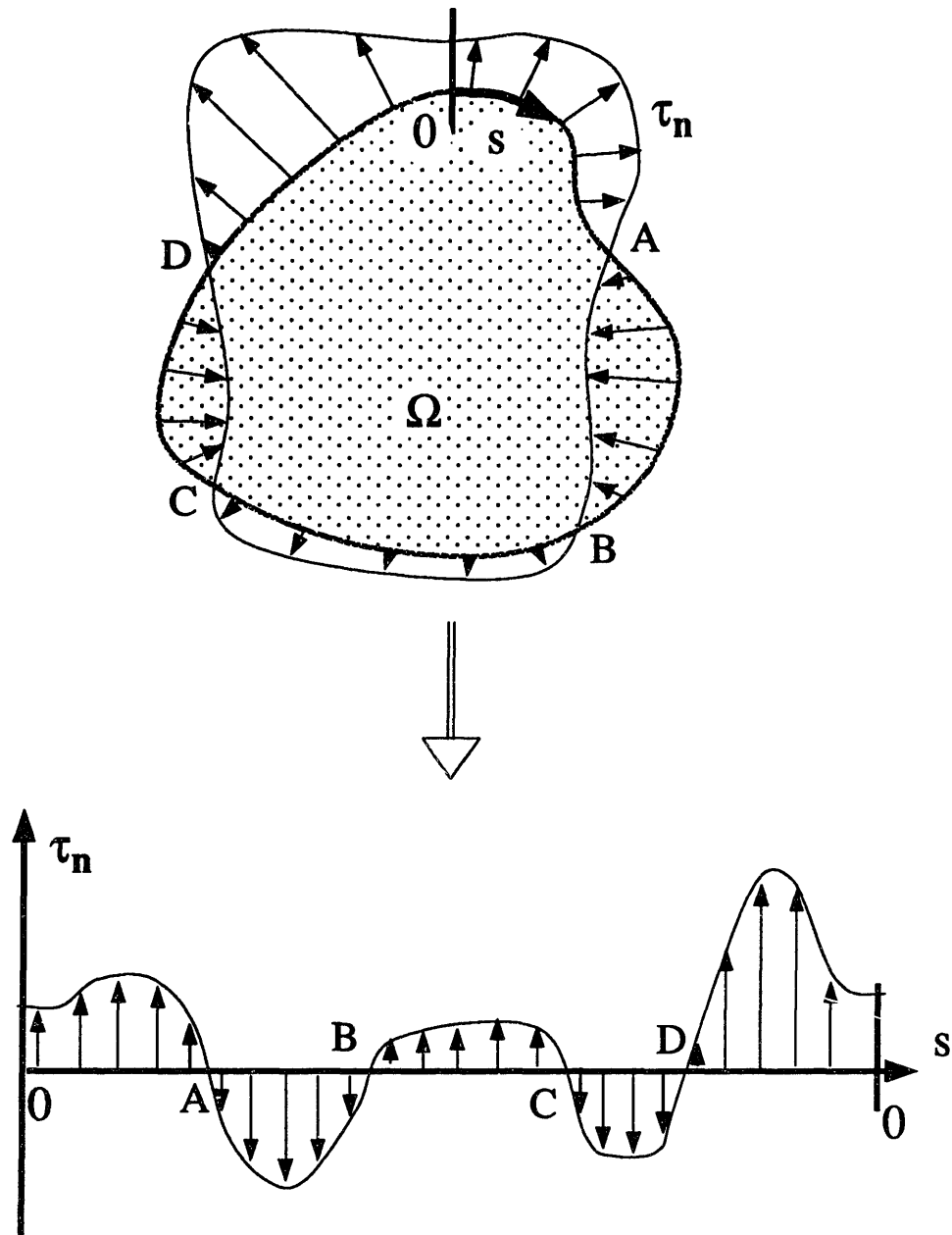


Figure 2.4 Schematic plot of the force along the interface for 2-D models .

CHAPTER 3

NUMERICAL METHODS

3.1 Introduction

In Chapter 2 we have defined a quantity, $\tau_{\mathbf{n}}$, which provides direct information on the driving force for morphology evolution of multi-phase materials. If we examine expressions (2.31), we can notice how the force on the interface can be obtained directly in terms of elastic field quantities evaluated at the material interface. This is indeed an extremely convenient feature of this approach, since we have an instrument, the Finite Element Method (FEM), that allows us to evaluate the elastic field around a material interface, for virtually any kind of morphology of the system, material constants, applied loads and internal stress state (eigenstrain field).

Throughout this thesis, the finite element program ABAQUS [39] has been used, so that, even if the methods are general, the software has been specifically developed to postprocess ABAQUS results.

For the present applications, we can limit our attention to small-deformation analysis, so that we can substitute the nominal Piola Kirchhoff stress, p_{ij} , with the Cauchy stress σ_{ij} and the expression for the EMT becomes

$$P_{kj} = W\delta_{kj} - \sigma_{ij}u_{i,k}. \quad (3.1)$$

The elastic strain energy density will be given by

$$W = \hat{W}(\epsilon_{ij}^e) = \int_0^{\epsilon_{ij}^e} \sigma_{ij} d\epsilon_{ij}^e, \quad (3.2)$$

where

$$\epsilon_{ij}^e = \epsilon_{ij} - \epsilon_{ij}^T \quad (3.3)$$

is the elastic part of the strain tensor ϵ_{ij} :

$$\epsilon_{ij} = \frac{1}{2}(u_{i,j} + u_{j,i}). \quad (3.4)$$

In this chapter we will first describe an extremely direct method to evaluate $\tau_{\mathbf{n}}$, then we will illustrate an alternative method which utilizes a domain integral representation for the energy perturbation δE_{EL}^T of exp. (2.30), and discuss its numerical implementation.

3.2 A Direct Approach: The Computer Program POSTABQ

Consider a generic boundary value problem (BVP) for which we intend to evaluate τ_n at the interface of an inclusion Ω (Fig. 3.1(a)). We first build a finite element model for the BVP, discretizing the domain under examination and applying appropriate boundary conditions (Fig. 3.1(b)). This model represents the input for the structural finite element code, ABAQUS, which will solve the BVP. ABAQUS provides, in output, values at nodes and integration points for the elastic energy density W , the displacement field \vec{u} and the stress tensor σ . Thus, one simple way to calculate the force on the interface would be to postprocess the ABAQUS output file, evaluating the quantities $[W], \vec{t}, [\frac{\partial \vec{u}}{\partial n}]$, and substitute these values in expression (2.31(b)) to directly obtain τ_n .

This method has been implemented in the computer program POSTABQ. The program POSTABQ has been conceived as a multi-purpose postprocessor for ABAQUS. The current version of the program can handle only 2-D problems with second-order eight-node isoparametric elements, but has been structured so that its applicability can be easily extended to cope with 3-D geometries. The user supplies a set of nodes (by way of their number in the F.E. model) which define a “path” — in our case the path will be the interface — and the program evaluates the path geometry: curvilinear coordinate and normal vector to the path, topology and connectivity of the elements around the path, etc. Then the user asks the program to perform a sequence of operations on a certain number of selected field variables along the path. These operations can include reading the quantities from the ABAQUS file and storing them in local arrays, evaluating gradients of scalar and vector fields, evaluating the components of vectors and second order tensors in a rotated reference frame, evaluating the dot product of vector and tensor fields with the normal to the path (thus calculating the normal component of these quantities), and printing the results of such operations in an ASCII file.

The user can also program a user-subroutine where he can process the quantities resulting from the previous operations. Thus, in order to calculate τ_n on the interface, the user will

- (a) provide an ordered list of the nodes along the interface;
- (b) require the program to:
 - read and store the values of the strain energy density W ;
 - read the values of the stress field and evaluate the components of the traction vector

$$t_i = \sigma_{ij}n_j;$$

- read the value of the displacement field \vec{u} , evaluate the gradient of the displacement field $\nabla\vec{u}$, and evaluate the derivative of \vec{u} along the normal direction:

$$\frac{\partial u_i}{\partial n} = u_{i,j}n_j;$$

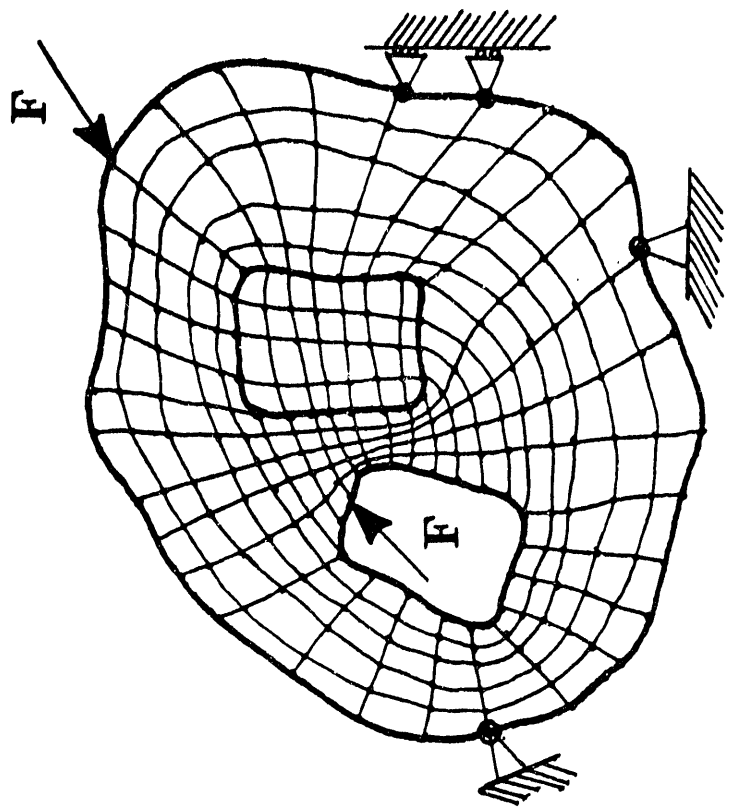
- (c) write a user subroutine where the results of the previous operations are combined to obtain

$$\tau_{\mathbf{n}} = [W] - t_i \left[\frac{\partial u_i}{\partial n} \right]$$

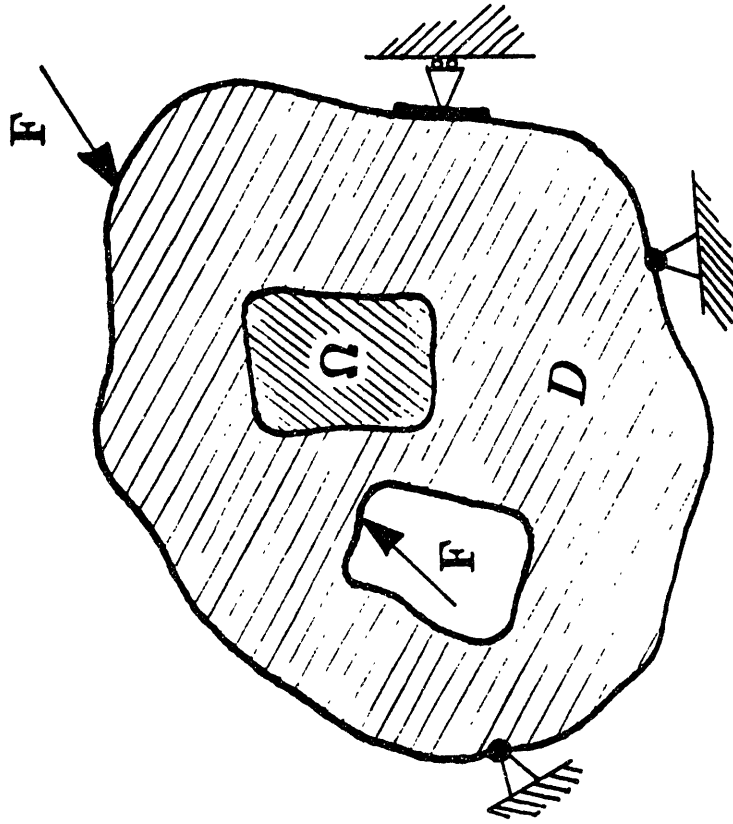
at all nodes along the interface.

The listing of the program POSTABQ is given in APPENDIX I.

The advantage of this method lies in its simplicity and therefore in the limited amount of calculations required. Unfortunately, it has one main drawback: since the evaluation of $\tau_{\mathbf{n}}$ directly relies on the determination of elastic field *at* the interface, we can expect that our results will be affected by some numerical noise. The area adjacent to the interface is in fact directly affected by numerical disturbances arising from the discontinuity of the elastic field. Extremely refined meshes, therefore, are required to limit this effect. An alternative approach which can overcome this kind of difficulty will be presented in the next section.



(a) Boundary value problem



(b) Finite element model

Figure 3.1 Finite element model of a boundary value problem

3.3 A Domain Integral Approach: The Computer Program DOMAIN

3.3.1 Historical perspective

The J -integral, introduced by Eshelby [45] together with a number of other path-independent contour integrals, has quickly become one of the most-used crack parameters in fracture mechanics.

Its role in the context of nonlinear fracture mechanics was introduced by Rice [40, 41] who has interpreted J as a measure of the intensity of the crack tip field: if evaluated on a contour placed within the region of HRR dominance [42, 43], the value of J serves as a unique scaling amplitude for the HRR singular fields. The initiation of crack growth in plastically deforming bodies can thus be correlated with a critical value of the J -integral.

The reason for the “success” of the J -integral lies mainly in the mentioned property of path-independence: the integrand is divergence-free for a material that admits a strain energy function, so that the J -integral has the same value for all open paths beginning on one face of the crack and ending on the opposite face. This feature plays an important role since it allows a direct computation of the strength of crack tip singularities by evaluating the integral in regions remote from the crack tip, where the numerical field solution is more reliable.

With the help of weighting functions, the J contour integral can be recast into a finite *domain* volume *integral*. This alternative formulation is naturally compatible with the finite element method.

In fact, the domain-approach first appeared already cast in its finite element implementation: the Virtual Crack Extension (VCE) technique, introduced by Parks [47], actually corresponds to a finite element formulation of the domain integral approach. By the VCE technique [48, 49, 50], accurate pointwise values of the energy release rate can be obtained.

This method has been interpreted in a somewhat more general context by deLorenzi [51, 52], who has obtained a more compact continuum formulation of the VCE technique.

The use of domain integral techniques in fracture mechanics has been subsequently addressed in several studies [44, 46, 53, 54], where thermal loads and kinetic energy have been rigorously incorporated in the formulation.

Here we present a straightforward extension of this methodology, which will allow us to evaluate the force acting on a material interface.

We are led to this approach by the same reasons which have brought about the use of contour and domain integrals in fracture mechanics. We must deal with a structural discontinuity (in our case, the interface; in fracture mechanics, the crack), which locally affects our numerically-determined field solutions. Thus we need to develop a formulation in which the desired local quantities are expressed in terms of the field solution in regions as remote as possible from the discontinuity.

In the next section, 3.3.2, we present a derivation of the domain integral expression for the energy variation, δE_{EL}^T , that corresponds to a migration of the interface. We then outline in Section 3.3.3 the finite element formulation of the domain integral method to determine the force on the interface. In Appendix II, we give the listing of the computer program DOMAIN in which this methodology has been implemented.

3.3.2 Derivation of a domain integral expression for the energy perturbation

Let S be the interface separating an inclusion Ω and an otherwise homogeneous medium (Fig. 3.2(a)). If \vec{n} is the unit outward normal to the interface, we can define a perturbation of the interface $\delta\vec{\xi}$ in terms of its normal component $\delta\xi_n$ as

$$\delta\vec{\xi}(\vec{x}) = \delta\xi_n(\vec{x}) \vec{n}(\vec{x}), \quad (3.5)$$

thus $\delta\vec{\xi}$ is a vector quantity defined at all locations \vec{x} along the interface.

In section 2.3 we have derived an expression for the change in the total energy, δE_{EL}^T , associated with the perturbation $\delta\vec{\xi}$:

$$\delta E_{EL}^T = \int_S \delta\xi_i [P_{ij}] n_j dS. \quad (3.6)$$

Let S^+ now be any surface completely surrounding S , and S^- any surface completely surrounded by S , as illustrated in Fig. 3.2(b). It is also assumed that the volume between S^+ and S^- is simply connected. In order to develop a volume integral expression for δE_{EL}^T , we first introduce the vector field \vec{q} defined over the domain V enclosed by S^- and S^+ . The vector field \vec{q} is defined so that it satisfies the following requirements:

- (a) $\vec{q}(\vec{x}) \equiv \delta\vec{\xi}(\vec{x})$; if \vec{x} identifies a point on S ;
- (b) $\vec{q}(\vec{x}) \equiv 0$; if \vec{x} identifies a point on S^+ or S^- ;
- (c) $\vec{q}(\vec{x})$ is a smooth function in V .

Then (3.5) can be written as

$$\delta E_{EL}^T = - \int_S q_i(\vec{x}) [P_{ij}] n_j dS. \quad (3.8)$$

We can recast (3.8) in the form

$$\delta E_{EL}^T = I^+ + I^-, \quad (3.9)$$

where

$$I^+ = - \int_S q_i P_{ij}^+ n_j dS \quad (3.10(a))$$

$$I^- = \int_S q_i P_{ij}^- n_j dS, \quad (3.10(b))$$

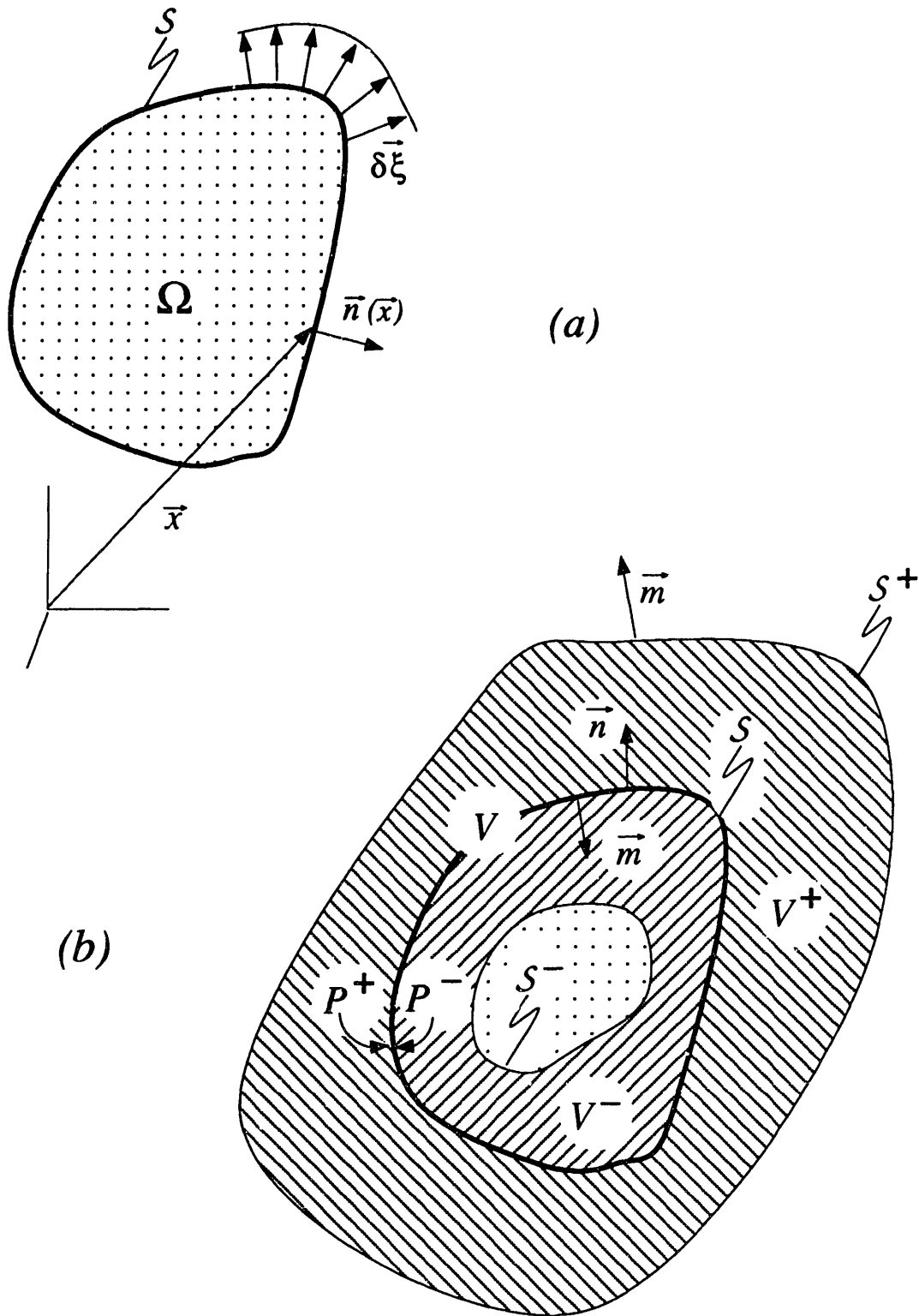


Figure 3.2 Definition of the domain of integration.

with P_{ij}^+ being the EMT on the “plus side” of the interface (Fig. 3.2(b)) and P_{ij}^- the EMT on the “minus side”.

Now consider the expression (3.10(b)) for I^- ; if we indicate with V^- the domain delimited by S^- and S , and with ∂V^- the boundary of V^- , since \vec{q} vanishes on S^- we can write:

$$I^- = \int_{\partial V^-} q_i P_{ij}^- n_j dS \quad (3.11)$$

and, applying the divergence theorem:

$$I^- = \int_{V^-} (q_i P_{ij})_{,j} dV \quad (3.12(a))$$

or

$$I^- = \int_{V^-} (P_{ij} q_{i,j} + P_{ij,j} q_i) dV. \quad (3.12(b))$$

In section 2.2 we have derived expression (2.16) for the divergence of P . If we substitute (2.18) in (2.16), we obtain

$$P_{ij,j} = \left(\frac{\partial W}{\partial X_i} \right)_{inhom} + \frac{\partial W}{\partial \epsilon_{mn}^T} \frac{\partial \epsilon_{mn}^T}{\partial X_i} + \rho b_k u_{k,i} \quad (3.13)$$

Using definition (3.2) for the strain energy density and substituting for the elastic strain (3.3) we obtain:

$$\frac{\partial W}{\partial \epsilon_{mn}^T} = - \frac{\partial W}{\partial \epsilon_{mn}} = -\sigma_{mn} \quad (3.14)$$

so that:

$$P_{ij,j} = \left(\frac{\partial W}{\partial X_i} \right)_{inhom} - \sigma_{mn} \epsilon_{mn,i}^T + \rho b_k u_{k,i}. \quad (3.15)$$

If the material within the domain V^- is homogeneous ($(\partial W / \partial X_j)_{inhom} = 0_j$), we have:

$$I^- = \int_{V^-} \{ P_{ij} q_{i,j} + (\rho b_k u_{k,i} - \sigma_{mn} \epsilon_{mn,i}^T) q_i \} dV. \quad (3.16)$$

We can perform an analogous sequence of operations on I^+ :

$$I^+ = \int_{\partial V^+} q_i P_{ij}^+ m_j dS, \quad (3.17)$$

where V^+ is the domain delimited by S and S^+ , ∂V^+ is its boundary, and \vec{m} is the unit outward normal to ∂V^+ ($\vec{m} = -\vec{n}$ on S).

By applying the divergence theorem and substituting for $P_{ij,j}$, if the material within V^+ is homogeneous, we obtain:

$$I^+ = \int_{V^+} \{P_{ij}q_{i,j} + (\rho b_k u_{k,i} - \sigma_{mn} \epsilon_{mn,i}^T)q_i\} dV. \quad (3.18)$$

Substituting (3.16) and (3.18) in (3.9) and noting that $V \equiv V^+ + V^-$ we obtain

$$\delta E_{EL}^T = \int_V \{P_{ij}q_{i,j} + (\rho b_k u_{k,i} - \sigma_{mn} \epsilon_{mn,i}^T)q_i\} dV, \quad (3.19(a))$$

or

$$\delta E_{EL}^T = \int_V \{(Wq_{i,i} - \sigma_{kj}u_{k,i}q_{i,j}) + (\rho b_k u_{k,i} - \sigma_{mn} \epsilon_{mn,i}^T)q_i\} dV. \quad (3.19(b))$$

We have thus obtained a volume-integral expression for δE_{EL}^T . Note how, as long as the \vec{q} -field and the domain V are chosen so that requirements (3.7) are satisfied, expressions (3.19) will give us the same value for δE_{EL}^T for any choice of the domain V . This *invariance of the domain integral* representation of δE_{EL}^T with respect to variation in domain size and shape will provide a useful independent check on the consistency and quality of our numerical calculations. This is indeed another attractive feature of the domain integral approach.

If we substitute expression (2.31(a)) in (2.30) we have

$$\delta E_{EL}^T = - \int_S \delta \xi_n \tau_n dS; \quad (3.20)$$

if we equate the right hand side of Eq. (3.20) and (3.19) we have

$$- \int_S \delta \xi_n \tau_n dS = \int_V \{(Wq_{i,i} - \sigma_{kj}u_{k,i}q_{i,j}) + (\rho b_k u_{k,i} - \sigma_{mn} \epsilon_{mn,i}^T)q_i\} dV. \quad (3.21)$$

The desired quantity, τ_n , appears on the left-hand side, while we can evaluate the expression on the right-hand side in terms of known field quantities: $W, \sigma, u, b, \epsilon^T$.

In the next section, 3.3.3, we will describe how, with an appropriate choice of the perturbation field ($\delta \vec{\xi}$ and \vec{q}), we can extract local values of τ_n from Eq. (3.21).

3.3.3 Finite element implementation

We will discuss a numerical implementation of the domain integral approach, for 2-D configurations, within the context of the displacement finite-element method using biquadratic Lagrangian shape functions.

We define on the interface S , N nodes and M biquadratic (3-node) isoparametric elements (Fig. 3.3(a)). For each element we can identify an isoparametric coordinate η — as shown in Fig. 3.3(b) — and define the basic shape functions:

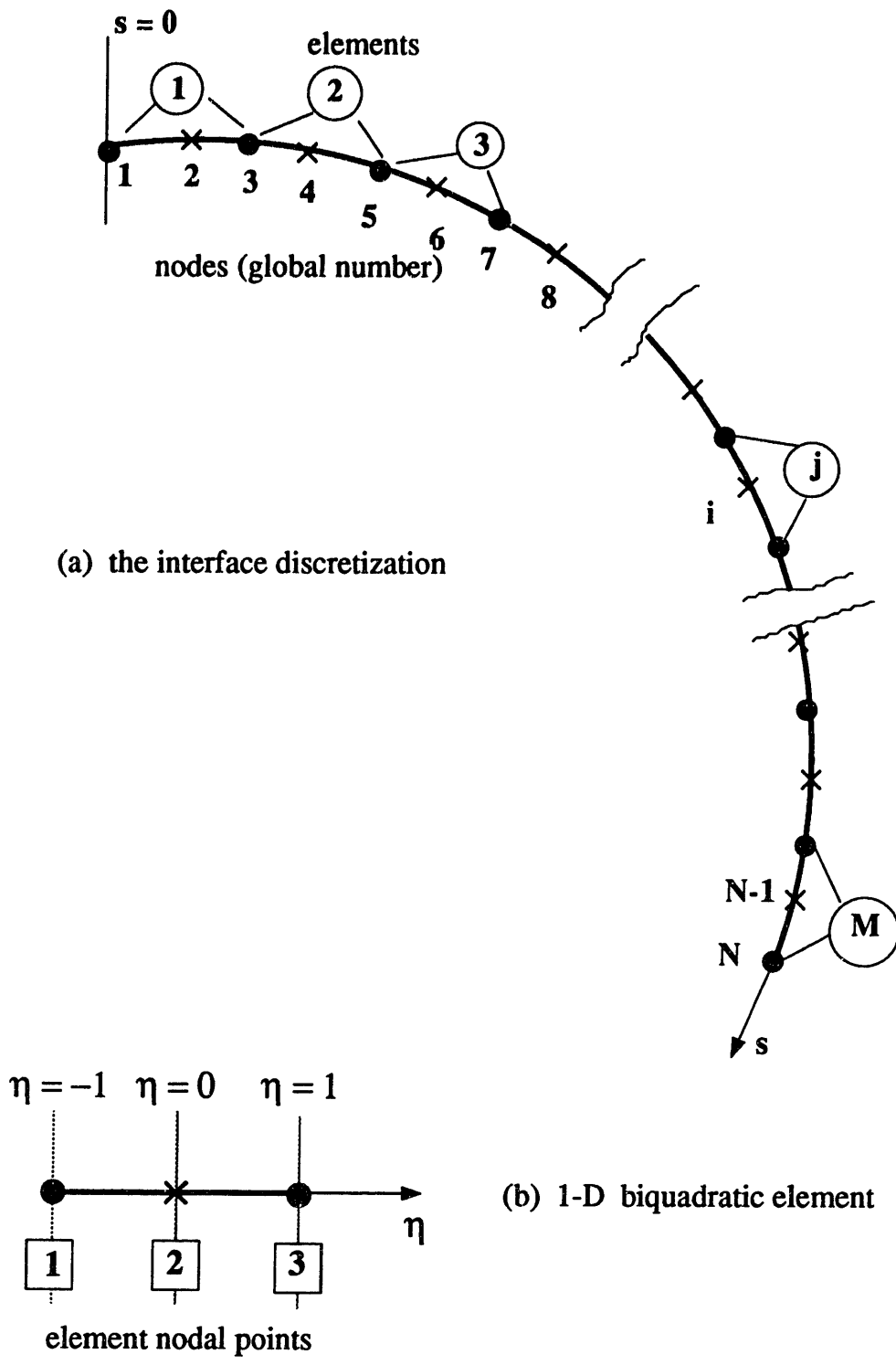


Figure 3.3 Finite element discretization of the interface.

$$N^1(\eta) = \frac{1}{2}\eta(\eta - 1)$$

$$N^2(\eta) = (1 - \eta)(1 + \eta)$$

$$N^3(\eta) = \frac{1}{2}\eta(\eta + 1).$$

Throughout our presentation, superscripts refer to the element nodal point number (as in Fig. 3.3(b)), while subscripts refer to the global node/element number along S .

We can express the value of any quantity, g , at location η along the element j in terms of the nodal values of g and of the shape functions:

$$g(\eta) = N^i(\eta)\langle g^i \rangle_j, \quad (3.22)$$

where the summation convention is implied also for superscripts and $\langle g^i \rangle_j$ is the value of g at node i of element j .

In particular, if s is the curvilinear coordinate along S , we have

$$s(\eta) = N^i(\eta)\langle s^i \rangle_j \quad (3.23)$$

and

$$ds = \frac{ds}{d\eta}d\eta = \frac{dN^i}{d\eta}\langle s^i \rangle_j d\eta. \quad (3.24)$$

We can also write:

$$\tau_{\mathbf{n}}(\eta) = N^i(\eta)\langle \tau_{\mathbf{n}}^i \rangle_j, \quad (3.25)$$

$$\delta\xi_{\mathbf{n}}(\eta) = N^i(\eta)\langle \delta\xi_{\mathbf{n}}^i \rangle_j. \quad (3.26)$$

We can then recast Eq. 3.20 in the form

$$\delta E_{EL}^T = \sum_{j=1}^M \left\{ - \int_{-1}^1 N^k(\eta)\langle \delta\xi_{\mathbf{n}}^k \rangle_j N^i(\eta)\langle \tau_{\mathbf{n}}^i \rangle_j \frac{dN^m}{d\eta}\langle s^m \rangle_j d\eta \right\}, \quad (3.27)$$

where we have extended the summation to all the elements of S and we have substituted the area element dS with the line element ds since we are modeling 2-D problems.

Now consider N different patterns for the perturbation $\delta\xi_{\mathbf{n}}$, defined so that, for the p^{th} perturbation pattern (Fig. 3.5(a)):

$$\begin{aligned} (\delta\xi_{\mathbf{n}})_p &\equiv 1 \text{ at the } p^{\text{th}} \text{ node} \\ (\delta\xi_{\mathbf{n}})_p &\equiv 0 \text{ at all other nodes.} \end{aligned}$$

If we write Eq. (3.27) for the p^{th} perturbation, only the elements j_p to which node p belongs will give a contribution to the p^{th} perturbation in energy $\delta E_{EL_p}^T$, so that we obtain

$$\delta E_{EL_p}^T = \sum_{j_p} \left\{ - \int_{-1}^1 N^l(\eta) N^i(\eta) \langle \tau_{\mathbf{n}}^i \rangle_{j_p} \frac{dN^m}{d\eta} \langle s^m \rangle_{j_p} d\eta \right\}, \quad (3.28)$$

where we are summing *only* over the elements j_p which contain node p and l is the position of node p in element j_p .

We can also write (3.28) as:

$$\delta E_{EL_p}^T = \sum_{j_p} [\tau_{\mathbf{n}}^i]_{j_p} [s^m]_{j_p} \left\{ - \int_{-1}^1 N^l(\eta) N^i(\eta) \frac{dN^m}{d\eta} d\eta \right\}, \quad (3.29)$$

and introduce the notation

$$B^{lim} = - \int_{-1}^1 N^l(\eta) N^i(\eta) \frac{dN^m}{d\eta} d\eta. \quad (3.30)$$

The quadratic form B^{lim} can be explicitly evaluated for all combinations of indices. The results are shown in Table 3.1. Eq. (3.29) can then be written in a more compact form as

$$\delta E_{EL_p}^T = \sum_{j_p} \langle \tau_{\mathbf{n}}^i \rangle_{j_p} \langle s^m \rangle_{j_p} B^{lim}. \quad (3.31)$$

If we write the same expression for all the N possible patterns, we obtain a system of N equations in the N unknown $\tau_{\mathbf{n}}$ nodal values:

$$M_{pr} \tau_{\mathbf{n}_r} = \delta E_{EL_p}^T, \quad (3.32(a))$$

or, in matrix notation:

$$[M] \{ \tau_{\mathbf{n}} \} = \{ \delta E_{EL}^T \}, \quad (3.32(b))$$

where

$\{ \delta E_{EL}^T \}$ is the vector of the energy perturbations, $\delta E_{EL_p}^T$

$\tau_{\mathbf{n}_r}$ is the nodal value of $\tau_{\mathbf{n}}$ at node r

M_{pr} is the p, r component of the coefficient matrix $[M]$ which is given by:

$$M_{pr} = \sum_{j_{p,r}} [s^m]_{j_{p,r}} B^{lim}. \quad (3.33)$$

Here the summation is extended only to the elements $j_{p,r}$ which contain *both* node r and node p (if $r \neq p$ there will be only one element) and t is the position of node r in element $j_{p,r}$.

We can thus easily construct the coefficient matrix $[M]$ from Table 3.1 and the curvilinear coordinates of the nodes.

Table 3.1

 B^{ijk} Values

$B^{111} = 1/3$	$B^{112} = -2/5$	$B^{113} = 1/15$
$B^{121} = 1/5$	$B^{122} = -4/5$	$B^{123} = 1/15$
$B^{221} = 8/15$	$B^{222} = 0$	$B^{223} = -8/15$
$B^{131} = -1/30$	$B^{132} = 0$	$B^{133} = 1/30$
$B^{231} = -1/15$	$B^{232} = 4/15$	$B^{233} = -1/5$
$B^{331} = -1/15$	$B^{332} = 2/5$	$B^{333} = -1/3$

To obtain the values of τ_n from system (3.32) we need now to evaluate the right-hand side vector $\{\delta E_{EL}^T\}$. Consider a finite element discretization of the region surrounding the interface, as shown in Fig. 3.4(a).

We use 2-D isoparametric 8-node elements, for which the nodal point numbers are shown in the isoparametric (η, ζ) -space in Fig. 3.4(b). The 2-D domain, V , around the interface can now be defined by considering a certain number of layers of elements around the interface as shown in Fig. 3.4(c). We can evaluate numerically each $\delta E_{EL,p}^T$, integrating expression 3.19(b) over V . We first define the perturbation field $(\vec{q})_p$ associated with the p^{th} pattern of interface perturbation $(\delta \xi_n)_p$. We can express the $(\vec{q})_p$ field in terms of nodal values $\langle \vec{q}^k \rangle_p$ and 2-D biquadratic shape functions as

$$(\vec{q})_p(\eta, \zeta) = \mathcal{N}^k(\eta, \zeta) \langle \vec{q}^k \rangle_p \quad (3.34)$$

where $\mathcal{N}^k(\eta, \zeta)$ are the 2-D shape functions expressed in terms of the isoparametric coordinates (η, ζ) (See Table 3.2). The nodal values of the p^{th} perturbation field, $\langle \vec{q}^k \rangle_p$, can be chosen freely as long as

1. $\langle \vec{q}^k \rangle_p \equiv 1 \cdot \vec{n}_p$ at node p on the interface
2. $\langle \vec{q}^k \rangle_p \equiv 0$ at all other nodes of the interface
3. $\langle \vec{q}^k \rangle_p \equiv 0$ at all nodes along the boundary of V .

A possible choice for the nodal values $\langle \vec{q}^k \rangle_p$ is shown in Fig. 3.5(b).

Table 3.2

2-D Shape Functions

$\mathcal{N}^1(\eta, \zeta) = (-1/4)(1 - \eta)(1 - \zeta)(1 + \eta + \zeta)$
$\mathcal{N}^2(\eta, \zeta) = (-1/4)(1 + \eta)(1 - \zeta)(1 + \eta + \zeta)$
$\mathcal{N}^3(\eta, \zeta) = (-1/4)(1 + \eta)(1 + \zeta)(1 + \eta - \zeta)$
$\mathcal{N}^4(\eta, \zeta) = (-1/4)(1 - \eta)(1 + \zeta)(1 + \eta - \zeta)$
$\mathcal{N}^5(\eta, \zeta) = (1/2)(1 - \eta)(1 + \eta)(1 - \zeta)$
$\mathcal{N}^6(\eta, \zeta) = (1/2)(1 - \zeta)(1 + \eta)(1 + \zeta)$
$\mathcal{N}^7(\eta, \zeta) = (1/2)(1 - \eta)(1 + \eta)(1 + \zeta)$
$\mathcal{N}^8(\eta, \zeta) = (1/2)(1 - \zeta)(1 + \zeta)(1 - \eta)$

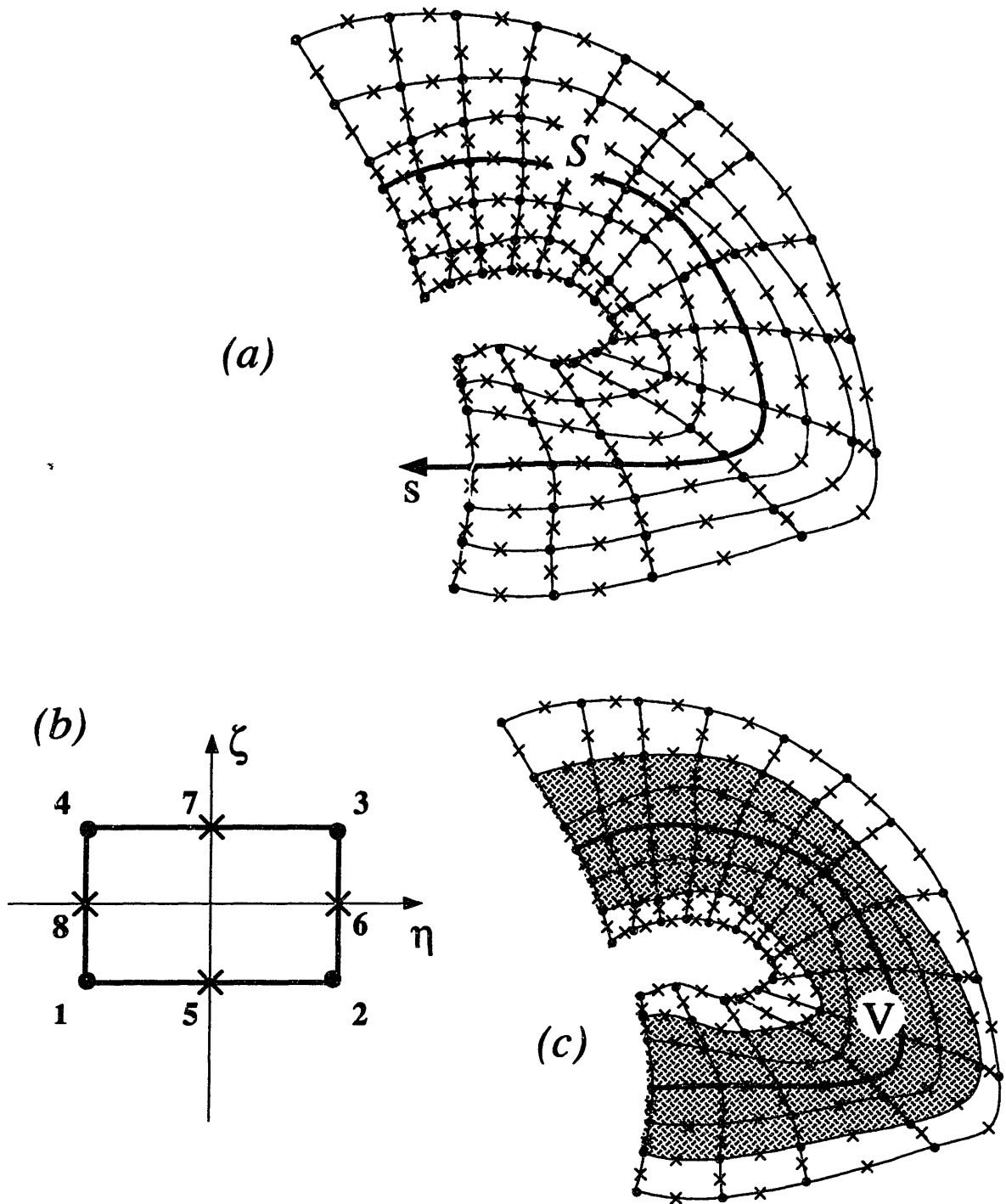
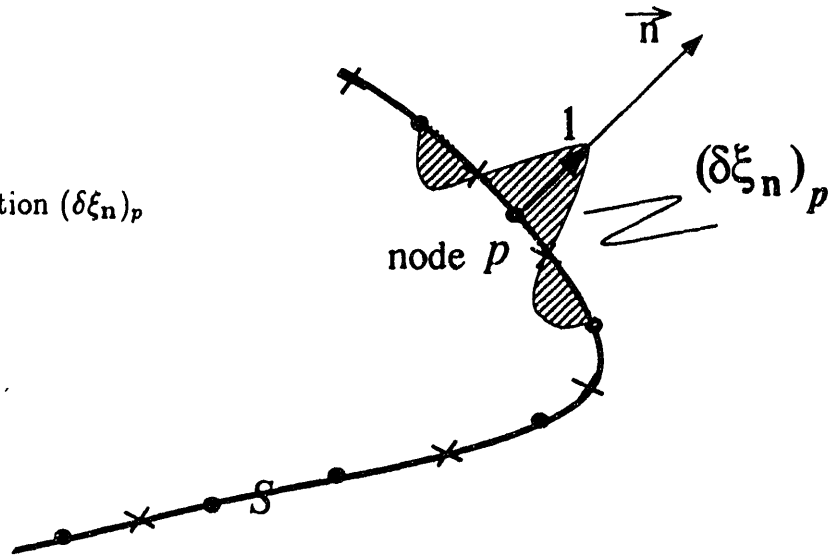


Figure 3.4 Finite element discretization of the domain of integration.

(a) Interface perturbation $(\delta\xi_n)_p$



(b) Perturbation field: $\langle \vec{q}^k \rangle_p$
 (only the nodes for which
 the vector \vec{q}^k is
 indicated are perturbed).

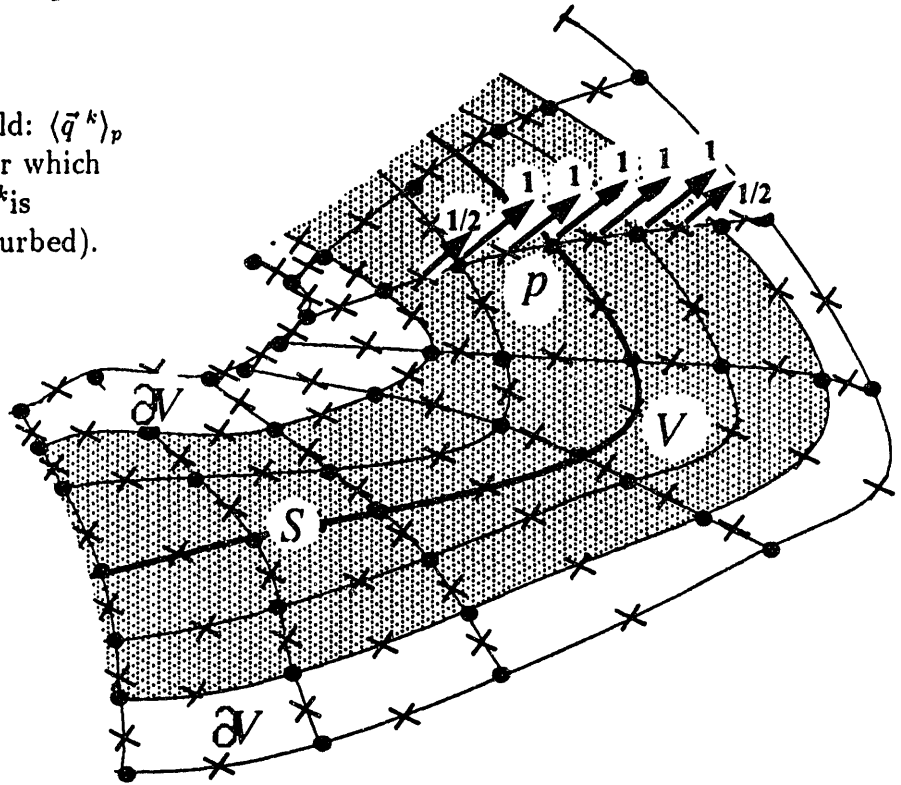


Figure 3.5 Perturbation patterns.

The integral form (3.19a) can now be written as

$$\delta E_{ELp}^T = \sum_V \int_{-1}^1 \int_{-1}^1 [P_{ij}(q_{i,j})_p + \{\rho b_k u_{k,i} - \sigma_{mn} \epsilon_{mn,i}^T\}(q_i)_p] |J| d\eta d\zeta, \quad (3.35)$$

where the sum is extended to all elements in V , and $|J|$ is the determinant of the Jacobian matrix:

$$|J| = \frac{\partial x}{\partial \eta} \frac{\partial y}{\partial \zeta} - \frac{\partial y}{\partial \eta} \frac{\partial x}{\partial \zeta}. \quad (3.36)$$

The integrand in (3.35) is, for each element, a function of the isoparametric coordinates η, ζ :

$$\mathcal{F}(\eta, \zeta) = P_{ij}(q_{i,j})_p + \{\rho b_k u_{k,i} - \sigma_{mn} \epsilon_{mn,i}^T\}(q_i)_p |J|, \quad (3.37)$$

so that each of the integrals can be evaluated numerically, e.g., by Gauss quadrature:

$$\int_{-1}^1 \int_{-1}^1 \mathcal{F}(\eta, \zeta) d\eta d\zeta = \sum_i \sum_j W_i W_j \mathcal{F}(\eta_i, \zeta_j), \quad (3.38)$$

where $\mathcal{F}(\eta_i, \zeta_j)$ is the value of \mathcal{F} at integration point (i, j) and the W_i, W_j are weights for Gauss quadrature.

Thus, if a finite element analysis has been performed on the body, we can calculate the values of \mathcal{F} at the integration points of the elements inside V , substitute these values in (3.38) and apply (3.35) to evaluate the right-hand side of system (3.32).

As we have already mentioned in section 3.32, we can use the invariance property of the domain integral expression for δE_{EL}^T as a check for the quality of our numerical calculations.

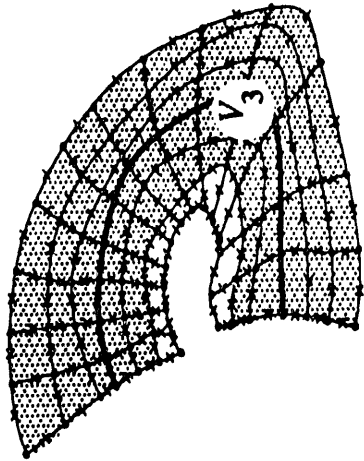
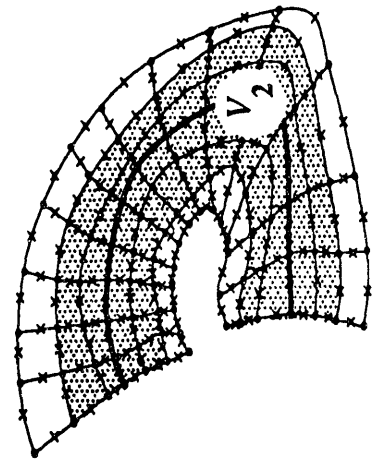
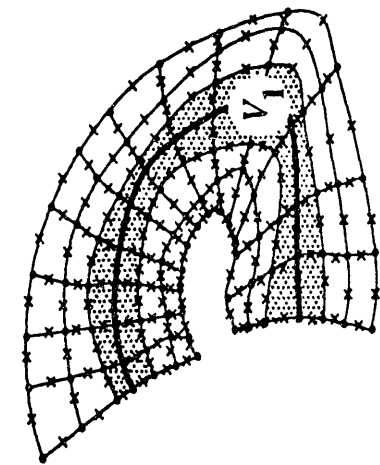
We can consider several choices for the domain of integration, V , and/or for the form of the perturbation field \vec{q} (See Fig. 3.6).

For each of these choices we can evaluate the RHS vector $\{\delta E_{EL}^T\}$ and solve the system (3.32) for the force on the interface $\{\tau_n\}$.

Differences in the values of the $\{\tau_n\}$ vectors can be regarded as a measure of the numerical error in the solution.

This method has been implemented in the computer program DOMAIN for which a listing of the symbolic code is given in Appendix II.

(a) varying the domain of integration



(b) varying the perturbation field

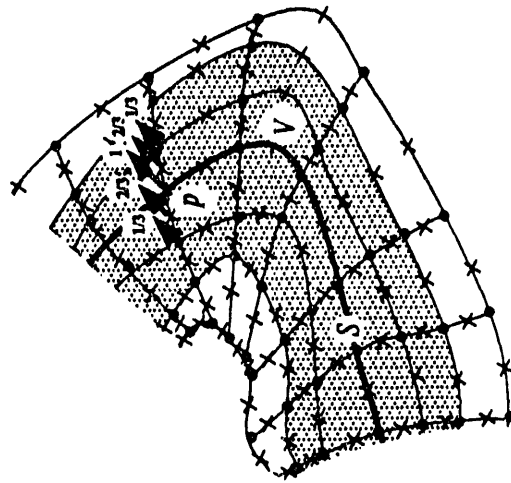
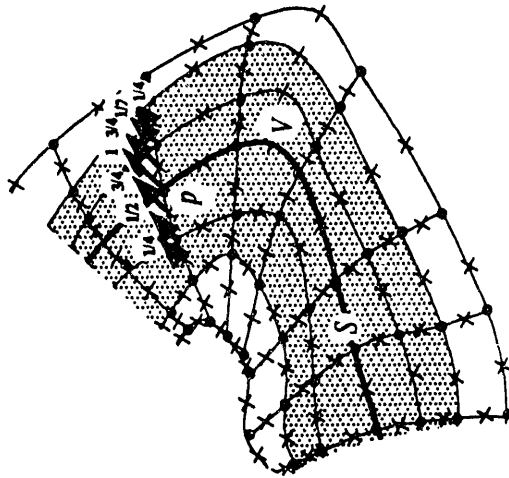
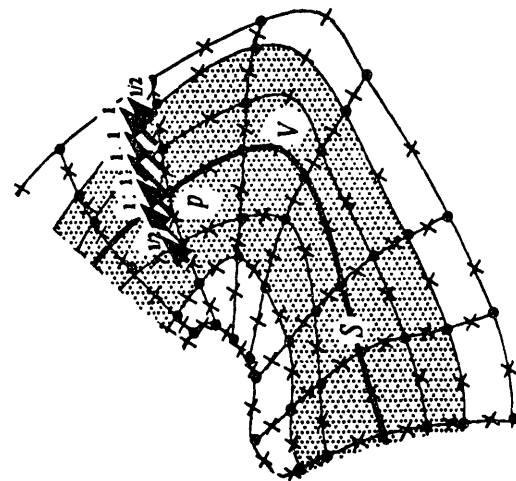


Figure 3.6 Test for the accuracy of the numerical solution.

CHAPTER 4

ANALYSIS OF RAFTING

4.1 Introduction

The numerical methods described in Chapter 3 allow us to evaluate the distribution of $\tau_{\mathbf{n}}$ over a material interface. As discussed in Chapter 2, this is a quantity directly related to the tendency of the interface to migrate and, with the convention used throughout our derivation, a positive value of $\tau_{\mathbf{n}}$, at a certain location, indicates a tendency for the inclusion to grow at that location. If the value of $\tau_{\mathbf{n}}$ along a precipitate-matrix interface is not uniform, this indicates a tendency for the inclusion to modify its morphology.

In this chapter we will apply these concepts to the analysis of rafting in $\gamma - \gamma'$ Ni-superalloys.

In paragraph 4.2, we will first assess the accuracy of our models by comparing data obtained by numerical calculations with analytical solutions for the simple case of a cylindrical inclusion in an infinite matrix. This test case will also provide the opportunity to construct an “evolution map” which interestingly compares with Pineau’s map (see Section 1.4).

In paragraph 4.3 we will then introduce the finite element model, for the $\gamma - \gamma'$ cuboidal morphology, that we will use to perform the rafting analysis, and we will identify the set of alloys for which we will carry out our calculations.

In paragraph 4.4 we will present and discuss the results of purely elastic analyses, where the force on the interface is evaluated for the initial conditions of applied stress and misfit, and no misfit-relaxation effect due to creep is considered.

In paragraph 4.5 we will follow the evolution of the driving force during the very first stage of primary creep in a simulated stress-annealing experiment.

In paragraph 4.6 we will finally discuss the results, draw our conclusions concerning the rafting process and offer a synoptic interpretation of numerical results and experimental data.

4.2 Test Case: A Cylindrical Inclusion in an Infinite Matrix

As a test case, we will consider the very simple problem of a cylindrical isotropic misfitting inclusion in an infinite isotropic matrix subjected, at infinity, to a state of uniaxial stress σ_∞ normal to the axis of the cylinder (Fig. 4.1(a)). The elastic solution for this problem has been first determined by Goodier [55].

In order to simplify our calculations, we will assume that the matrix and the inclusion have the same Poisson ratio ν . Then the state of stress and strain at any location $(r/r^\Omega; \theta)$, where r^Ω is the radius of the inclusion, can be determined in terms of:

- E_p : the stiffness (Young's modulus) of the precipitate
- E_m : the stiffness (Young's modulus) of the matrix
- σ_∞ : the applied stress
- δ : the misfit
- ν : the Poisson ratio (assumed common to matrix and precipitate)

From the analytical expression for the elastic field, given in [55], the quantity τ_n can be readily evaluated at all locations along the interface using eq. (2.31(b)).

These calculations have been implemented in the simple program GOODIER, listed in Appendix III, which evaluates τ_n at N locations along the interface (N is a user-defined quantity).

Due to the symmetry of the problem, only one fourth of the geometry needs to be considered. (We have chosen the quadrant shown in Fig. 4.1(b)).

The values of τ_n along the interface can be plotted against a normalized arclength s as shown in Fig. 4.2. The origin for s is at the very top of the particle (see Fig. 4.1(b)) so that, in the graphs in Fig. 4.2, the left part of the graph roughly corresponds to the "top" of the particle, while the right part corresponds to the "side".

Then, graph 4.2(a), where the average value of τ_n on the "top" is larger than the average value of τ_n on the "side", indicates a tendency toward a "type P" rafting behavior, with rafts aligned in the direction of the applied stress; graph 4.2(b) indicates a tendency toward an isotropic rafting behavior; and graph 4.2(c) indicates a tendency toward a "type N" rafting behavior with plates forming in the direction normal to the applied stress.

Since, for this case, the analytical distribution of τ_n can be readily found, we have been able to perform a brief parametric study varying the same characteristic quantities chosen by Pineau to construct his map (see paragraph 1.4), namely $\sigma_\infty/E_m\delta$ and E_p/E_m . The results of this study, obtained with a value of the misfit $\delta = 0.1\%$, are summarized in Fig. 4.3 and, with a broader spectrum of E_p/E_m values, in Fig. 4.4.

For each small plot two numerical values are given; the first represents the magnitude (in MPa) of the difference between the average values of τ_n on the top and on

the side: this is a measure of the tendency to coarsen with a preferential orientation; the second value represents the average value of $\tau_{\mathbf{n}}$ (in MPa) along the interface: this is a measure of the average tendency for the particle to grow in order to decrease the total elastic energy.

From this set of results, we can sketch the map shown in Fig. 4.5 that can be compared with Pineau's map of Fig. 1.8. Besides the differences in the geometry of the problems (spherical inclusion for Pineau; cylindrical inclusion for our test case), the two maps differ for a fundamental reason: Pineau's map is a *stability map*: it is constructed by determining the configuration that minimizes the energy. Our map is an *evolution map*: it is constructed by evaluating the tendency toward shape evolution for the precipitate in the actual initial configuration.

Still, bearing in mind this basic difference, the patterns of the two maps show striking similarities.

We have also explored the effects of varying the sign and magnitude of the misfit. A mere change of the sign of the misfit does not affect the results, as can be noted by comparing Fig. 4.6, obtained with a misfit $\delta = -0.1\%$, and Fig. 4.3. Conversely, if we change the magnitude of the misfit, while the pattern of the map is not modified, the magnitude of the driving force is remarkably altered.

The plots in Fig. 4.7 have been obtained with a misfit $\delta = 0.3\%$: if we compare the numerical values of $\tau_{\mathbf{n}}$ with those in Fig. 4.3 we can notice that the force on the interface is increased by almost one order of magnitude. This result should have been expected since, for a purely elastic problem, $\tau_{\mathbf{n}}$ is a quadratic form in the stress field so that, if we increase the misfit (and thus σ_{∞} to keep $\sigma_{\infty}/E_m\delta$ constant) of a factor 3, we can expect that $\tau_{\mathbf{n}}$ will increase of a factor $3^2 = 9$.

After this digression we will now return to our original task of assessing the accuracy of the numerical methods introduced in Chapter 3 to evaluate $\tau_{\mathbf{n}}$.

A boundary value problem to be solved using the finite element program ABAQUS has been defined as shown in Fig. 4.8. Plane-strain, eight-node isoparametric element have been used. Symmetry conditions are applied at the axes; the nodes along the top of the domain of analysis are constrained to have equal vertical displacement and to these nodes the external load σ_{∞} is applied; the nodes along the outer edge are constrained to have equal horizontal displacements.

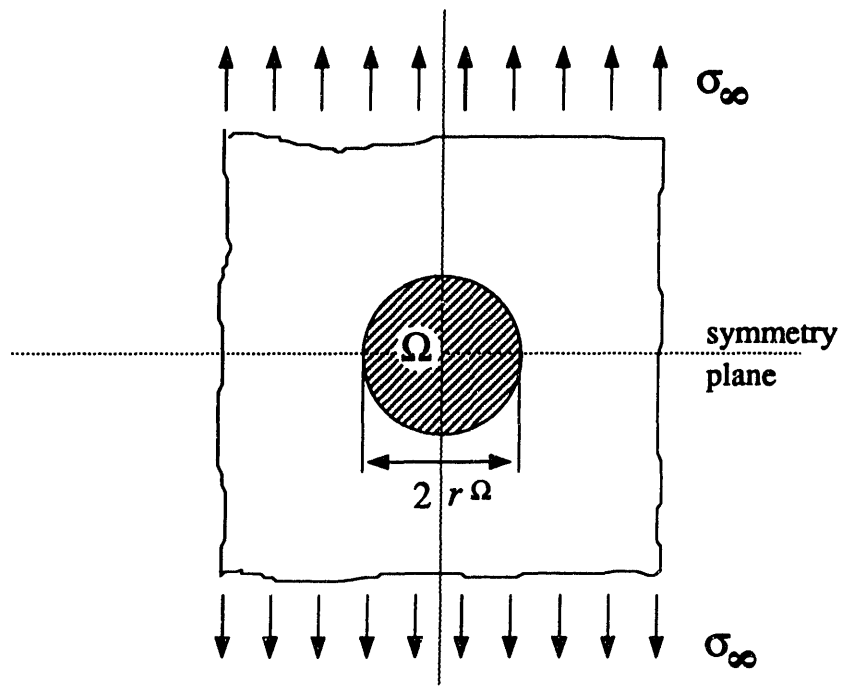
In this analysis the ratio of the particle radius, r^{Ω} , to the dimension of the domain of analysis, L_{∞} , is $1/20$. This ratio is low enough to insure "far field" conditions on the outer boundary of the domain. The finite element mesh used for this problem is shown in Fig. 4.9. A listing of the ABAQUS input file is given in Appendix IV.

The results of the finite element analysis have been post processed using both the program POSTABQ and the program DOMAIN to obtain the distribution of $\tau_{\mathbf{n}}$ along the interface.

A comparison of analytical and numerical results, for a representative case, is shown in Fig. 4.10. In general, the domain integral method yields smoother results,

but the agreement with the analytic solution is satisfactory also for the direct method. No appreciable difference in the results obtained using the domain integral method is observed when varying the domain of integration, thus confirming the good level of accuracy of the calculations. However, as we will discuss in the next paragraph, there exist particular cases in which the direct method can yield more consistent results than the domain integral method.

a) Test problem



b) Representative section to be modeled

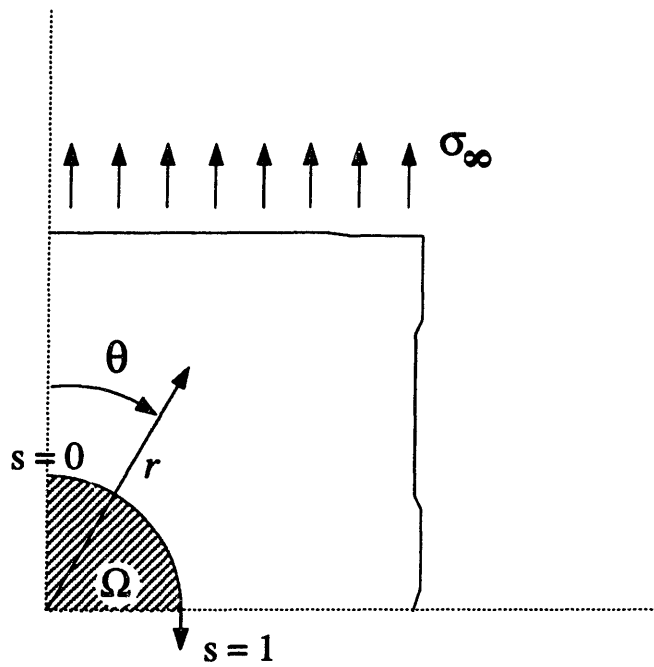


Figure 4.1 Cylindrical inclusion in an infinite matrix.

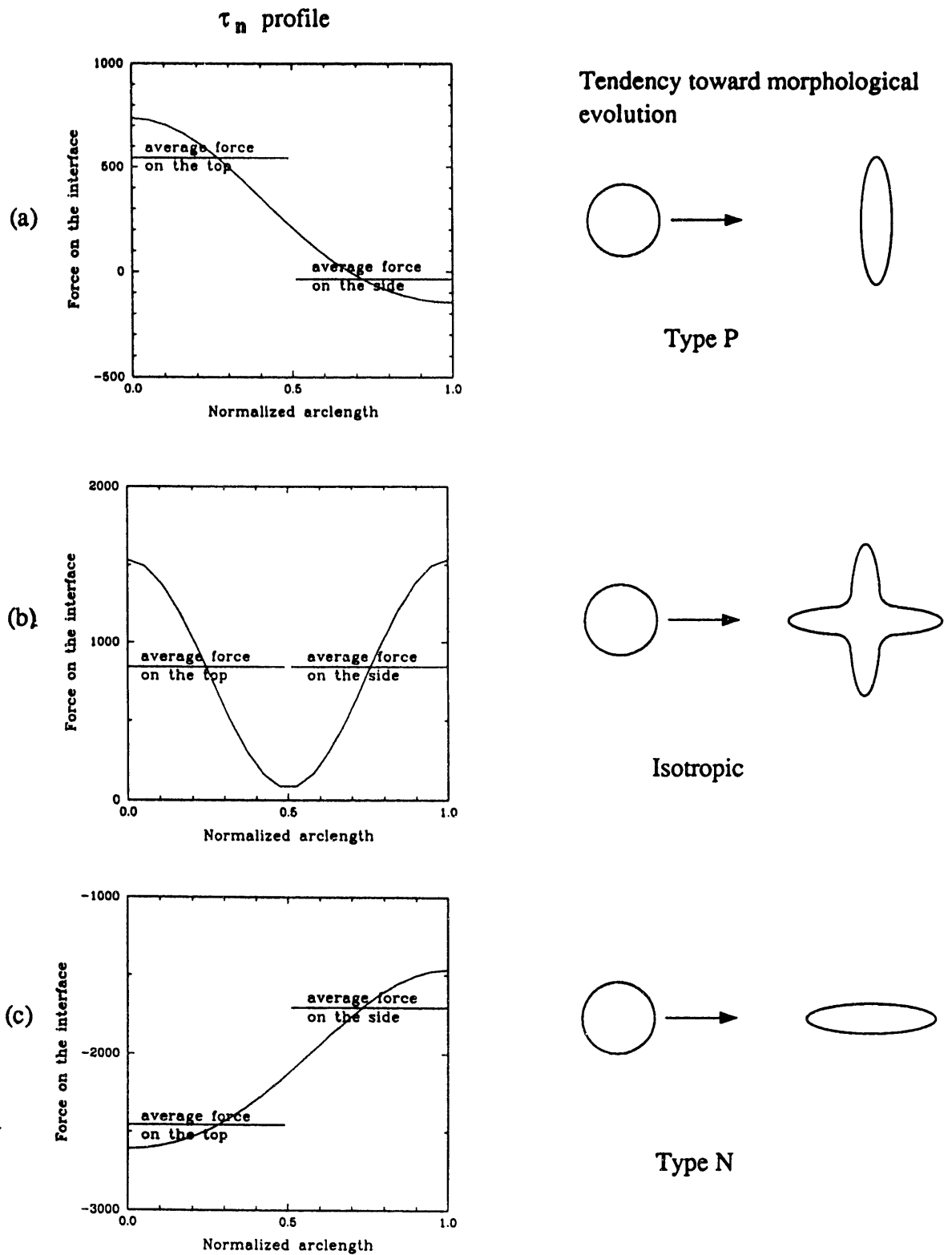


Figure 4.2 Relation between the profile of τ_n along the interface and the tendency toward morphological evolution.

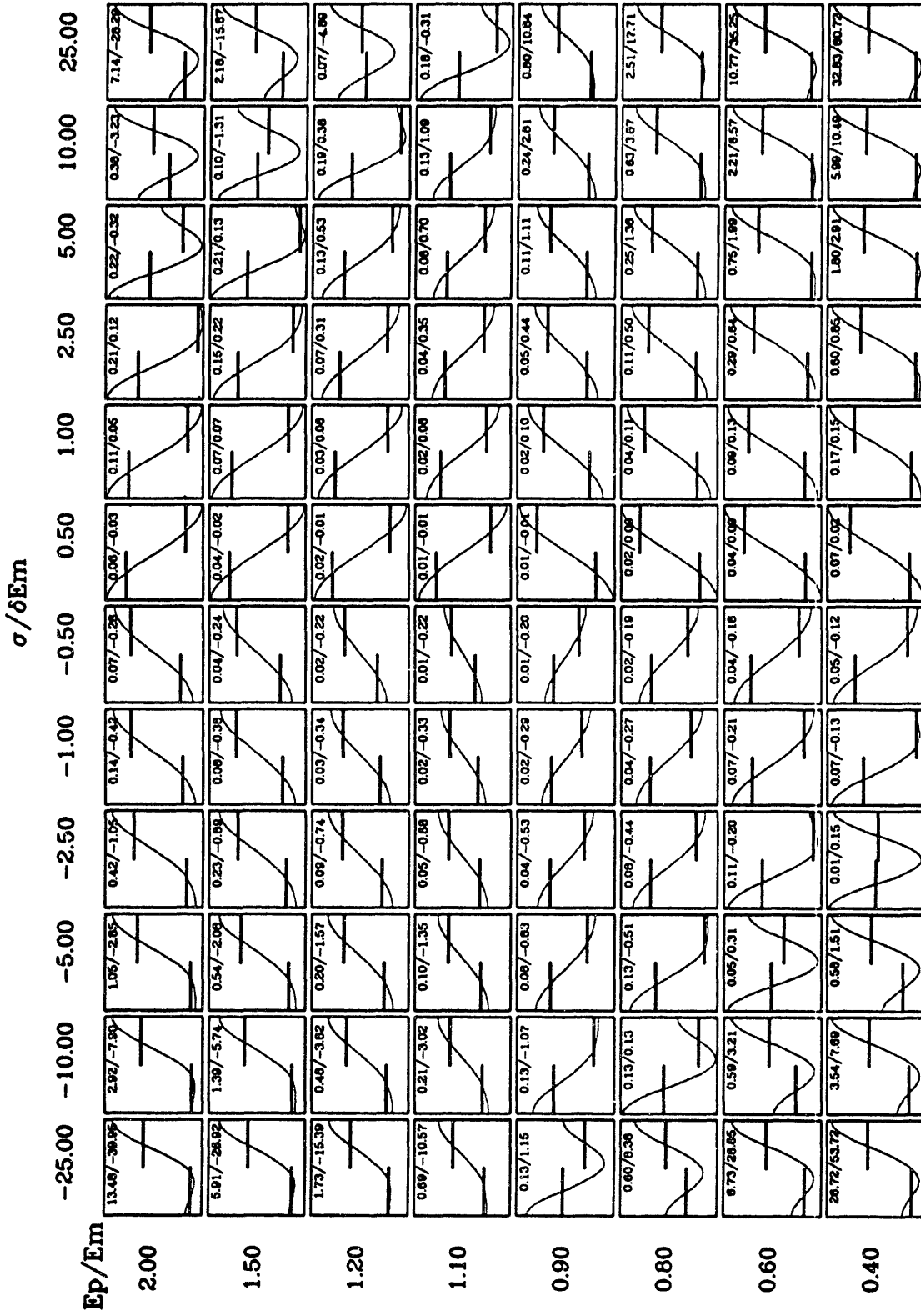


Figure 4.3 Parametric study of τ_n profile for: $\delta = 0.1\%$; $E_m = 100$ GPa;
 $0.4 \leq E_p/E_m \leq 2.0$.

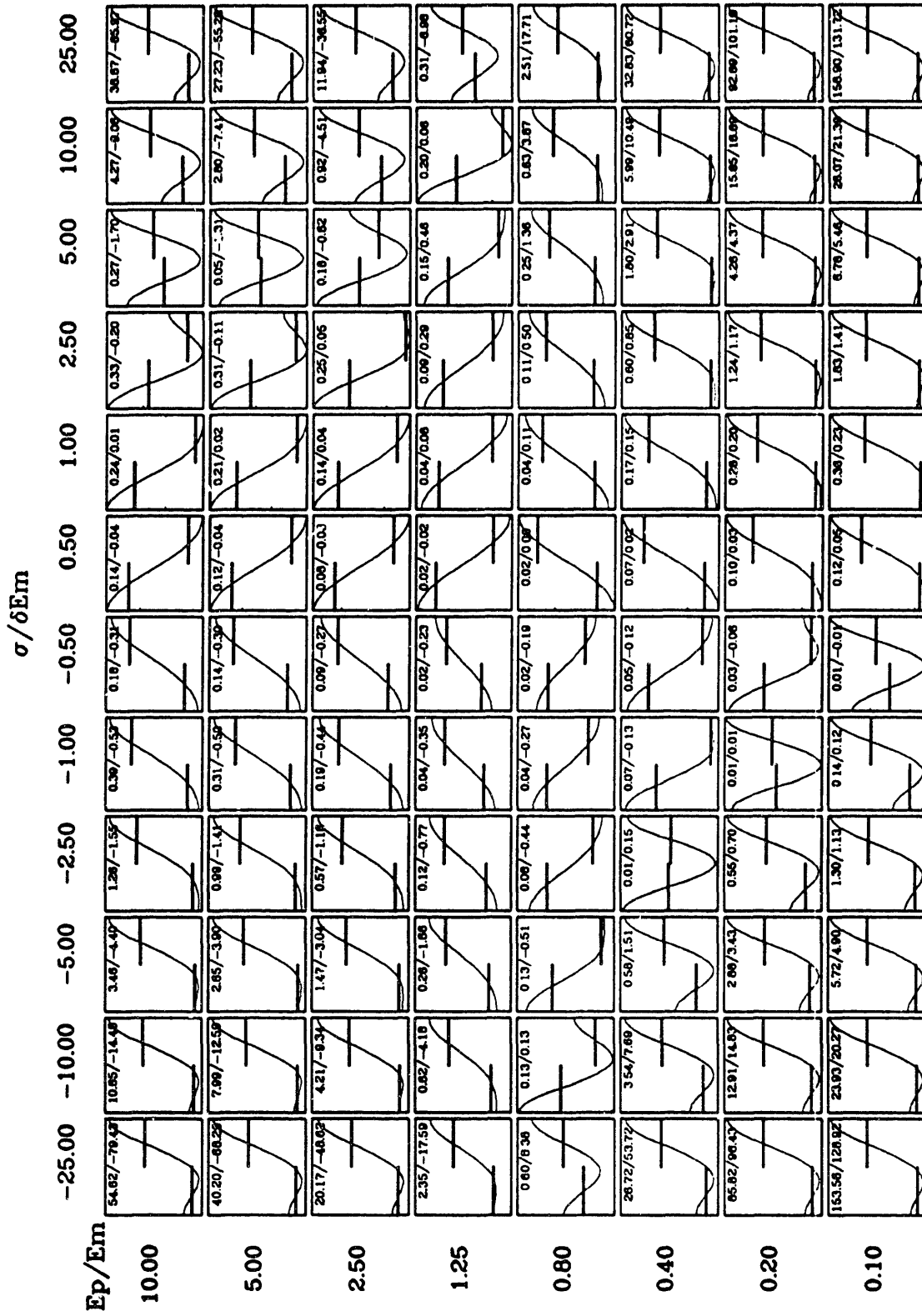


Figure 4.4 Parametric study of τ_n profile for: $\delta = 0.1\%$; $E_m = 100$ GPa; $0.1 \leq E_p/E_m \leq 10.0$.

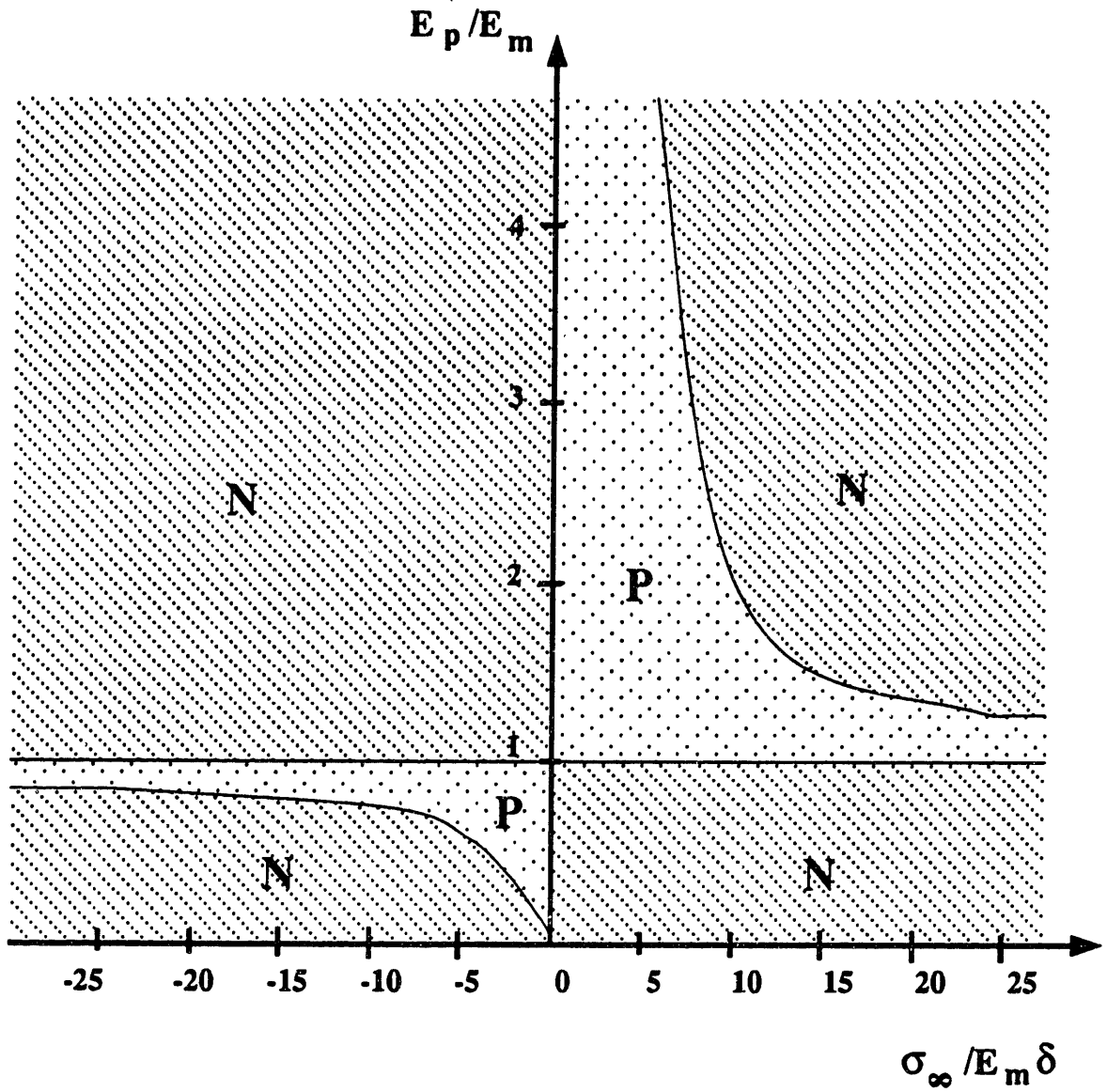


Figure 4.5 Evolution map for an isotropic cylindrical inclusion in an infinite matrix.

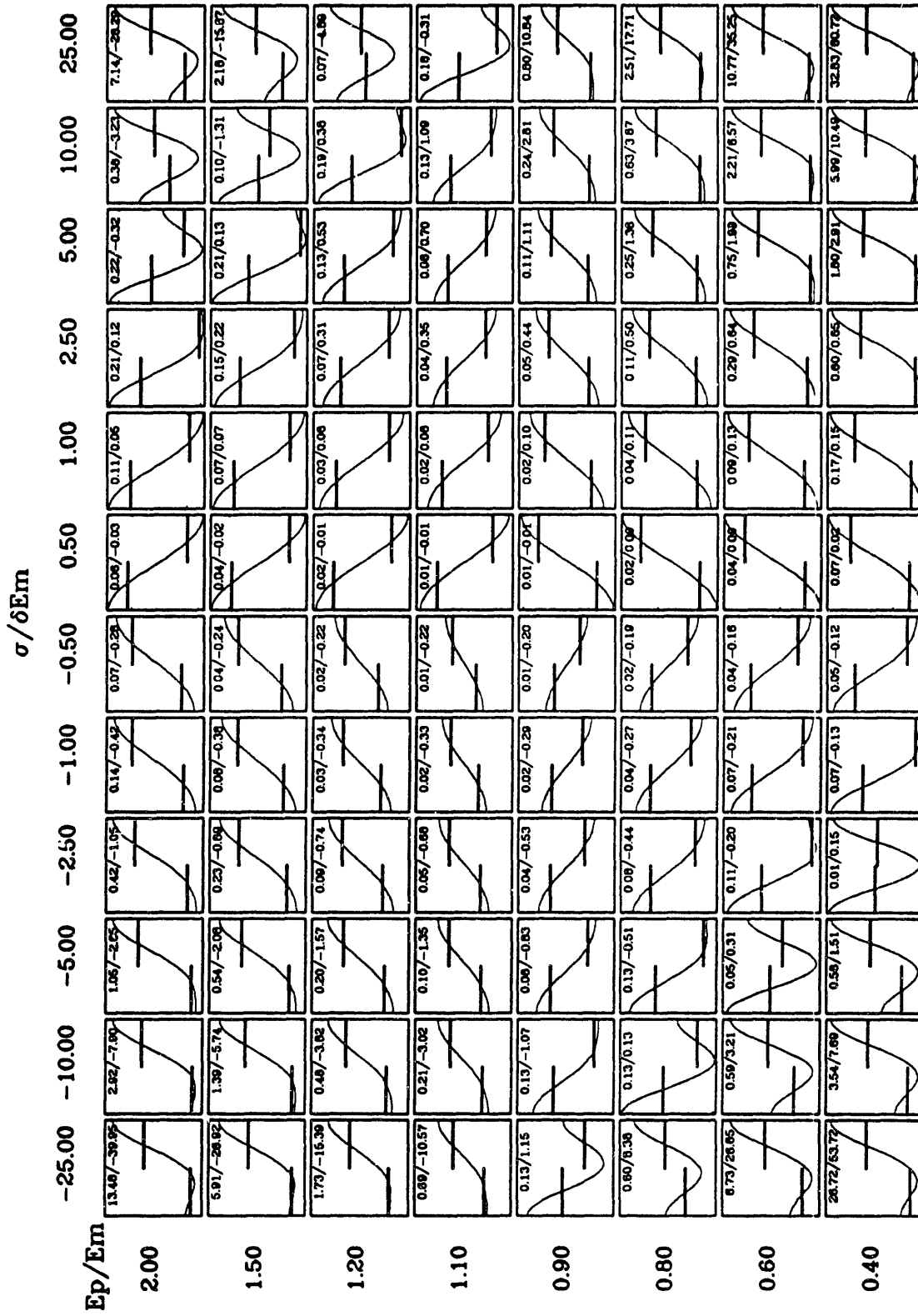


Figure 4.6 Parametric study of τ_n profile for $\delta = -0.1\%$; $E_m = 100$ GPa; $0.4 \leq E_p/E_m \leq 2.0$.

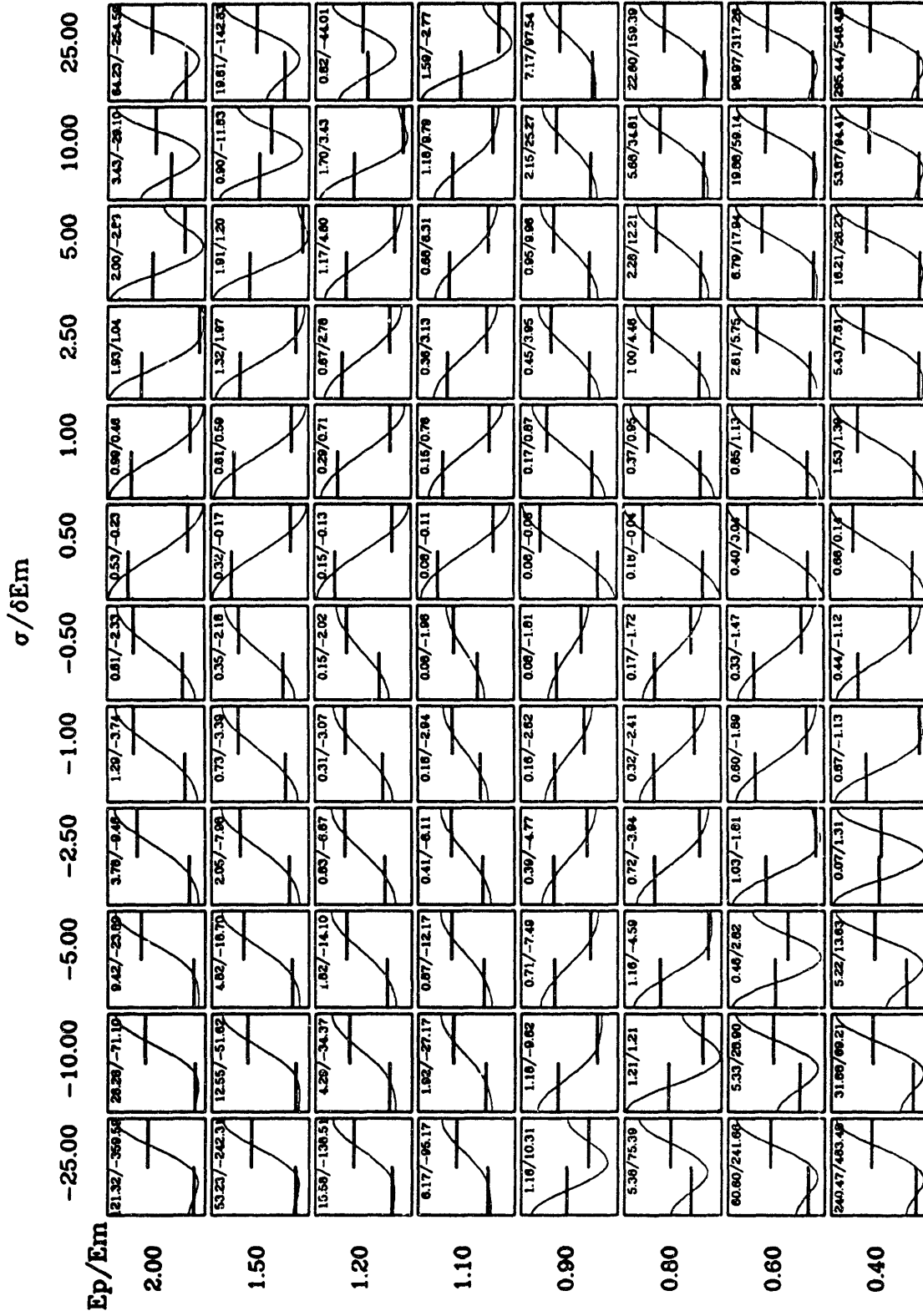


Figure 4.7 Parametric study of τ_n profile for $\delta = 0.3\%$; $E_m = 100$ GPa
 $0.4 \leq E_p/E_m \leq 2.0$.

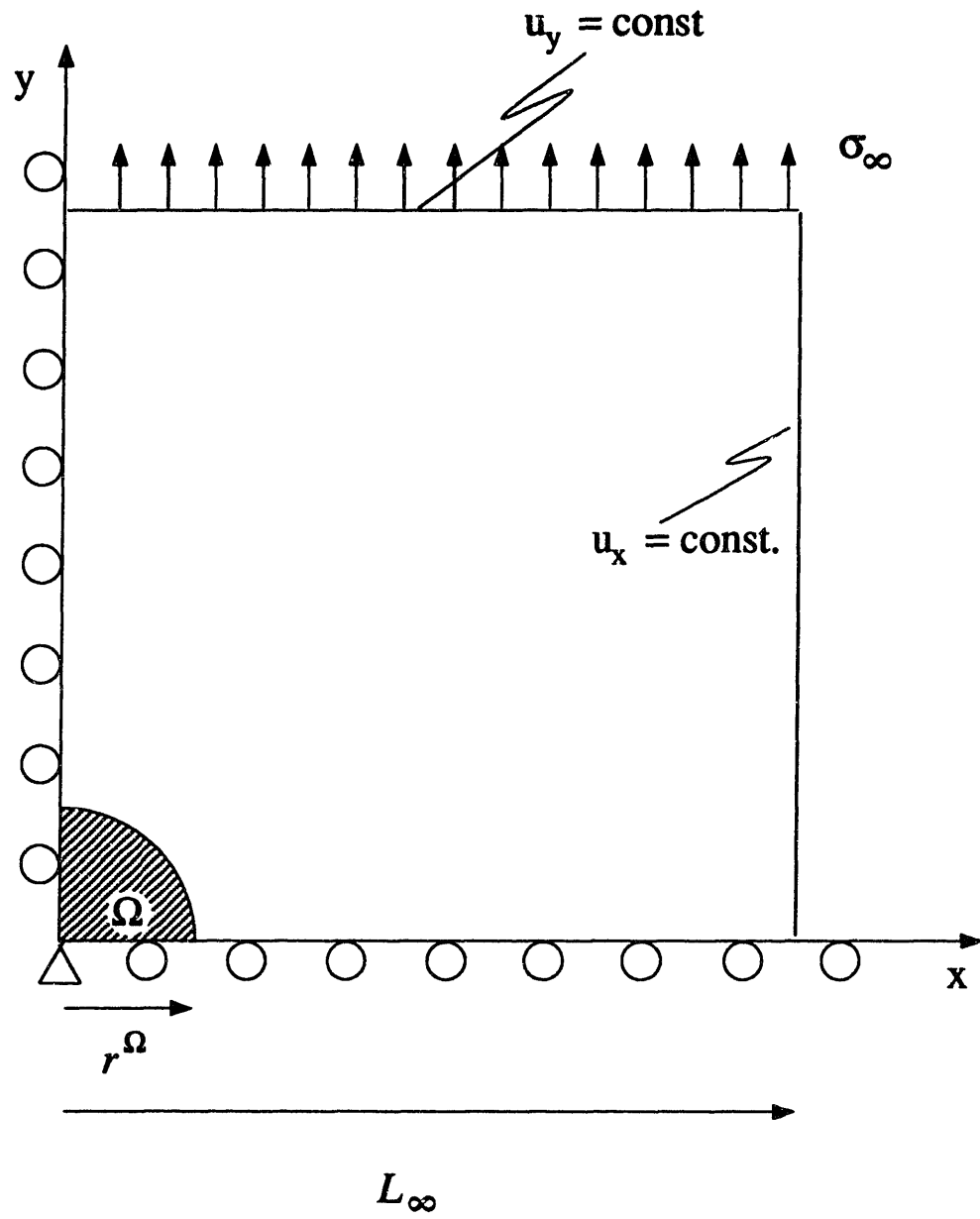


Figure 4.8 Schematic description of the cylindrical inclusion problem modeled, with the boundary conditions indicated ($r^\Omega / L_\infty = 1/20$).

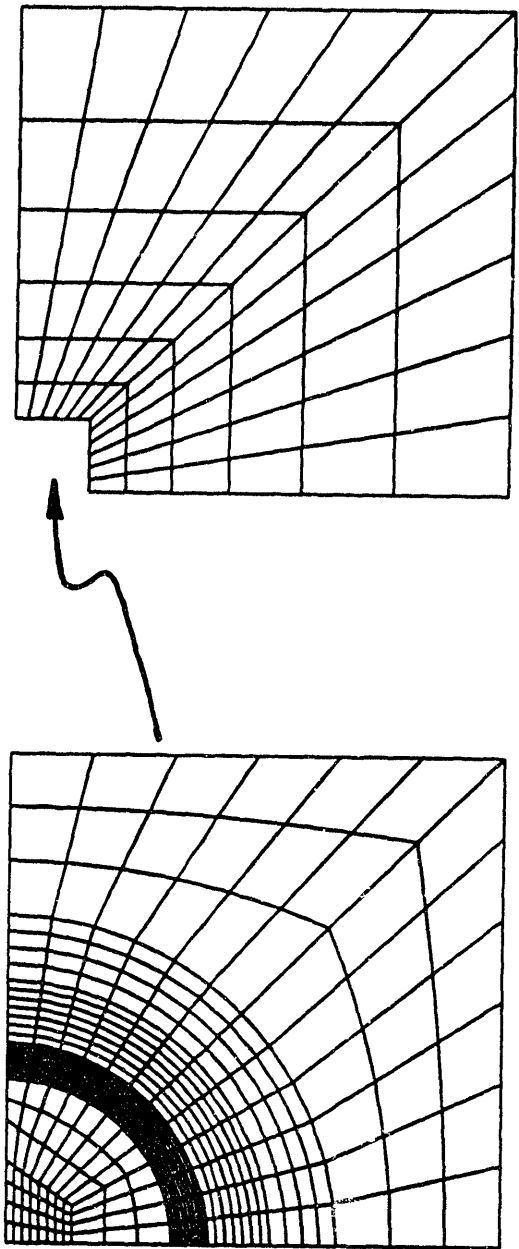


Figure 4.9 Finite element mesh for the cylindrical inclusion problem modeled. In this Figure the bottom mesh (“near-particle” region) fits into the indicated area of the top mesh (“nominal far-field” region).

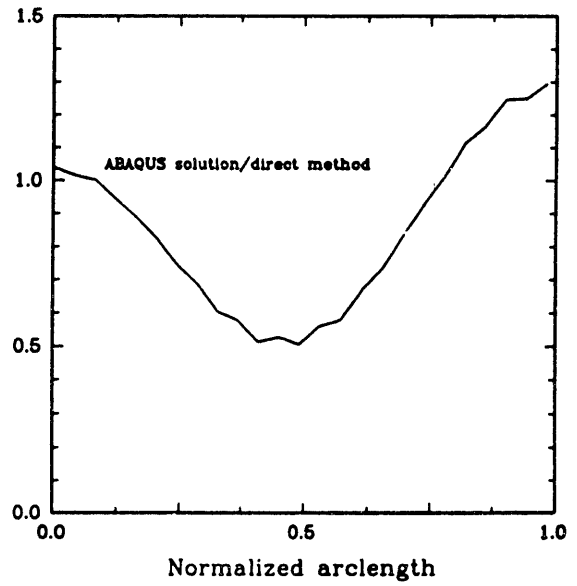
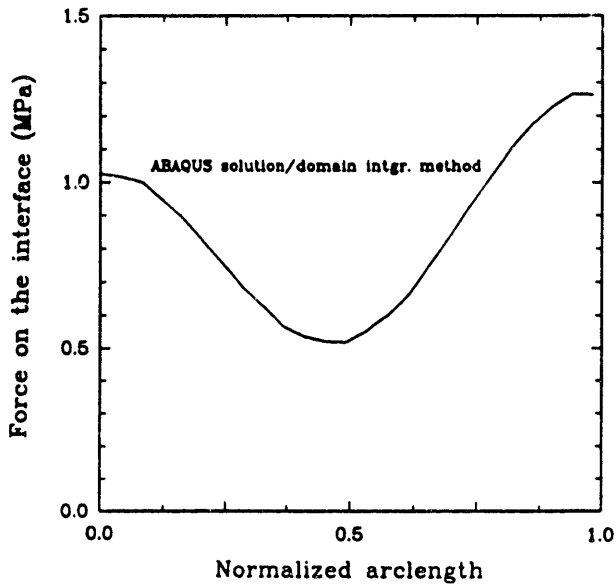
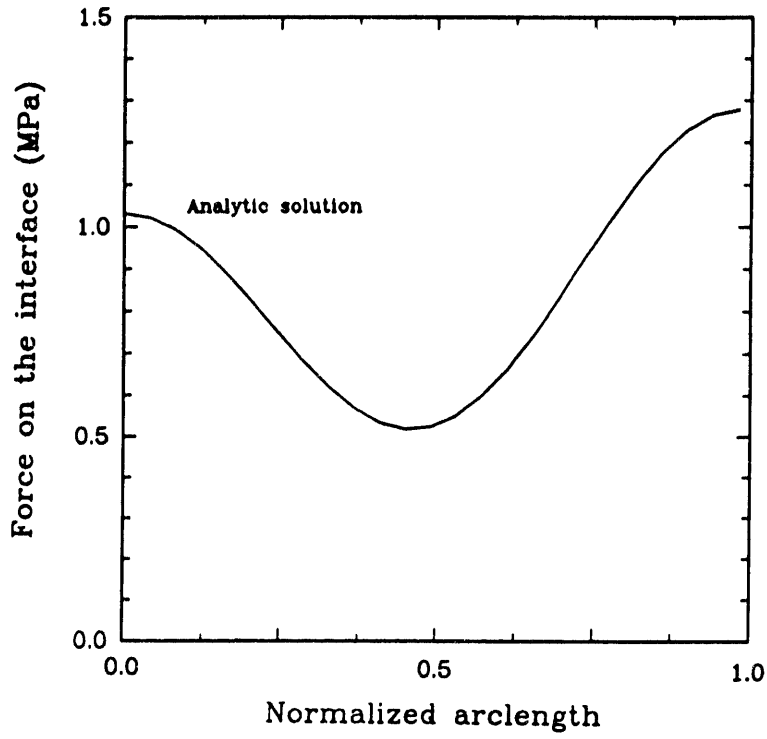


Figure 4.10 Comparison of analytical and numerical results
 (for $E_m = 200$ GPa; $E_p/E_m = 0.5$; $\sigma_\infty = 1000$ MPa;
 $\delta = -0.1\%$).

4.3 Problem Description

In the previous paragraph we have assessed the reliability of the proposed numerical procedures, by direct confrontation of numerical results and analytical solutions in a simple test problem. We can now apply these numerical methods to analyze the morphological evolution of γ' precipitates in Ni-superalloys.

The first step will be to construct a finite element model of the array of cuboidal γ' precipitates. We have simplified the problem by considering a 2-D model using generalized plane strain elements.

These elements permit uniform displacements in the “thickness” direction (normal to the mesh-plane), thus allowing expansion in the third dimension as well as the development of normal stresses and strain in this direction.

Due to the symmetry and periodicity of the microstructure, we can confine our analysis to the “unit cell” depicted in Fig. 4.11(a).

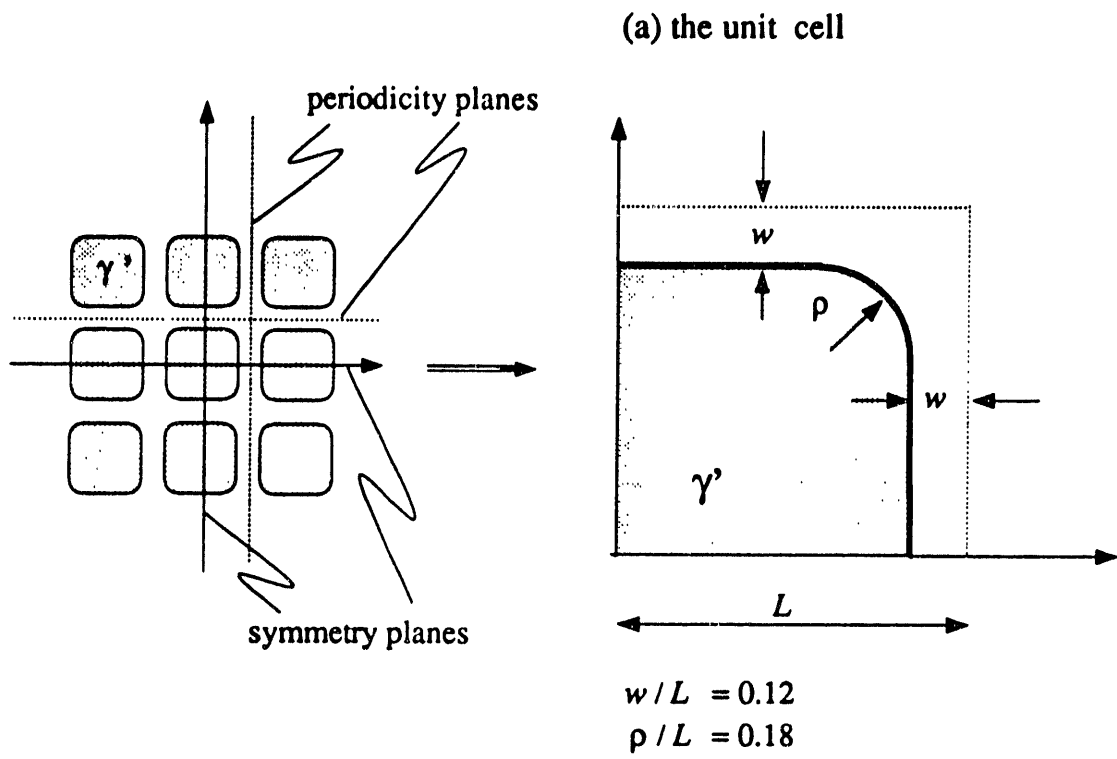
Two different meshes have been generated: a coarse mesh (Fig. 4.11(b)), used in the “tune-up” stage of the research to obtain first order approximations of the τ_n profile with a limited amount of required computational time, and a more refined mesh (Fig. 4.11(c)) for the final calculations.

The level of numerical noise associated with different choices of mesh and/or numerical method can be appreciated by comparing the τ_n profiles in Fig. 4.12.

All of the plots shown in the following paragraphs have been obtained using the refined mesh. Most of them have been obtained by applying the domain integral method. However, as previously mentioned, there exist particular cases in which the level of numerical noise in the domain integral solution is particularly high: if we consider the integral expression for δE^T in Eq. (3.19 (a)), we can see that δE^T depends on the gradient of the transformation strains $\epsilon_{mn,i}^T$. When we will perform the stress-annealing analyses, the transformation strains will be given by the superposition of misfit strains and creep strains ϵ^{creep} . In the very last stage of the analyzed transients, extremely steep ϵ^{creep} -gradients develop around the corners of the γ' precipitates (see Figs 4.34 and 4.38). For these particular conditions the finite element mesh is not refined enough to allow a precise numerical evaluation of the gradient of ϵ^{creep} so that, for these particular cases, the direct method yields more reliable results than the domain integral approach.

In order to perform a finite element analysis of the $\gamma - \gamma'$ crystal, we need the following set of data:

- elastic constants of matrix and precipitate;
- misfit at test temperature;
- loading conditions;



(b) coarse mesh

(c) refined mesh

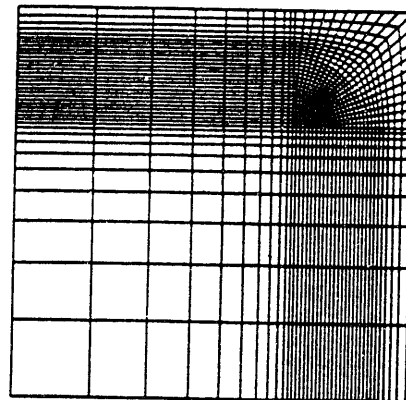
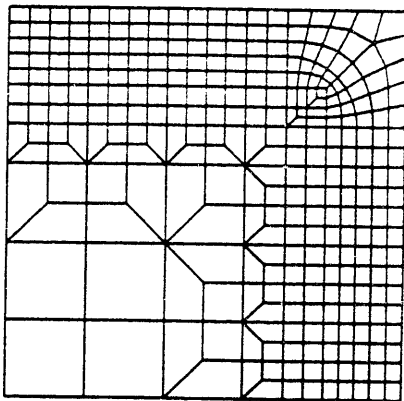


Figure 4.11 Finite element discretization of the unit cell.

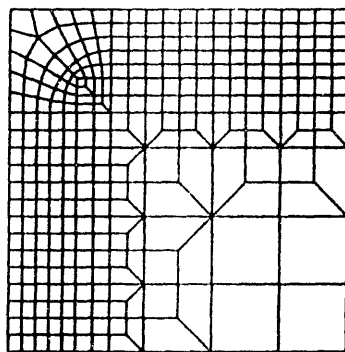
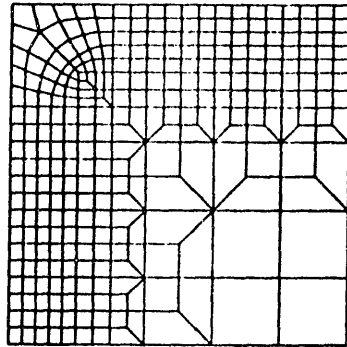
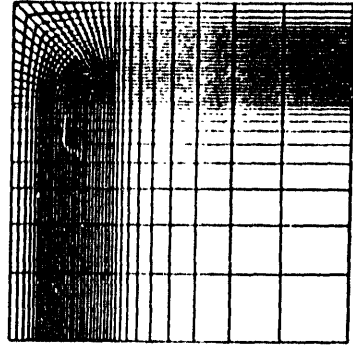
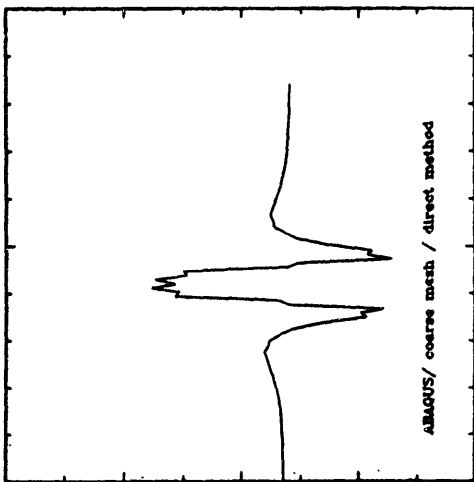
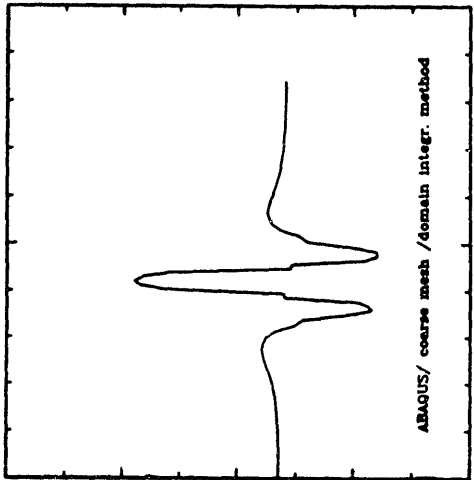
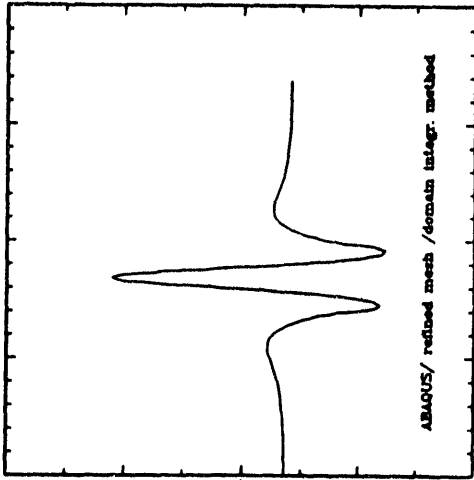


Fig. 4.12 Comparison of τ_n profiles obtained with different choices of mesh and/or numerical method.

- creep properties;
- microstructure geometry (dimensions of the γ' cubes and of the γ channels).

While a simulation of actual γ - γ' crystals is of extreme interest because the results of the analysis can be directly compared with experimental data, we are limited, in this approach, by the extremely exiguous number of well-characterized alloys available in the literature. Values for the elastic constants of the γ and of the γ' phases are available only for three alloys on which rafting experiments have been carried out. These are:

- a. The negative-misfit alloy studied by Pollock [25]
- b. The alloy studied by Tien and Copley [13]
- c. The alloys studied by Miyazaki, Nakamura and Mori [15]

For these alloys the loading conditions and the test temperature are available as well; also the value of the misfit at test temperature is given (alloys (a) and (c)) or can be evaluated (alloy (b): see the end of paragraph 1.2). In Table 4.1 we have summarized the characteristics of these alloys, together with the rafting behavior observed in the experiments. Thus we have only six cases, to which we have assigned an acronym that we will use to identify each case, that we can use to compare our results with experimental data.

In order to explore a wider range of possibilities, we have “created” a few *hypothetical* alloys by altering some of the characteristics of the alloys of Table 4.1.

Altering the characteristics of the alloy studied by Miyazaki Nakamura and Mori, we have “created” an alloy with positive misfit and soft precipitates by switching the elastic constants of the two phases, and an alloy with negative misfit and hard precipitates by changing the sign of the misfit.

For the alloy studied by Tien and Copley, we have explored the effect of assuming the value of the misfit reported in the paper: in this way we have studied the behavior of an alloy with soft particle and small positive misfit. Finally, we have explored the effect of varying the crystal symmetry by considering for both phases isotropic crystal lattices with elastic constants *equivalent* to those of the cubic lattices of the alloy studied by Pollock; we have evaluated an equivalent Young’s modulus as

$$E_{eq} = \frac{(C_{11} - C_{12})(3 + (C_{11} - C_{12})/C_{12})}{2 + (C_{11} - C_{12})/C_{12}} \quad (4.1)$$

and an equivalent Poisson’s ratio as

$$\nu_{eq} = \frac{1}{2 + (C_{11} - C_{12})/C_{12}} \quad (4.2)$$

where C_{11} and C_{12} are the elastic constants of the cubic lattice [58].

researchers	crystal symmetry	elastic constants of the γ' -phase	elastic constants of the γ -phase	misfit	applied load (along $\langle 001 \rangle$)	type of observed rafting behavior	case no.	case acronym
Miyazaki, Nakamura, Mori [16]	cubic	$C_{11} = 167$ GPa $C_{12} = 106$ GPa $C_{44} = 99$ GPa	$C_{11} = 112$ GPa $C_{12} = 63$ GPa $C_{44} = 57$ GPa	+0.56%	+ 147 MPa	P	1	MNMT
					- 147 MPa	N	2	MNMC
Tien, Copley [13]	isotropic	$E = 144$ GPa $\nu = 0.3$	$E = 158$ GPa $\nu = 0.3$	-0.30%	+ 155 MPa	N	3	TCT
					- 155 MPa	P	4	TCC
Pollock [25]	cubic	$C_{11} = 179$ GPa $C_{12} = 120$ GPa $C_{44} = 88$ GPa	$C_{11} = 202$ GPa $C_{12} = 139$ GPa $C_{44} = 95$ GPa	-0.38%	+ 50 MPa	N	5	PLT
					+ 138 MPa	N	6	PHT

Table 4.1 Characteristics of experimental alloys and observed rafting behavior.

notes	crystal symmetry	elastic constants of the γ' -phase	elastic constants of the γ -phase	misfit	applied load (along $\langle 001 \rangle$)	case no.	case acronym
Same as MNMT case, but with the elastic constants of the γ' and γ phases inverted (soft precipitate)	cubic	$C_{11} = 112$ GPa $C_{12} = 63$ GPa $C_{44} = 57$ GPa	$C_{11} = 167$ GPa $C_{12} = 106$ GPa $C_{44} = 99$ GPa	+0.56%	+ 147 MPa	7	MNMT _{INV}
Same as MNMT case, but with negative misfit	cubic	$C_{11} = 167$ GPa $C_{12} = 106$ GPa $C_{44} = 99$ GPa	$C_{11} = 112$ GPa $C_{12} = 63$ GPa $C_{44} = 57$ GPa	-0.56%	+ 147 MPa	8	MNMT _{NMS}
Same as TCT,TCC cases, but with the positive value of misfit given in [13]	isotropic	$E = 144$ GPa $\nu = 0.3$	$E = 158$ GPa $\nu = 0.3$	+0.02%	+ 155 MPa	9	TCT _{PMS}
					- 155 MPa	10	TCC _{PMS}
Same as the PLT case, but with equivalent isotropic crystal symmetry	isotropic	$E = 82$ GPa $\nu = 0.3$	$E = 89$ GPa $\nu = 0.3$	-0.38%	+ 50 MPa	11	PLT _{iso}

Table 4.2 Characteristics of hypothetical alloys examined in the rafting analysis.

The characteristics of these hypothetical alloys and the loading conditions for which the simulations have been carried out are summarized in Table 4.2

Regarding the creep properties, in the range of loading conditions that will be explored, the predominant creep mechanism involves dislocation motion primarily in the γ -matrix. TEM studies [25] show that the γ' cuboids are not sheared by dislocations until the latest stage of steady state creep. Thus in our model of the very first stage of the stress-annealing transient, the γ' precipitate is allowed to deform only elastically while the matrix material can deform by creep.

Since the $\langle 001 \rangle$ orientation of the applied load is a multiple slip orientation, a simple isotropic power-law relation has been used to characterize the creep properties of the matrix:

$$\dot{\epsilon}^{cr} = A\sigma^n. \quad (4.3)$$

In all our stress annealing transients the creep properties given by Johnson et al., [56] for Ni-6W tested at 854° have been used, with:

$$n = 4.8$$

$$A = 5.4E - 15(s^{-1}MPa^{-4.8})$$

Actually, since we are not particularly interested in “real time” simulation of the stress-annealing transient, the accuracy of the pre-exponential coefficient A , is of secondary relevance; the stress exponent, n , is a more important quantity but it should not exhibit significant modifications when the alloying of the γ phase is slightly modified.

Regarding the microstructure geometry, we have relied on the data obtained by Pollock [25] by TEM study of CMSX3. This choice will not yield an accurate simulation of the Tien and Copley and of the Miyazaki-Nakamura-Mori alloys which are characterized by a lower volume fraction of the γ' phase. However, we believe that this inaccuracy will not affect the basic pattern of the results. This point should be, however, proved by further simulations in which the γ' volume fraction is modified.

According to Pollock's data, the γ' precipitates have an average cube length of 0.45 μm and the matrix passages have an average thickness of 60 nm, giving a γ' volume fraction of 0.68. The finite element models shown in Fig. 4.11 have been formulated so as to preserve these dimensions, so that since a generalized plane strain analysis is done, the volume fraction of the γ' in the model is somewhat higher than in the real material because the matrix channels parallel to the plane of the mesh are neglected. While we are aware of the fact that our models still present a certain degree of inaccuracy, and that the eleven cases that we will analyze do not constitute a complete parametric study, we will see in the following paragraphs how the results of our simulations fit in a logical pattern that can yield significant insight to the rafting phenomenon.

4.4 Elastic Analysis

An elastic analysis for the eleven cases characterized in Tables 4.1 and 4.2, has been carried out. Both the matrix and the precipitate are only allowed to deform elastically and coherency at the matrix-precipitate interface is enforced. A typical ABAQUS input file for this type of analysis is listed in Appendix V. The particular file listed is relative to case 1 (MNMT), but all the other cases can be easily obtained by correcting the values of misfit, elastic constants and applied load, according to the data of Tables 4.1 and 4.2.

The results of the elastic analyses have been postprocessed to obtain the distribution of the force on the interface. Profiles of τ_n for each of the eleven cases as shown in Figs. 4.13 through 4.23. A synopsis of the results is given in Table 4.3.

We can notice observing the τ_n profiles, that the value of the difference of driving force on the top and on the side of the particle is always very limited: at most it is of the order of 0.3 MPa for the “MNM” – cases and it is as low as 0.006 MPa for the TCT_{PMS} and TCC_{PMS} cases.

If we evaluate the “Pineau’s parameters” E_p/E_m and $\sigma/E_m\delta$ for all the eleven cases (for the cubic crystals an equivalent Young’s modulus can be calculated using Eq. (4.1)), we can see how the type of rafting behavior indicated by the τ_n profiles is perfectly consistent with the behavior predicted by our simple evolution map of Fig. 4.5.

This suggests that a very similar map could be constructed by performing a parametric study on the actual $\gamma - \gamma'$ morphology.

Table 4.3 Synopsis of the Elastic Analysis

Case #	Case Acronym	E_p/E_m	$\sigma/E_m\delta$	Rafting behavior predicted by the model	Consistency with the evolution map of Fig. 4.5	Consistency with experimental results
1	MNMT	1.23	0.388	P	YES	YES
2	MNMC	1.23	-0.388	N	YES	YES
3	TCT	0.91	-0.327	P	YES	NO
4	TCC	0.91	+0.327	N	YES	NO
5	PLT	0.92	-0.148	P	YES	NO
6	PHT	0.92	-0.399	P	YES	NO
7	MNMT _{INV}	0.81	+0.314	N	YES	
8	MNMT _{NMS}	1.23	-0.388	N	YES	
9	TCT _{PMS}	0.91	+4.9	N	YES	
10	TCC _{PMS}	0.91	-4.9	P	YES	
11	PLT _{ISO}	0.92	-0.148	P	YES	

Unfortunately, such a map would be totally inadequate to predict the rafting behavior of the crystals since, as indicated in Table 4.3, our predictions based on elastic calculation of the τ_n profile are not always in agreement with the available experimental data.

This leads us toward a more accurate simulation of the actual conditions in which the rafting behavior is observed, as will be discussed in the next paragraph.

It is interesting to note that if we assume, for the alloy studied by Tien and Copley, the erroneous value of the misfit given in the paper, the rafting behavior predicted by our evolution map, and by the τ_n profiles, is consistent with the experimental observations.

This unfortunate contingency has represented, in the past, a confusing source of misplaced confidence in the methods based on purely elastic calculations.

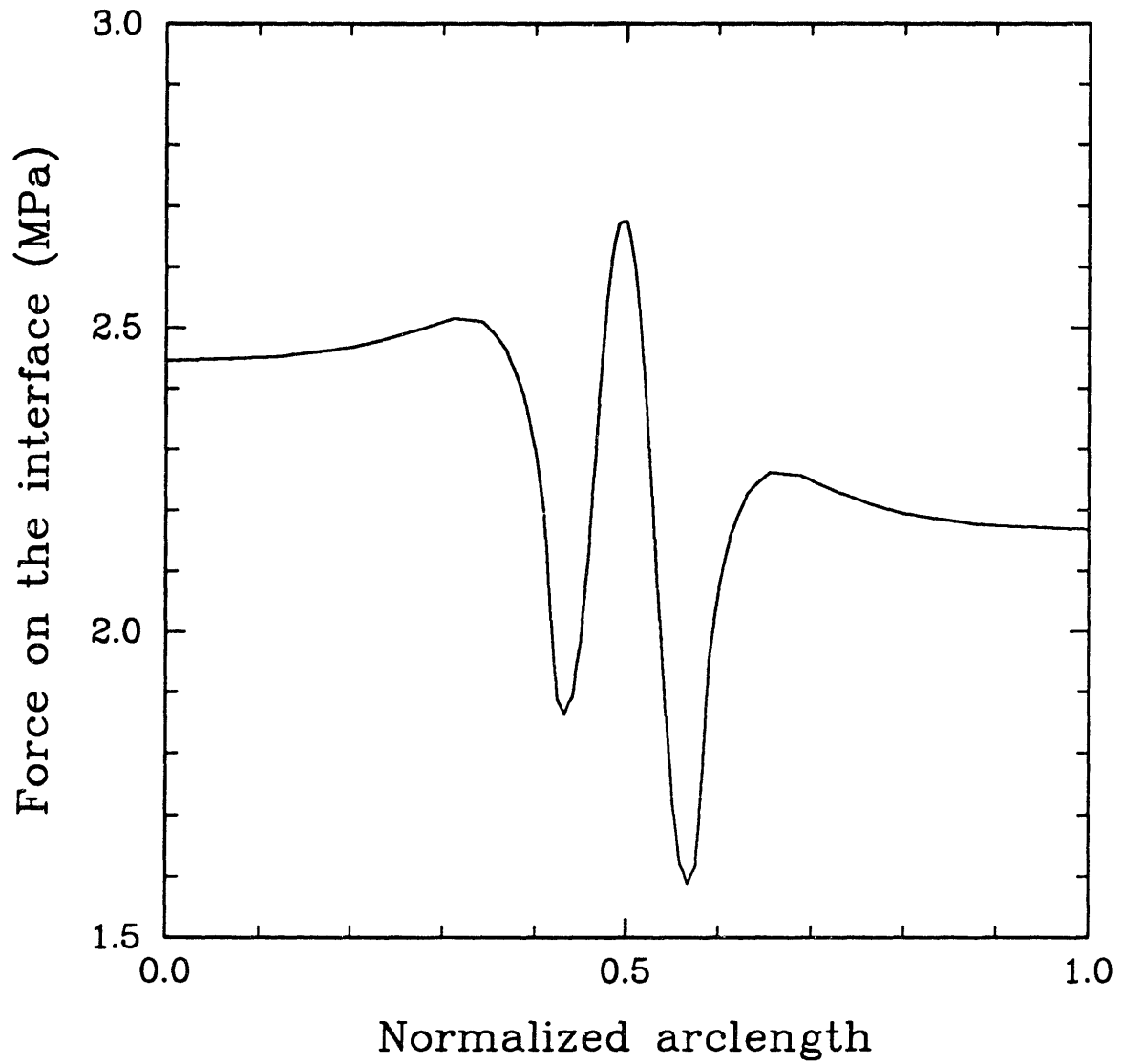


Figure 4.13 τ_n profile for the elastic analysis of case 1 (MNMT).

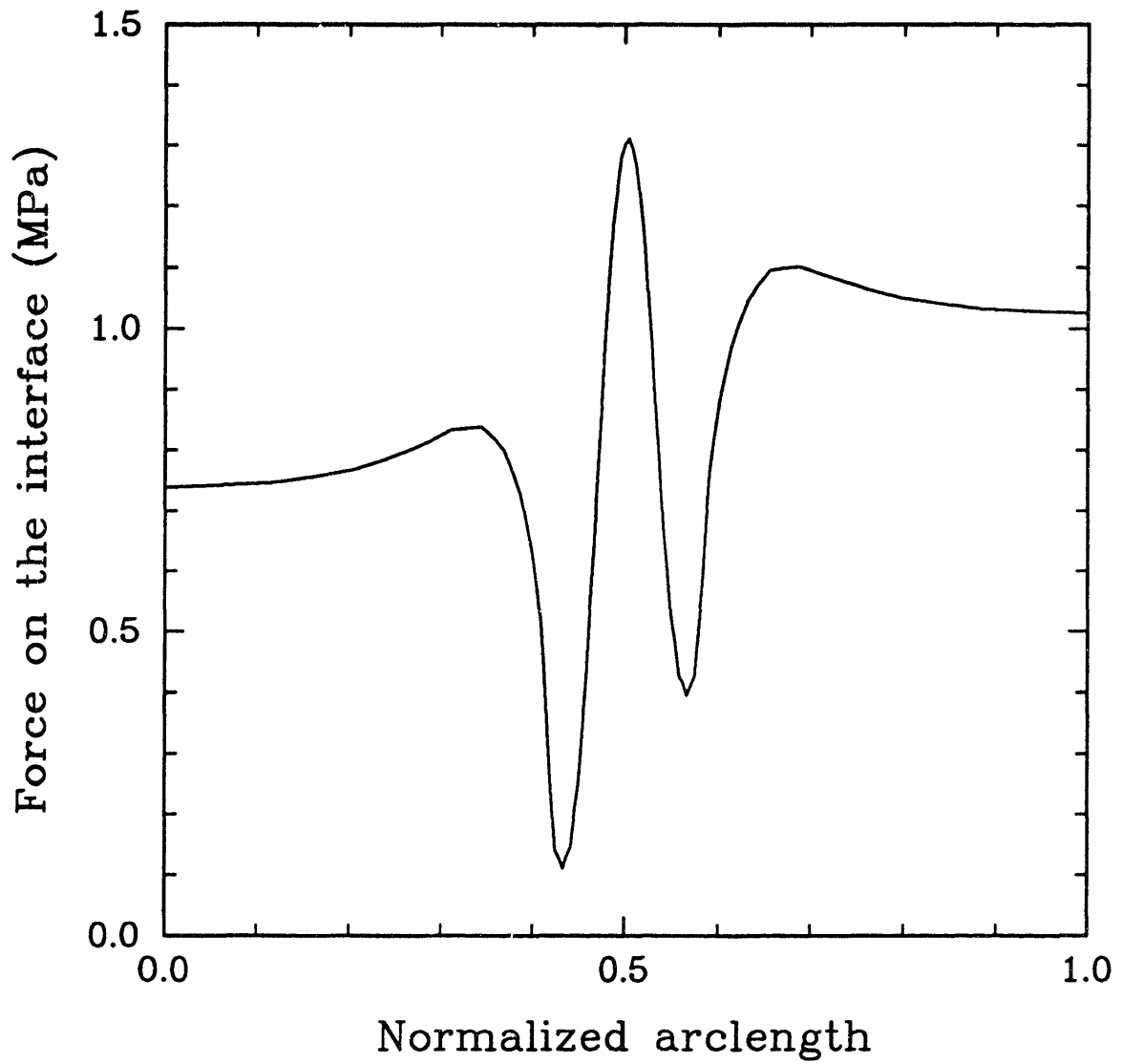


Figure 4.14 τ_n profile for the elastic analysis of case 2 (MNNC).

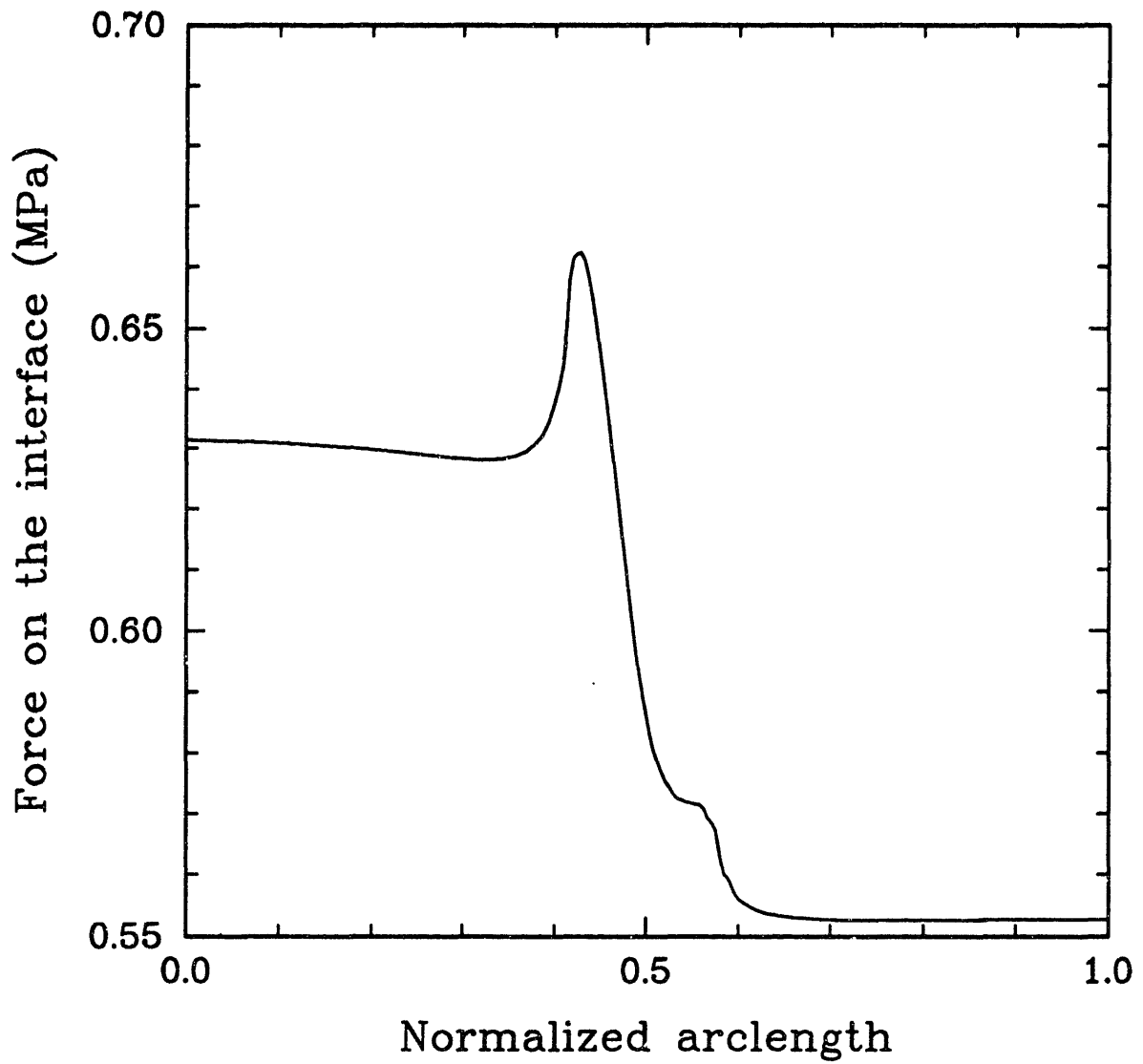


Figure 4.15 τ_n profile for the elastic analysis of case 3 (TCT).

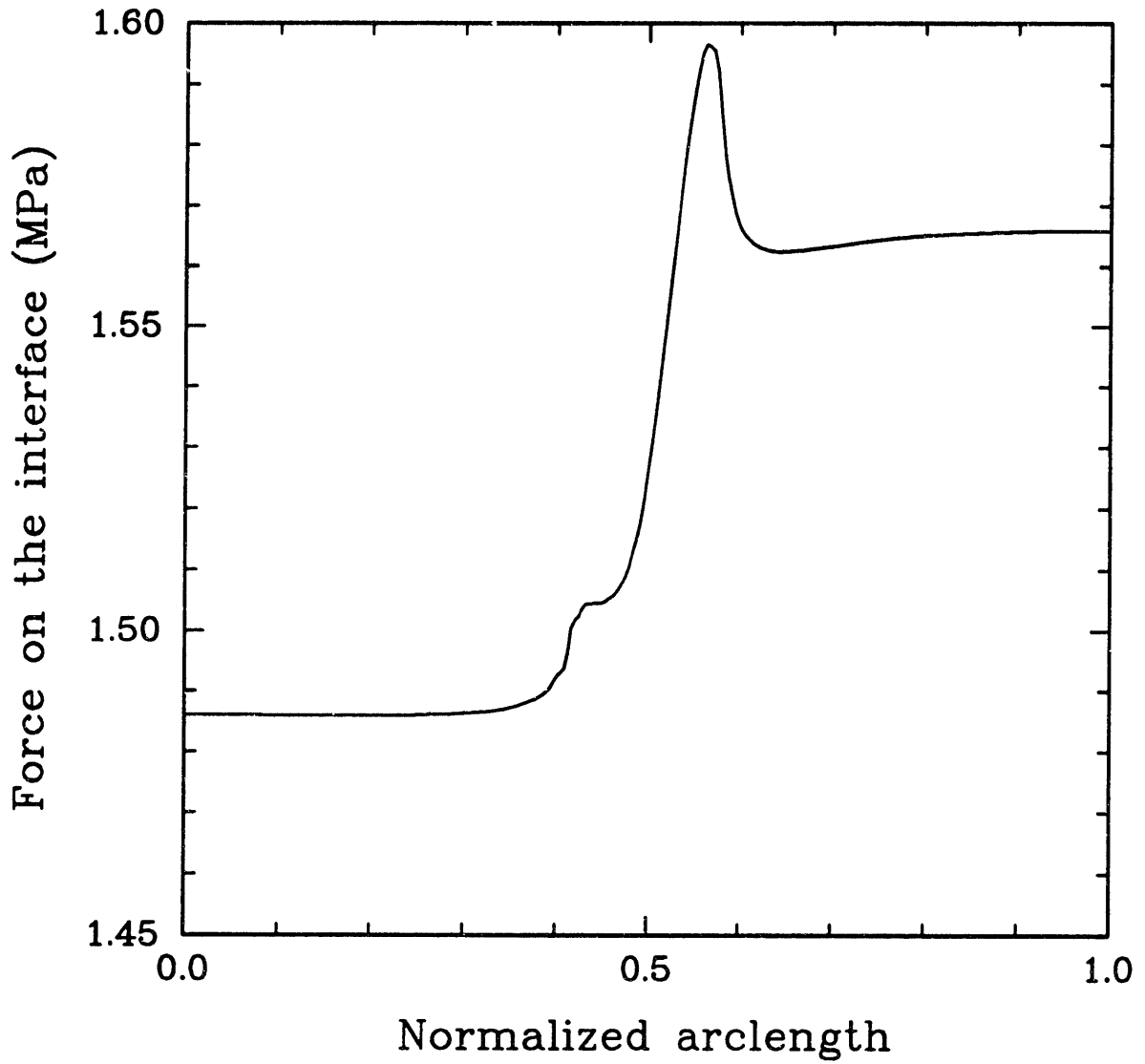


Figure 4.16 τ_n profile for the elastic analysis of case 4 (TCC).

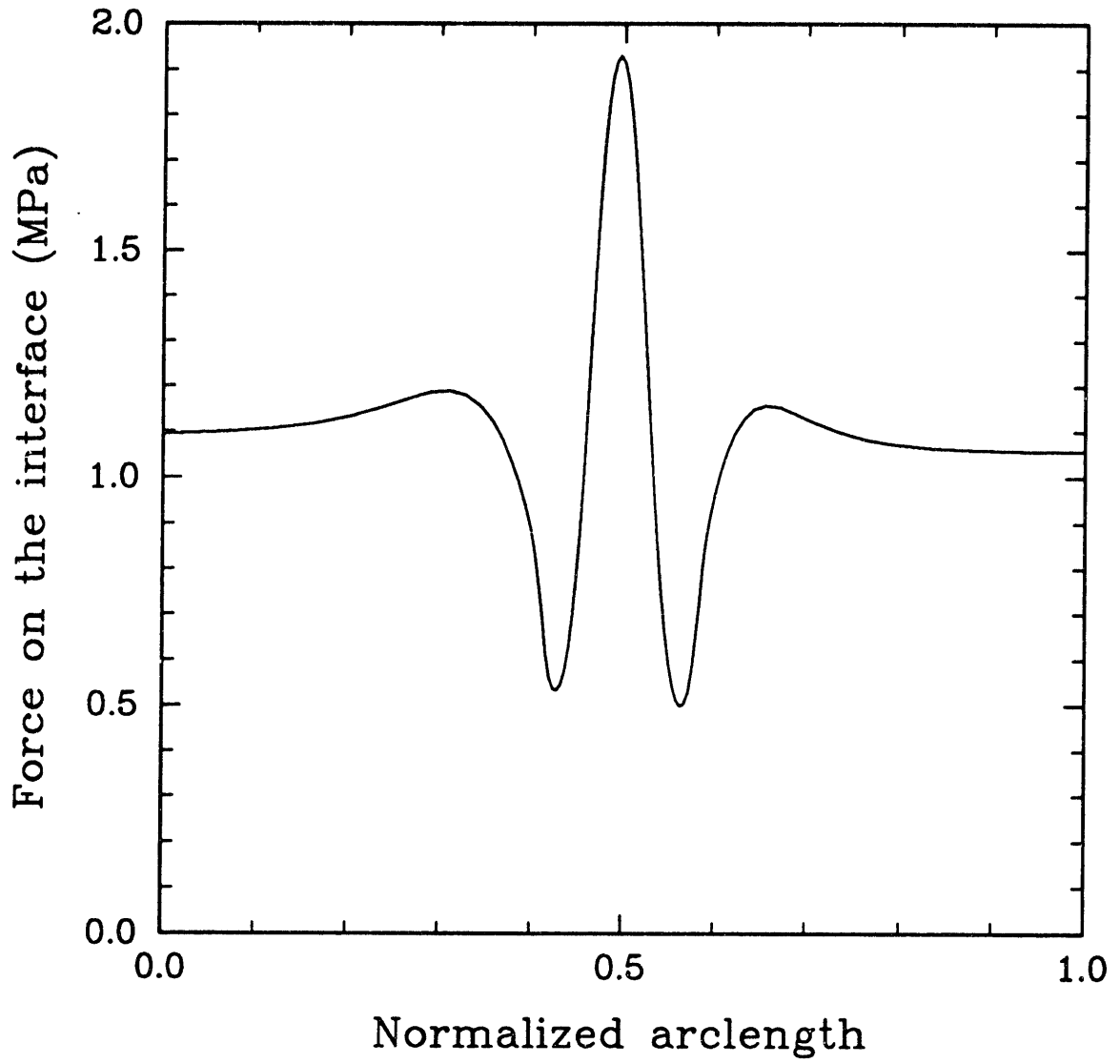


Figure 4.17 τ_n profile for the elastic analysis of case 5 (PLT).

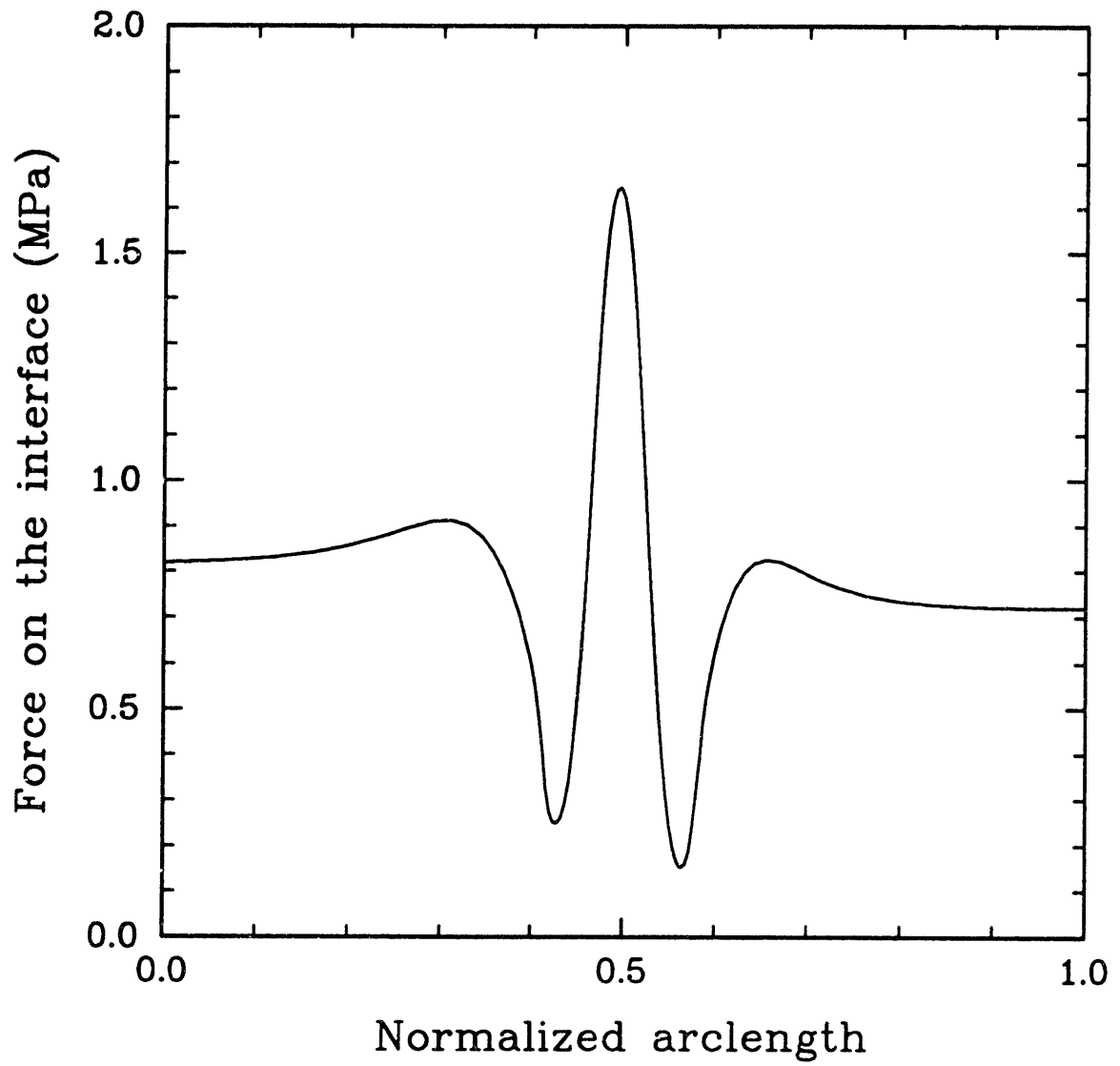


Figure 4.18 τ_n profile for the elastic analysis of case 6 (PHT).

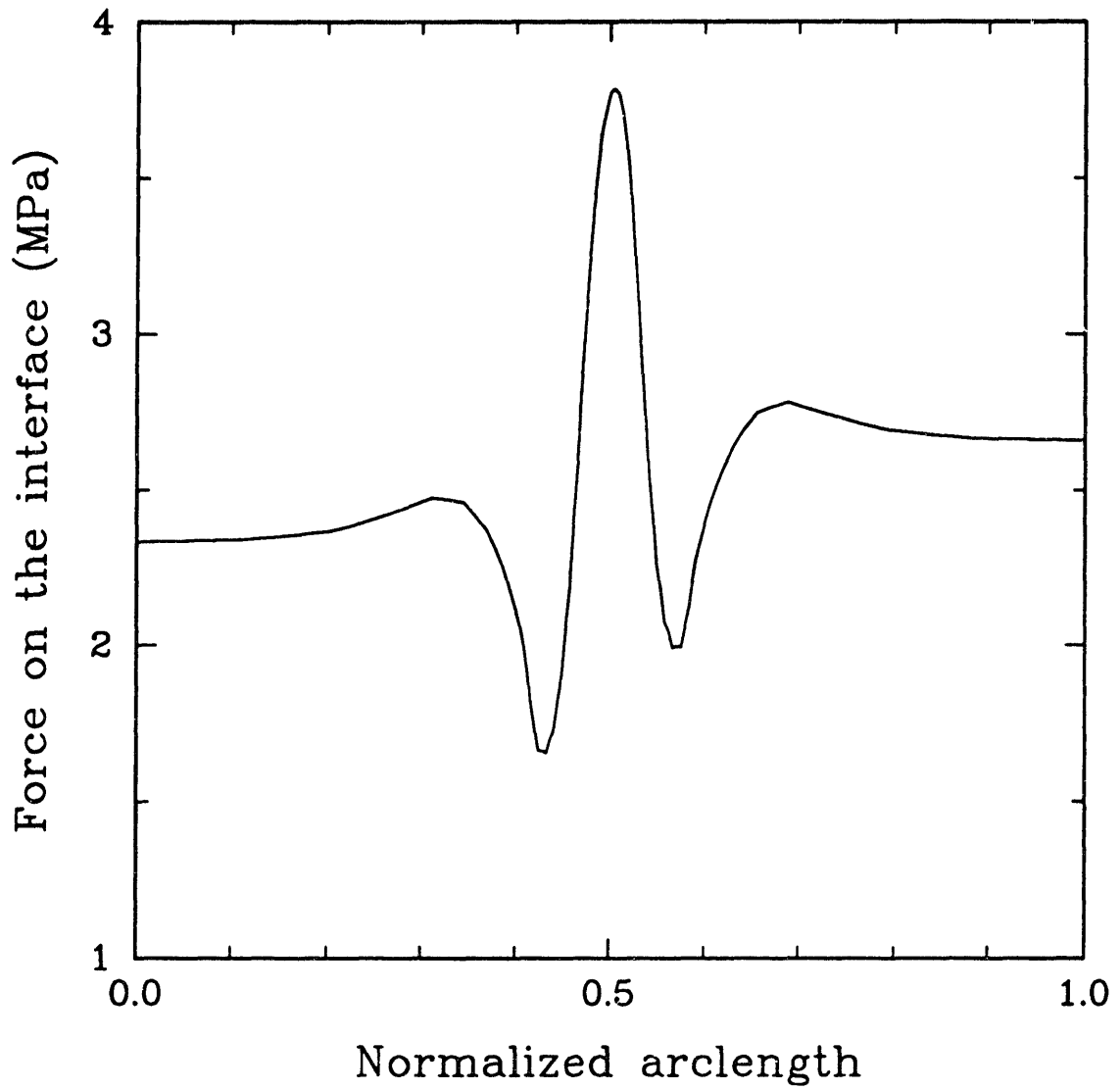


Figure 4.19 τ_n profile for the elastic analysis of case 7 (MNM_{INV}).

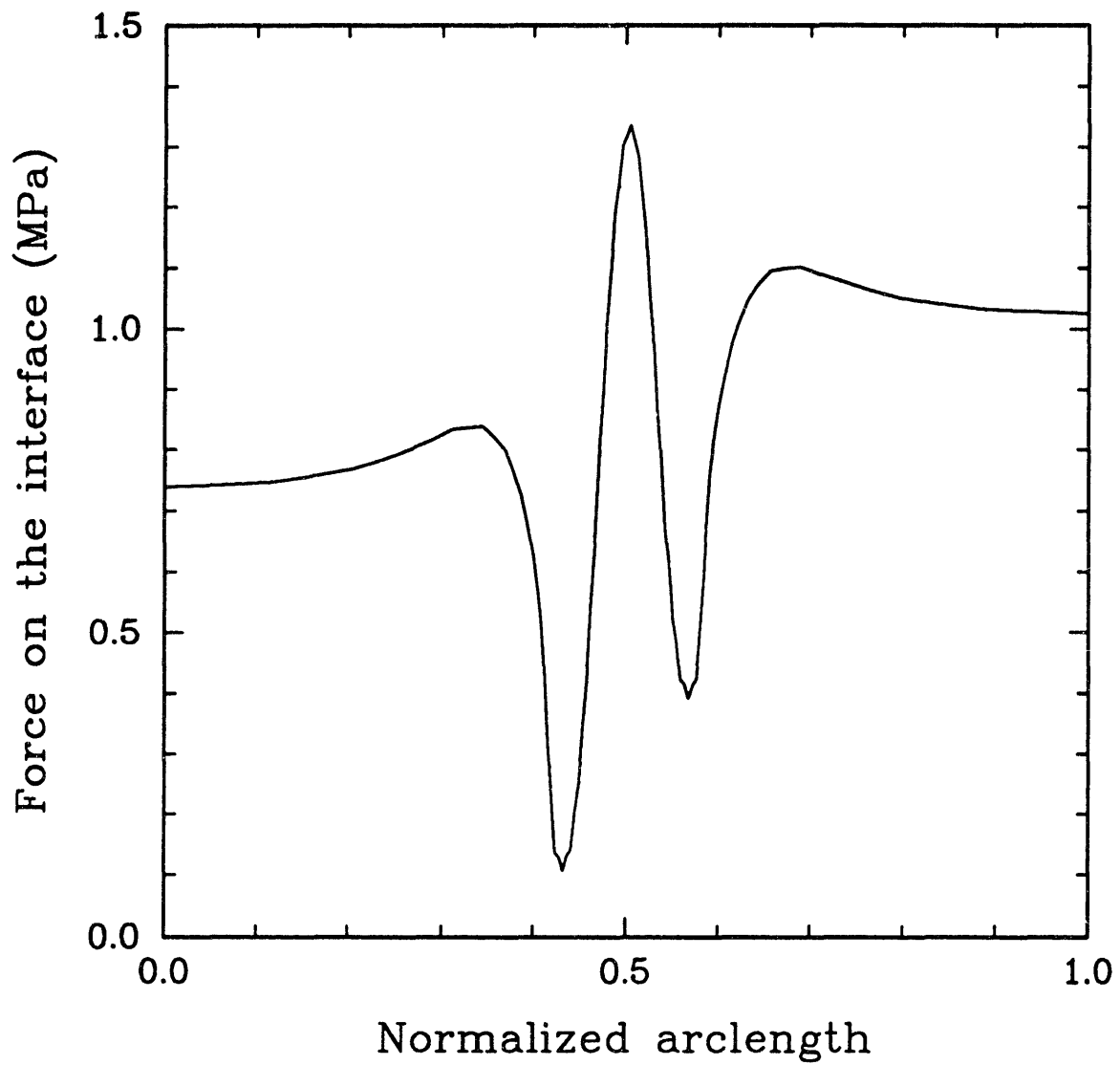


Figure 4.20 τ_n profile for the elastic analysis of case 8 (MNMT_{NMS}).

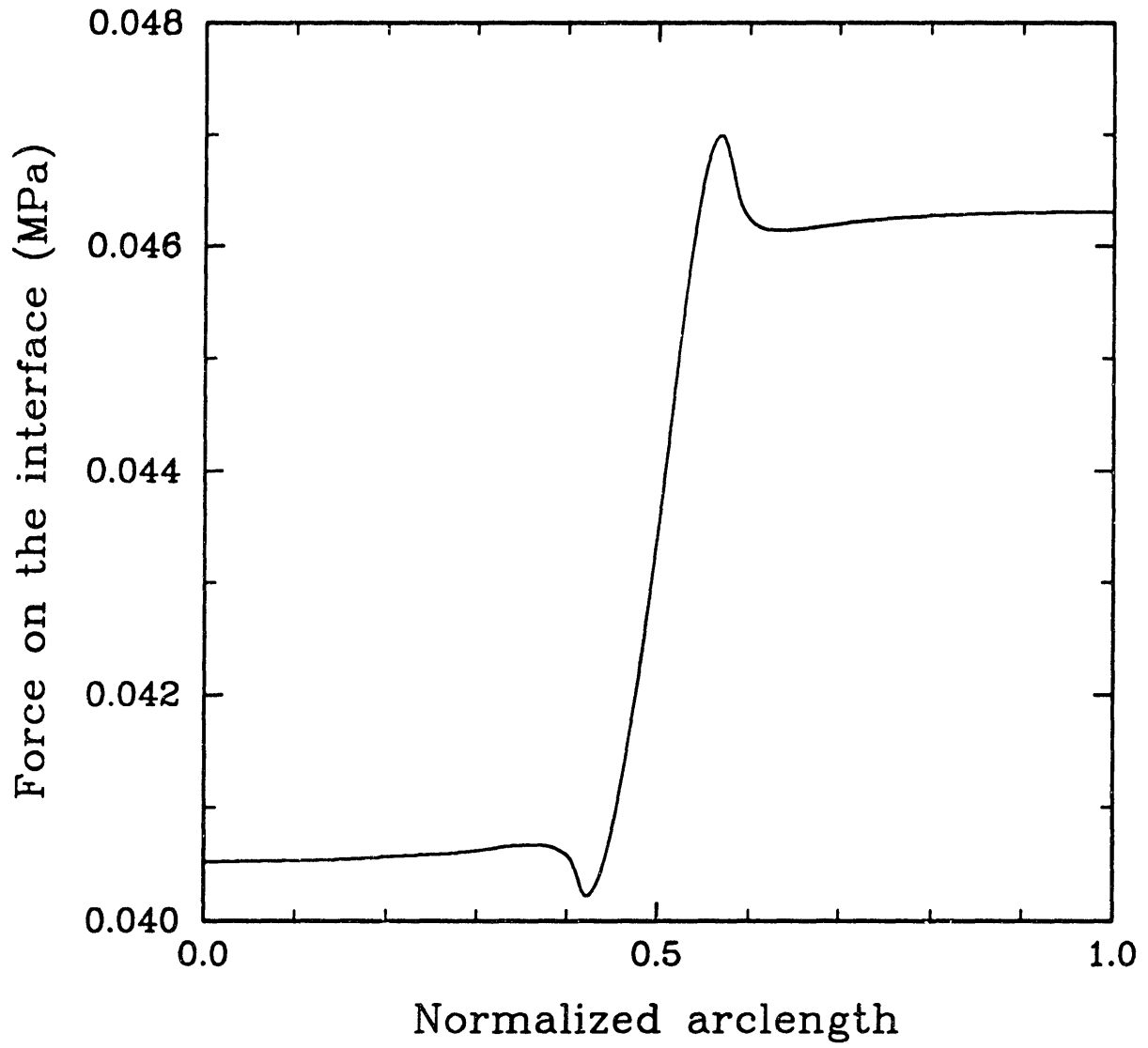


Figure 4.21 τ_n profile for the elastic analysis of case 9 (TCT_{PMS}).

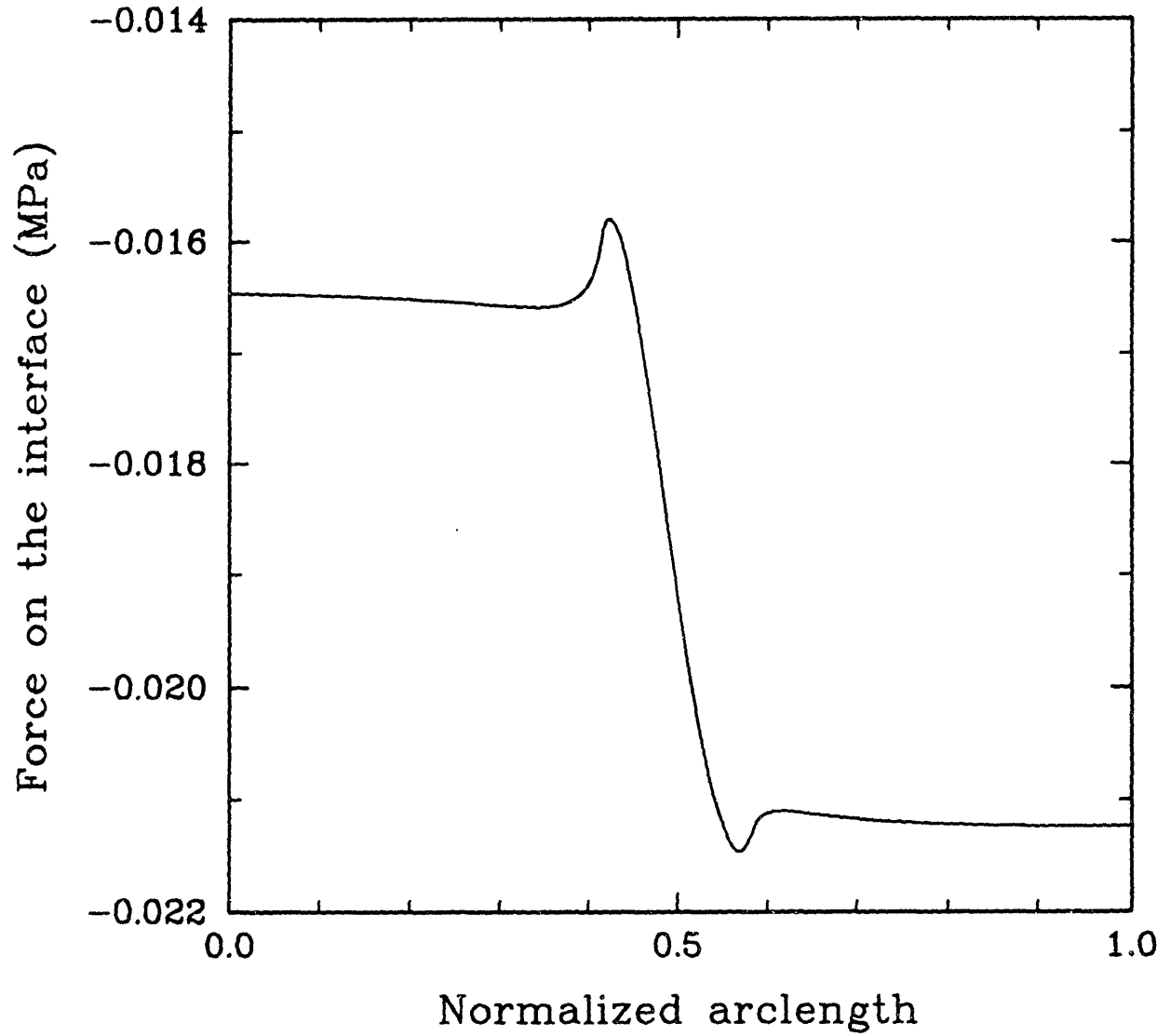


Figure 4.22 τ_n profile for the elastic analysis of case 10 (TCC_{PMS}).

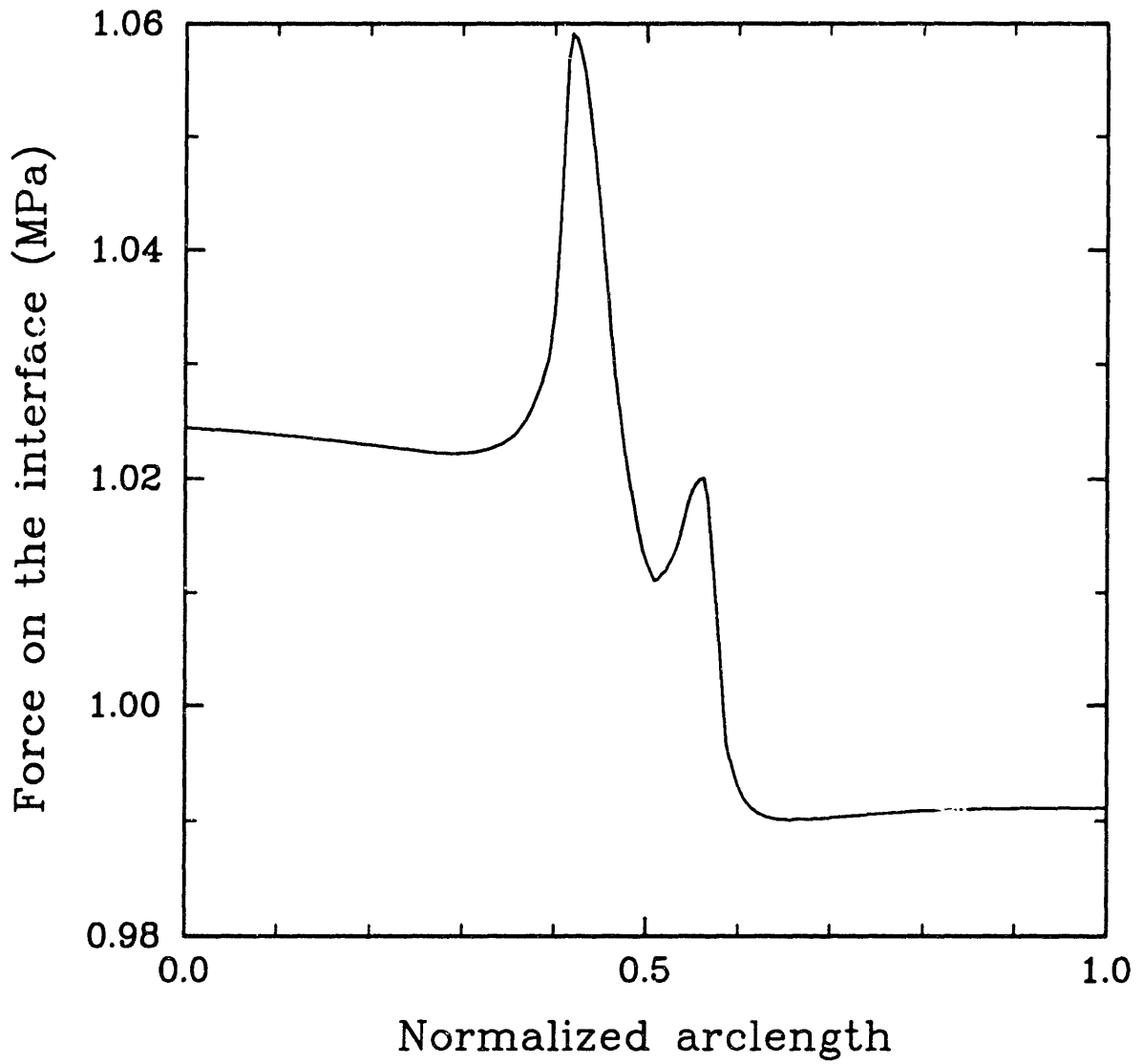


Figure 4.23 τ_n profile for the elastic analysis of case 11 (PLT_{ISO}).

4.5 Analysis of the Stress-Annealing Transients

As previously discussed in paragraph 1.2, TEM observations of $\gamma-\gamma'$ crystals show how, in the very first stage of stress-annealing tests, mobile dislocations start to form and multiply in the γ matrix. As soon as the crystal is brought to test temperature, networks of dislocations form at the $\gamma-\gamma'$ interfaces, wrapping the γ' cuboids and relieving most of the shear component of the misfit strain. When an external load is applied, dislocations glide and climb in the narrow γ channels so that a macroscopic creep flow in the γ matrix is observed.

As a result of this process, the elastic fields in the crystal are dramatically modified. Therefore a meaningful evaluation of the force on the interface should be based on these altered fields.

Even if, considering the scale of the microstructure, an accurate simulation of the process should be based on a model capable to treat discrete dislocations, some interesting results can be obtained by considering a simplified macroscopic creep model for the γ phase. As we have already mentioned in paragraph 4.3, we have modeled the creep behavior of the matrix with the simple isotropic power-law relation (4.3).

We have carried out a simulation of the very first stage of the stress annealing transients, using the ABAQUS code, and analyzed the corresponding evolution of the τ_n profile.

A typical ABAQUS input file for this kind of analysis is listed in Appendix VI. The particular file listed corresponds to case 1 (MNMT).

As *initial* conditions for the simulated transients we have considered the elastic field in the crystal associated with the misfit strain at test temperature, enforcing perfect coherency at the interfaces. We have then applied the test load, over a short linear ramp of one second, and let the matrix creep according to equation 4.3.

Typical contour plots of the *initial* stress state, due to the misfit only, are shown in Figs. 4.24 through 4.29 for a positive-misfit alloy (Miyazaki-Nakamura-Mori alloy: Cases 1,2,7) and for a negative-misfit alloy (Pollock alloy: Case 5).

As schematically indicated in Fig. 4.30(a), the main components of stress in the matrix, σ_0 in the Figure, are in the planes of the channels (tensile for positive-misfit alloys, compressive for negative-misfit alloys). The magnitude of the biaxial stress σ_0 in the γ channels varies with the misfit and the elastic constants of the two phases but typically is of the order of 400 - 500 MPa in most commercial alloys. The component of stress normal to the planes of the channels is one order of magnitude smaller and of opposite sign. The γ' precipitates are almost in a state of hydrostatic stress of the same magnitude as the normal stress in the γ channels.

Thus in the very first stage of a stress-annealing transient with an applied stress, σ , in the range 50-200 MPa, the effect of the misfit stresses dominates over the effect of the applied load, and the γ matrix creeps so as to accommodate the misfit (Fig.

4.30(b)). This stage corresponds to the formation of dislocation networks at the $\gamma-\gamma'$ interfaces.

In Figs. 4.31 through 4.38, a sequence of contour plots of the equivalent creep strain in the matrix, ϵ_{eq}^{creep} , at subsequent stages of the primary creep transient for case 1 (MNMT) and case 2 (MNMC) is shown.

The equivalent creep strain in the matrix is defined as:

$$\epsilon_{eq}^{creep} = \sqrt{\frac{2}{3} \epsilon_{ij}^{creep} \epsilon_{ij}^{creep}}, \quad (4.4)$$

where ϵ_{ij}^{creep} are the components of the creep strain tensor.

The steep gradient of ϵ_{eq}^{creep} in the direction normal to the interface, particularly noticeable around the corner of the precipitate, is the “continuum” analogy to the network of dislocations at the interface. The gradient would be even steeper with a higher creep exponent, n , in expression 4.3.

As the creep transient progresses, and the deviatoric components of the stress tensor are accommodated by the creep strains, a state of hydrostatic stress builds up in the matrix channels. Regardless of the sign of the misfit and of the relative stiffnesses of matrix and precipitates, all the transients evolve toward a stress state, at the end of the primary creep stage, in which (Fig. 4.30 (c)):

- if a *tensile* stress is applied, there is a build up of *negative* pressure in the *horizontal* channels (the channels normal to the applied stress) and of *positive* pressure in the *vertical* channels (the channels parallel to the applied stress);
- if a *compressive* stress is applied, there is a build up of *positive* pressure in the *horizontal* channels and of *negative* pressure in the *vertical* channels.

The magnitude of the stress in the horizontal channels is higher than the applied stress, while the magnitude of the stress in the vertical channels is much lower than the applied stress.

In Figs. 4.39 through 4.54, typical contour plots of the stress state at the end of the primary creep stage are shown for applied tensile loads (Cases 1,3,5,6,9) and compressive loads (Cases 2,4,6).

As the stress state evolves, the force on the interface is modified as well. Plots of the evolution of the τ_n profile during the stress annealing transient for the eleven cases considered are shown in Figs. 4.55 through 4.65. For each case, nine plots are given of the τ_n profile at successive times of the transient. As a normalized measure of the stage of evolution of the creep transient we have chosen the ratio between the average equivalent creep strain in the matrix and the initial misfit ($\bar{\epsilon}^{creep}/\delta$). The average creep strain in the matrix is evaluated as a volume average, over the γ phase, of the equivalent creep strain:

$$\bar{\epsilon}^{\text{creep}} = \frac{1}{V_\gamma} \int_{V_\gamma} \epsilon_{\text{eq}}^{\text{creep}} dV_\gamma, \quad (4.5)$$

where V_γ is the volume occupied by the γ phase.

We have chosen the parameter $\bar{\epsilon}^{\text{creep}}/\delta$ rather than a more immediate quantity, such as the creep time, because it is more directly related to the evolution of the τ_n profile, as we will discuss in the next paragraph.

Let's now consider the evolution of the τ_n profiles for the first six cases, relative to the simulation of stress annealing tests performed on experimental alloys.

We can notice how the profiles quickly evolve toward configurations that show a marked driving force for directional coarsening. If we compare these graphs with those obtained in our purely elastic analyses, we can see that the *absolute values* of the differences between the force on the top and on the side of the precipitates, $\Delta\tau_n$, are generally increased by one order of magnitude; however, the most important result is that the *signs* of $\Delta\tau_n$ are inverted for several cases so that now for *all* the experimental alloys we have perfect agreement between the observed rafting behavior and the tendency toward directional coarsening that can be inferred from the τ_n profiles.

If we now consider the evolution of the τ_n profiles for the hypothetical alloys of cases 7 through 11, we can list a number of considerations:

- comparing case 7 (MNMT_{INV}) and case 1 (MNMT) we can see that, if we invert the relative stiffnesses of matrix and precipitate, the driving force for rafting remains virtually identical. This result is in antithesis to that of a purely elastic calculation for which an inversion of the elastic constants brings about a parallel inversion of the rafting tendency (see map in Fig. 4.5);
- conversely, comparing case 8 (MNMT_{NMS}) and case 1 (MNMT) we see that if we change the sign of the misfit the τ_n profiles result totally reversed;
- we compare now case 9 (TCT_{PMS}) and case 7 (MNMT_{INV}). Both cases are relative to positive-misfit alloys with soft precipitates but the misfit for case 9 is about 1/20th of the misfit for case 7. We can see that the fourth plot of Fig. 4.63 (case 9), relative to a stage of the transient for which $\bar{\epsilon}^{\text{creep}}/\delta = 1.88$ shows a profile similar to that of the eighth plot of Fig. 4.61 (case 7), for which $\bar{\epsilon}^{\text{creep}}/\delta = 1.83$. However, the value of $\Delta\tau_n$ for this stage of case 9 is only a few percent of the correspondent value for case 7;
- comparing case 10 (TCC_{PMS}) and case 9 (TCT_{PMS}) we see that if we invert the direction of the applied load, the τ_n profiles are reversed. (This can be also noted comparing cases 1 and 2 and cases 3 and 4).
- comparing case 11 (PLT_{ISO}) and case 5 (PLT) we see that a change in the symmetry of the crystal brings about only minor changes in the τ_n profiles which are mainly localized around the corners of the precipitate.

In the next paragraph, we will reinterpret these observations, as well as other features of the τ_n profiles, within the context of a more general framework and we will offer a general discussion of the rafting phenomenon.

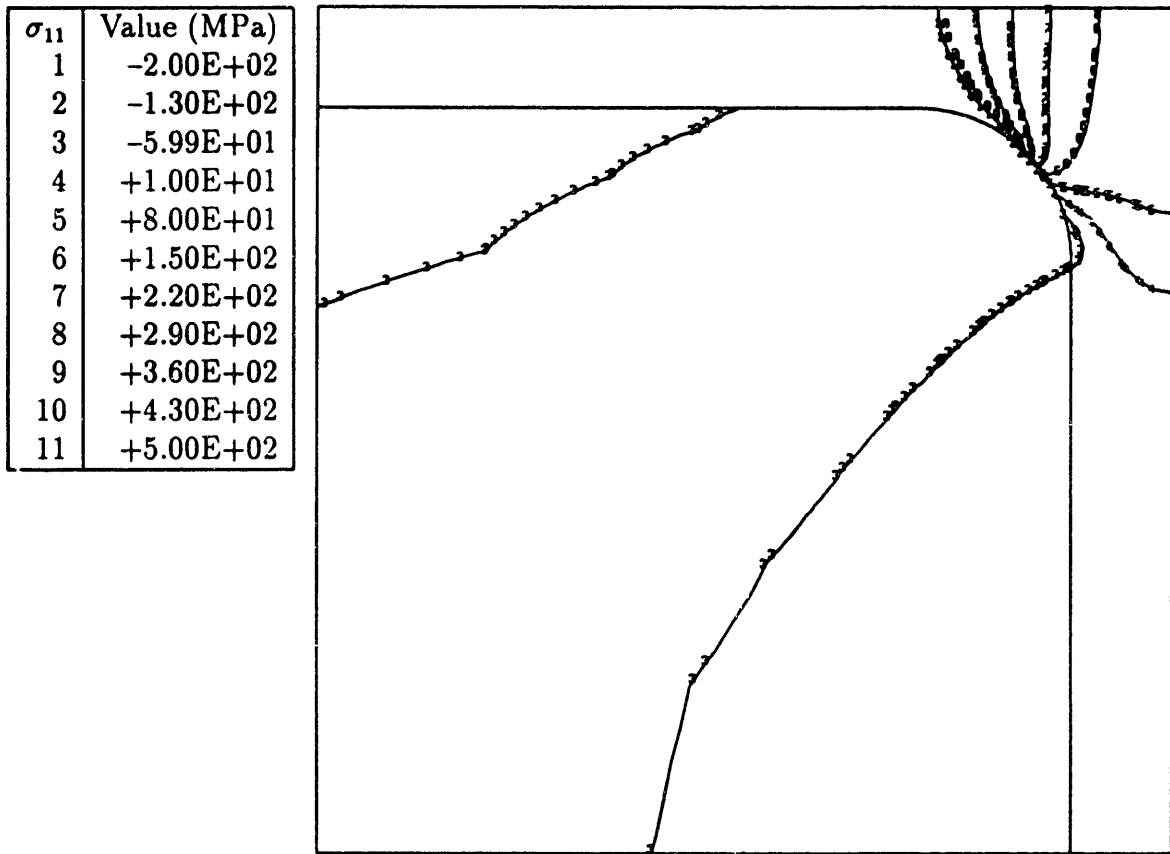


Figure 4.24 Contours of σ_{11} due to misfit only ($\delta = +.56\%$)
for the alloy tested by Miyazaki, Nakamura and Mori [16].

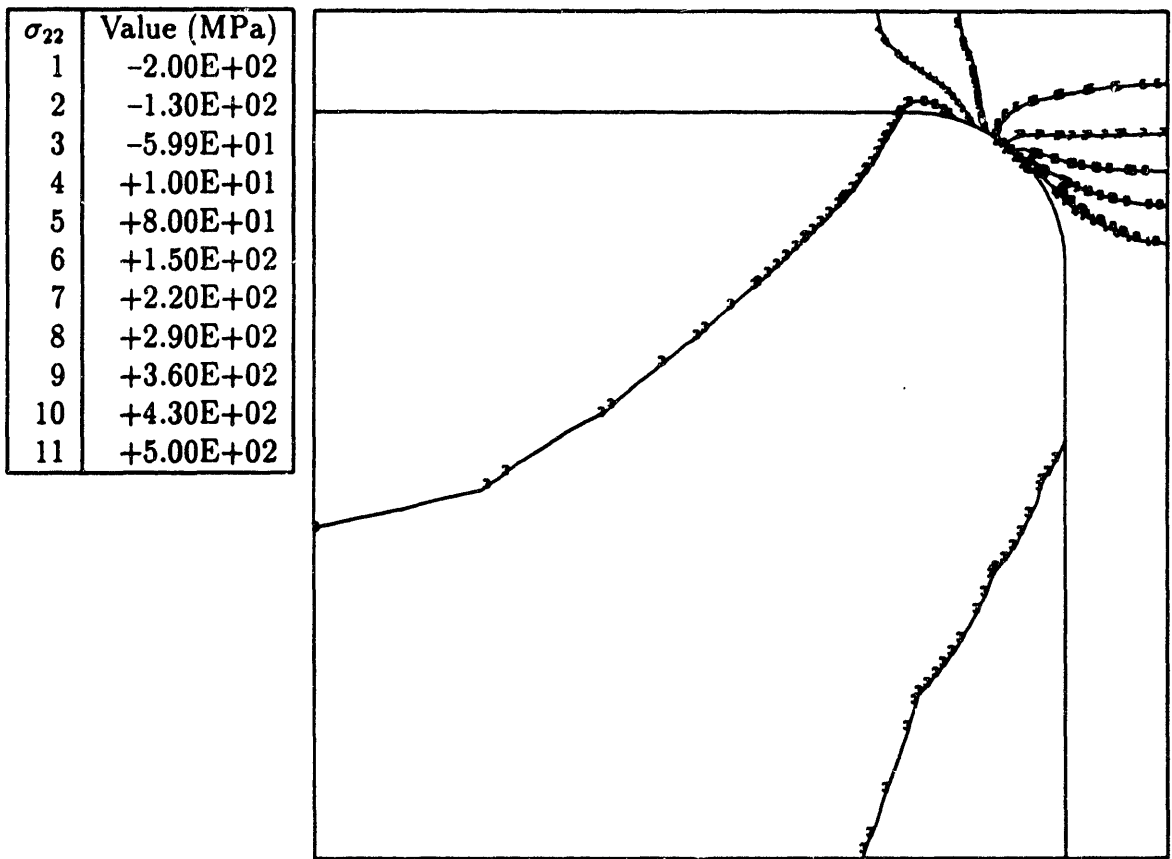


Figure 4.25 Contours of σ_{22} due to misfit only ($\delta = +.56\%$)
for the alloy tested by Miyazaki, Nakamura and Mori [16].

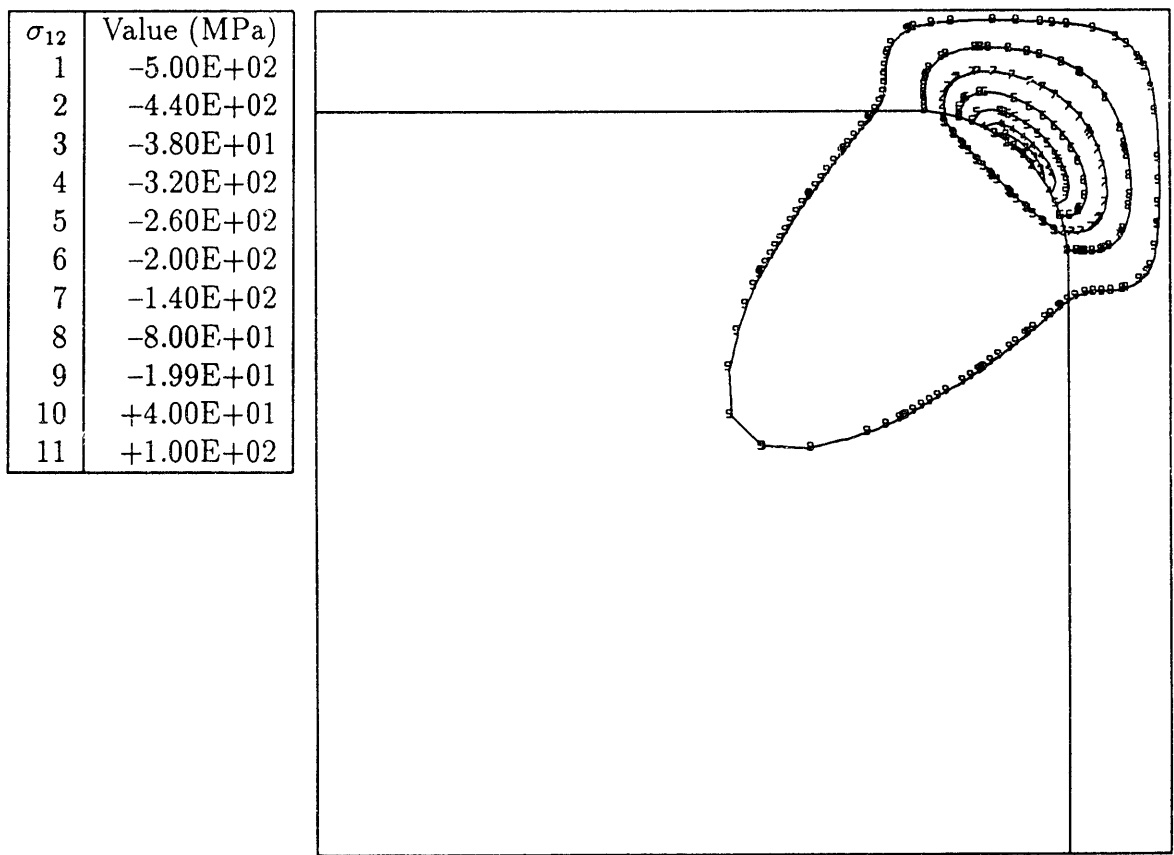


Figure 4.26 Contours of σ_{12} due to misfit only ($\delta = +.56\%$) for the alloy tested by Miyazaki, Nakamura and Mori [16].

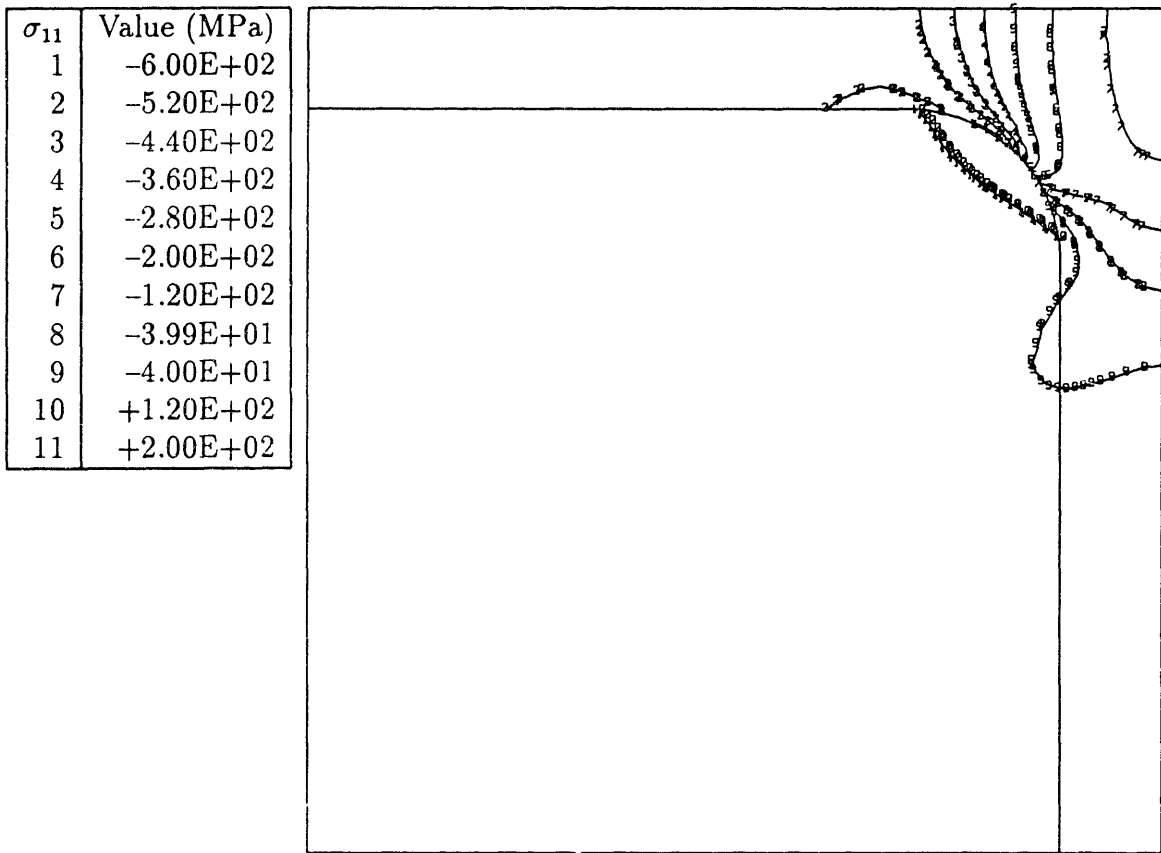


Figure 4.27 Contours of σ_{11} due to misfit only ($\delta = -0.38\%$) for the alloy tested by Pollock [25].

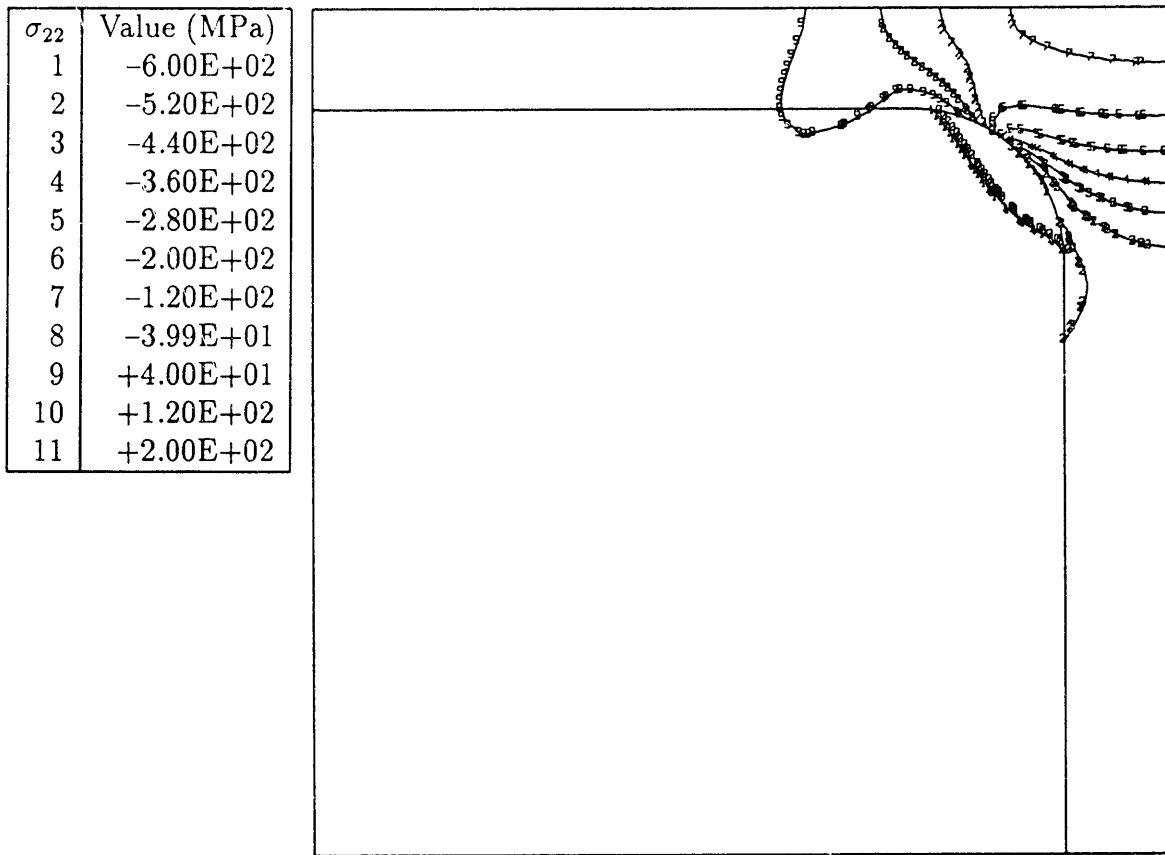


Figure 4.28 Contours of σ_{22} due to misfit only ($\delta = -0.38\%$) for the alloy tested by Pollock [25].

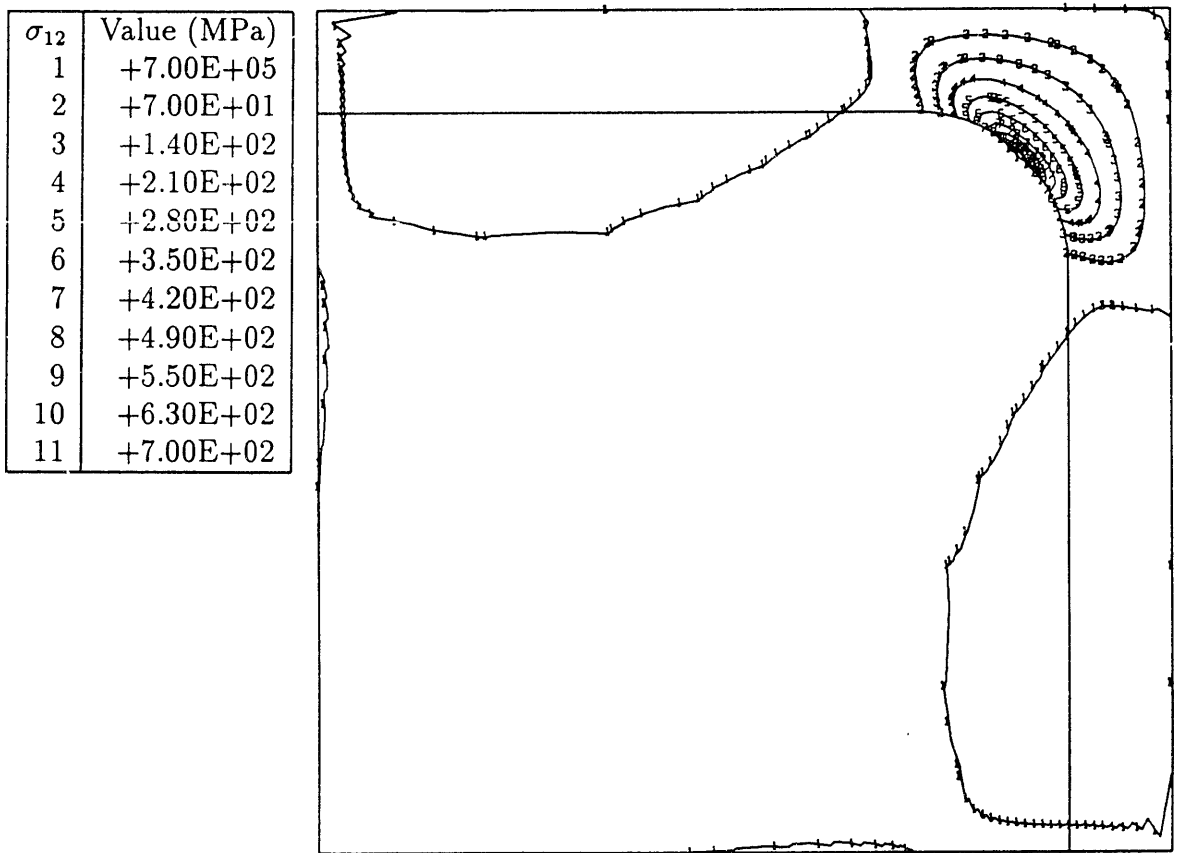


Figure 4.29 Contours of σ_{12} due to misfit only ($\delta = -0.38\%$) for the alloy tested by Pollock [25].

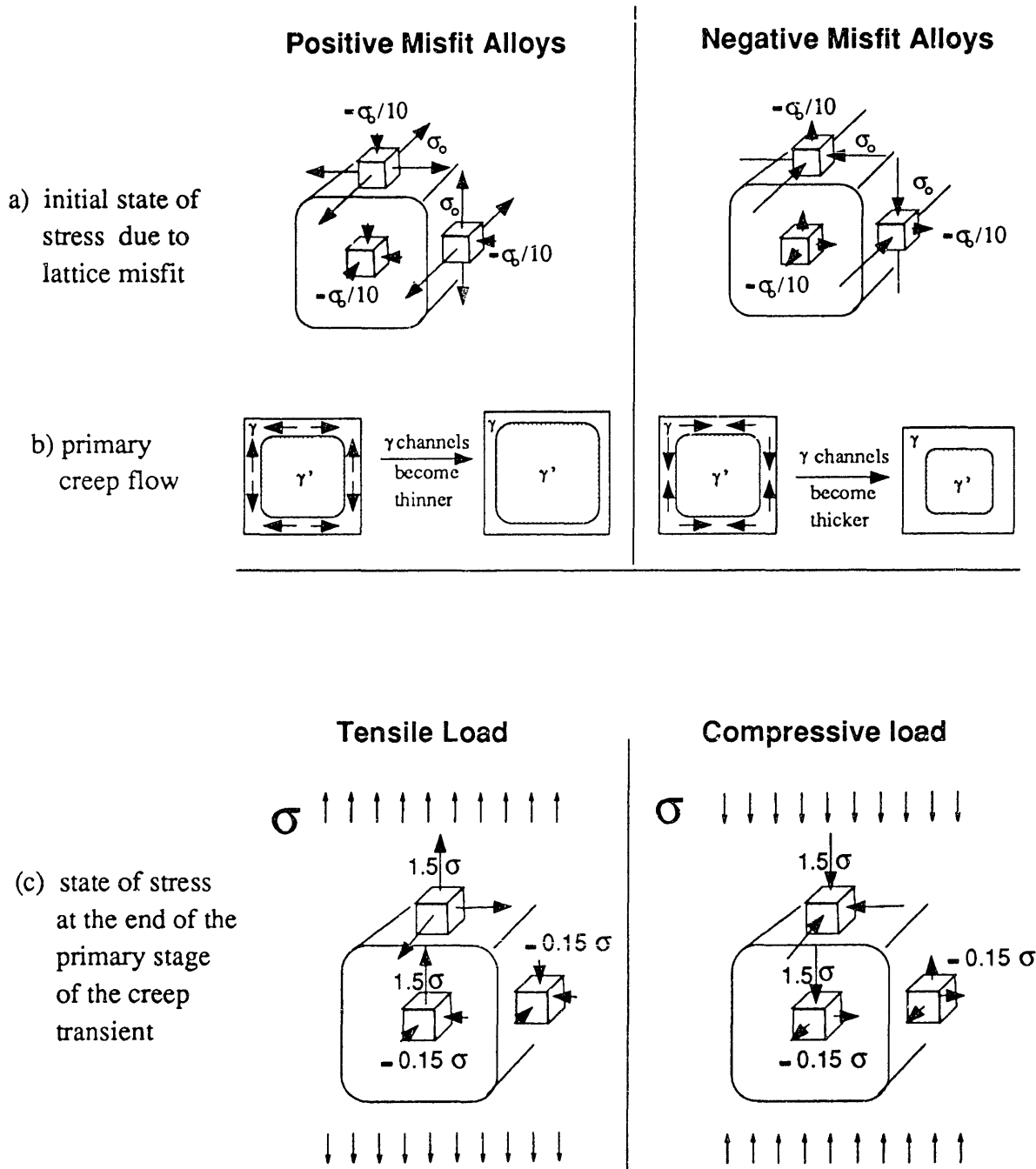


Figure 4.30 Schematic representation of the evolution of the stress and strain fields in the primary stage of the creep transient.

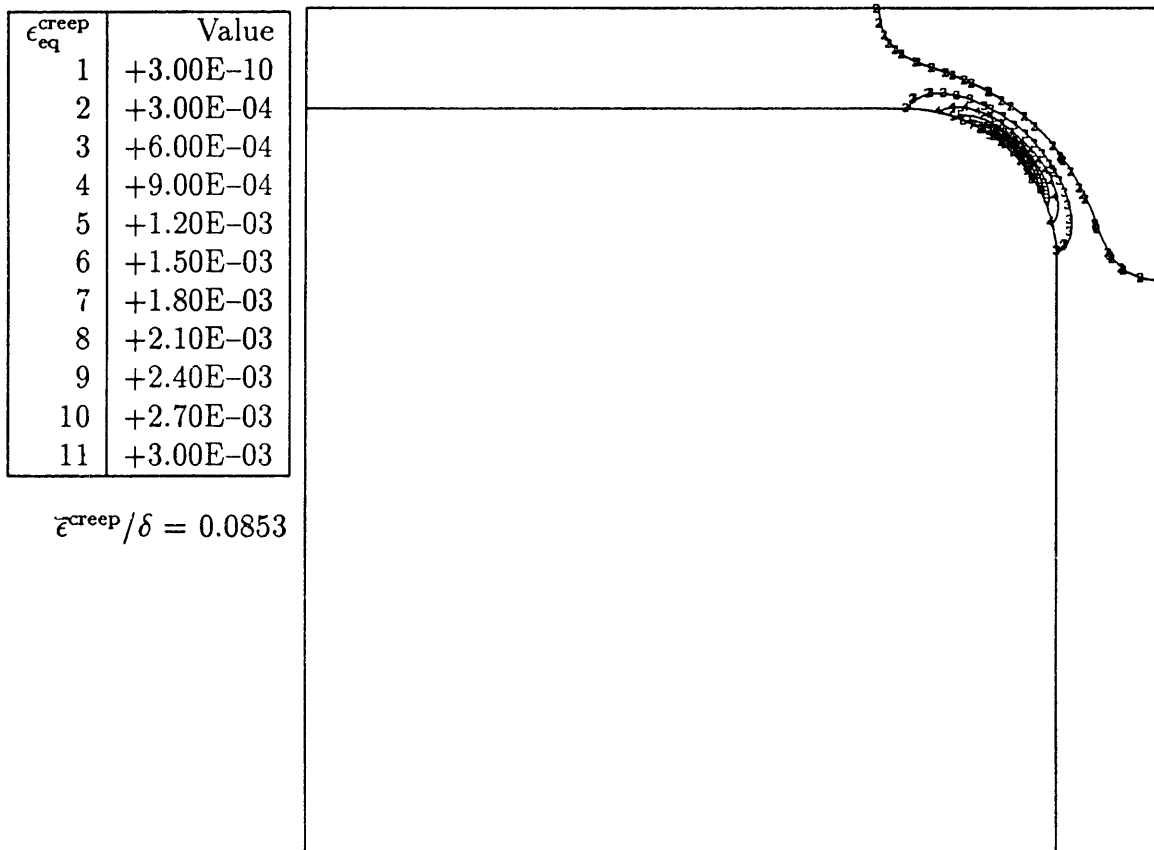


Figure 4.31 Contours of ϵ_{eq}^{creep} for the transient analyzed in case 1 (MNMT) at creep time $t = 0.011$ sec.

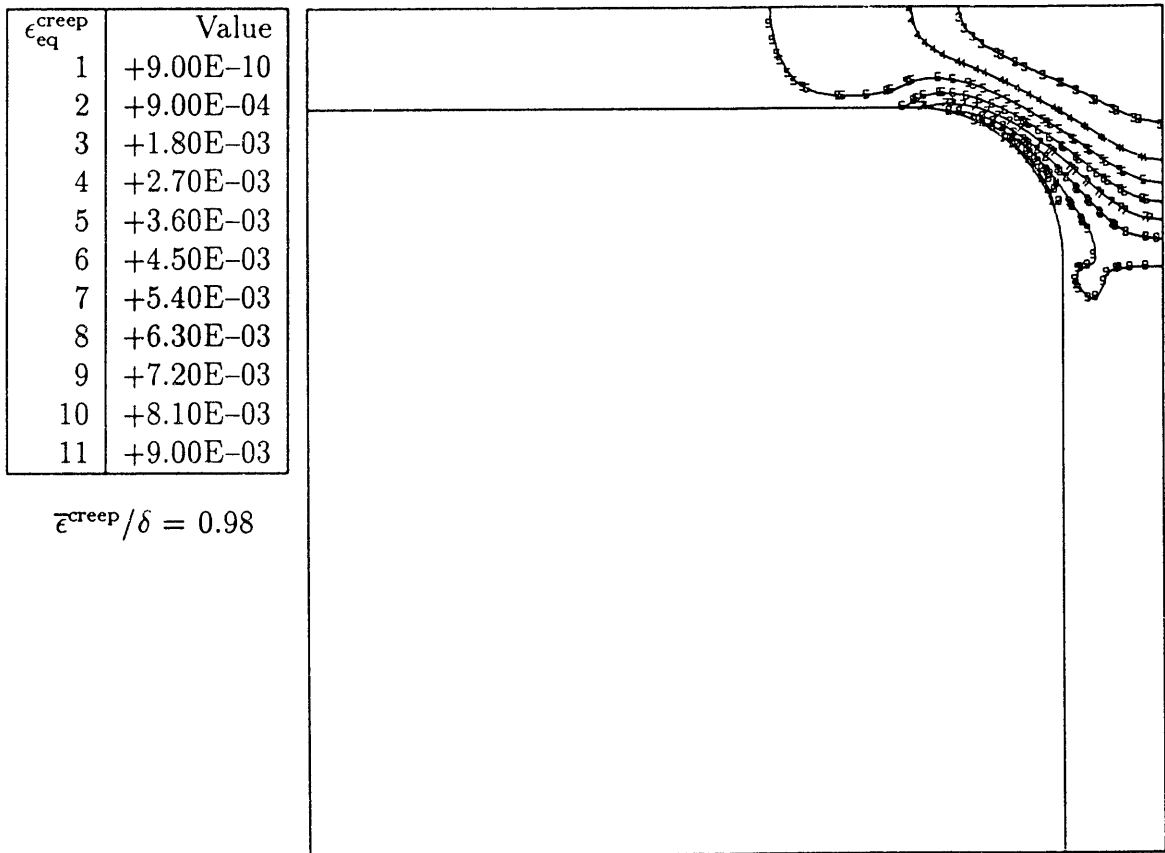


Figure 4.32 Contours of ϵ_{eq}^{creep} for the transient analyzed in case 1 (MNMT) at creep time $t = 4.46$ sec.

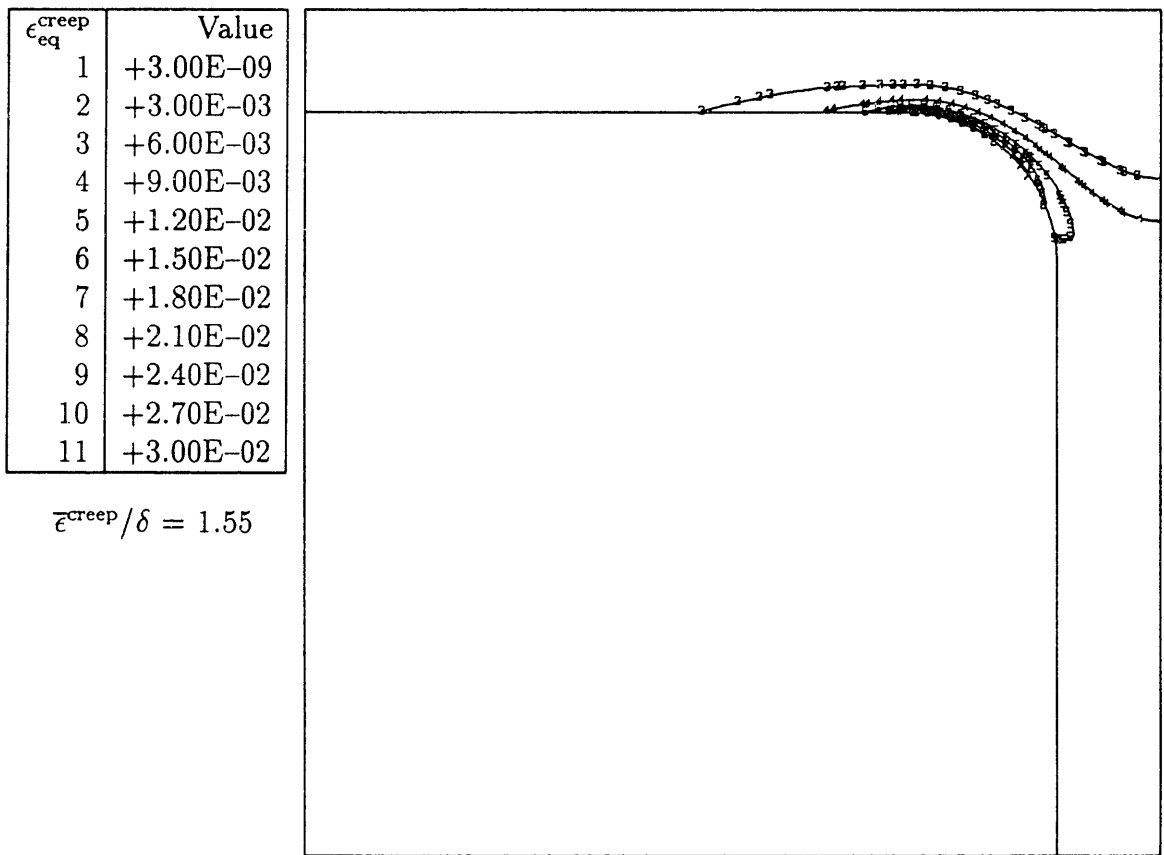


Figure 4.33 Contours of ϵ_{eq}^{creep} for the transient analyzed in case 1 (MNMT) at creep time $t = 63.47$ sec.

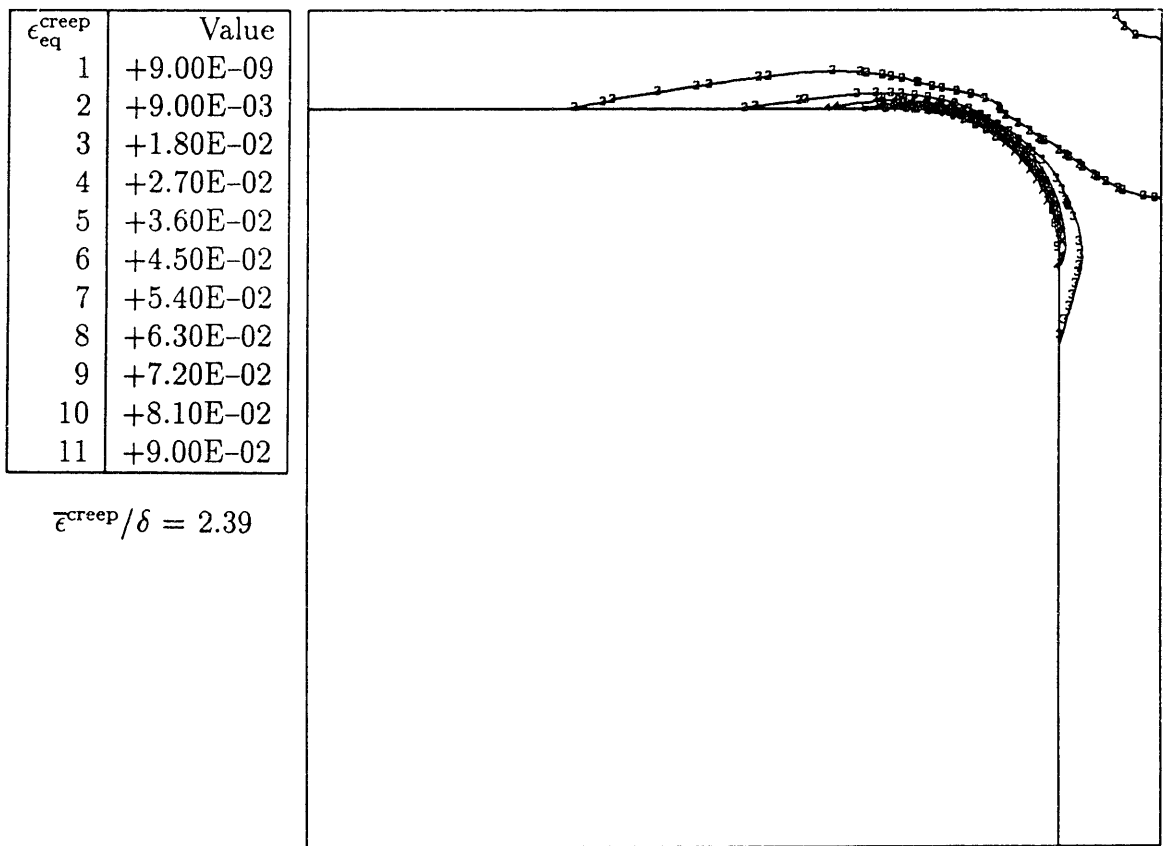


Figure 4.34 Contours of ϵ_{eq}^{creep} for the transient analyzed in case 1 (MNMT) at creep time $t = 50,000$ sec.

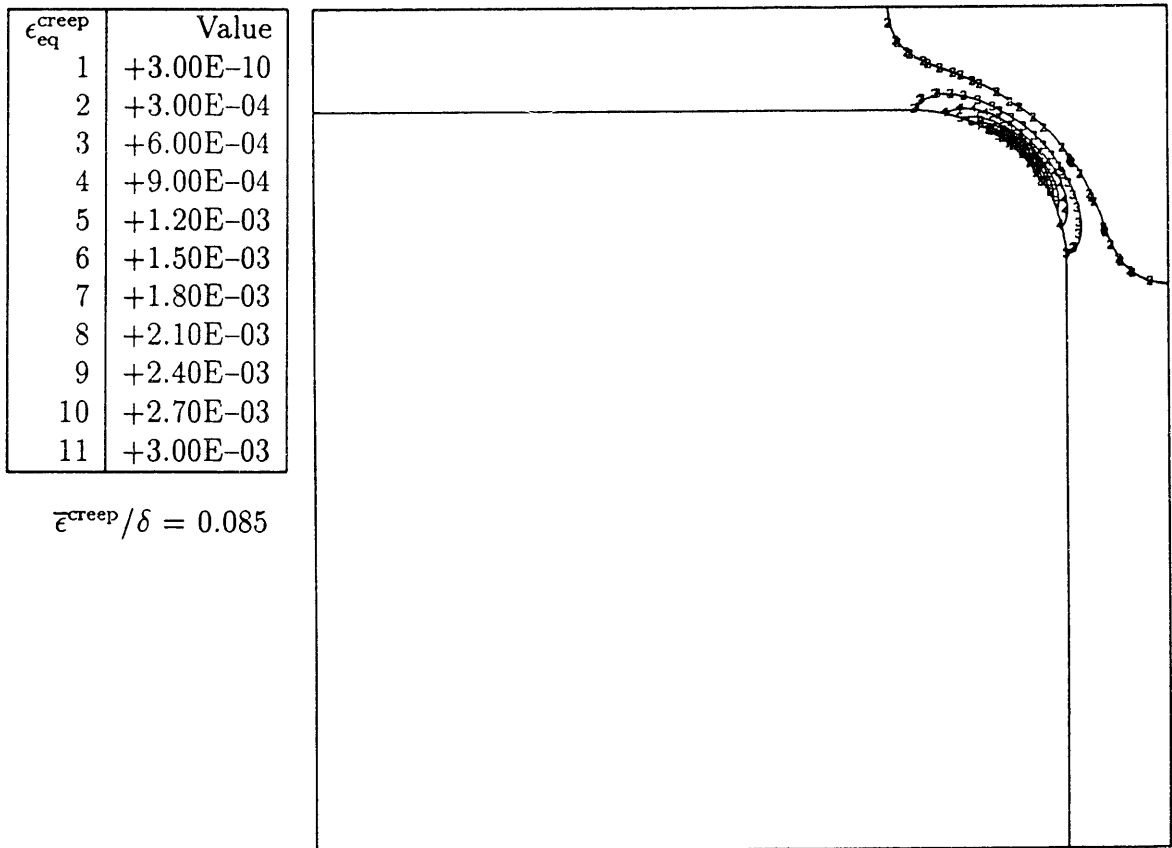


Figure 4.35 Contours of ϵ_{eq}^{creep} for the transient analyzed in case 2 (MNMIC) at creep time $t = 0.011$ sec.

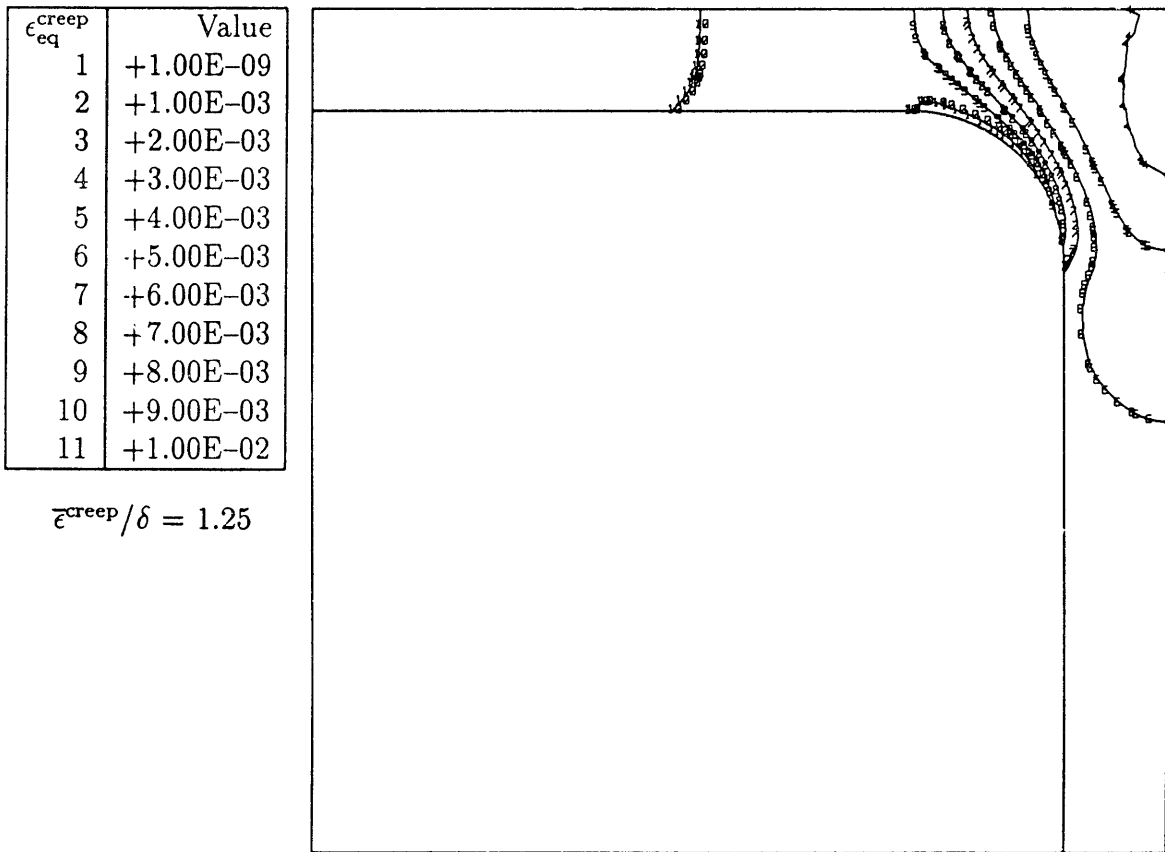


Figure 4.36 Contours of ϵ_{eq}^{creep} for the transient analyzed in case 2 (MNMC) at creep time $t = 3.86$ sec.

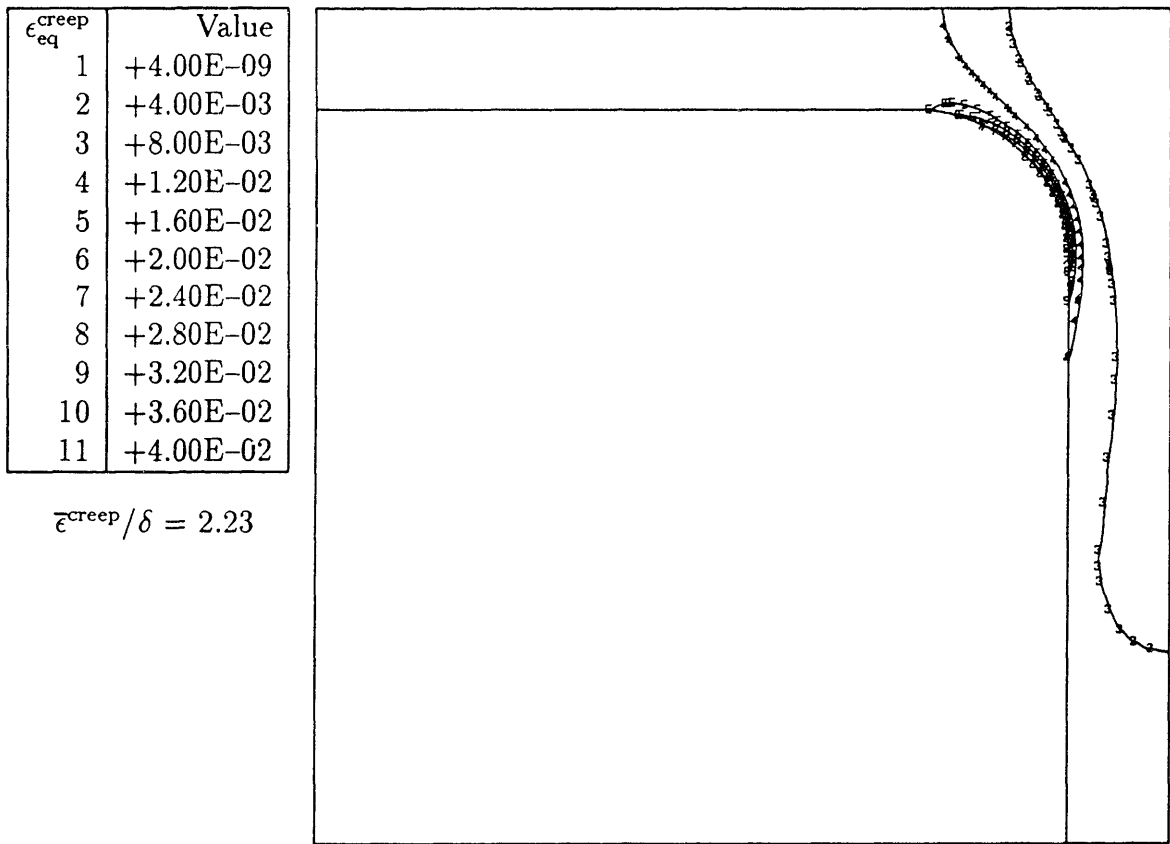


Figure 4.37 Contours of ϵ_{eq}^{creep} for the transient analyzed in case 2 (MNMC) at creep time $t = 252$ sec.

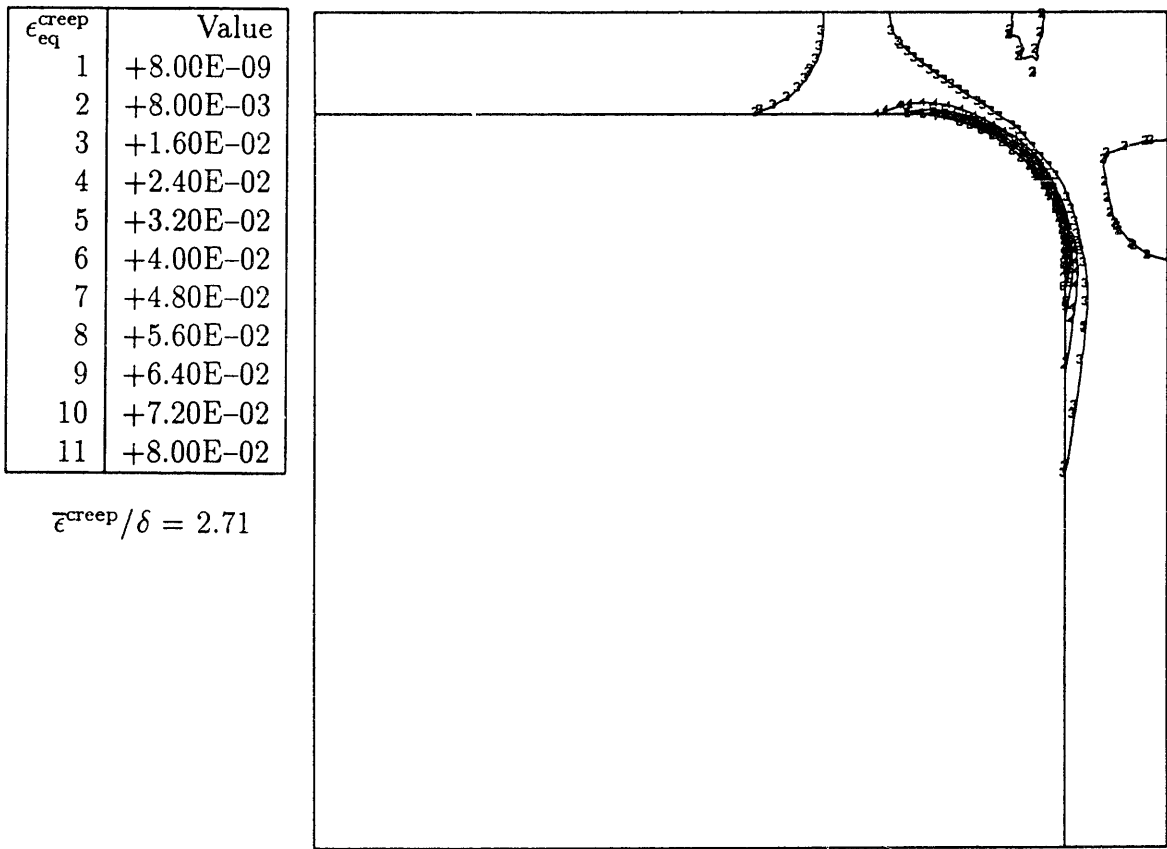


Figure 4.38 Contours of ϵ_{eq}^{creep} for the transient analyzed in case 2 (MNNC) at creep time $t = 50,000$ sec.

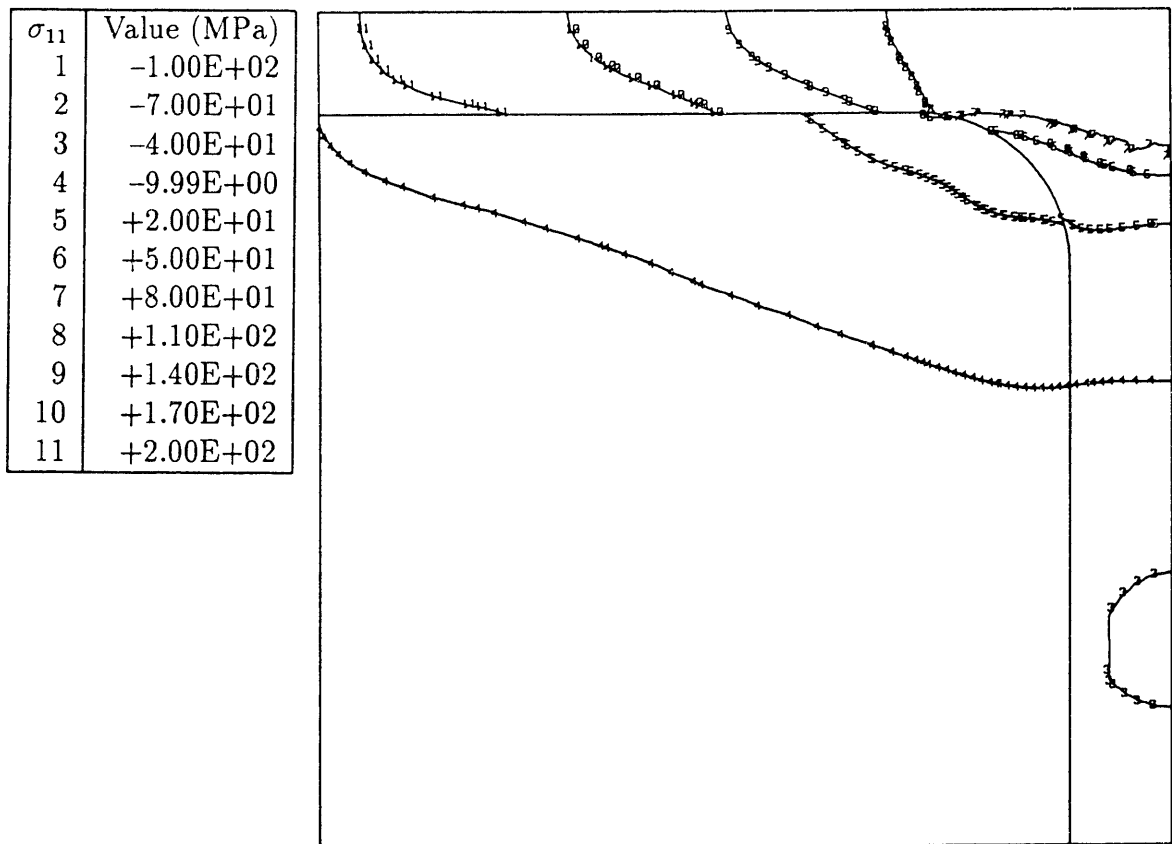


Figure 4.39 Contours of σ_{11} at the end of the analyzed transient for case 1 (MNMT).

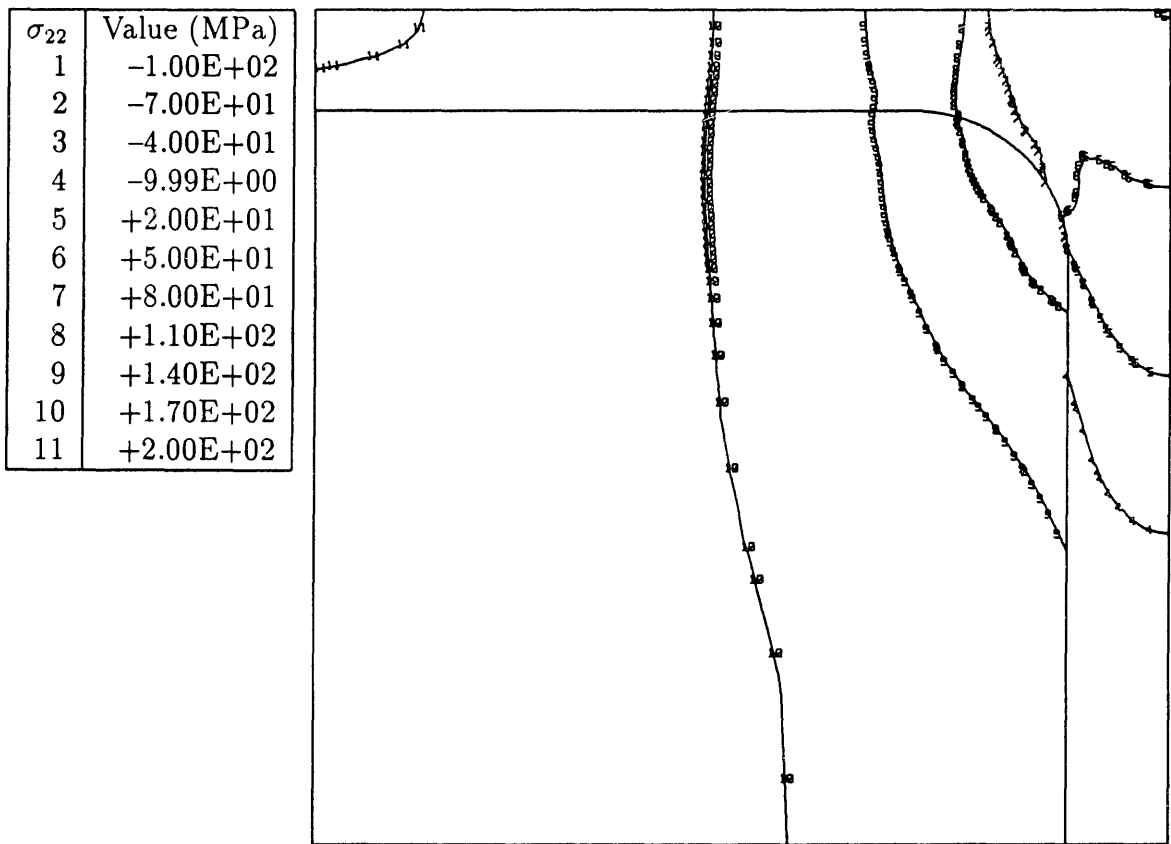


Figure 4.40 Contours of σ_{22} at the end of the analyzed transient for case 1 (MNMT).

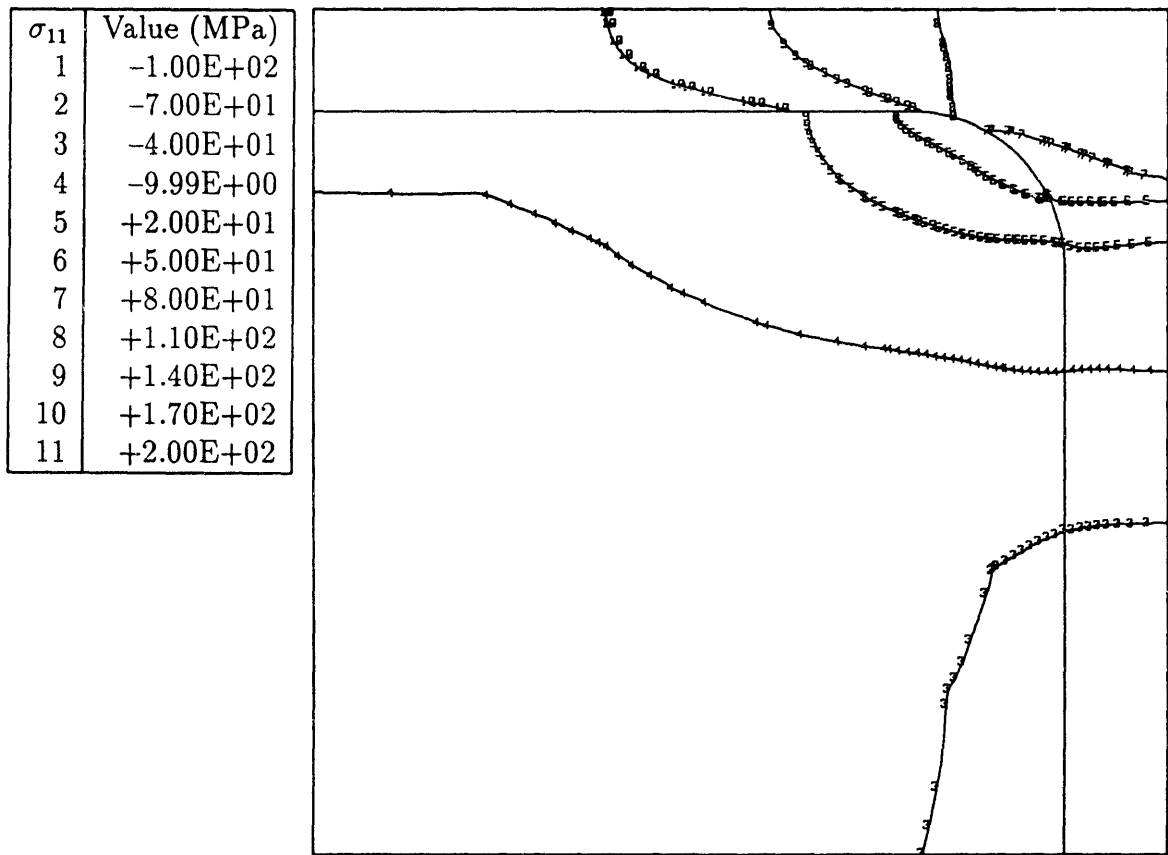


Figure 4.41 Contours of σ_{11} at the end of the analyzed transient for case 3 (TCT).

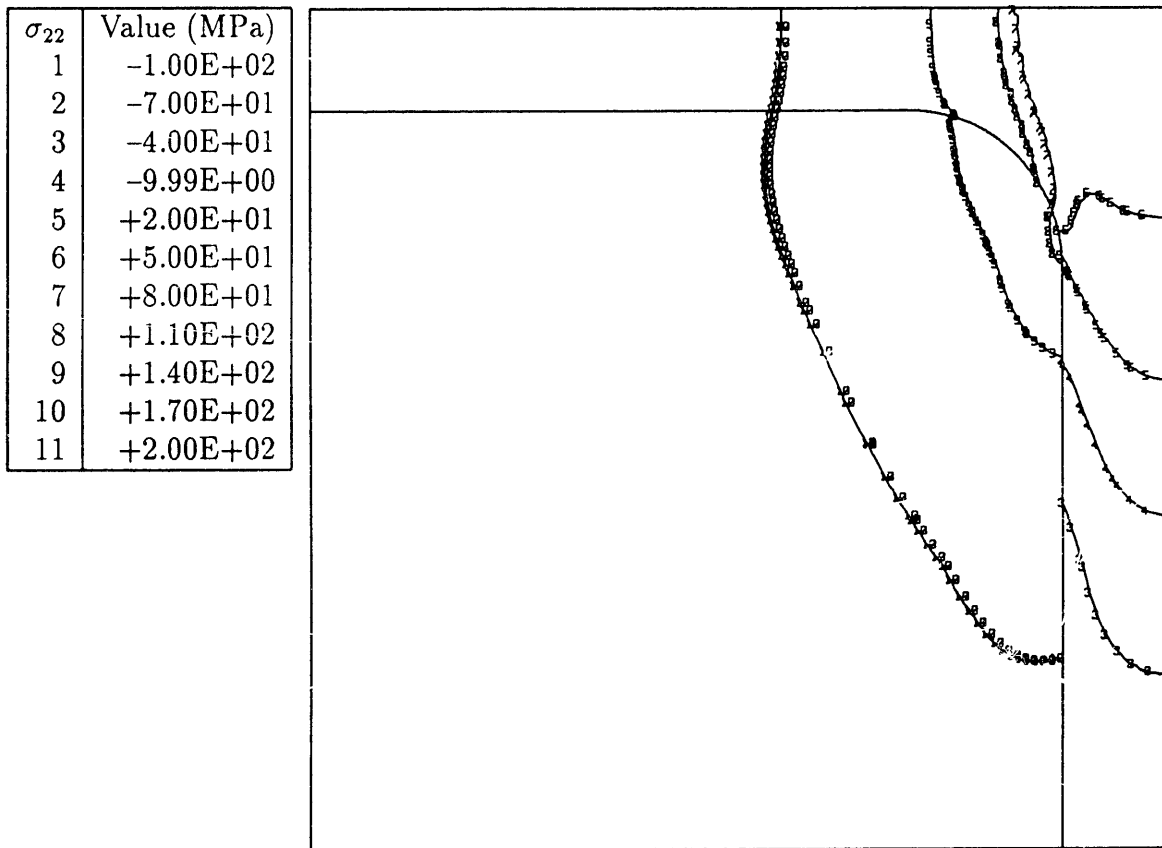


Figure 4.42 Contours of σ_{22} at the end of the analyzed transient for case 3 (TCT).

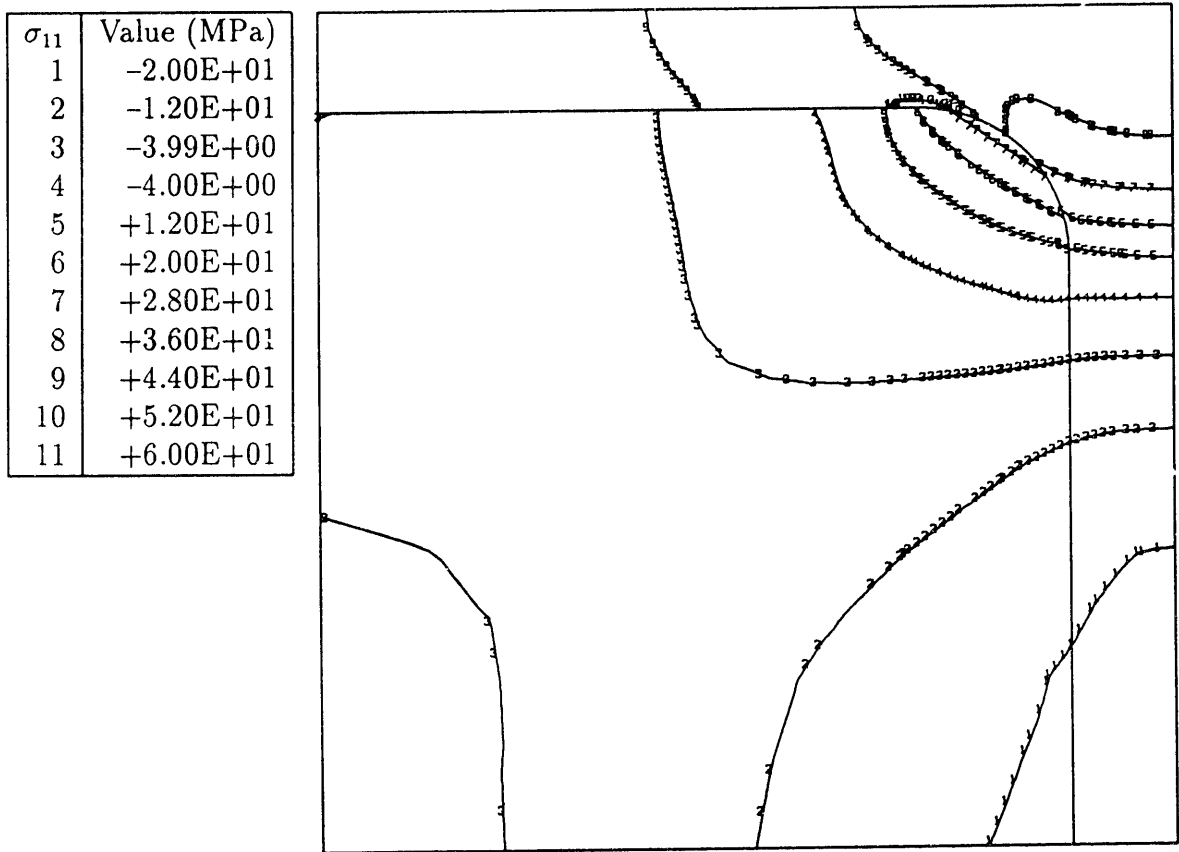


Figure 4.43 Contours of σ_{11} at the end of the analyzed transient for case 5 (PLT).

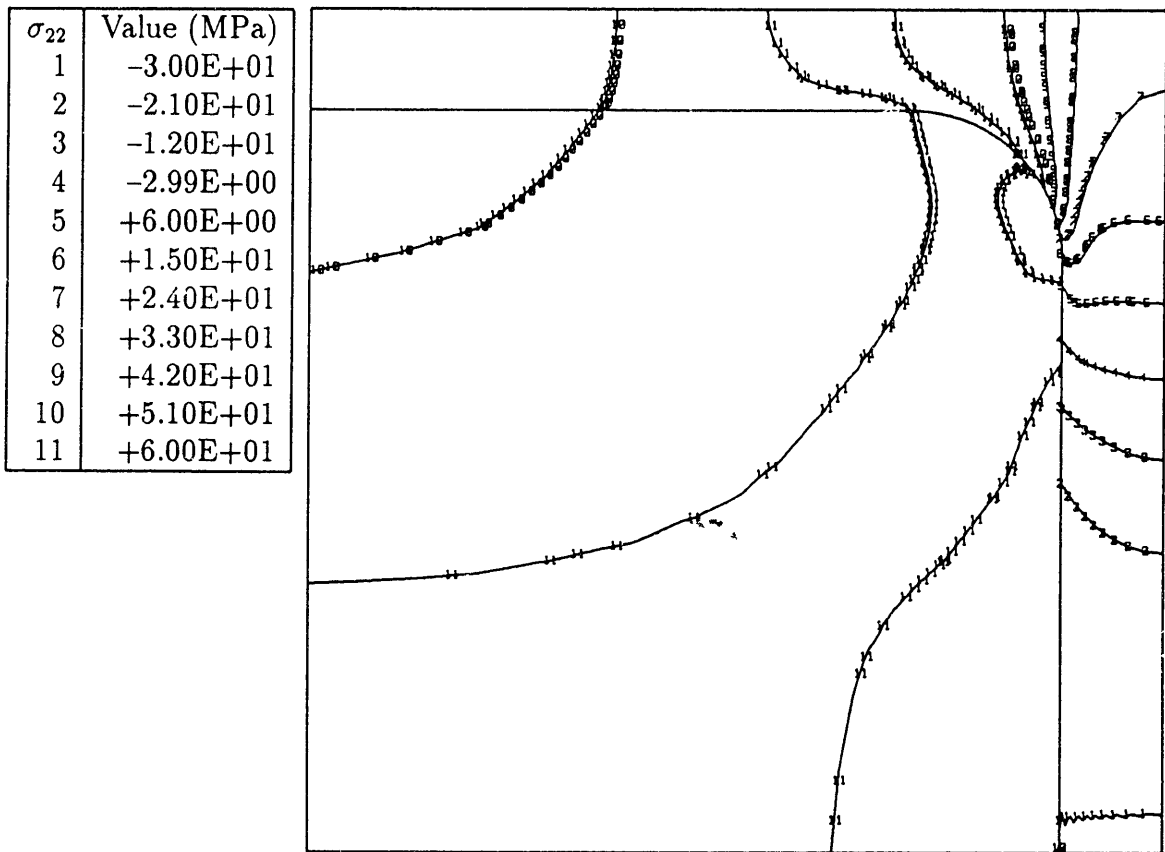


Figure 4.44 Contours of σ_{22} at the end of the analyzed transient for case 5 (PLT).

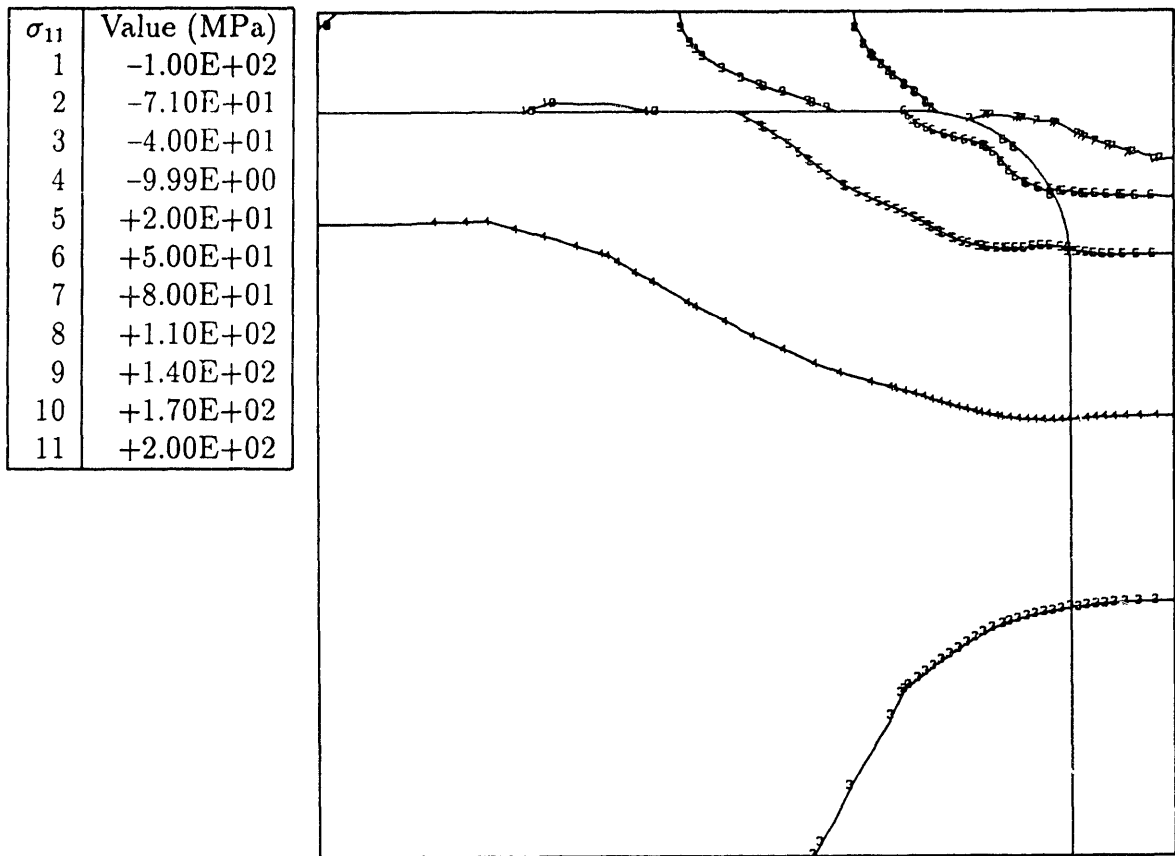


Figure 4.45 Contours of σ_{11} at the end of the analyzed transient for case 6 (PHT).

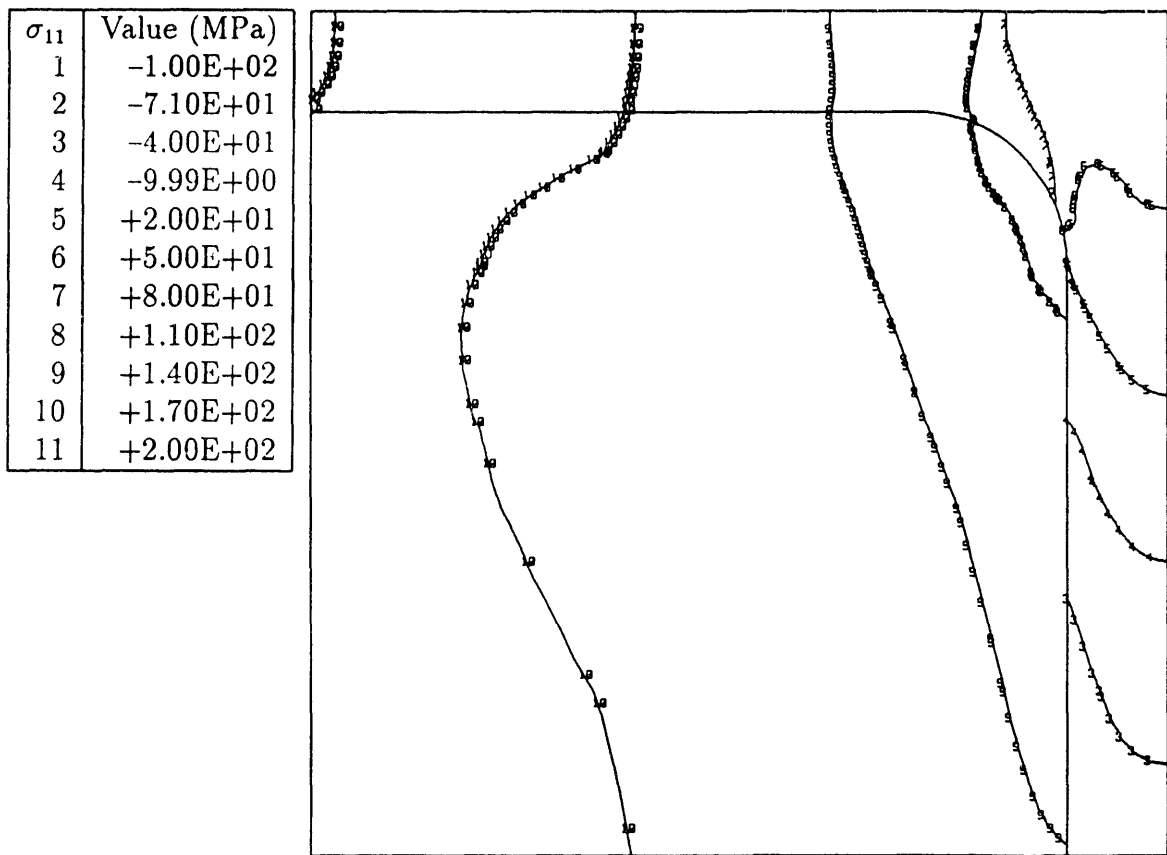


Figure 4.46 Contours of σ_{22} at the end of the analyzed transient for case 6 (PHT).

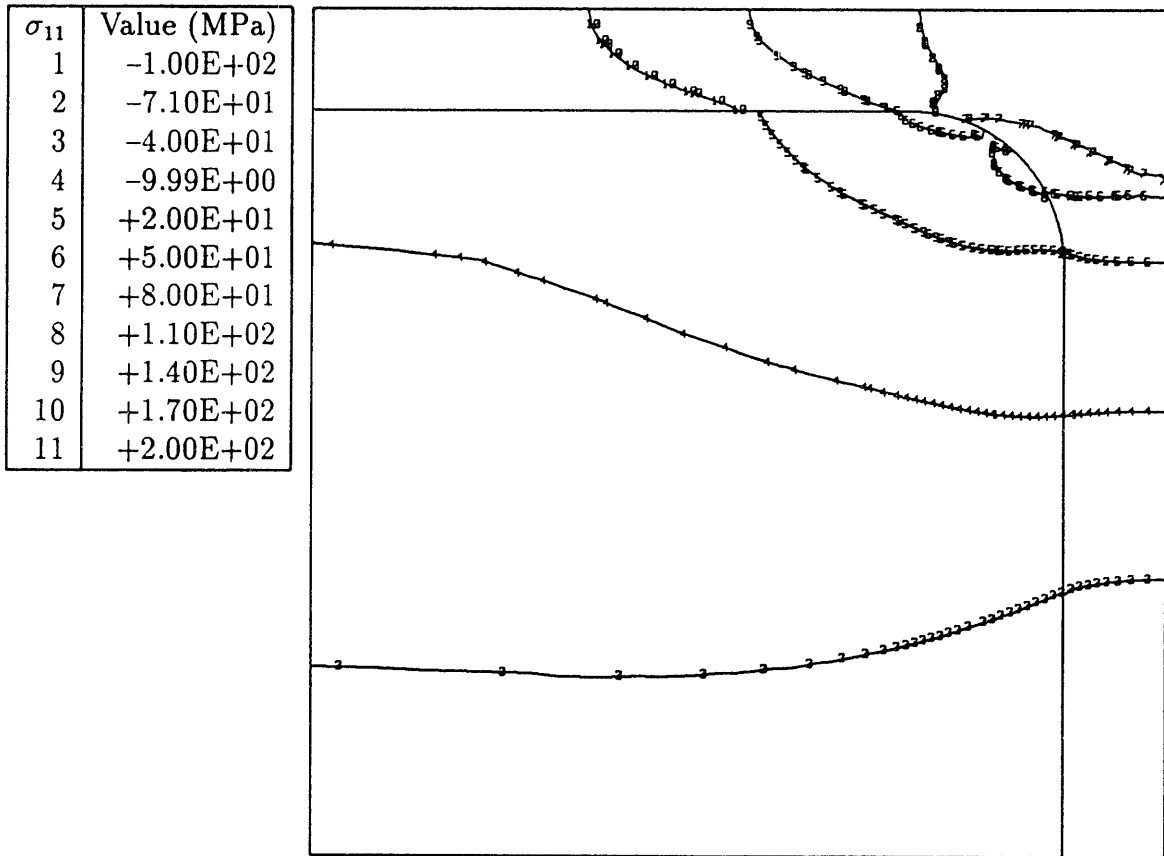


Figure 4.47 Contours of σ_{11} at the end of the analyzed transient for case 9 (TCT_{PMS}).

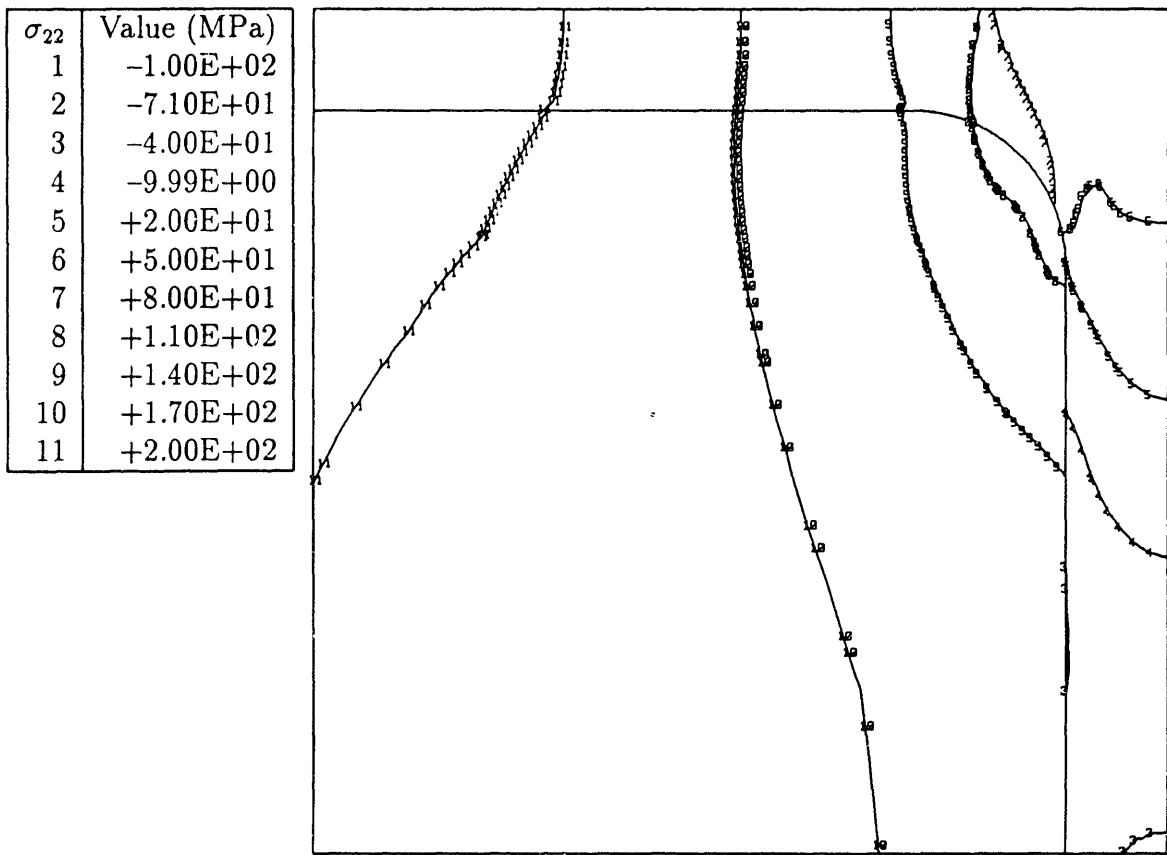


Figure 4.48 Contours of σ_{22} at the end of the analyzed transient for case 9 (TCT_{PMS}).

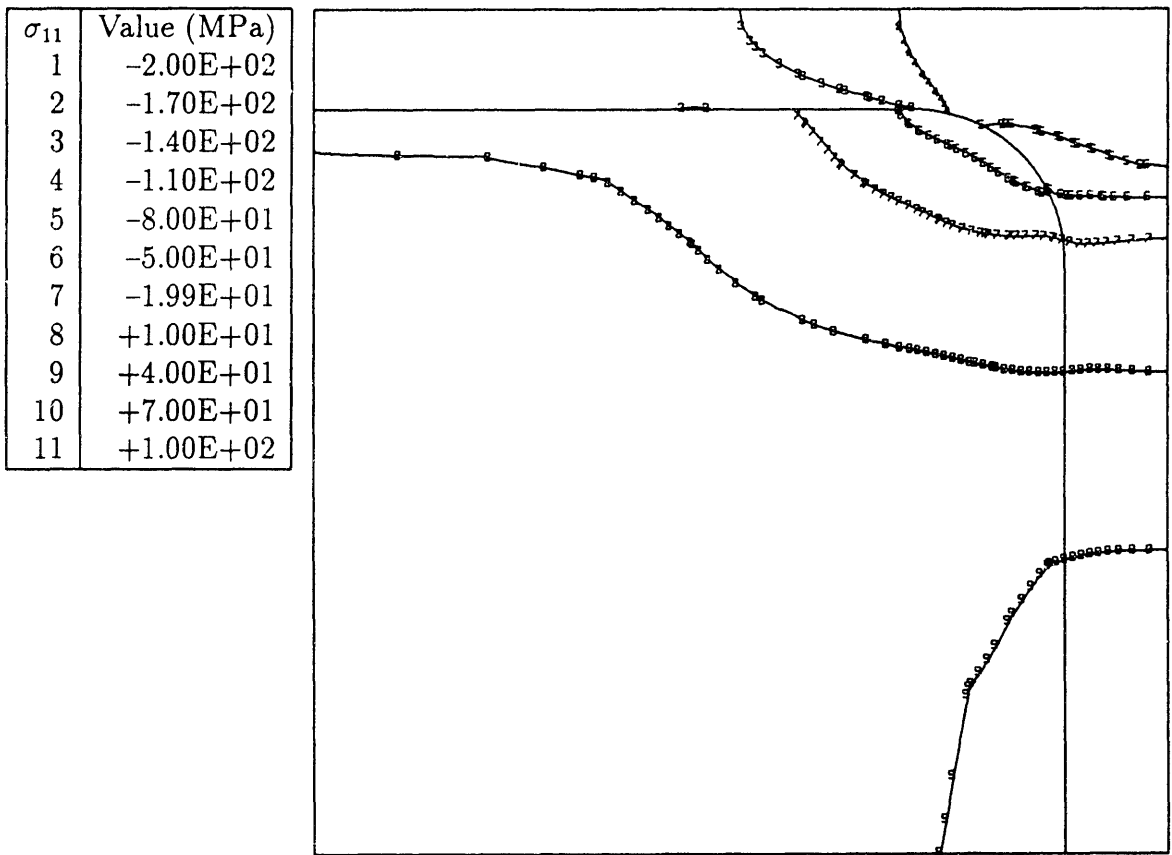


Figure 4.49 Contours of σ_{11} at the end of the analyzed transient for case 2 (MNMC).

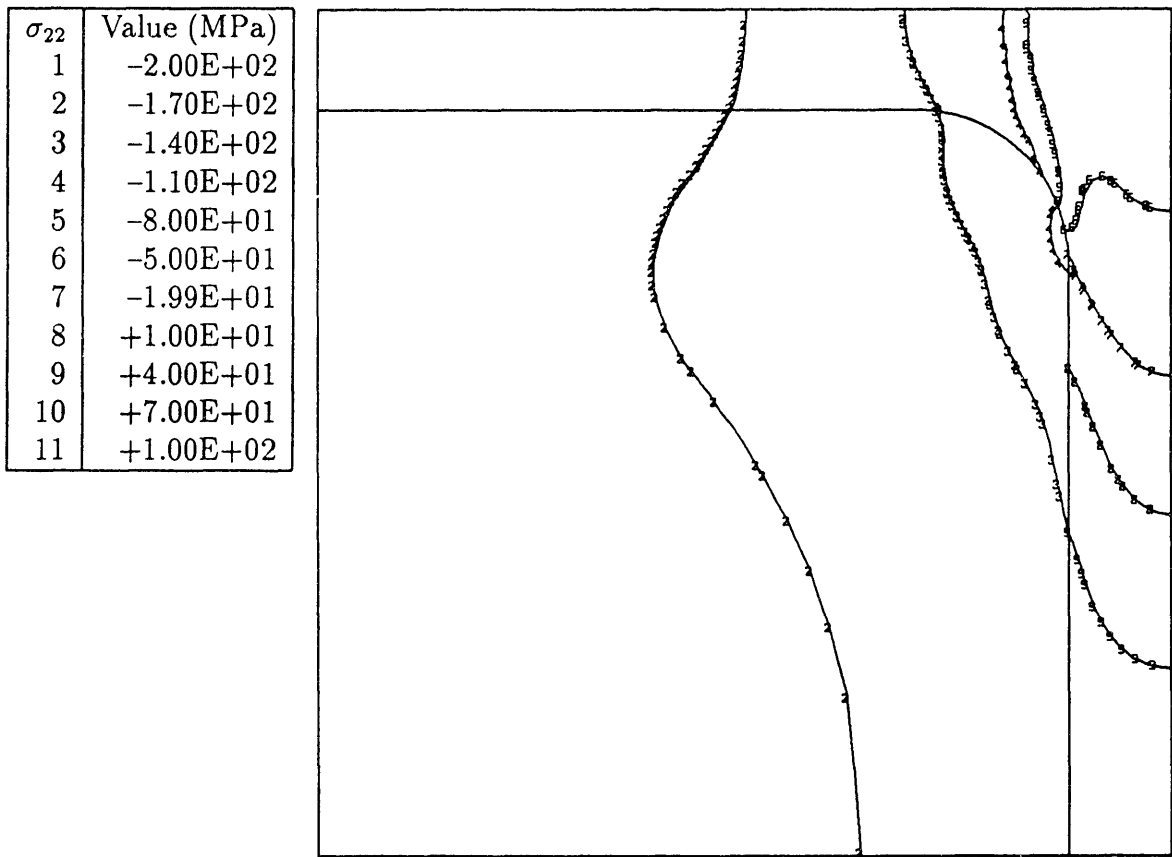


Figure 4.50 Contours of σ_{22} at the end of the analyzed transient for case 2 (MNMC).

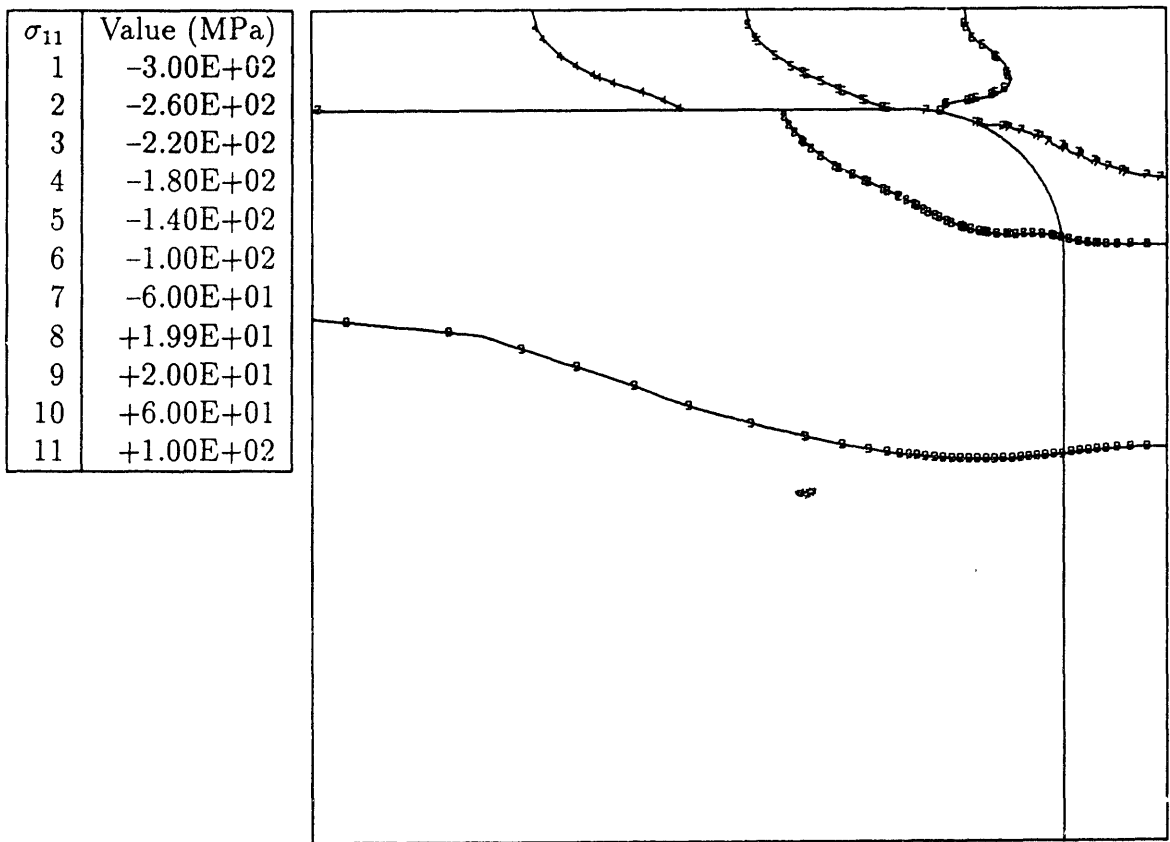


Figure 4.51 Contours of σ_{11} at the end of the analyzed transient for case 4 (TCC).

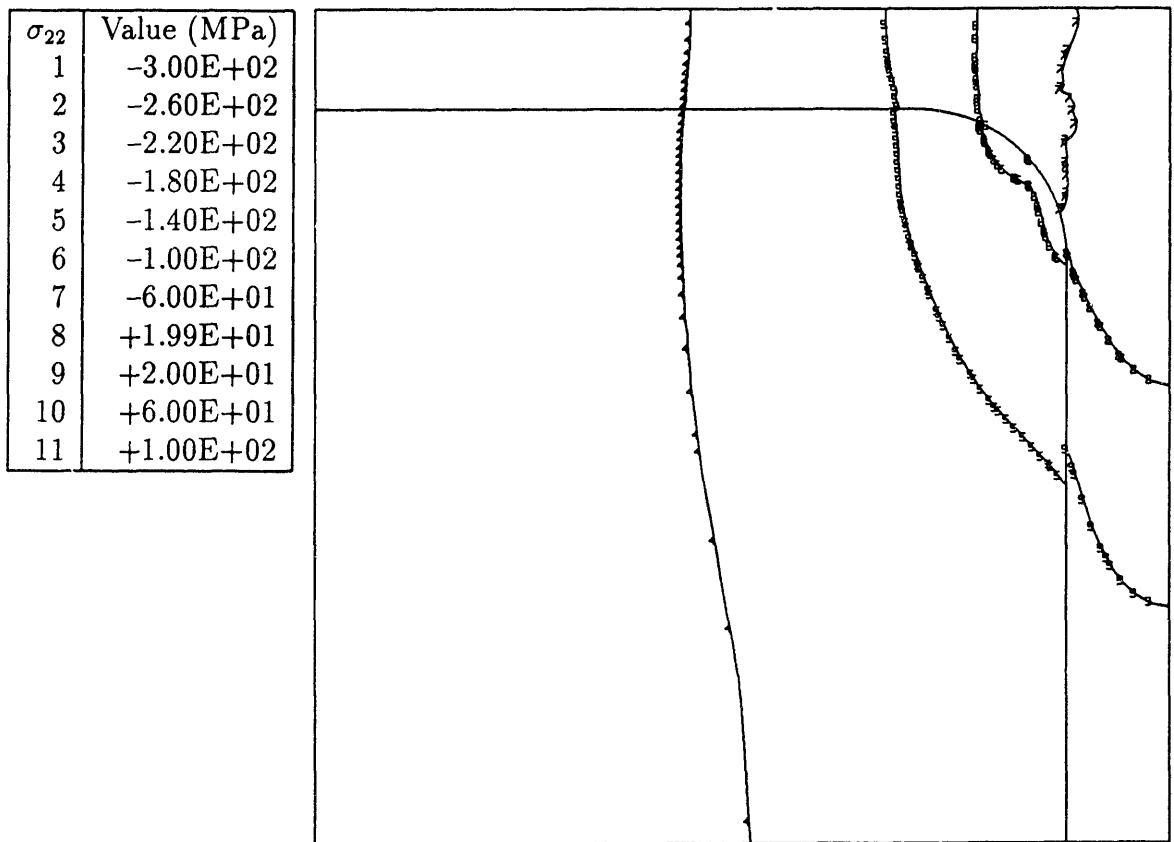


Figure 4.52 Contours of σ_{22} at the end of the analyzed transient for case 4 (TCC).

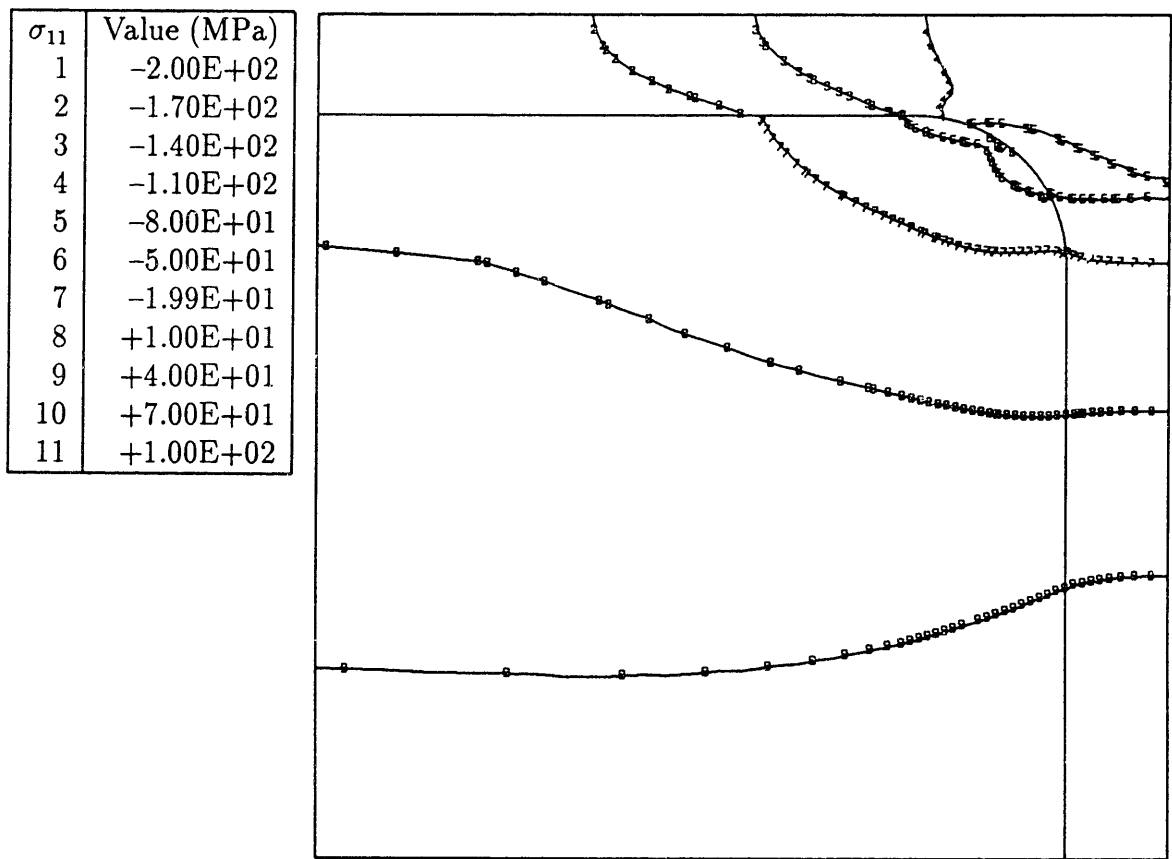


Figure 4.53 Contours of σ_{11} at the end of the analyzed transient for case 10 (TCC_{PMS}).

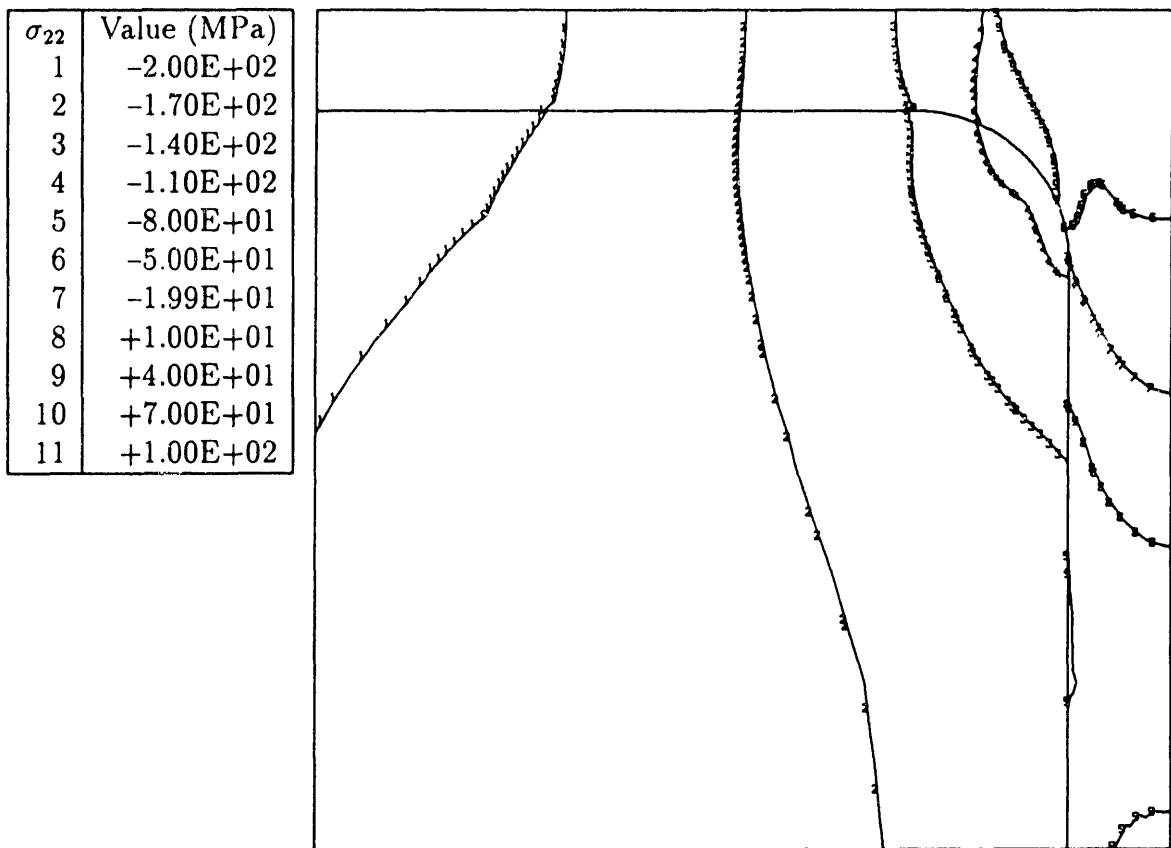


Figure 4.54 Contours of σ_{22} at the end of the analyzed transient for case 10 (TCC_{PMS}).

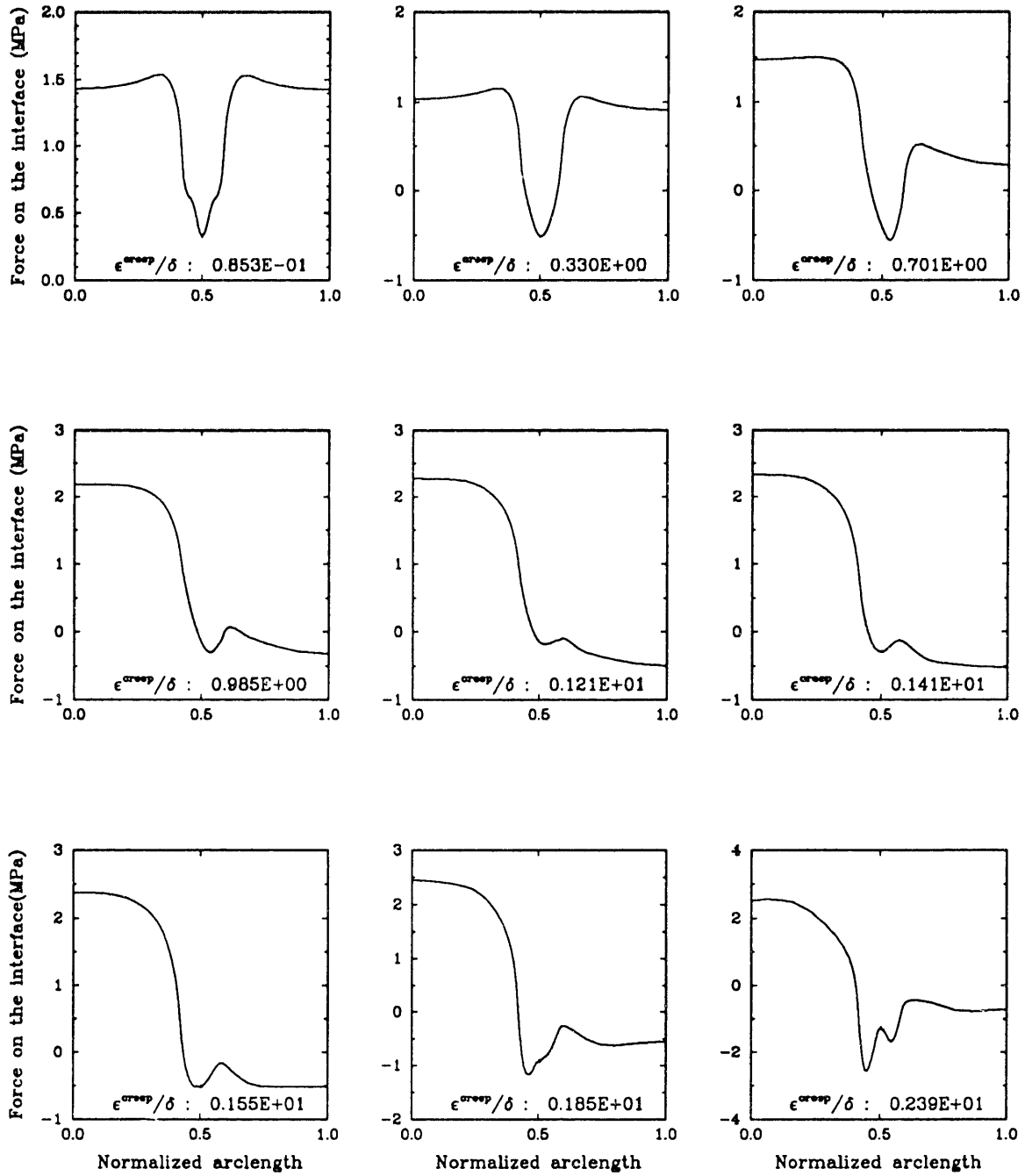


Figure 4.55 Evolution of the τ_n profile during the stress-annealing transient for case 1 (MNMT).

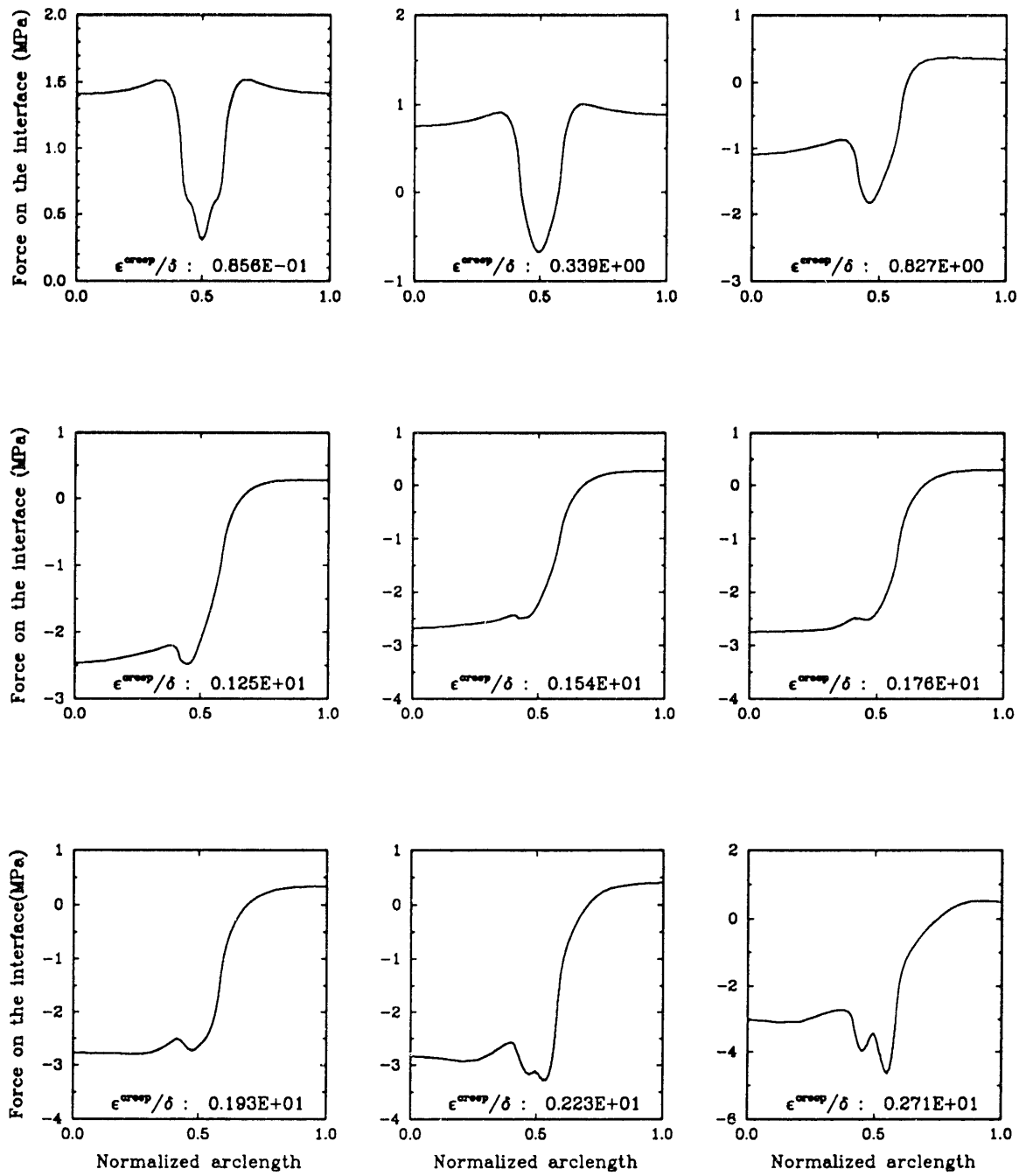


Figure 4.56 Evolution of the τ_n profile during the stress-annealing transient for case 2 (MNMN).

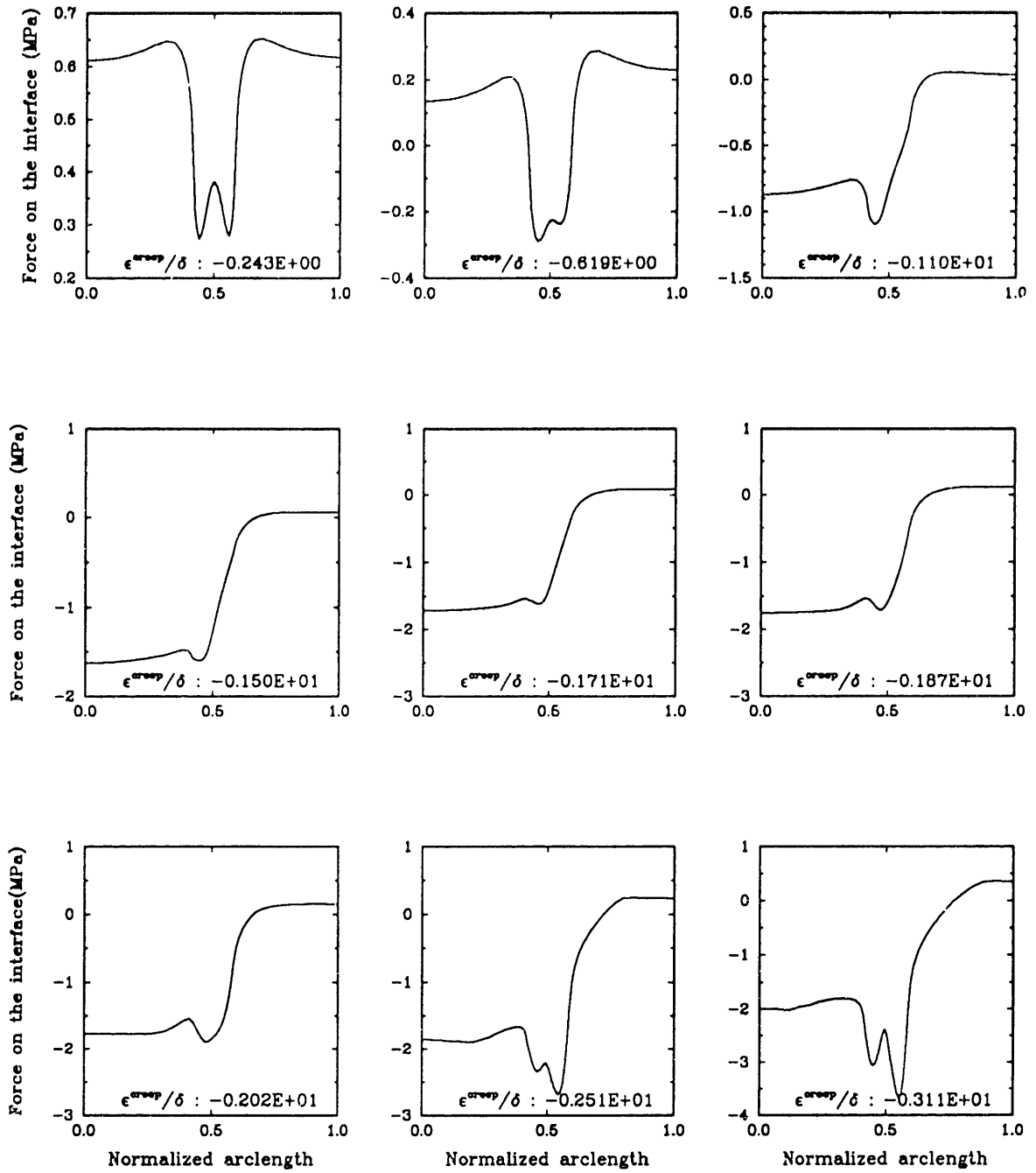


Figure 4.57 Evolution of the τ_n profile during the stress-annealing transient for case 3 (TCT).

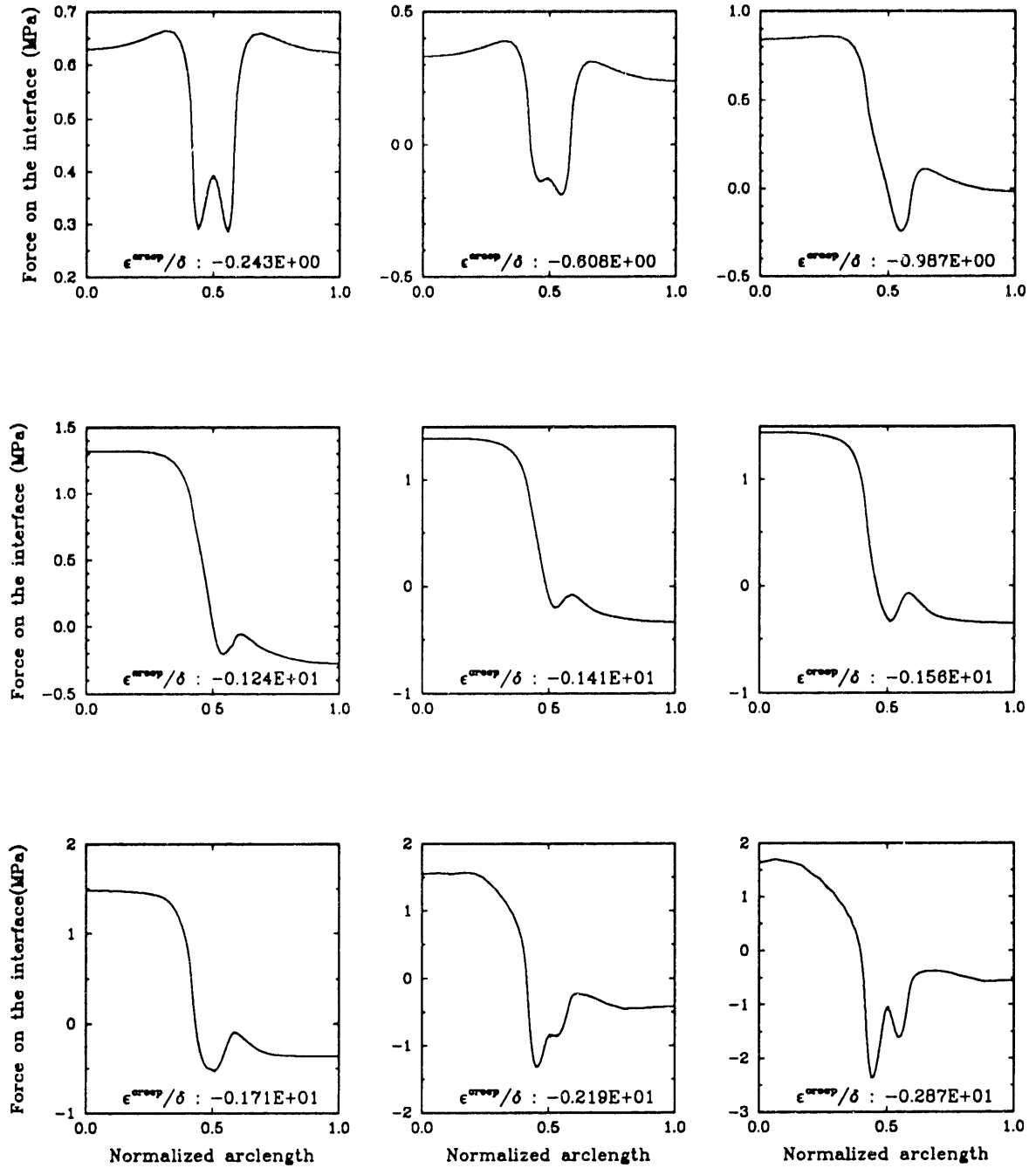


Figure 4.58 Evolution of the τ_n profile during the stress-annealing transient for case 4 (TCC).

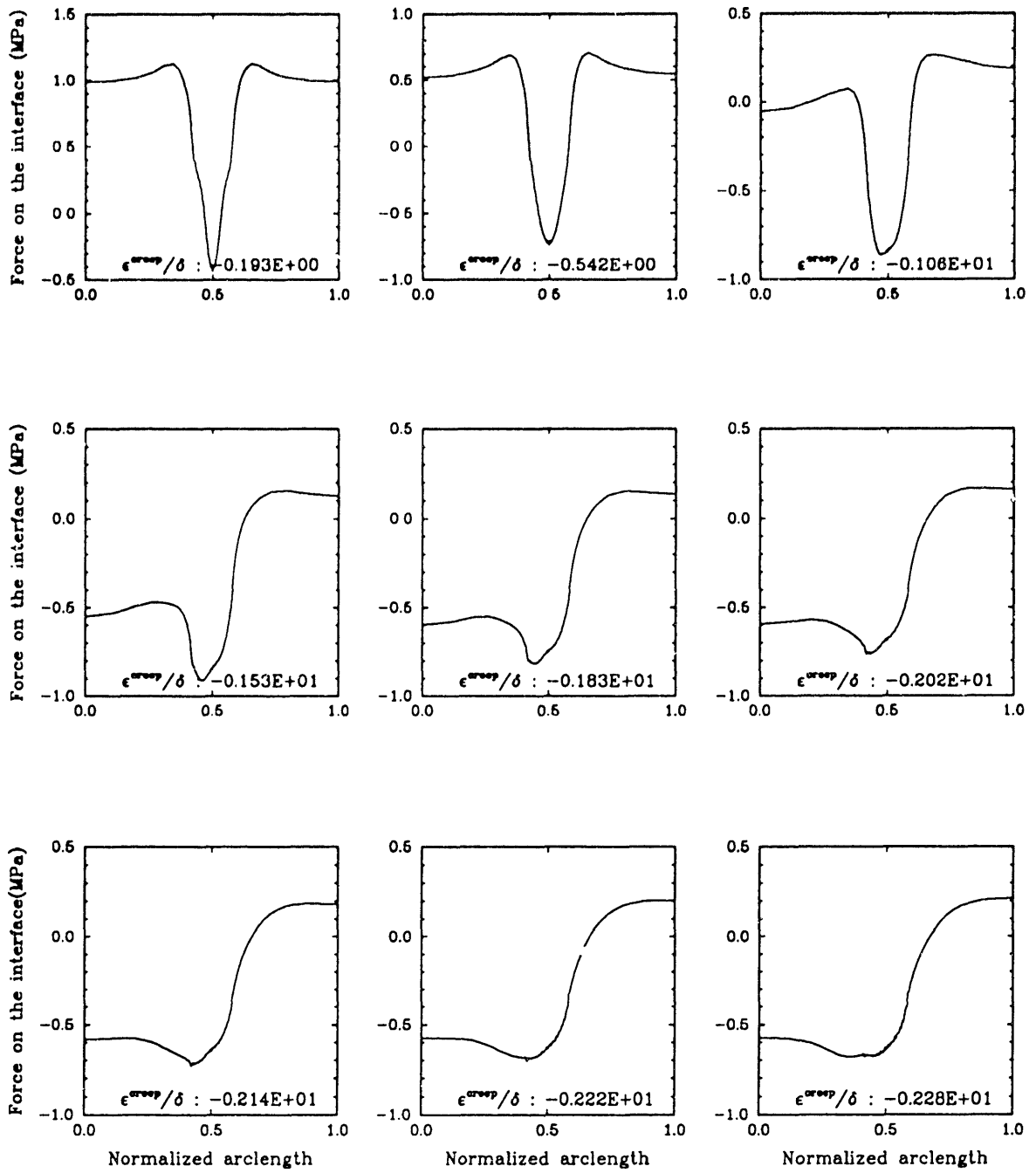


Figure 4.59 Evolution of the τ_n profile during the stress-annealing transient for case 5 (PLT).

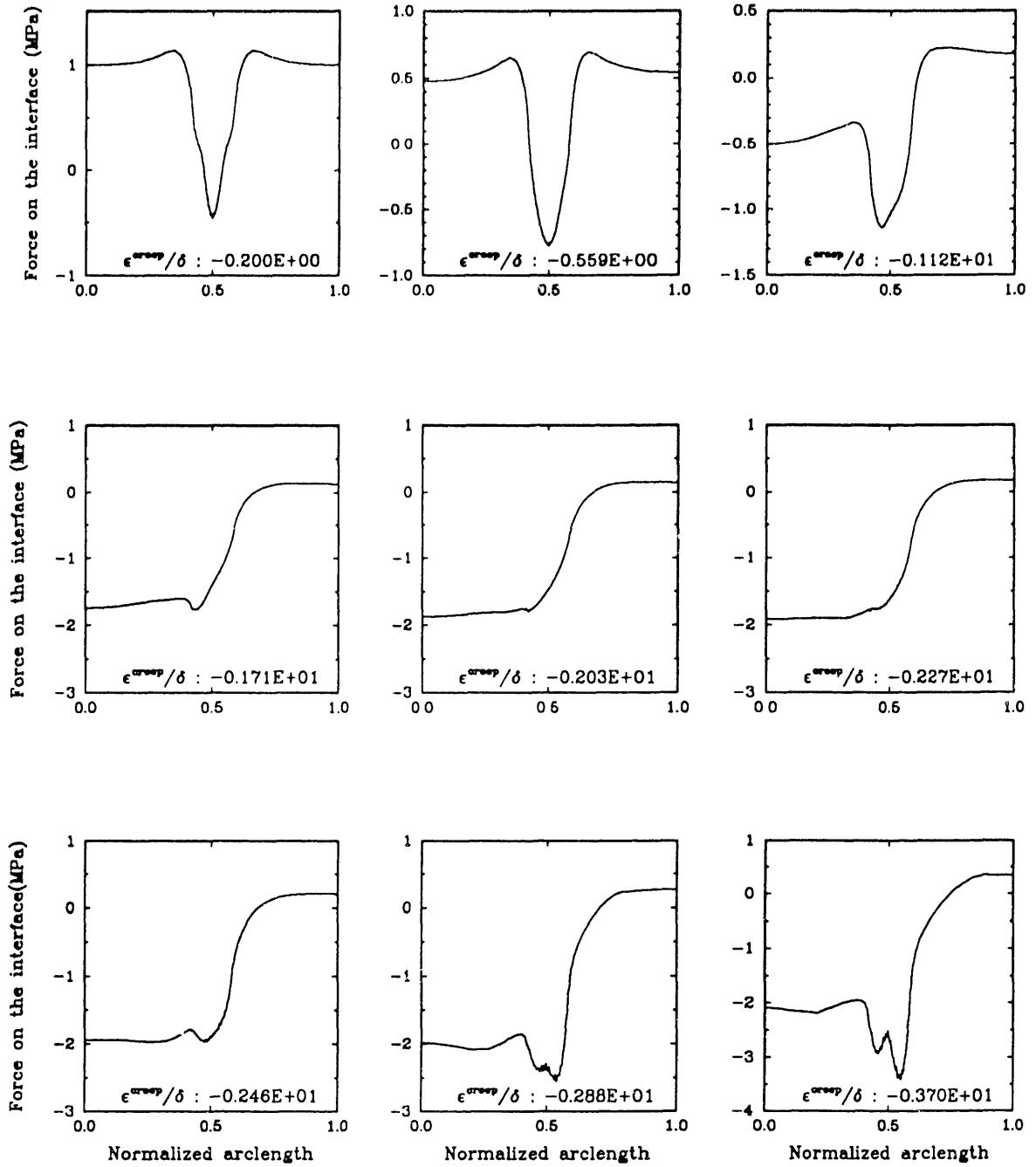


Figure 4.60 Evolution of the τ_n profile during the stress-annealing transient for case 6 (PHT).

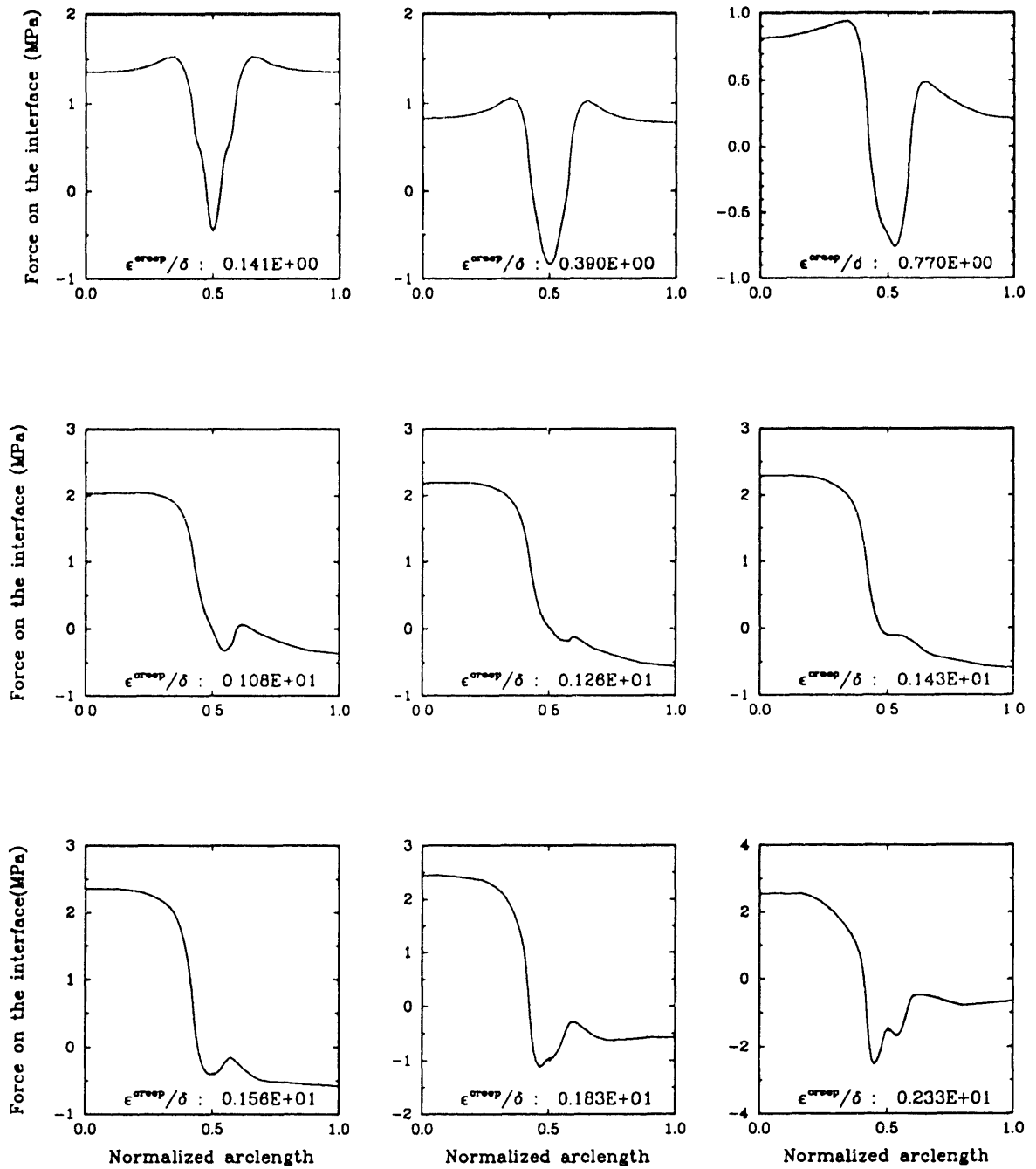


Figure 4.61 Evolution of the τ_n profile during the stress-annealing transient for case 7 ($MNMT_{INV}$).

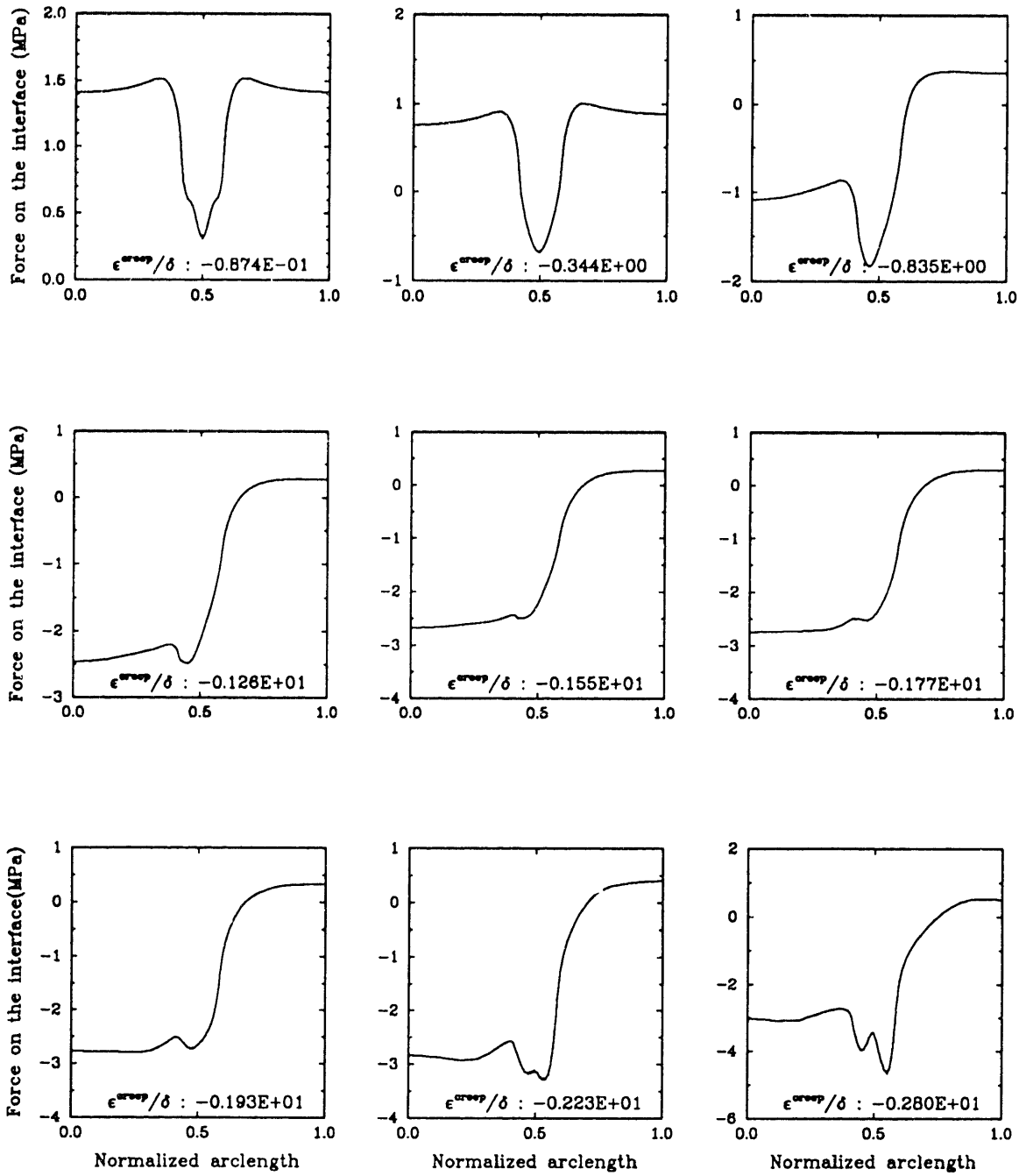


Figure 4.62 Evolution of the τ_n profile during the stress-annealing transient for case 8 (MNMT_{NMS}).

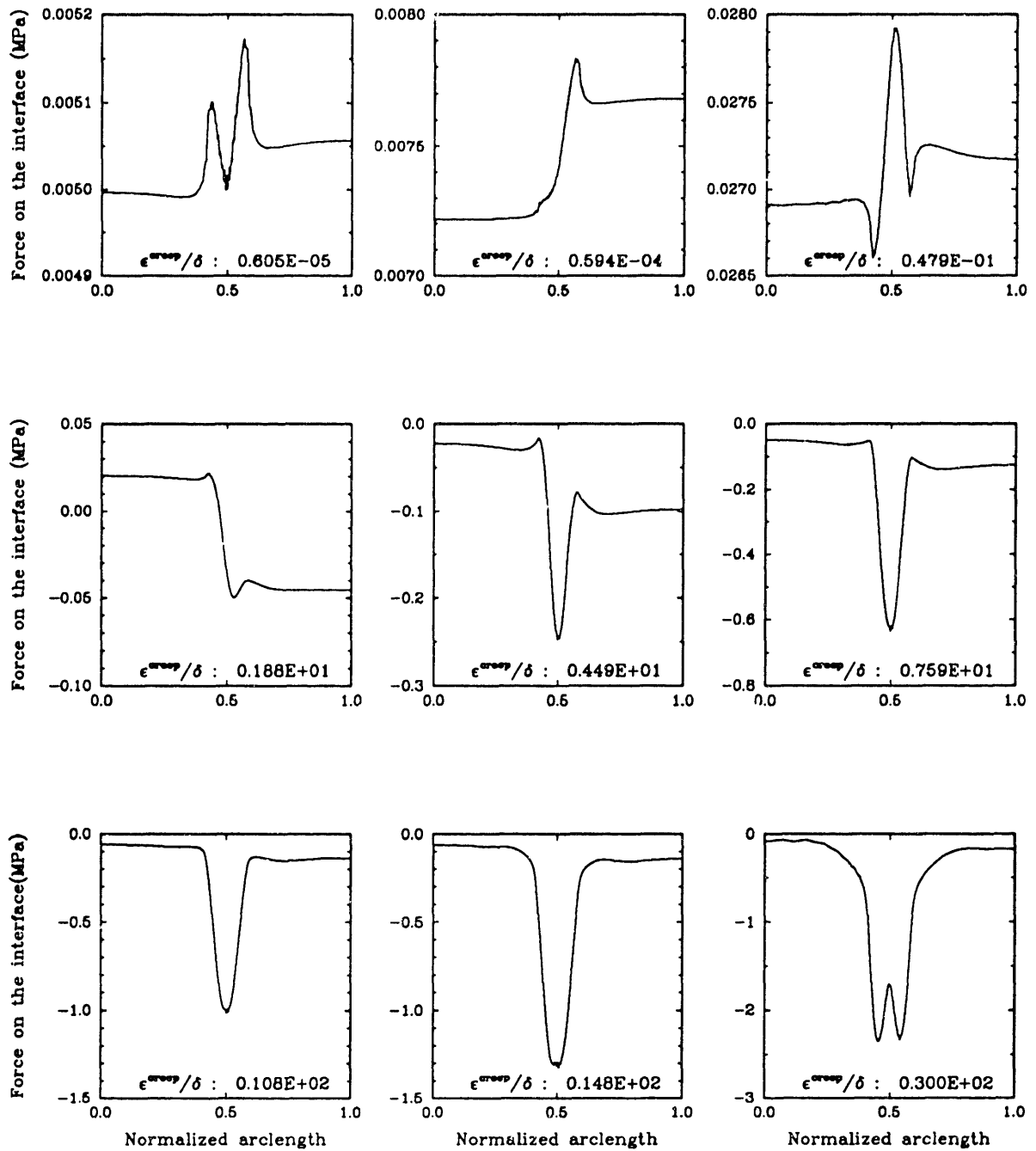


Figure 4.63 Evolution of the τ_n profile during the stress-annealing transient for case 9 (TCT_{PMS}).

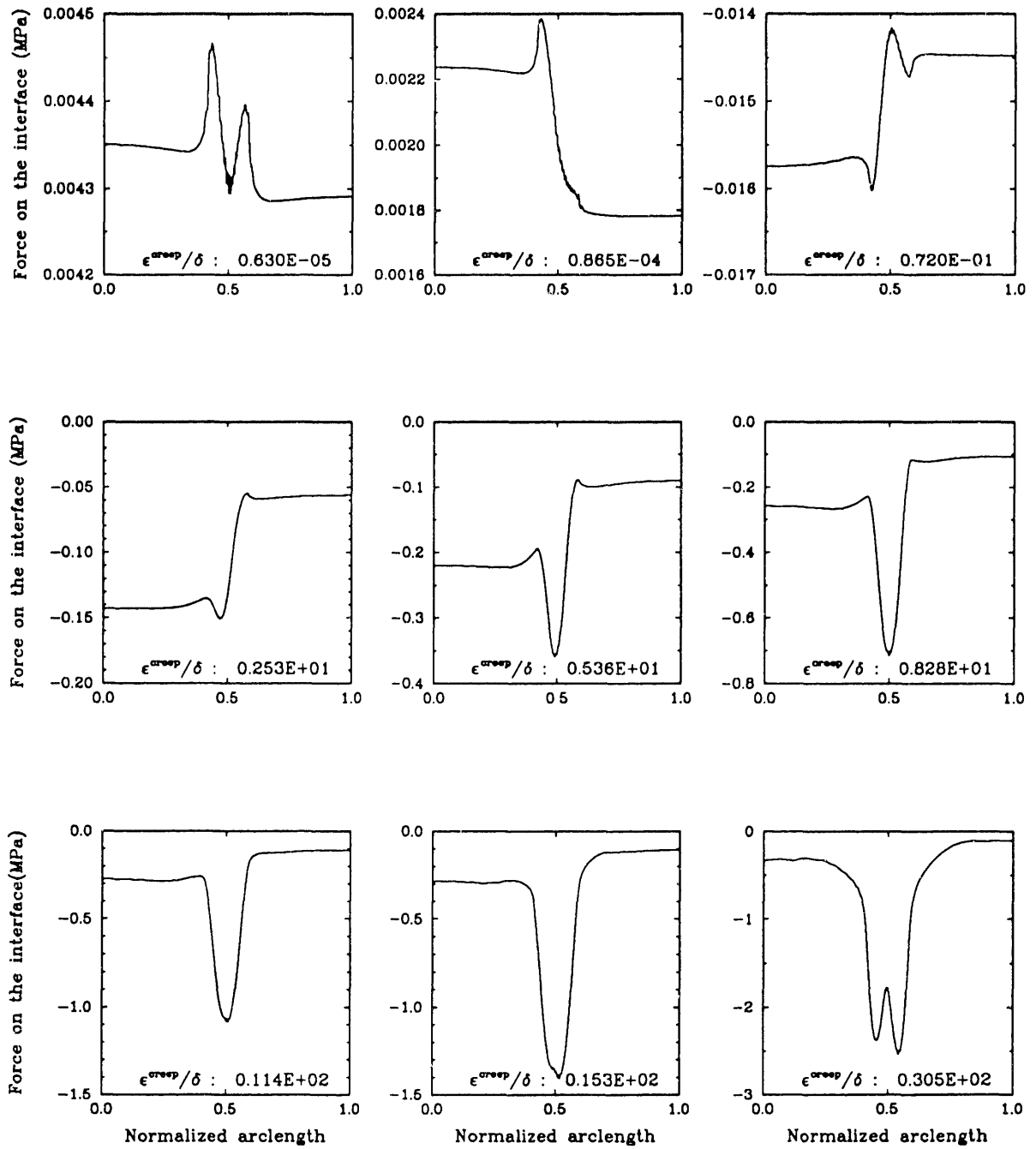


Figure 4.64 Evolution of the τ_n profile during the stress-annealing transient for case 10 (TCC_{PMS}).

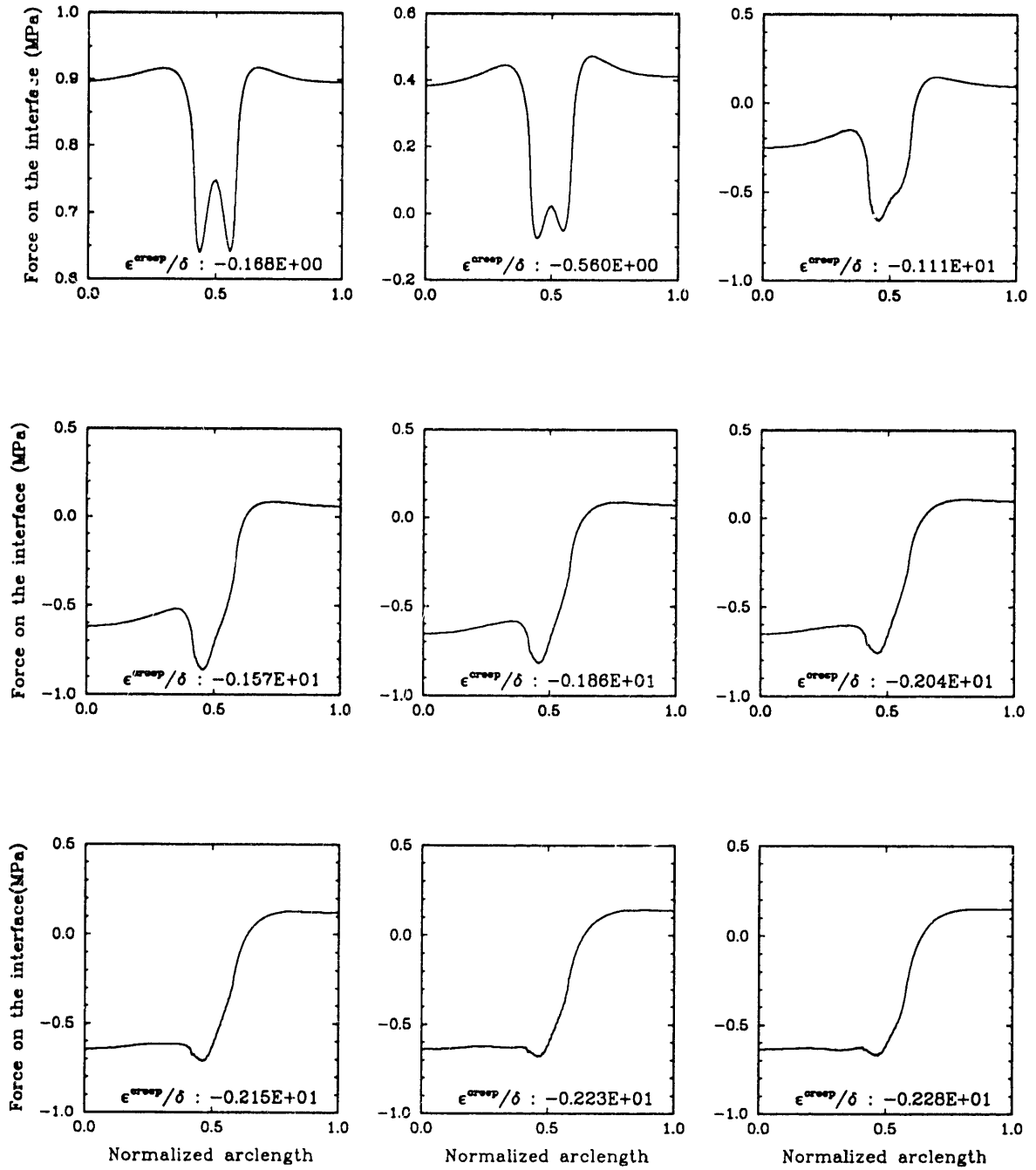


Figure 4.65 Evolution of the τ_n profile during the stress-annealing transient for case 11 (PLT_{iso}).

4.6 Discussion

As we have repeatedly mentioned, experimental observations show that the rafting process initiates in the primary stage of the creep transient.

Figure 4.66 shows a typical creep curve with corresponding micrographs illustrating the development of rafting as observed by MacKay and Ebert [22]. Figure 4.67 shows a similar curve obtained by Fredholm and Strudel [23] with the corresponding changes in microstructure.

From these and several other observations [17-24,27], we can infer that the driving force for directional coarsening sets in early in the transient and that the morphology evolution ensues within an extent of time which is determined by the kinetics of the process – in particular by the diffusion properties of the crystal [57]. We can then expect to be able to explain the tendency toward directional coarsening by analyzing the state of strain and stress in the crystal at the end of the primary creep.

The primary stage of creep corresponds to the formation of networks of dislocations which relieve the misfit stresses; in our continuum model, we can identify this stage by comparing the value of the average equivalent creep strain in the matrix $\bar{\epsilon}^{\text{creep}}$ as defined in (4.5), with the initial value of the misfit, δ : we can assume that the misfit stresses are relieved when $\bar{\epsilon}^{\text{creep}}$ and δ are of the same order of magnitude. Actually, from the results of our finite element analysis, we can conclude that the primary stage of creep is completed when $\bar{\epsilon}^{\text{creep}}/\delta \simeq 2$.

Let's now analyze the state of stress and strain at this stage of the transient, and the corresponding effects on the $\tau_{\mathbf{n}}$ profile. We recall that the value of $\tau_{\mathbf{n}}$ is given by the expressions (2.31) that we repeat here for convenience:

$$\tau_{\mathbf{n}} = [W] - t_i \left[\frac{\partial u_i}{\partial n} \right]. \quad (4.6)$$

We will first consider the case of an applied tensile load and we will afterward discuss the case of an applied compressive load.

(a) Applied Tensile Load

It is convenient to independently analyze the conditions on the “top” of the precipitates (corresponding to the channels normal to the applied load) and on the “side” of the precipitates (corresponding to the channels parallel to the applied load).

- On the *top* of the precipitates, due to the high level of hydrostatic stress in the matrix (see Fig. 4.30(c)), the $t_i \left[\frac{\partial u_i}{\partial n} \right]$ term in expression (4.6) largely dominates. The $[W]$ term ranges between one and five percent of the $t_i \left[\frac{\partial u_i}{\partial n} \right]$ term for the analyzed alloys.

The value of the component of the traction vector normal to the interface, $t_{\mathbf{n}}$, is large and positive, while the tangential component is negligible. The

magnitude of the normal component of $[\frac{\partial \vec{u}}{\partial n}]$, which we will indicate as $[u_{\mathbf{n},\mathbf{n}}]$, is larger than the magnitude of the original misfit since the primary creep flow acts so as to enhance the jump in $u_{\mathbf{n},\mathbf{n}}$ across the interface, initially due to the lattice misfit (see Fig. 4.30(b)). Thus for *negative-misfit* alloys $[u_{\mathbf{n},\mathbf{n}}]$ is positive so that the force on the interface on the top of the precipitate results negative. The magnitude of the force scales with the applied load (which directly affects the magnitude of $t_{\mathbf{n}}$) and with the misfit (which directly affects $[u_{\mathbf{n},\mathbf{n}}]$). As the transient progresses past the primary stage, and the matrix starts creeping under the effect of the applied load, the creep flow keeps acting so as to increase $[u_{\mathbf{n},\mathbf{n}}]$ and therefore $\tau_{\mathbf{n}}$ will assume increasingly larger negative values.

Conversely, for *positive-misfit* alloys $[u_{\mathbf{n},\mathbf{n}}]$ is initially negative so that the force on the interface on the top of the precipitate results positive. The magnitude of $\tau_{\mathbf{n}}$ scales again with the applied load and with the misfit. As the transient progresses past the primary stage, the matrix starts creeping under the effect of the applied load. This process gives a positive contribution to $[u_{\mathbf{n},\mathbf{n}}]$ so that the magnitude of $\tau_{\mathbf{n}}$ starts to decrease and, for $\bar{\epsilon}^{\text{creep}}/\delta \simeq 4$, $\tau_{\mathbf{n}}$ becomes negative.

- On the *side* of the precipitates, since the traction vector is approximately one order of magnitude smaller than that of the top, the two terms in (4.6) are comparable and the magnitude of the force on the interface is much lower. The $[W]$ term always gives a negative contribution to $\tau_{\mathbf{n}}$ because the state of stress in the precipitate gives rise to an elastic energy level higher than that in the matrix channels, which are essentially in a state of moderate hydrostatic stress.

The normal component of the traction vector, $t_{\mathbf{n}}$, is negative and the tangential component is negligible.

For *negative-misfit alloys*, the $[u_{\mathbf{n},\mathbf{n}}]$ term at the end of primary creep is large and positive (for what concerns this term, the primary creep flow acts in the same sense of the misfit) so that the $(-t_i[\frac{\partial u_i}{\partial n}])$ term is positive and counterbalances the $[W]$ term.

Thus for alloys characterized by a small negative misfit, the $[W]$ term initially dominates and $\tau_{\mathbf{n}}$ is negative, while for alloys with large negative misfit the $(-t_i[\frac{\partial u_i}{\partial n}])$ term dominates and $\tau_{\mathbf{n}}$ is positive (this is normally the case for most commercial alloys). As the transient progresses, the matrix material creeps under compressive stress so that negative contributions are added to $[u_{\mathbf{n},\mathbf{n}}]$ and thus to the force $\tau_{\mathbf{n}}$.

For *positive-misfit alloys*, the $[u_{\mathbf{n},\mathbf{n}}]$ term at the end of the primary creep is large and negative so that the $(-t_i[\frac{\partial u_i}{\partial n}])$ term is negative as well and adds up with $[W]$ to give a negative value for $\tau_{\mathbf{n}}$. As the transient evolves, negative contributions are added to $[u_{\mathbf{n},\mathbf{n}}]$ so that $\tau_{\mathbf{n}}$ assumes increasingly larger negative values.

(b) Applied Compressive Loads

The patterns according to which $\tau_{\mathbf{n}}$ evolves are essentially symmetrical to those for tensile loads due to the fact that the sign of the traction vector is inverted

- on the *top* of the precipitates, the $t_i[\frac{\partial u}{\partial n}]$ term dominates; $t_{\mathbf{n}}$ is large and negative while the tangential component of the traction vector is negligible.

For *negative-misfit* alloys $[u_{\mathbf{n},\mathbf{n}}]$ at the end of primary creep is positive so that the force on the interface results positive, and its magnitude scales with the applied load and the initial value of the misfit.

As the transient evolves, the matrix material creeps under the applied compressive loads and negative contributions are added to $[u_{\mathbf{n},\mathbf{n}}]$ so that the magnitude of $\tau_{\mathbf{n}}$ starts to decrease and $\tau_{\mathbf{n}}$ will eventually become negative.

For *positive-misfit* alloys $[u_{\mathbf{n},\mathbf{n}}]$ at the end of the primary creep is negative so that the force on the interface is negative as well. As the transient progresses past the primary stage of creep, the matrix creeps in compression under the applied load so that negative contributions are added to $[u_{\mathbf{n},\mathbf{n}}]$ and $\tau_{\mathbf{n}}$ will assume increasingly larger negative values.

- On the *side* of the precipitates the two terms in (4.6) are comparable and the magnitude of $\tau_{\mathbf{n}}$ is much lower. The $[W]$ term always gives a negative contribution to $\tau_{\mathbf{n}}$. The normal component of the traction vector, $t_{\mathbf{n}}$, is positive and the tangential component is negligible. For *negative-misfit* alloys, the $[u_{\mathbf{n},\mathbf{n}}]$ term at the end of primary creep is positive so that the $(-t_i[\frac{\partial u}{\partial n}])$ term is negative and adds up with $[W]$ to give a negative value for $\tau_{\mathbf{n}}$. As the transient evolves, $\tau_{\mathbf{n}}$ will assume increasingly larger negative values due to the positive contributions to $[u_{\mathbf{n},\mathbf{n}}]$ as the matrix creep under tensile stress.

For *positive-misfit* alloys, the $[u_{\mathbf{n},\mathbf{n}}]$ term at the end of primary creep is negative so that the $(-t_i[\frac{\partial u}{\partial n}])$ term counterbalance the $[W]$ term and $\tau_{\mathbf{n}}$ will be positive or negative depending on the value of the initial misfit. As the transient evolves negative contributions will be added to $\tau_{\mathbf{n}}$.

In Fig. 4.68, we give a schematic synoptic diagram showing the levels of $\tau_{\mathbf{n}}$ on the top and on the side of the precipitates at the end of the primary stage of the creep transient for the possible combinations of tensile/compressive load and positive/negative misfit.

From this diagram we can see how under a tensile load a negative-misfit alloy will tend to exhibit a “type N” rafting behavior, while a positive-misfit alloy will tend to exhibit a “type P” rafting behavior and vice versa for a compressive load.

These simple patterns are indeed in agreement with all the available experimental data listed in Table 1.1.

The arrows in Fig. 4.68 indicate how the levels of $\tau_{\mathbf{n}}$ will decrease as the creep transient evolves toward higher levels of creep strains under the effect of the applied

loads. If we consider this further evolution of the τ_n profiles we can conclude that we can always expect to observe a “Type N” rafting behavior for a negative-misfit alloy under a tensile load and for a positive-misfit alloy under a compressive load. However, if we consider the case of negative-misfit alloys under compressive loads and positive-misfit alloys under tensile loads, we can expect to observe a marked tendency toward a “type P” rafting behavior only if we conduct our test so as to maintain the crystal at a low level of creep for the time needed by the kinetics of the process to accomplish, at least partially, the morphology evolution.

In fact, if we compare micrographs of “Type P” rafts and “Type N” rafts, the latter are generally characterized by a higher aspect ratio and a more regular structure.

With regard to the evolution of $\Delta\tau_n$, since the magnitude of τ_n essentially scales with the misfit, δ , and the applied stress, σ , and the sign of $\Delta\tau_n$ changes with the sign of δ and σ as shown in Fig. 4.68, we can expect that plots of the normalized quantity $\Delta\tau_n/\sigma\delta$ versus the magnitude of $\bar{\epsilon}^{\text{creep}}/\delta$ will show similar patterns for all the different alloys that we have analyzed. These curves are shown in Fig. 4.69, and it can be noted how all the data correlates within a very narrow band.¹

This result also agrees with the experimental observations that indicate how the rate of directional coarsening scales with the lattice misfit and the applied stress (see paragraph 1.2): the process is accelerated when the driving force is increased. The hastening of the rafting process observed when the test temperature is increased and when the microstructure is refined, is most probably related to a reduction of the characteristic diffusion time, namely, to an increase in diffusivity and to a shortening of the diffusion path.

In Fig. 4.69 we can notice a substantial increase in $\Delta\tau_n$ within the very first stage of primary creep, when $0.5 \leq |\bar{\epsilon}^{\text{creep}}/\delta| \leq 2.0$. After this sharp rise, which corresponds to the period in which the misfit stresses are relieved, the creep flow in the matrix becomes dominated by the applied stress and the behavior of “Type N” evolutions and “Type P” evolutions branches: the driving force for “Type N” coarsening keeps increasing, while the force for “Type P” coarsening will eventually reach a saturation level.

These trends can be already qualitatively observed in the last portion of the curves in Fig 4.69. If we compare correspondent pairs of “Type N” and “Type P” plots (see Fig. 4.70) we can notice that the last section of the “Type P” curves (MNMT, TCC) dips below the last section of the “Type N” curves (MNMC, TCT) which still exhibit an upward curvature.

We have chosen not to continue our analysis beyond this stage because experimental observations show that at the end of primary creep, relevant morphological changes are already occurring: if we extend our analysis, based on the initial cuboidal

¹Note that we have not included the data for case 9 (TCT_{PMS}) and case 10 (TCC_{PMS}). This is because the misfit that we have chosen for this hypothetical alloy is exceedingly small—the misfit strains and the elastic strains have comparable magnitude. It is obvious how, in the limit of zero misfit, quantities normalized by the misfit itself lose their significance.

shape of the precipitates, to the steady state creep we would not obtain a reliable simulation of this subsequent stage of the process.

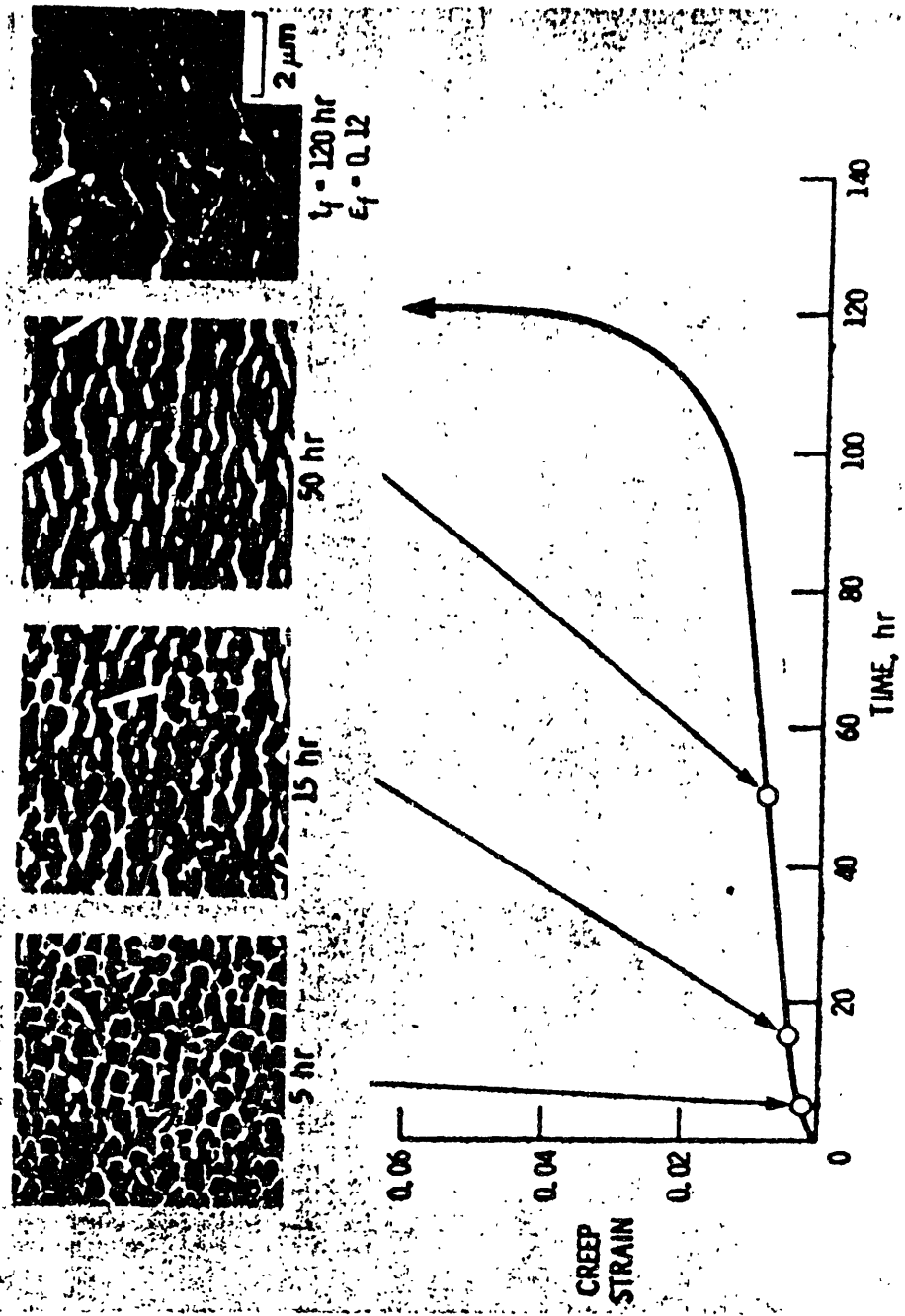


Figure 4.66 A typical creep curve with corresponding micrographs which show the development of directional coarsening [22].

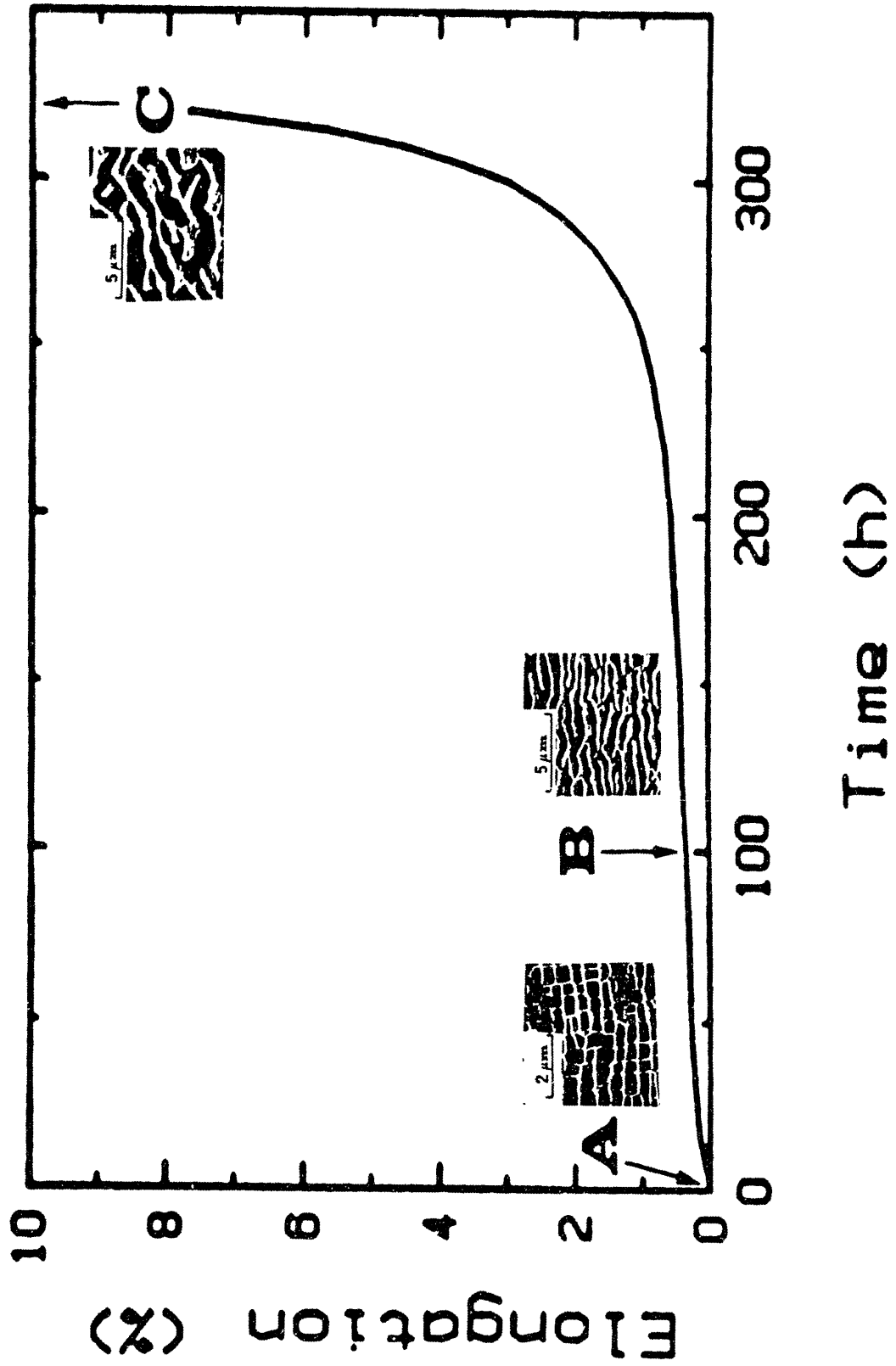


Figure 4.67 Creep curve and correspondent changes in microstructure [23].

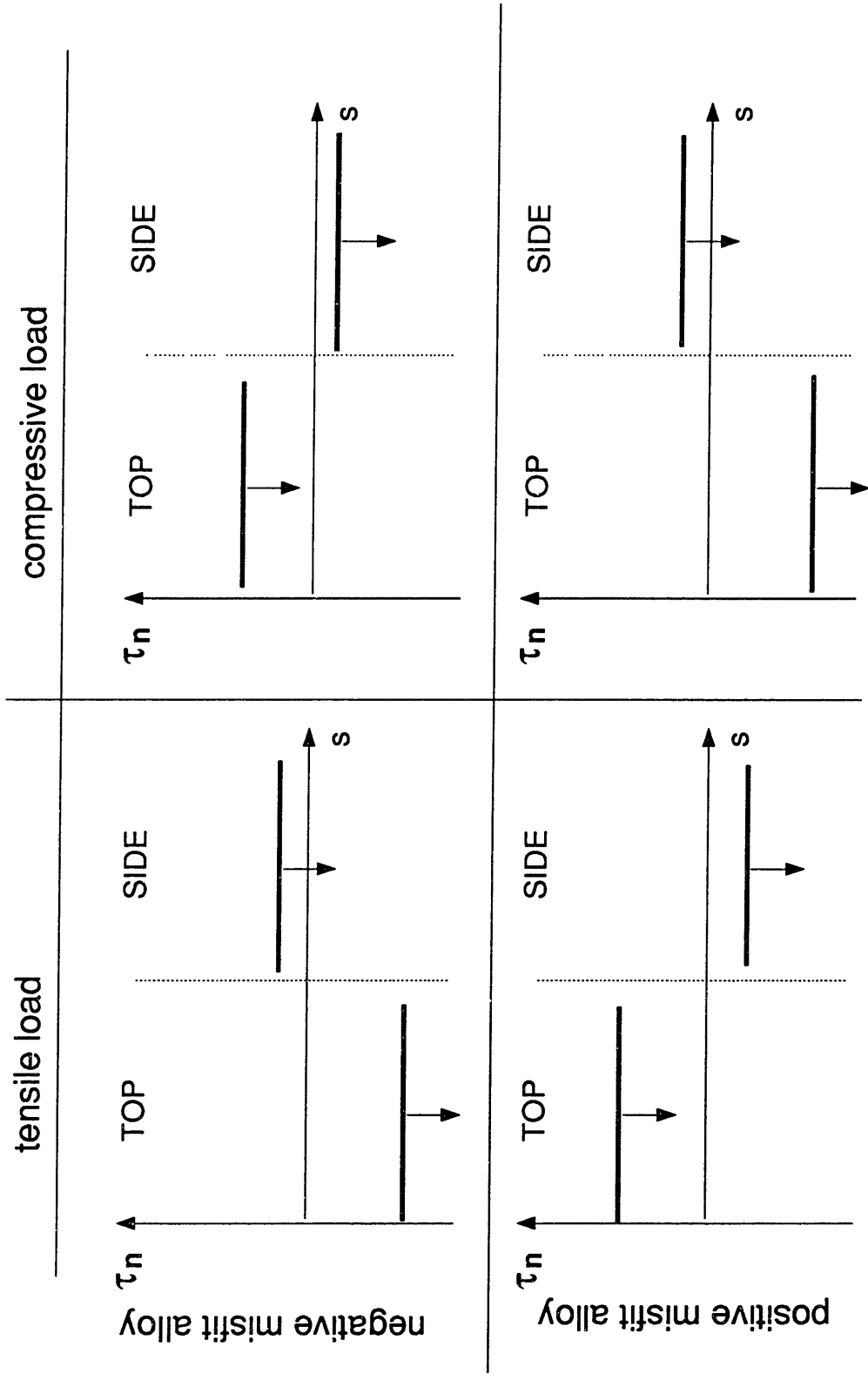


Figure 4.68 A schematic diagram showing the τ_n levels at the end of the primary stage of the creep transient . Vertical arrows indicate sense of expected evolution of τ_n with on-going creep.

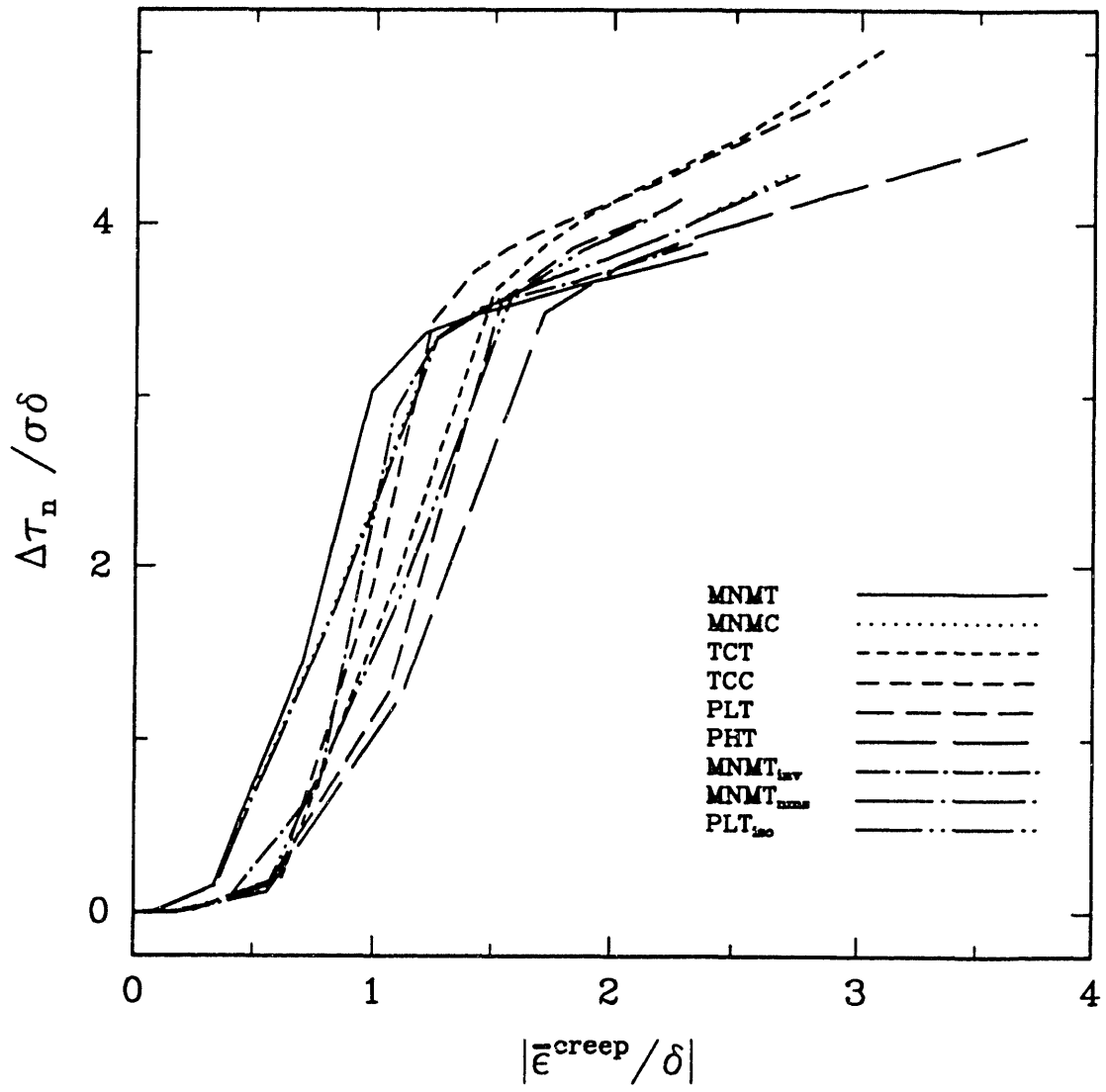


Figure 4.69 Evolution of $\Delta\tau_n / \sigma\delta$ for the analyzed creep transients

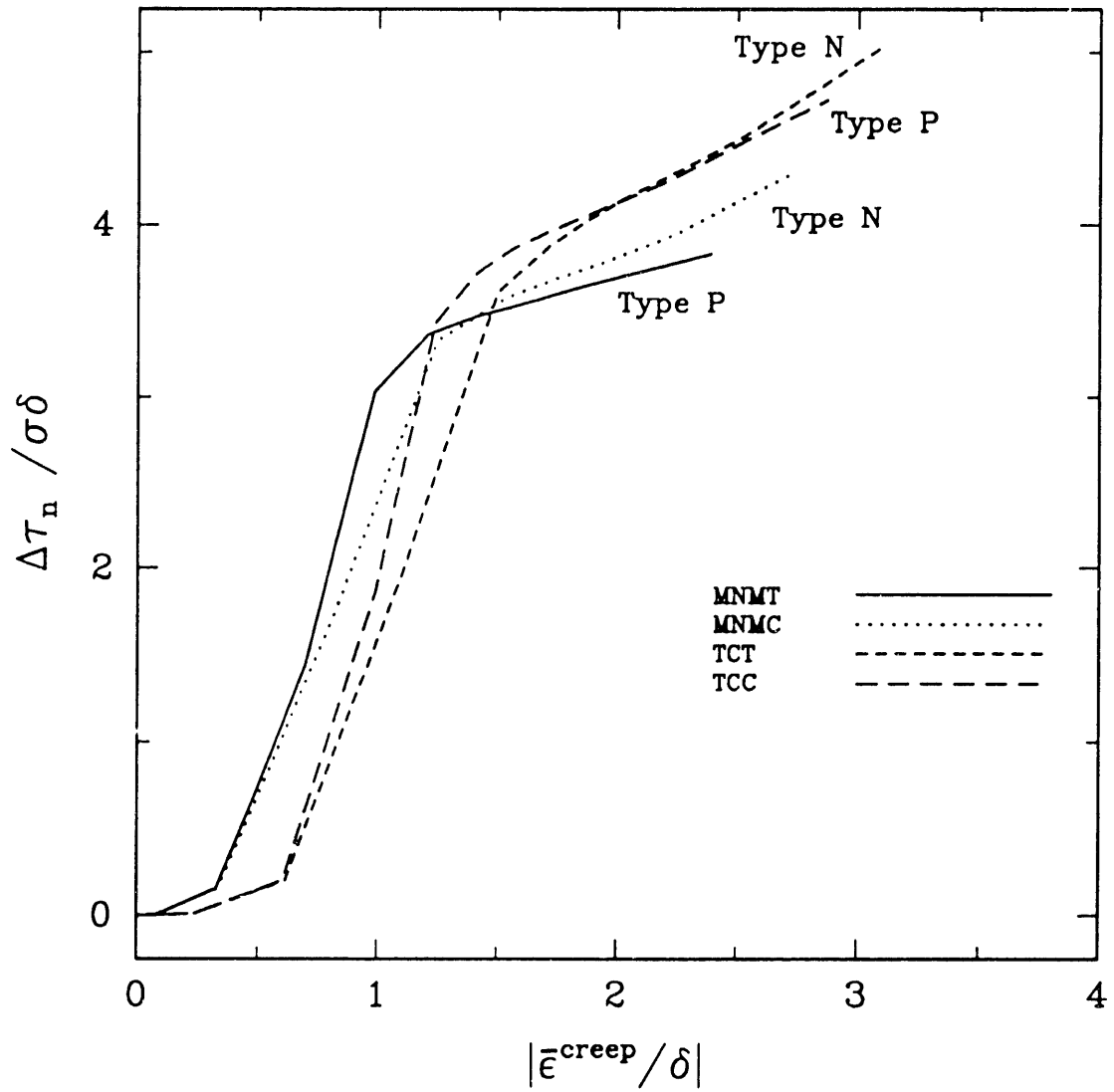


Figure 4.70 Comparison of “Type P” and “Type N” evolution curves for $\Delta\tau_n / \sigma\delta$

CHAPTER 5

CONCLUSIONS

5.1 Summary of Results

We have developed numerical techniques, in the framework of the finite element method, which allows us to evaluate local values of the generalized force acting on a material interface which is work-conjugate with the normal displacement of the interface itself.

This quantity is a direct measure of the tendency for the interface to migrate, and thus of the driving force for morphological evolutions of the microstructure.

We have applied these methods to the study of rafting in $\gamma - \gamma'$ Ni-superalloys.

The flexibility of the proposed methods has readily allowed us to closely model the actual microstructural morphology of the alloys and to account for the effects of applied boundary conditions, lattice misfit, elastic anisotropy and inelastic behavior of the crystals during the stress annealing transients.

We have modeled some experimental alloys, for which we have positively compared the indications of our model with the experimental data, and we have conducted a circumscribed parametric study which has allowed us to formulate a more general interpretation of the rafting phenomenon, which appears to give a satisfactory explanation for all the available experimental observations.

According to the results of our analysis, it is of fundamental importance, in modeling the rafting phenomenon, to consider the effects of the creep flow in the γ -matrix and in particular the evolution of the stress and strain fields during the primary creep stage of the stress-annealing transients.

Earlier attempts to interpret the rafting behavior of these alloys have indeed failed essentially because these effects were neglected.

In summary, the proposed methodology has proved itself successful for our particular application and appears suitable to be used in the analysis of parallel phenomena concerning microstructural evolutions in multi-phase materials.

5.2 Suggestions for Future Study

We can identify two main topics that we have addressed in our research. The first is the development of the numerical techniques *per se*; the second is the analysis of the rafting phenomenon. Regarding the development of numerical techniques for the evaluation of local forces acting on maternal interfaces, the first and most immediate development is the extension of the computer programs to cope with 3-D geometries. A more ambitious and substantial development, more closely related to the study of rafting, would be the implementation of a kinetic model to follow the evolution of the microstructure morphology. In such a model, the evaluation of the driving force would represent only one of several steps in the procedure.

With regard to the analysis of the rafting phenomenon, more involved creep models could be implemented, and the effects of modifications of the volume fraction of the precipitates could be investigated.

Finally, we should recognize that a continuum model for creep is not entirely adequate to model the discrete nature of motion and multiplication of dislocations in the narrow γ' channels.

The development of a discrete model for dislocation mechanics conceived so that it could be interactively superposed to the finite element solutions of continuum elastic behavior, would represent a substantial contribution to the analysis of this process as well as of other phenomena characterized by creep processes with a small length scale.

REFERENCES

1. M. V. Nathal: *Metal. Trans.***18A**, 1961, (1987).
2. G. A. Webster and C. P. Sullivan: *J. Inst. Metals*, **95**, 138, (1967).
3. Y. Nakada and W. C. Leslie: *Trans. ASM*, **60**, 223, (1961).
4. I. L. Mirkin and O. D. Kancheev: *Met. Sci. Heat Treatment*, **1**, 10, (1967).
5. C. P. Sullivan, G. A. Webster and B. J. Pearcey: *J. Inst. Metals*, **96**, 274, (1968).
6. J. R. Mihalisin and D. L. Pasquine: *Proc. International Symposium on Structural Stability in Superalloys*, Seven Springs, PA, **1**, 131 (1968).
7. W. Danesi and M. Donachie: *J. Inst. Metals*, **97**, 107, (1969).
8. R. G. Davies and T. L. Johnson: *Proc. Third. Landing Conf. on Ordered Alloys*, Baton Rouge, LA, 447, (1970).
9. R. A. Stevens and P. E. Flewitt: *Mat. Sci. Eng.*, **37**, 237, (1979).
10. G. A. Webster and B. J. Pearcey: *Trans. ASM*, **59**, 847, (1966).
11. J. K. Tien and R. P. Gamble: *Met. Trans.*, **3**, 2157, (1972).
12. J. K. Tien and S. M. Copley: *Met. Trans*, **2**, 215, (1971).
13. J. K. Tien and S. M. Copley: *Met. Trans.*, **2**, 543, (1971).
14. A. Pineau: *Acta Met.*, **24**, 550, (1976).
15. T. Miyazaki, K. Nakamura and H. Mori: *J. Mat. Sci.*, **14**, 1827, (1979).
16. C. Carry and J. L. Strudel: *Acta. Met.*, **25**, 767, (1977).
17. C. Carry and J. L. Strudel: *Acta. Met.*, **26**, 859, (1978).
18. D. D. Pearson, F. D. Lemkey and B. H. Kear: *Proc. Fourth International Symposium on Superalloys*, Metals Park, OH, 513, (1980).
19. D. D. Pearson, B. H. Kear and F. D. Lemkey: **Creep and Fracture of Engineering Materials and Structure**, (B. Wilshire and D. R. Owen, Ed.), Pineridge Press, Ltd., Swansea, U. K., 213, (1983).
20. M. V. Nathal and L. J. Ebert: *Scripta Met.*, **17**, 115, a, (1983).
21. P. Caron and T. Khan: *Mat. Sci. Eng.*, **61**, 173, (1983).
22. R. A. MacKay and L. J. Ebert: **Superalloys 1984**, (M. Gell, et al., Ed.), 135, (1984).
23. A. Fredholm and J. L. Strudel: **Superalloys 1984**, (M. Gell, et al., Ed.), 211, (1984).
24. R. A. MacKay and L. J. Ebert: *Met. Trans.*, **16A**, 1968, (1985).
25. T. M. Pollock: "Creep Deformation in Nickel-base Superalloys Single Crystal", Ph.D. Thesis, Dept. Mat. Sci. Eng., MIT, (1989).

26. J. M. Oblak and B. H. Kear: *Trans. Quart. ASM*, **61**, 519, (1968).
27. M. V. Nathal, R. A. MacKay, R. G. Garlick: *Mat. Sci. Eng.*, **75**, 195, (1985).
28. D. A. Grose and G. S. Ansell: *Metall. Trans*, **A12**, 1631, (1981).
29. M. P. Arbuzov and I. A. Zelenkov: *Phys. Met. Metalloved*, **16**, 65, (1963).
30. **Superalloys II**, C.T. Sims, N. S. Stoloff, W. C. Hagel Ed., (1987).
31. J. K. Lee, D. M. Barnett and H. I. Aaronson: *Met. Trans.*, **8A**, 963, (1977).
32. A. F. Jankowski, E. M. Wingo and T. Tsakalakos: *Computer Simulation of Microstructural Evolution*, (D. J. Srolovitz, Ed.), MS-AIME, 125, (1985).
33. G. Faivre: *Phys. Stat. Sol*; **35**, 249, (1964).
34. W. C. Johnson: "The Elastic and Diffusional Interaction of Spherical Inhomogeneities in a Uniaxial Stress Field", in **Micromechanics Inhomogeneity. Toshio Mura anniversary Volume**, (G. Weng, Ed.), Springer Verlag (1989).
35. J. C. Chang: "Elastic Energy Changes Accompanying Gamma-Prime Rafting in Nickel-Base Superalloys", Ph.D. Thesis, Dept. Mat. Sci. Eng., MIT, (1989).
36. J. D. Eshelby: *Phil. Trans.*, **A244**: 87 (1951).
37. J. D. Eshelby: "Energy Relations and the Energy Momentum Tensor in Continuum Mechanics", in **Inelastic Behavior of Solids**, (M. F. Kanninen, et al., Ed.), 77-115, McGraw-Hill, New York (1970).
38. T. Mura: **Micromechanics of Defects in Solids**, Martinus Nijhoff Publishers, Dordrecht (1987).
39. ABAQUS version 4.7, Hibbitt, Karlsson and Sorensen, Inc., Providence, R. I.
40. J. R. Rice: "Mathematical Analysis in the Mechanics of Fracture" in **Fracture: An Advanced Treatise**, (H. Liebowitz, Ed.), Academic Press, New York (1968).
41. J. R. Rice: *J. Appl. Mech.*, **35**, 379, (1968).
42. J. W. Hutchinson: *J. Mech. Phys. Solids*, **16**, 13, (1968).
43. J. R. Rice and G. F. Rosengren: *J. Mech. Phys. Solids*, **16**, 1, (1968).
44. C. F. Shih, B. Moran, T. Nakamura: *Int. J. Fracture*, **30**, 79, (1986).
45. J. D. Eshelby: "Calculation of Energy Release Rate" in **Prospects of Fracture Mechanics**, (Sih, Van Elst and Broek, Ed.), Noordhoff (1974).
46. T. Nakamura, C. F. Shih, L. B. Freund, *Int. J. Fracture*, **27**, 229, (1985).
47. D. M. Parks: *Int. J. Fracture*, **10**, 487, (1974).

48. D. M. Parks: *Comp. Meth. Appl. Mech. Eng.*, **12**, 353, (1977).
49. D. M. Parks: "Virtual Crack Extension: A General Finite Element Technique for the J -Integral Evaluation" in **Numerical Methods in Fracture Mechanics**, (Luxmore A. R. and Owen D. R. J., Ed.), University College of Wales, Swansea (1978).
50. T. K. Hellen: *Int. J. Numer. Method. Eng.*, **9**, 187, (1975).
51. H. G. deLorenzi: *Int. J. Fracture*, **19**, 183, (1982).
52. H. G. deLorenzi: "Energy Release Rate Calculations by the Finite Element Method", General Electric Company, TIS, Rep. 82 CRD205 (1982).
53. F. Z. Li, C. F. Shih, A. Needleman: *Engineering Fracture Mechanics*, **21**, 405, (1985).
54. B. Moran and C. F. Shih: *Engineering Fracture Mechanics*, **27**, 615, (1987).
55. J. N. Goodier: *Trans. ASME*, **55**, 39, (1933).
56. W. R. Johnson, C. R. Barrett, W.D. Nix: *Metall. Trans.*, **3A**, 693, (1972).
57. F. G. Haubensak: S. M. Thesis, Dept. Mat. Sci. Eng., M.I.T., (1990).
58. F. A. McClintock and A. S. Argon: **Mechanical Behavior of Materials**, Addison-Wesley, (1966).

**APPENDIX I: THE COMPUTER PROGRAM
POSTABQ**


```

10      GO TO 20
      PRINT*, '
      PRINT*, '
      PRINT*, 'Unable to open file : ',FILIMP
      PRINT*, '
      PRINT*, '
      PRINT 1000, ' Do you want to try again? [Y],
      READ (*,2000)IUTIL, RESP
      IF (RESP.EQ.'N'.OR.RESP.EQ.'n') STOP
      PRINT 1000, ' Choose another Job_name ,
      READ (*,2000) IJM,FILM

C      FILE_NAME(1:IJM) = FILM(1:IJM)
      FILE_NAME(IJM+1:IJM+6) = TABQ(1:6)
      FILE_NAME(IJM+7:25) = ' ,

C      FILIMP(1:IJM) = FILM(1:IJM)
      FILIMP(IJM+1:IJM+6) = TIMP(1:6)
      FILIMP(IJM+7:32) = ' ,

C      FILDAT(1:IJM) = FILM(1:IJM)
      FILDAT(IJM+1:IJM+6) = TDAT(1:6)
      FILDAT(IJM+7:32) = ' ,

C      FILCHK(1:IJM) = FILM(1:IJM)
      FILCHK(IJM+1:IJM+6) = TCHK(1:6)
      FILCHK(IJM+7:25) = ' ,

C      FILOUT(1:IJM) = FILM(1:IJM)
      FILOUT(IJM+1:IJM+6) = TOUT(1:6)
      FILOUT(IJM+7:32) = ' ,

C      FILGEO(1:IJM) = FILM(1:IJM)
      FILGEO(IJM+1:IJM+6) = TGEO(1:6)
      FILGEO(IJM+7:25) = ' ,

C      FILP01(1:IJM) = FILM(1:IJM)
      FILP01(IJM+1:IJM+6) = TP01(1:6)
      FILP01(IJM+7:32) = ' ,
      FILP02(1:IJM) = FILM(1:IJM)
      FILP02(IJM+1:IJM+6) = TP02(1:6)
      FILP02(IJM+7:32) = ' ,
      FILP03(1:IJM) = FILM(1:IJM)
      FILP03(IJM+1:IJM+6) = TP03(1:6)

      FILP03(IJM+7:32) = ' ,
      FILP04(1:IJM) = FILM(1:IJM)
      FILP04(IJM+1:IJM+6) = TP04(1:6)
      FILP04(IJM+7:32) = ' ,
      FILP05(1:IJM) = FILM(1:IJM)
      FILP05(IJM+1:IJM+6) = TP05(1:6)
      FILP05(IJM+7:32) = ' ,
      FILP06(1:IJM) = FILM(1:IJM)
      FILP06(IJM+1:IJM+6) = TP06(1:6)
      FILP06(IJM+7:32) = ' ,
      FILP07(1:IJM) = FILM(1:IJM)
      FILP07(IJM+1:IJM+6) = TP07(1:6)
      FILP07(IJM+7:32) = ' ,
      FILP08(1:IJM) = FILM(1:IJM)
      FILP08(IJM+1:IJM+6) = TP08(1:6)
      FILP08(IJM+7:32) = ' ,
      FILP09(1:IJM) = FILM(1:IJM)
      FILP09(IJM+1:IJM+6) = TP09(1:6)
      FILP09(IJM+7:32) = ' ,
      FILP10(1:IJM) = FILM(1:IJM)
      FILP10(IJM+1:IJM+6) = TP10(1:6)
      FILP10(IJM+7:32) = ' ,
      FILP11(1:IJM) = FILM(1:IJM)
      FILP11(IJM+1:IJM+6) = TP11(1:6)
      FILP11(IJM+7:32) = ' ,
      FILP12(1:IJM) = FILM(1:IJM)
      FILP12(IJM+1:IJM+6) = TP12(1:6)
      FILP12(IJM+7:32) = ' ,
      FILP13(1:IJM) = FILM(1:IJM)
      FILP13(IJM+1:IJM+6) = TP13(1:6)
      FILP13(IJM+7:32) = ' ,
      FILP14(1:IJM) = FILM(1:IJM)
      FILP14(IJM+1:IJM+6) = TP14(1:6)
      FILP14(IJM+7:32) = ' ,
      FILP15(1:IJM) = FILM(1:IJM)
      FILP15(IJM+1:IJM+6) = TP15(1:6)
      FILP15(IJM+7:32) = ' ,
      FILP16(1:IJM) = FILM(1:IJM)
      FILP16(IJM+1:IJM+6) = TP16(1:6)
      FILP16(IJM+7:32) = ' ,
      FILP17(1:IJM) = FILM(1:IJM)
      FILP17(IJM+1:IJM+6) = TP17(1:6)
      FILP17(IJM+7:32) = ' ,
      FILP18(1:IJM) = FILM(1:IJM)
      FILP18(IJM+1:IJM+6) = TP18(1:6)

```

```

FILP18(IEM+7:32) = ' ,
FILP19(I: IEM) = FILM(1: IEM)
FILP19(IEM+1: IEM+6) = TP19(1: 6)
FILP19(IEM+7: 32) = ' ,
C
C
C
OPEN(UNIT = 10, FILE = FILLIP, STATUS = 'OLD', ERR=10)
20
C
CONTINUE
C
OPEN(UNIT = 11, FILE = FILDAT)
OPEN(UNIT = 13, FILE = FILCHK)
OPEN(UNIT = 14, FILE = FILOUT)
OPEN(UNIT = 15, FILE = FILGEO)
OPEN(UNIT = 16, FILE = FILP01)
OPEN(UNIT = 17, FILE = FILP02)
OPEN(UNIT = 18, FILE = FILP03)
OPEN(UNIT = 19, FILE = FILP04)
OPEN(UNIT = 20, FILE = FILP05)
OPEN(UNIT = 21, FILE = FILP06)
OPEN(UNIT = 22, FILE = FILP07)
OPEN(UNIT = 23, FILE = FILP08)
OPEN(UNIT = 24, FILE = FILP09)
OPEN(UNIT = 25, FILE = FILP10)
OPEN(UNIT = 26, FILE = FILP11)
OPEN(UNIT = 27, FILE = FILP12)
OPEN(UNIT = 28, FILE = FILP13)
OPEN(UNIT = 30, FILE = FILP15)
OPEN(UNIT = 31, FILE = FILP16)
OPEN(UNIT = 32, FILE = FILP17)
OPEN(UNIT = 33, FILE = FILP18)
OPEN(UNIT = 34, FILE = FILP19)
C
C
C
MORI = 10
MORD = 11
MOWC = 13
MOWO = 14
MOWG = 15
MOWP(1) = 16
MOWP(2) = 17
MOWP(3) = 18
MOWP(4) = 19
MOWP(5) = 20
FILP18(IEM+7:32) = 21
MOWP(7) = 22
MOWP(8) = 23
MOWP(9) = 24
MOWP(10) = 25
MOWP(11) = 26
MOWP(12) = 27
MOWP(13) = 28
MOWP(14) = 29
MOWP(15) = 30
MOWP(16) = 31
MOWP(17) = 32
MOWP(18) = 33
MOWP(19) = 34
C
C
MELT = 8
MDIM = 2
KERROR = 0
C
Accessing file 8
C
MRU = 1
LRUNIT(1,1) = 8
LRUNIT(2,1) = 2
CALL INITPF(MRU, LRUNIT, LOUFP)
JUNIT = 8
CALL DRRMU(JUNIT)
C
Geometry input. Connectivity matrices
C
CALL GEOPAT
C
IF(ERROR.GT.0) GO TO 200
C
C
Path geometry. Curvilinear coordinate and normal to the path.
C
CALL GEOPAT
C
IF(ERROR.GT.0) GO TO 200
C
C
Shape function matrices
C
C

```

```

C          CALL PRESFW
C
C          IF(ERROR.GT.0) GO TO 200
C
C          IF(KPSTOP.EQ.1) GO TO 300
C
C          Input the control variables of the procedure
C
C          CALL CTRIMP
C
C          IF(ERROR.GT.0) GO TO 200
C
C          Processing the variables for all the step/increment required by user
C
C          DO 150 MOUT = 1, MFGUT
C
C              reset to zero flags and variables
C
C              CALL RESETV
C
C              WRITE(MOWO,4000) MSTEP(MOUT), MMINCR(MOUT)
C
C                  DO 100 IVAR = 1, NVAR
C
C                      CALL PROGES(MOUT,IVAR)
C
C                          IF(ERROR.GT.0) GO TO 200
C
C                  CONTINUE
C
C          Executing the user routine
C
C          IF (JSUB.EQ.0) GO TO 300
C
C          CALL USRSUB(MOUT,FILM)
C
C          IF(ERROR.GT.0) GO TO 200
C
C          150 CONTINUE
C          STOP

```

```

C
C
C 200 CONTINUE
C
C      WRITE (MOWC,3000) MERROR
C      WRITE (MOWO,3000) MERROR
C
C 300 CONTINUE
C
C      1000 FORMAT($,A,' : ')
C      2000 FORMAT(Q,A)
C      3000 FORMAT(IH1,/,/,10X,','* * * ERROR DETECTED. PROGRAM STOP : MERROR',
C      &'= ',15,' * * *')
C      4000 FORMAT(IH1,/,/,10X,','* * * STEP',13,' MCR.',14,' * * *',/)
C
C      STOP
C      END
C
C      NOTE : Routines follow in alphabetical order
C
C
C
C

```



```

C      Mode input set
C
C      100 CONTINUE
C
C      DO 150 IN = 1, NTOTIS
C      IF(NCOMM(1,IN).NE.NAB) GO TO 150
C      NLC = IN
C      GO TO 300
C
C      150 CONTINUE
C      GO TO 300
C
C      Mode set
C
C      200 CONTINUE
C
C      DO 250 IN = 1, NTMOD
C      IF(NABAQ(IN).NE.NAB) GO TO 250
C      NLC = IN
C      GO TO 300
C
C      250 CONTINUE
C
C      300 CONTINUE
C      RETURN
C      END

```

```

*****
*
*      S U B R O U T I N E   C K P E R M
*
*****

```

```

SUBROUTINE CKPERM(ID,IMOVE,INEV,B,X)
C
C      Check if in the matrix AN rows have been permuted. If yes (IMOVE=1)
C      it permutes the Right Hand Side B according to the order given by
C      vector INEV
C
C      DIMENSION INEV(ID),B(ID),X(ID)
C
C      IF(IMOVE.NE.1) GO TO 500
C
C      DO 100 NR = 1, ID
C      X(NR) = B(INEV(NR))
C      DO 200 NR = 1, ID
C      B(NR) = X(NR)
C
C      500 CONTINUE
C
C      RETURN
C      END

```

```

C
C
C *****
C *
C * SUBROUTINE COMM E C
C *
C *
C *****
C
C SUBROUTINE COMM EC(IFISH0, IDOME)
C
C Evaluates the connectivity matrices MCONM & IELTOP
C Evaluates the total number of nodes NTFMOD and element NTELT
C
C Parameters
C I/ IFISH0(10000) :local input-set-number for abaqus nodes
C O/ IDOME(10000) :local number for abaqus nodes
C
C INCLUDE 'post_common'
C DOUBLE PRECISION ARRAY
C DIMENSION IFISH0(10000), IDOME(10000)
C DIMENSION ARRAY(513), JRRAY(2,513)
C EQUIVALENCE (ARRAY(1), JRRAY(1,1))
C
C Rewind file 8
C CALL DBFILE(2,ARRAY,JRCD)
C
C Scanning file 8
C
C NTFMOD = 0
C NTELT = 1
C DO 500 K = 1,99999
C
C CALL DBFILE(0,ARRAY,JRCD)
C IF(JRCD.NE.0) GO TO 600
C
C LR = JRRAY(1,1)
C KEY = JRRAY(1,2)

```

```

IF(KEY.NE.1900) GO TO 500
IEAB = JRRAY(1,3)

Check if any of the nodes of IEAB is a node of the input set
IADD = 1
DO 200 NN = 1,NTELT
  JRRAB = JRRAY(1,NN+4)
  IF(IFISH0(JRRAB).EQ.0) GO TO 200
  IADD = IADD+0
  JRRAB is a node of the input set -> fill MCONM
  NTELT = IFISH0(JRRAB)
  KP = 4 + MCONM(3,NTELT)*3
  MCONM(3,NTELT) = MCONM(3,NTELT) + 1
  check max number of element to which NTELT belongs
  IF(MCONM(3,NTELT).LE.6) GO TO 100
  KERROR = KERROR + 1
  WRITE(NOPC,1000) JRRAB
  GO TO 700
  CONTINUE
  filling MCONM
  MCONM(KP,NTELT) = IEAB
  MCONM(KP+1,NTELT) = NTELT
  MCONM(KP+2,NTELT) = NN
  CONTINUE

Check if the elt is on the path -> if yes fill IELTOP

IF (IADD.GT.0) GO TO 500
IELTOP(1,NTELT) = IEAB

DO 400 NN = 1,NTELT
  JRRAB = JRRAY(1,NN+4)
  Check if the node has been already numbered in the
  local list. If not -> put it in the list.
  IF(IDOME(JRRAB).NE.0) GO TO 300
  NTFMOD = NTFMOD+1

```

```

IDONE(MMAB) = MTHOD
MABAQ(MTHOD) = MMAB

IF(IFISHO(MMAB).EQ.0) GO TO 300
MMIS = IFISHO(MMAB)
MCON(2,MMIS) = MTHOD
CONTINUE
C
300
IA = 2+(MM-1)*2
IELTOP(IA,MTELT) = MMAB
IELTOP(IA+1,MTELT) = IDONE(MMAB)
CONTINUE
MTELT = MTELT + 1
C
500 CONTINUE
600 CONTINUE
C
MTELT = MTELT - 1
C
C Check max number of elt's (100) and nodes (800)
C
C
IF(MTELT.LE.100.AND.MTHOD.LE.800) GO TO 700
KERROR = KERROR + 1
WRITE(MONG,2000) MTELT,MTHOD
C
700 CONTINUE
C
IF (IOUTG.EQ.0) GO TO 900
WRITE(MONG,3000)
C
DO 750 MMIS = 1,MTOTIS
IMAX = MCON(3,MMIS)*3+3
WRITE(MONG,4000) MMIS,(MCON(I,MMIS),I=1,IMAX)
C
750
WRITE(MONG,5000)
C
DO 800 IELC = 1,MTELT
IMAX = MTELT*2 + 1
WRITE(MONG,6000) IELC,(IELTOP(I,IELC),I = 1,IMAX)
C
800
WRITE(MONG,7000)
C
DO 850 MMLC = 1,MTHOD

```

```

850 WRITE(MONG,8000) MMLC,MABAQ(MMLC)
C
900 CONTINUE
C
1000 FORMAT(1H1,///,20X,'** ERROR IN SBR. CONNEC * * *',//,
& 10X,'MAX NUMBER OF ELEMENTS CONNECTED TO ONE NODE EXCEEDED',//,
& 10X,'MORE THAN 6 ELEMENTS ARE CONNECTED TO NODE ',I4)
2000 FORMAT(1H1,///,20X,'** ERROR IN SBR. CONNEC * * *',//,
& 10X,'MAX NUMBER OF ELEMENTS and/or NODES EXCEEDED',//,
& 10X,'TOTAL NUMBER OF ELEMENTS = ',I4,' (MAX : 100)',//,
& 10X,'TOTAL NUMBER OF NODES = ',I4,' (MAX: 800)')
3000 FORMAT(1H1,///,40X,'* * * M C O M * * *',//,
& 1X,'MMIS MMAB MMLC MBE IAB1 LC1 P1 IAB2 LC2 P2 IAB3 LC3 P3 ',
& 'IAB4 LC4 P4 IAB5 LC5 P5 IAB6 LC6 P6',/)
4000 FORMAT(1X,I3,2X,I4,1X,I3,1X,I3,6(1X,I4,1X,I3,1X,I2))
5000 FORMAT(1H1,///,40X,'* * * I E L T O P * * *',//,
& 1X,'IELC IEAB MAB1 MLC1 MAB2 MLC2 MAB3 MLC3 MAB4 MLC4 MAB5 ',
& 'MLC5 MAB6 MLC6 MAB7 MLC7 MAB8 MLC8',/)
6000 FORMAT(18(1X,I4))
7000 FORMAT(1H1,///,40X,'* * * M A B A Q * * *',//,
& 1X,'MMLC MMAB ',/)
8000 FORMAT(2(1X,I4))
C
RETURN
END

```

```

C C *****
C C *
C C *
C C *
C C *
C C *
C C *
C C *
C C *****
C C
C C SUBROUTINE CTRIMP
C C Reads the contro. variables of the procedure
C C
C C INCLUDE 'post_common'
C C
C C READ(MORI,6000) NVAR,JSUB
C C
C C DO 100 NV = 1, NVAR
C C
C C READ(MORI,7000) IVAR,IV,K
C C
C C IVDIM(IVAR) = IV
C C KAB (IVAR) = K
C C
C C READ(MORI,8000) (KPPP(J,IVAR),J=1,8)
C C
C C DO 10 J =1,8
C C IF(KPPP(J,IVAR).NE.0) GO TO 10
C C MPROC(IVAR) = J-1
C C GO TO 20
C C
C C CONTINUE
C C CONTINUE
C C
C C Check the consistency of the procedure
C C
C C IF(KPPP(1,IVAR).EQ.1.OR.KPPP(1,IVAR).EQ.2) GO TO 30
C C ERROR = KERROR +1
C C WRITE(MONC,1000) IVAR,KPPP(1,IVAR)
C C CONTINUE
C C
C C IGRST(IVAR) = 0
C C IGRAD = 0
C C DO 60 J = 2,MPROC(IVAR)
C C *****
C C *
C C *
C C *
C C *
C C *
C C *
C C *
C C *****
C C
C C IF(KPPP(J,IVAR).NE.1.AND.KPPP(J,IVAR).NE.2) GO TO 40
C C KERROR = KERROR +1
C C WRITE(MONC,2000) J,IVAR,KPPP(J,IVAR)
C C CONTINUE
C C
C C 40
C C
C C IF(KPPP(J,IVAR).NE.3) GO TO 60
C C IF(IGRAD.EQ.0) GO TO 50
C C KERROR = KERROR +1
C C WRITE(MONC,3000) IVAR
C C CONTINUE
C C
C C 50
C C IGRAD = 1
C C IGRST(IVAR) = J
C C CONTINUE
C C
C C IF(IGRST(IVAR).LE.1) GO TO 100
C C DO 80 J = 1,IGRST(IVAR)-1
C C IF(KPPP(J,IVAR).NE.4) GO TO 70
C C KERROR = KERROR + 1
C C WRITE (MONC,4000) IVAR
C C CONTINUE
C C
C C 70
C C IF(KPPP(J,IVAR).NE.5) GO TO 80
C C KERROR = KERROR + 1
C C WRITE (MONC,5000) IVAR
C C CONTINUE
C C
C C 80
C C 100 CONTINUE
C C
C C C
C C C
C C C
C C READ(MORI,9000) NTOUT
C C
C C DO 200 NOUT = 1,NTOUT
C C READ(MORI,6000)NSTEP(NOUT),NINCH(NOUT)
C C
C C 200
C C
C C 1000 FORMAT(1H1,///,20X,'* * ERROR IN SBR. CTRIMP * *',//,
C C & 10X,'THE FIRST STEP OF THE PROCEDURE MUST BE A READING STEP',//,
C C & 10X,'BAD FIRST STEP FOR VARIABLE N.',I4,'FIRST STEP = ',I4)
C C 2000 FORMAT(1H1,///,20X,'* * ERROR IN SBR. CTRIMP * *',//,
C C & 10X,'ONLY THE FIRST STEP OF THE PROC. CAN BE A READING STEP',//,
C C & 10X,'BAD STEP N.',I4,' FOR VARIABLE N.',I4,' STEP = ',I4)
C C 3000 FORMAT(1H1,///,20X,'* * ERROR IN SBR. CTRIMP * *',//,
C C & 10X,'ONLY ONE GRADIENT STEP IS ALLOWED FOR EACH VARIABLE',//,
C C & 10X,'MORE THAN ONE GRADIENT STEP FOR VARIABLE N.',I4)
C C 4000 FORMAT(1H1,///,20X,'* * ERROR IN SBR. CTRIMP * *',//,
C C & 10X,'ROTATION STEP IS NOT ALLOWED FOR ALL NODES',//,
C C & 10X,'A ROT. STEP PRECED. GRADIENT STEP FOR VARIABLE N.',I4)
C C 5000 FORMAT(1H1,///,20X,'* * ERROR IN SBR. CTRIMP * *',//,

```



```

C          ERROR = ERROR + 1
          WRITE(NOWC,3000) K
          GO TO 400

C
C 210 CONTINUE
      DLISCO = -1.
      GO TO 400

C
C 220 CONTINUE
      DLISCO = 1.
      GO TO 400

C
C 230 CONTINUE
      DLISCO = 1.
      GO TO 400

C
C 240 CONTINUE
      DLISCO = -1.
      GO TO 400

C
C 250 CONTINUE
      DLISCO = 0.
      GO TO 400

C
C 260 CONTINUE
      DLISCO = 1.
      GO TO 400

C
C 270 CONTINUE
      DLISCO = 0.
      GO TO 400

C
C 280 CONTINUE
      DLISCO = -1.
      GO TO 400

C
C          Second coordinate : H
C
C 300 CONTINUE
      GO TO (310,320,330,340,350,360,370,380) K

C          ERROR = ERROR + 1
          WRITE(NOWC,3000) K

          GO TO 400

C 310 CONTINUE
      DLISCO = -1.
      GO TO 400

C
C 320 CONTINUE
      DLISCO = -1.
      GO TO 400

C
C 330 CONTINUE
      DLISCO = 1.
      GO TO 400

C
C 340 CONTINUE
      DLISCO = 1.
      GO TO 400

C
C 350 CONTINUE
      DLISCO = -1.
      GO TO 400

C
C 360 CONTINUE
      DLISCO = 0.
      GO TO 400

C
C 370 CONTINUE
      DLISCO = 1.
      GO TO 400

C
C 380 CONTINUE
      DLISCO = 0.
      GO TO 400

C
C 400 CONTINUE
      GO TO 400

C
1000 FORMAT(1H1,///,20X,'* * ERROR IN FWC.DLISCO * *',//,
* 10X,'ONLY ELEMENT-TYPE 8 IS IMPLEMENTED',//,
* 10X,'ELEMENT-TYPE = ',I4)
2000 FORMAT(1H1,///,20X,'* * ERROR IN FWC.DLISCO * *',//,
* 10X,'THE REQUIRED-COORDINATE-CODE MUST BE 1 (G) OR 2(H)',//,
* 10X,'REQUIRED COORDINATE CODE = ',I4)
3000 FORMAT(1H1,///,20X,'* * ERROR IN FWC.DLISCO * *',//,
* 10X,'FOR THIS EL-TYPE THE NODE NUMBER MUST BE BETW. 1 AND 8',//,
* 10X,'NODE NUMBER = ',I4)

```



```

C          MCOMP = 1
          IF(ID.EQ.1) MCOMP = 3
          IF(ID.EQ.2) MCOMP = 9
C          Scanning data file
C
C          DO 400 K = 1,99999
            READ(NORD,3000,END = 500) I,MAB,(VECT(I),I=1,MCOMP)
            IF(I.NE.IV) GO TO 400
C          Check if the node belongs to the input set:if YES->Fill VAR
C
C          CALL CHKSET(1,MAB,MNIS)
            IF(MNIS.EQ.0) GO TO 200
            JW(MNIS) = 1
            DO 100 I = 1,MCOMP
              VAR(I,MNIS) = VECT(I)
            CONTINUE
          100
          200
C
C          Check if CURALL is required and if MAB belongs to the node
C          set: If YES -> Fill ALL
C
C          IF(IA.EQ.0) GO TO 400
            CALL CHKSET(2,MAB,MNLC)
            IF(MNLC.EQ.0) GO TO 400
              JA(MNLC) = 1
              DO 300 I = 1,MCOMP
                ALL(I,MNLC) = VECT(I)
            CONTINUE
          300
          400
C          Check if all nodes have been found
C
C          DO 600 K = 1,NTOTIS
            IF(JV(K).EQ.1) GO TO 600
            ERROR = ERROR + 1
            WRITE(MWC,1000) K,IV
          600
          CONTINUE
C
          IF(IA.LE.0) GO TO 800
          DO 700 K = 1,NTOTD
            IF(JA(K).EQ.1) GO TO 700
          700
          CONTINUE
          800
          CONTINUE
C          ERROR = ERROR + 1
          WRITE(MWC,2000) K,IV
          700
          CONTINUE
C          800
          CONTINUE
C
          1000
          FORMAT(1H1,///<,20X,'* * ERROR IN SBR. DSVRI * *',//,
            & 10X,'MODE NUMBER',I4,'OF THE INPUT SET HAS NOT BEEN FOUND',
            & ' FOR IVAR = ',I4)
          2000
          FORMAT(1H1,///<,20X,'* * ERROR IN SBR. DSVRI * *',//,
            & 10X,'MODE NUMBER',I4,'OF THE NODE SET HAS NOT BEEN FOUND',
            & ' FOR IVAR = ',I4)
          3000
          FORMAT(2IS),9(F10.0))
C
          RETURN
          END

```

```

C *****
C *
C *          S U B R O U T I N E   F I L L I N
C *
C *
C *****
C
C SUBROUTINE FILLIN(KEY,LR,ARRAY,MLC,CUR)
C
C Fills CUR(j,MLC) with the values given by ARRAY according to rules
C defined by KEY
C
C Parameters
C I/    KEY : Abaqus file-8-reading key
C I/    LR  : Record length of ARRAY
C I/    ARRAY : Input record read from file 8
C I/    MLC : local identification number : number of the
C         column of CUR to be filled with ARRAY
C I/O   CUR : internal variable input array
C
C INCLUDE 'post_common'
C DOUBLE PRECISION ARRAY
C DIMENSION ARRAY(513),CUR(9,800)
C
C   DO 10 I = 1,9
C     CUR(I,MLC) = 0.
C
C   IF(KEY.GE.100) GO TO 400
C
C Element variable
C
C   IF(KEY.EQ.2.OR.KEY.EQ.14) GO TO 100
C   IF(KEY.EQ.11) GO TO 200
C   IF(KEY.GE.21.AND .KEY.LE.25) GO TO 300
C
C KERROR = KERROR + 1
C WRITE (N0WC,1000) KEY
C GO TO 700
C
C 1 component-variable
C
C 100 CONTINUE
C
C *****
C *
C *          S U B R O U T I N E   S T R E S S
C *
C *
C *****
C
C CUR(1,MLC) = ARRAY(3)
C GO TO 700
C
C Stress tensor
C
C CONTINUE
C
C CUR(1,MLC) = ARRAY(3)
C CUR(2,MLC) = ARRAY(4)
C CUR(3,MLC) = ARRAY(5)
C CUR(4,MLC) = ARRAY(6)
C CUR(7,MLC) = ARRAY(6)
C IF(MDIM.LT.3) GO TO 700
C CUR(5,MLC) = ARRAY(7)
C CUR(6,MLC) = ARRAY(7)
C CUR(8,MLC) = ARRAY(8)
C CUR(9,MLC) = ARRAY(8)
C GO TO 700
C
C Strain tensor
C
C CONTINUE
C
C CUR(1,MLC) = ARRAY(3)
C CUR(2,MLC) = ARRAY(4)
C CUR(3,MLC) = ARRAY(5)
C CUR(4,MLC) = ARRAY(6)*0.5
C CUR(7,MLC) = ARRAY(6)*0.5
C IF(MDIM.LT.3) GO TO 700
C CUR(5,MLC) = ARRAY(7)*0.5
C CUR(6,MLC) = ARRAY(7)*0.5
C CUR(8,MLC) = ARRAY(8)*0.5
C CUR(9,MLC) = ARRAY(8)*0.5
C GO TO 700
C
C Mode variable
C
C CONTINUE
C
C DO 500 J = 4,LR
C   IC = J-3
C   IF(IC.LT.9) GO TO 500
C   KERROR = KERROR + 1
C   WRITE(N0WC,2000)

```

```

          GO TO 700
500  CUR(IC,ELC) = ARRAY(J)
C
700  CONTINUE
C
      1000 FORMAT(1H1,///,20X,'** ERROR IN SBR. FILLIN * * ',//,
      & 10X,'ONLY KEY = 2,11,14,21,22,23,24,25 OR FEY GT. 100',
      & ' ARE IMPLEMENTED OPTIONS',//,10X,'KEY = ',(4)
2000  FORMAT(1H1,///,20X,'** ERROR IN SBR. FILLIN * * ',//,
      & 10X,'FOR MODE VARIABLES ONLY 9 COMPONENTS CAN BE READ ')
C
      RETURN
      END
C
SUBROUTINE F8VRIN(NOUT,KREQ,IA,CURVAR,CURALL)
C
C Read variable data from Abaqus-file 8
C
C Parameters
C  I/ KREQ : Abaqus file 8-read-key for the required variable
C  I/ IA  : All-flag:
C              IA = 0 -> values required only at path-nodes
C              IA = 1 -> values required at all nodes
C  O/ CURVAR: Variable values at path nodes
C  O/ CURALL: Variable values at all nodes
C
C INCLUDE 'post_common'
C
DOUBLE PRECISION ARRAY
DIMENSION ARRAY(513),JRRAY(2,513),CURVAR(9,200),CURALL(9,800)
DIMENSION JV(200),JA(800)
EQUIVALENCE (ARRAY(1),JRRAY(1,1))
C
DO 10 K=1,200
  JV(K) = 0
C
DO 20 K = 1,800
  JA(K) = 0
C
C Rewind file 8
C
CALL DBFILE(2,ARRAY,JRCD)
C
C Scanning file 8
C
DO 330 K = 1,999999
  CALL DBFILE(0,ARRAY,JRCD)
  IF(JRCD.NE.0) GO TO 350
C

```



```

2000 FORMAT(1H1,///,20X,'** ERROR IN SBR. F8VRIN **',//,
& 10X,'MODE NUMBER',I4,'OF THE MODE SET HAS NOT BEEN FOUND',
& ' FOR KEY = ',I4)
C
3000 FORMAT(1H1,///,20X,'** ERROR IN SBR. F8VRIN **',//,
& 10X,'INCREMENT ',I4,' OF STEP',I4,' HAS NOT BEEN FOUND')
C
RETURN
END
*****
*
* SUBROUTINE GEIIMP
*
*****
SUBROUTINE GEIIMP
C
C Manages the geometric input
C
C INCLUDE 'post_common'
C
C DIMENSION IFISHO(10000),IDONE(10000)
C
C READ(NORI,1000) ITYPE,MPSTOP,IOUTG
C
C Path definition
C
C CALL PATDEF(IFISHO)
C
C IF (KERROR.GT.0) GO TO 100
C
C Connectivity matrices
C
C CALL CONNOC(IFISHO,IDONE)
C
C IF (KERROR.GT.0) GO TO 100
C
C
C Mode cartesian components
C
C CALL NCARCO(IDONE)
C
C
C 100 CONTINUE
C
C 1000 FORMAT(3(I5))

```

RETURN
END

```

C
C
C *****
C *
C *          S U B R O U T I N E   G E O P A T
C *
C *
C *
C *****
C
C
C SUBROUTINE GEOPAT
C
C Evaluates curvilinear coordinate , normal and tangent vector to
C the path.
C
C NOTE!!! ONLY FOR 2nd ORDER - 8 NODES - ISOPARAMETRIC 2D ELEMENTS
C =====
C INCLUDE 'post_common'
C
C DIMENSION N(3), X(2,3), T(2,3), AL(2), TOLD(2)
C
C TOLD(1) = 0.
C TOLD(2) = 0.
C SCURV(1) = 0.
C BELT = (NTOTIS-1)/2
C
C Following the path
C
C DO 500 NE = 1, BELT
C   DO 100 I = 1, 3
C     N(I) = (NE-1)*2 + I
C     N(I) = NCON(N(2), N(I))
C   DO 100 J = 1, 2
C     X(J, I) = COORDS(J, N(I))
C
C   Evaluating the cart. comp. of the tang. at the three nodes
C
C     CALL TANG2D(X, T)
C
C     Average value of the tangent vector at node 1
C
C     IF(NE.EQ.1) GO TO 200
C     T(1,1) = (T(1,1)+TOLD(1))/2.

```

```

2000 FORMAT(1X,I4,1X,F10.5,6(1X,F6.3))
C
      T(2,1) = (T(2,1)+TOLD(2))/2.
CONTINUE
C
      TOLD(1) = T(1,3)
      TOLD(2) = T(2,3)
C
      Cartesian component of the normal at nodes 1,2,3
C
      DO 300 I =1,3
        NDIS = (NE-1)*2+I
        PATANG(1,NDIS) = T(1,I)
        PATANG(2,NDIS) = T(2,I)
        PATANG(3,NDIS) = 0.
        PATNOR(1,NDIS) = -T(2,I)
        PATNOR(2,NDIS) = T(1,I)
        PATNOR(3,NDIS) = 0.
      CONTINUE
C
      Evaluating the arclength (1-2) and (2-3) : AL(2)
      CALL CCIEC2(X,AL)
C
      IF (KERROR.GT.0) GO TO 600
      Curvilinear coordinate
C
      DO 400 I =2,3
        NDIS = (NE-1)*2 +I
        SCURV(NDIS) = SCURV(NDIS-1) +AL(I-1)
      CONTINUE
C
      CONTINUE
C
      IF (IOUTG.EQ.0) GO TO 800
      WRITE(NONG,1000)
C
      DO 700 NDIS = 1,NTOTIS
        WRITE(NONG,2000) NDIS,SCURV(NDIS),(PATANG(I,NDIS),I = 1,3),
          & (PATNOR(I,NDIS),I = 1,3)
C
      800 CONTINUE
C
      1000 FORMAT(1H1,////,40X,'* * * P A T H   G E O M E T R Y * * *',//
        & 1X,'NDIS CURV. COOR  T(1) T(2) T(3)  N(1) N(2)  N(3)')//

```

```

C      x(I) : Ith cartesian coordinate
C      Fj(k) : Jth comp. of input field at node k
C
C      *****
C      *
C      * SUBROUTINE GRADIE
C      *
C      *
C      *
C      *
C      *****
C      SUBROUTINE GRADIE(IDIM,F,OU)
C
C      Evaluates the gradient of a scalar field or of a vector field at
C      the nodes of the path.
C
C      Parameters
C      I/ IDIM : Dimension flag of the input field
C           0 : scalar field
C           1 : vector field
C      I/ F : Input field at all nodes
C      O/ OU : Output gradient field at the nodes of the path
C
C      INCLUDE 'post_common'
C
C      DIMENSION F(9,800), OU(9,200), AM(3,3), AU(3,3), AL(3,3), B(3), X(3)
C      DIMENSION GR(3,3,6), GRN(3,3), INEW(3)
C
C      Local array :
C      AM : coeff. matrix -> AM(I,J) = [d N(k)/d c(I)] * X(k)(J)
C      AL,AU : Triang. fact. matr. AM = AL*AU
C      B : RHS -> Bj(I) = [d N(k)/d c(I)] * Fj(k)
C      X : Unknown vect -> Xj(I) = d Fj/d x(I)
C      GR : Gr. at the node ev. for each elt ->
C           GR(J,I,L) = d Fj/d x(I)
C           for elt L
C
C      GRM : mean gr. value at the node -> GRM(J,I) = d Fj/d x(I)
C
C      M(k) : Kth shape function
C      c(I) : Ith isop. coord.
C      X(k)(J) : Jth cart coord of the Kth node
C
C      *****
C      NOTE : max numb. of element at a node : 6 [GR(3,3,6)]
C      *****
C
C      DO 10 N = 1,200
C      DO 10 I = 1,9
C      OU(I,N) = 0.
C
C      DO 20 I = 1,3
C      DO 20 J = 1,3
C      GRM(I,J) = 0.
C      DO 20 N = 1,6
C      GR(I,J,N) = 0.
C
C      MCOMP = EDIM
C      IF(IDIM.EQ.0) MCOMP = 1
C
C      Following the path
C
C      DO 400 NP = 1,NTOTIS
C      DO 100 NE = 1,MCONH(3,NP)
C      NIELC = 5+(NE-1)*3
C      NRP = 6+(NE-1)*3
C      IELC = MCONH(NIELC,NP)
C      KP = MCONH(NRP ,NP)
C
C      Evaluate the coefficient matrix AM
C      CALL GRMAT(IELC,KP,AM)
C
C      LU factorization
C      KER = KERROR
C      CALL LUFACT(KER,3,INOVE,INEW,AM,AU,AL)
C      KERROR = KER
C      IF(KERROR.GT.0) GO TO 500
C
C      Solving the system for all the components of F
C
C      DO 100 ID = 1,MCOMP
C
C      Evaluating the RHS

```



```

C
C
C *****
C *
C *
C *   S U B R O U T I N E   P A T D E F
C *
C *
C *
C *****
C
C SUBROUTINE PATDEF(IFISNO)
C
C Reads input set nodes. Find total number of input set nodes
C
C Parameters
C   0/   IFISNO(10000) :local input-set-number for abaqus nodes
C
C INCLUDE 'post_common'
C DIMENSION IFISNO(10000),NIIMP(15)
C
C NIIS = 0
C READ(NORI,1000) NSET
C DO 100 NS = 1,NSET
C   READ(NORI,2000) IN,(NIIMP(K),K=1,15)
C   IF(IN.NE.O) THEN
C     NI = NIIMP(1)
C     NL = NIIMP(2)
C     NT = 1+(NL-NI)/IN
C     DO 130 NN = 1,NT
C       NIIS = NIIS+1
C       NNAB = NI + (NN-1)*IN
C       NCOMM(1,NIIS) = NNAB
C       IFISNO(NNAB) = NIIS
C     CONTINUE
C   ELSE
C     DO 160 NN=1,15
C       IF(NIIMP(NN).EQ.O) GO TO 160
C       NNAB = NIIMP(NN)
C       NIIS = NIIS +1
C       NCOMM(1,NIIS) = NNAB
C       IFISNO(NNAB) = NIIS
C     CONTINUE
C   ENDIF
C 100 CONTINUE
C   NTOTIS = NIIS

```

```

C
C Check the max number of nodes
C
C IF (NTOTIS.LE.200) GO TO 200
C   ERROR = ERROR +1
C   WRITE(NOWC,3000) NTOTIS
C 200 CONTINUE
C
C 1000 FORMAT(15)
C 2000 FORMAT(16(15))
C 3000 FORMAT(181,///,20X,'* * ERROR IN SBR. PATDEF * *',//,
C   & 10X,'MAX NUMBER OF INPUT SET NODES EXCEEDED',//,
C   & 10X,'TOTAL NUMBER OF I.S. NODES = ',I4,' (MAX: 200)')
C
C RETURN
C END

```



```

      & 10X,'ONLY ELEMENT-TYPE 8 IS IMPLEMENTED',//,
      & 10X,'ELEMENT-TYPE = ',I4)
2000 FORMAT(1H1,////,20X,'* * * ERROR IN FNC.PDSHFN * * *',//,
      & 10X,'THE REQUIRED-COORDINATE-CODE MUST BE 1 (G) OR 2(H)',//,
      & 10X,'REQUIRED COORDINATE CODE = ',I4)
3000 FORMAT(1H1,////,20X,'* * * ERROR IN FNC.PDSHFN * * *',//,
      & 10X,'FOR THIS EL-TYPE THE NODE NUMBER MUST BE BETW. 1 AND 8',//,
      & 10X,'NODE NUMBER = ',I4)
C
      RETURN
      END
C
      SUBROUTINE PRESFN
C
C      Evaluate partial derivative of the shape function at the nodes
      (SFDER)
C
      INCLUDE 'post_common'
      DIMENSION C(3)
C
      DO 50 I = 1,3
50   C(I) = 0.
C
      IT = ITYPE
C
      DO 200 I = 1,NEELT
        DO 100 M = 1,NDIM
          C(M) = DLISCO(I,M,IT)
100   DO 200 K = 1,NEELT
          DO 200 J = 1,NDIM
            SFDER(I,K,J) = PDSHFN(C(1),C(2),C(3),K,J,IT)
200   CONTINUE
C
C
      IF (IOUTG.EQ.0) GO TO 400
      WRITE(NOUTG,1000)
        DO 300 I = 1,NEELT
          DO 300 K = 1,NEELT
            DO 300 J = 1,NDIM
              WRITE(NOUTG,2000) I,K,J,SFDER(I,K,J)
300   CONTINUE
400   CONTINUE
C
1000 FORMAT(1H1,////,40X,'* * * SHAPE FUNCTION DERIVATIVE * * *',//,
      & 1X,'NODE SH.FN J D(SH.NF)/D(COORD.J)',//)
2000 FORMAT(1X,I4,3X,I2,4X,I1,4X,F10.5)

```



```

C          ROW 7      /      /      /      t(2,1)
C          ROW 8      /      /      /      t(3,1)
C          ROW 9      /      /      /      t(3,2)
C
C          INCLUDE 'post_common'
C
C          DIMENSION IALL(7),CURVAR(9,200),OLDVAR(9,200)
C          DIMENSION CURALL(9,800),OLDALL(9,800)
C
C          DO 5 IST = 1,7
C          IALL(IST) = 0
C
C          IF(IGRST(IVAR).LE.1) GO TO 20
C          DO 10 J = 1,IGRST(IVAR)-1
C          IALL(J) = 1
C          20 CONTINUE
C
C          DO 900 NSTEP = 1,NPROC(IVAR)
C          IA = IALL(NSTEP)
C          GO TO (100,200,300,400,500,600) KPRP(NSTEP,IVAR)
C
C          Read from file 8
C          CONTINUE
C          IVCDIM = IVDIM(IVAR)
C          KEY = KAB(IVAR)
C          CALL FSVRIN(MOUT,KEY,IA,CURVAR,CURALL)
C          IF(ERROR.GT.0) GO TO 999
C          GO TO 700
C
C          read variable from data set
C          CONTINUE
C          IVCDIM = IVDIM(IVAR)
C          ID = IVCDIM
C          IV = IVAR
C          CALL DSVRIN(IV,ID,IA,CURVAR,CURALL)
C          IF(ERROR.GT.0) GO TO 999
C          GO TO 700
C
C          Evaluate the gradient of OLDALL : CURVAR = grad(OLDALL)
C
C          300 CONTINUE
C          IF(IVODIM.LE.1) GO TO 350
C          KERROR = KERROR + 1
C          WRITE (NOMC,1000) IVAR,NSTEP
C          GO TO 700
C
C          350 CONTINUE
C          IVCDIM = IVODIM + 1
C          CALL GRADIE(IVODIM,OLDALL,CURVAR)
C          IF(ERROR.GT.0) GO TO 999
C          GO TO 700
C
C          Rotate the reference frame
C          CONTINUE
C          400 CONTINUE
C          IF(IVODIM.GT.0) GO TO 450
C          KERROR = KERROR + 1
C          WRITE (NOMC,2000) IVAR,NSTEP
C          GO TO 700
C          CONTINUE
C          450 CONTINUE
C          IVCDIM = IVODIM
C          CALL ROTATE(IVCDIM,OLDVAR,CURVAR)
C          IF(ERROR.GT.0) GO TO 999
C          GO TO 700
C
C          Evaluate the dot product with the normal to the path
C          CONTINUE
C          500 CONTINUE
C          IF(IVODIM.GT.0) GO TO 550
C          KERROR = KERROR + 1
C          WRITE (NOMC,3000) IVAR,NSTEP
C          GO TO 700
C          CONTINUE
C          550 CONTINUE
C          IVCDIM = IVODIM-1
C          CALL NORPR(IVODIM,OLDVAR,CURVAR)
C          IF(ERROR.GT.0) GO TO 999
C          GO TO 700
C
C          Write CURVAR on file 'postout'
C
C
C

```

```

600          CONTINUE
C
C      CALL VPRINT(MOUT,IVAR,NSTEP,IA,IVCDIM,CURVAR,CURALL)
C
700          CONTINUE
C
      IVODIM = IVCDIM
      DO 800 NC = 1,9
        DO 730 NMS = 1,NTOTIS
          OLDVAR(MC,NMS) = CURVAR(MC,NMS)
        IF(IA.NE.1) GO TO 800
        DO 760 NMLC = 1,NTHOD
          OLDALL(MC,NMLC) = CURALL(MC,NMLC)
        C
800          CONTINUE
900          CONTINUE
C
      DO 950 NMS = 1,NTOTIS
        DO 950 NC = 1,9
          OUTVAR(IVAR,NC,NMS) = CURVAR(MC,NMS)
C
999          CONTINUE
C
1000         FORMAT(1H1,///,2O1,'* * * ERROR IN SBR. PROCES * * *',//,
& 10X,'A GRADIENT STEP IS NOT ALLOWED ON A TENSOR VARIABLE',//,
& 10X,'BAD PROCEDURE FOR VARIABLE N.',I4,' STEP N.',I4)
2000         FORMAT(1H1,///,2O1,'* * * ERROR IN SBR. PROCES * * *',//,
& 10X,'A ROTATION STEP IS NOT ALLOWED ON A SCALAR VARIABLE',//,
& 10X,'BAD PROCEDURE FOR VARIABLE N.',I4,' STEP N.',I4)
3000         FORMAT(1H1,///,2O1,'* * * ERROR IN SBR. PROCES * * *',//,
& 10X,'A NORM. DOT. PROD. STEP IS NOT ALLOWED ON A SCALAR VR.',//,
& 10X,'BAD PROCEDURE FOR VARIABLE N.',I4,' STEP N.',I4)
C
          RETURN
          END

```

```

C
C      *****
C      *
C      *      S U B R O U T I N E  R E S E T V
C      *
C      *
C      *****
C
      SUBROUTINE RESETV
C
      Reset to zero the memory used in the loop over the step/increment
C
      INCLUDE 'post_common'
C
      DO 200 N = 1,200
        DO 200 J=1,9
          DO 200 K=1,10
            OUTVAR(K,J,N) = 0.
          C
200          CONTINUE
C
      RETURN
      END

```

```

C
C
C *****
C *
C *     S U B R O U T I N E   R O T A I E
C *
C *
C *****
C
C     SUBROUTINE ROTATE(I,OLD,CUR)
C
C     Find the components of vector and tensors in a rotated frame with
C     e1 = unit vector tangent to the path (t)
C     e2 = unit vector normal to the path (n)
C     e3 = e1xe2 (z)
C
C     Parameters
C     I/  ID : Dimension flag of the input field
C         1 : vector field
C         2 : tensor field
C     I/  OLD : Input field -> coords in the main cartesian frame
C     O/  CUR : Output field -> coords in the t,n,z frame
C
C     INCLUDE 'post_common'
C     DIMENSION OLD(9,200),CUR(9,200),Q(3,3),Z(3),V(3),T(3,3),TI(3,3)
C     DIMENSION VP(3),TP(3,3),QT(3,3)
C
C     DO 600 NP = 1,NTOTIS
C     DO 100 NR = 1,9
C     CUR(NR,NP) = 0.
C
C     Components of the third axis z normal to t & n (z = t x n)
C
C     Z(1) = PATANG(2,NP)*PATNR(3,NP)-PATANG(3,NP)*PATNR(2,NP)
C     Z(2) = PATANG(3,NP)*PATNR(1,NP)-PATANG(1,NP)*PATNR(3,NP)
C     Z(3) = PATANG(1,NP)*PATNR(2,NP)-PATANG(2,NP)*PATNR(1,NP)
C
C     Store the components of the transformation matrix Q and the
C     transpose QT
C
C     DO 200 NC = 1,3
C     Q(1,NC) = PATANG (NC,NP)
C     Q(2,NC) = PATNR (NC,NP)
C     Q(3,NC) = Z (NC)
C     QT(NC,1) = Q(1,NC)
C
C *****
C
C     QT(NC,2) = Q(2,NC)
C     QT(NC,3) = Q(3,NC)
C
C     CONTINUE
C
C     IF(ID.EQ.2) GO TO 500
C
C     OLD is a vector
C
C     DO 300 I = 1,3
C     V(I) = OLD(I,NP)
C
C     CALL DOTPRO(3,1,2,3,9,3,V,Q,VP)
C
C     DO 400 I = 1,3
C     CUR(I,NP) = VP(I)
C
C     GO TO 600
C
C     CONTINUE
C
C     OLD is a tensor
C
C     T(1,1) = OLD(1,NP)
C     T(2,2) = OLD(2,NP)
C     T(3,3) = OLD(3,NP)
C     T(1,2) = OLD(4,NP)
C     T(1,3) = OLD(5,NP)
C     T(2,3) = OLD(6,NP)
C     T(2,1) = OLD(7,NP)
C     T(3,1) = OLD(8,NP)
C     T(3,2) = OLD(9,NP)
C
C     CALL DOTPRO(3,2,2,9,9,9,I,QT,TI)
C     CALL DOTPRO(3,2,2,9,9,9,Q,TI,TP)
C
C     CUR(1,NP) = TP(1,1)
C     CUR(2,NP) = TP(2,2)
C     CUR(3,NP) = TP(3,3)
C     CUR(4,NP) = TP(1,2)
C     CUR(5,NP) = TP(1,3)
C     CUR(6,NP) = TP(2,3)
C     CUR(7,NP) = TP(2,1)
C     CUR(8,NP) = TP(3,1)
C     CUR(9,NP) = TP(3,2)
C

```

```
C
600 CONTINUE
C
```

```
RETURN
END
```

```
C
C
C *****
C *
C * SUBROUTINE R W P E R M
C *
C *
C *
C *****
C
SUBROUTINE RWPERM(ID,IMOVE,IJNEW,AM,AP,AN)
C
C Change the order of the rows of AM if ZERO elements are on the
C main diagonal.
C
C Parameters:
C I/ ID : matrix dimension
C O/ IMOVE : row permutation code (=1 : row permuted )
C O/ IJNEW : perm. record :IJNEW(J)= old # of new row #J
C I/O AM : square input/output matrix
C / AP : matrix used locally to keep record of non-zero
C pivots
C / AN : matrix used locally to store the new perm. matr.
C
C
C DIMENSION AM(ID,ID),AP(ID,ID),AN(ID,ID),IJNEW(ID)
C
DO 10 IR = 1, ID
IJNEW(IR) = 0
DO 10 IC = 1, ID
AP(IC,IR) = 0.
AN(IC,IR) = 0.
10 CONTINUE
C
IMOVE = 0
PIVMIN = 1.E-06
C
C Check if matrix AM has zero elements on the main diagonal
C
DO 50 IR = 1, ID
IF (ABS(AM(IR,IR)).GE.PIVMIN) GO TO 50
IMOVE = 1
50 CONTINUE
C
IF (IMOVE.EQ.0) GO TO 900
```

```

C
C      Permutation required
C
C      Prepare matrix AP with the position of non-zero pivots and
C      vector INEW with the # of rows which have non-zero pivots
C
C      DO 100 MPIV = 1, ID
C      DO 100 MR = 1, ID
C          IF (ABS(AM(MR, MPIV)).LT. PIVMIN) GO TO 100
C          IPOS = INEW(MPIV)+1
C          INEW(MPIV) = IPOS
C          AP(MPIV, IPOS) = FLOAT(MR)
100      CONTINUE
C
C      Permutation
C      MP = 0
C
C      DO 200 CONTINUE
C
C      DO 700 MPIV = 1, ID
C
C          IF (INEW(MPIV).NE. MP) GO TO 700
C
C          IF (MP.EQ. 0) THEN
C              IMOVE = -1
C              WRITE(13, 1000) MPIV
C              WRITE(13, *) AM
C              GO TO 900
C          ENDIF
C          PIVMAX = PIVMIN
C
C      DO 300 MCP = 1, MP
C          MR = INT(AP(MPIV, MCP))
C          PIVOT = ABS(AM(MR, MPIV))
C          IF (PIVOT.GE. PIVMAX) THEN
C              PIVMAX = PIVOT
C              MRCH = MR
C          ENDIF
300      CONTINUE
C
C          INEW(MPIV) = -MRCH
C          DO 350 MC = 1, ID
C              AM(MPIV, MC) = AM(MRCH, MC)

```

```

C
C      Packing of AP
C
C      DO 600 MR = 1, ID
C          IF (INEW(MR).LT. 0) GO TO 600
C          DO 500 MC = 1, ID
C              IF (INT(AP(MR, MC)).EQ. MRCH) THEN
C                  INEW(MR) = INEW(MR) - 1
C                  DO 400 MLC = MC, ID-1
C                      AP(MR, MLC) = AP(MR, MLC+1)
C                      AP(MR, ID) = 0.
C                  GO TO 600
C              ENDIF
C              CONTINUE
C          CONTINUE
C
C      MP = MP-1
C      GO TO 200
C
C      MP = MP+1
C
C      Check if all the pivot have been found
C
C      INEG = 1
C      DO 750 MR = 1, ID
C          IF (INEW(MR).GT. 0) INEG = 0
C
C      IF (INEG.EQ. 1) GO TO 800
C
C      IF (MP.LE.ID) GO TO 200
C
C      IMOVE = -1
C      WRITE(13, 2000)
C      WRITE(13, *) INEW
C      WRITE(13, 3000)
C      WRITE(13, *) AM
C      WRITE(13, 4000)
C      WRITE(13, *) AP
C      WRITE(13, 5000)
C      WRITE(13, *) AM
C
C      CONTINUE
C
C      DO 850 MR = 1, ID

```

```

C      INEW(NR) = -INEW(NR)
C      DO 850 NC = 1, ID
C      AM(NR, NC) = AM(NR, NC)
C      850 CONTINUE
C      900 CONTINUE
C      1000 FORMAT(1H1,///,20X,'** ERROR IN SBR. RWPERM **',//,
C      & 20X,'NO PIVOT AVAILABLE FOR ROW N.',14,///,
C      & 20X,'INPUT MATRIX AM FOLLOWS',//)
C      2000 FORMAT(1H1,///,20X,'** ERROR IN SBR. RWPERM **',//,
C      & 20X,'P GREATER THAN ID. NP =',14,' ID =',14,///,
C      & 20X,'PERMUTATION RECORD VECTOR INEW FOLLOWS',//)
C      3000 FORMAT(1X,///,20X,'INPUT MATRIX AM FOLLOWS',//)
C      4000 FORMAT(1X,///,20X,'PIVOT MATRIX AP FOLLOWS',//)
C      5000 FORMAT(1X,///,20X,'OUTPUT MATRIX AN FOLLOWS',//)
C      RETURN
C      END
C      *****
C      *
C      * SUBROUTINE SOLVER
C      *
C      *****
C      SUBROUTINE SOLVER(ID, IMOVE, INEW, AU, AL, B, I)
C      Solve the systems  $AL \cdot C = B$  and  $AU \cdot X = C$ 
C      If matrix AM has been permuted, the RHS is permuted too
C      Parameters
C      I/ ID : matrix/vector dimension
C      I/ IMOVE : row permutation code (=1 : row permuted)
C      I/ INEW : perm. record : INEW(J) = old # of new row #J
C      I/ AL : lower triang. matrix AL(ID, ID)
C      I/ AU : upper triang. matrix AU(ID, ID)
C      I/ B : RHS of the system  $AL \cdot AU + X = B$ 
C      O/ X : unknown vector
C      DIMENSION AU(ID, ID), AL(ID, ID), B(ID), X(ID), INEW(ID)
C      Check if rows of AM have been permuted. If YES, permute B
C      CALL CKPERM(ID, IMOVE, INEW, B, X)
C      DO 10 NC = 1, ID
C      X(NC) = 0.
C      Evaluate X ->  $AL \cdot X = B$ 
C      DO 200 NR = 1, ID
C      SUM = 0.
C      IF (NR.EQ.1) GO TO 200
C      DO 100 NC = 1, NR-1
C      SUM = SUM + X(NC) * AL(NR, NC)
C      X(NR) = B(NR) - SUM
C      Copy X in B

```

```

C
C      DO 250 I = 1, ID
C      B(I) = X(I)
250  X(I) = 0.
C
C      Evaluate X -> AU*X = B
C
C      DO 400 NR = ID, 1, -1
C          SUM = 0.
C          IF (NR.EQ.ID) GO TO 400
C          DO 300 NC = NR+1, ID
C              SUM = SUM + X(NC) * AU(NR, NC)
300  X(NR) = (B(NR)-SUM)/AU(NR, NR)
400
C
C      RETURN
C      END

```

```

*****
*
*      S U B R O U T I N E   T A N G 2 D
*
*
*****
SUBROUTINE TANG2D(X,T)
C
C      Evaluates the components of the unit tangent vector at the three
C      subsequent nodes on a side of a 2nd ord. isop 2D elt
C
C      Parameters
C      I/   X : Cartesian coordinate of the nodes
C      O/   T : Cartesian components of the unit tangent vector
C            at the nodes
C
C      NOTE!!! ONLY FOR 2nd ORDER - 8 NODES - ISOPARAMETRIC 2D ELEMENTS
C      =====
C      DIMENSION X(2,3), T(2,3), DXDS(2,3), SQMOD(3)
C
C      First node
C
C      SQMOD(1) = 0.
C      DO 100 I = 1, 2
C          DXDS(I,1) = -1.5 * X(I,1) + 2 * X(I,2) - 0.5 * X(I,3)
100  SQMOD(1) = SQMOD(1) + DXDS(I,1)**2
C
C      second node
C
C      SQMOD(2) = 0.
C      DO 200 I = 1, 2
C          DXDS(I,2) = -0.5 * X(I,1) + 0.5 * X(I,3)
200  SQMOD(2) = SQMOD(2) + DXDS(I,2)**2
C
C      third node
C
C      SQMOD(3) = 0.
C      DO 300 I = 1, 2
C          DXDS(I,3) = 0.5 * X(I,1) - 2 * X(I,2) + 1.5 * X(I,3)

```



```

300 SQMOD(3) = SQMOD(3) + DXDS(I,3)**2
C
DO 400 N = 1,3
DO 400 I = 1,2
400 T(I,N) = DXDS(I,N)/SQRT(SQMOD(N))
C
RETURN
END

*****
*
* SUBROUTINE USRSUB
*
*****
SUBROUTINE USRSUB(MOUT,FILM)
C
Parameter
C
I/ MOUT : Serial number of the current step/increment
I/ FILM : Job name
C
Evaluate the energy momentum tensor with:
C
OUTVAR(1,J,NIIS) = W
OUTVAR(2,J,NIIS) = t
OUTVAR(3,J,NIIS) = du/dn
C
INCLUDE 'post_common'
DIMENSION ENMT(200),T(3),DUDN(3)
CHARACTER*20 FILM
C
WRITE(MORD,1000) NKSTEP(MOUT),NKINCR(MOUT)
WRITE(MOWP(MOUT),4000) FILM,NKSTEP(MOUT),NKINCR(MOUT)
C
C
C
C
DO 100 NIIS = 1,NTOTIS
C
DO 10 K = 1,3
T(K) = OUTVAR(2,K,NIIS)
DUDN(K) = OUTVAR(3,K,NIIS)
CONTINUE
CALL DOTPRO(3,1,1,3,3,1,T,DUDN,PR)
C
WRITE(MORD,3000) OUTVAR(1,1,NIIS),PR
C
ENMT(NIIS) = OUTVAR(1,1,NIIS) - PR

```

```

C          SCOR=SCURV(NNIS)/SCURV(NTOTIS)
C          WRITE(MWP(MOUT),6000) SCOR,ENHIN(NNIS)
C
C
C          1000 FORMAT(1H1,////,20X,'** STEP',I3,' INCR.',I4,' ** ',//,
C          & 10X,'ELAST.EMER.',10X,' T*du/dn ',//)
C          2000 FORMAT(12X,F8.4,T35,E12.5)
C          3000 FORMAT(10X,E12.5,10X,E12.5)
C          4000 FORMAT(1X,'normalized arclength',/,'1X','normal component of the',
C          & ' EMT (MPa)',/,'TYPE 3',/,'LABL 2',/,'.5 .5 .1',/
C          & ' A',/,'.5 .2 .1',/,'NSTEP : ',I2,' NINCR : ',I3,/, 'END')
C          6000 FORMAT(1X,F8.4,2X,E12.5)
C          RETURN
C          END
C
C          SUBROUTINE VPRINT(MOUT,IV,MST,IA,IDIM,VAR,ALL)
C
C          Print the current value of variable IVAR in file 'postout'
C
C          Parameters
C          I/ MOUT : Serial number of the current abqstep/increment
C          I/ IV  : Variable ID number
C          I/ MST : Step number
C          I/ IDIM: Dimension flag of the output field
C
C          0 : scalar field
C          1 : vector field
C          2 : tensor field
C
C          I/ IA  : All-flag
C          IA = 0 -> values to be printed only at path-nodes
C          IA = 1 -> values to be printed at all nodes
C          I/ VAR : Variable values at path nodes
C          I/ ALL : Variable values at all nodes
C
C          INCLUDE 'post-common'
C
C          DIMENSION VAR(9,200),ALL(9,800)
C
C          WRITE (HOWO,1000) IV,MST
C
C          DO 100, NNIS = 1,NTOTIS
C
C          100 WRITE (HOWO,2000) NNIS,NGOEN(1,NNIS),SCURV(NNIS),
C          & (VAR(I,NNIS),I = 1,9)
C
C          IF(IA.EQ.C) GO TO 300
C
C          WRITE(HOWO,3000) IV,MST
C
C          DO 200 NNLC = 1,NTNOD

```

```

C
200 WRITE(NOWO,4000) NMLC,MABAQ(NMLC),(ALL(I,NMLC),I = 1,9)
C
300 CONTINUE
C
1000 FORMAT(1H1,////,1X,T10,'** * V A R I A B L E N . ',I2,
& ' S T E P N . ',I2,' ** *',//,
& 1X,T30,'OUTPUT VARIABLE AT PATH NODES',//,
& 1X,'THIS MAB CURV. COORD ',5X,'11',9X,'22',9X,'33',9X,
& '12',9X,'13',9X,'23',9X,'21',9X,'31',9X,'32',//)
2000 FORMAT(2(I5),F10.5,2X,9(E11.4))
3000 FORMAT(1H1,////,1X,T10,'** * V A R I A B L E N . ',I2,
& ' S T E P N . ',I2,' ** *',//,
& 1X,T30,'OUTPUT VARIABLE AT ALL NODES',//,
& 1X,'NMLC MAB',10X,'11',10X,'22',10X,'33',10X,
& '12',10X,'13',10X,'23',10X,'21',10X,'31',10X,'32',//)
4000 FORMAT(2(I5),5X,9(E12.5))
C
RETURN
END
C
C
C
C
C
C
*****
*
*
* C O M M O N B L O K S O F P R O G R A M P O S T A B Q *
*
*****
Common variables
COMMON / COMM / NCOMM(21,200),IELTOP(17,100),MABAQ(800)
COMMON / COOR / COORDS(3,800)
COMMON / CTRL / NVAR,JSUB,ITYPE,IOUTG,KPSTOP
COMMON / CTRV / KPKP(8,10),IVDIM(10),KAB(10),NPROC(10),IGRST(10)
COMMON / ERRO / KERRDI
COMMON / MUMB / NMBL,MDIM,MTOTIS,MTMOE,MTFLT
COMMON / PATH / PATHOR(3,200),PATANG(3,200),SCURV(200)
COMMON / SHEW / SHEW / SFDER(8,8,2)
COMMON / STEP / NKSTEP(19),NKINCR(19),NTOUT
COMMON / UNIT / NURI,NUWD,NUWC,NUWO,NUWG,NUWP(19)
COMMON / VARI / OUTVAR(10,9,200)
C
C
C
C
C
C

```

**APPENDIX II: THE COMPUTER
PROGRAM DOMAIN**


```

DATA TP12 /',.p12'/
DATA TP13 /',.p13'/
DATA TP14 /',.p14'/
DATA TP15 /',.p15'/
DATA TP16 /',.p16'/
DATA TP17 /',.p17'/
DATA TP18 /',.p18'/
DATA TP19 /',.p19'/

C
PRINT *,',',
PRINT *,',', * * *
PRINT *,',', PROGRAM DOMAIN * * *
PRINT *,',', ABAQUS OUTPUT (FILE 8) MUST BE NAMED Job_name.abq'
PRINT *,',', DOMAIN INPUT FILE MUST BE NAMED Job_name.inp'
PRINT *,',', DOMAIN OUTPUT FILE WILL BE NAMED Job_name.out'
PRINT *,',', DOMAIN CHECK FILE WILL BE NAMED Job_name.chk'
PRINT *,',', DOMAIN GEOM. FILE WILL BE NAMED Job_name.geo'
PRINT *,',', DOMAIN PLOT FILES WILL BE NAMED Job_name.p**'
PRINT *,',',

C
PRINT 1000,' Please enter the Job_name (MAX 20 Char.)'
READ(*,2000) INH,FILE

FILIMP(1:INH) = FILM(1:INH)
FILIMP(INH+1:INH+4) = TIMP(1:4)

FILE_NAME(1:INH) = FILM(1:INH)
FILE_NAME(INH+1:INH+4) = TABQ(1:4)

FILCHK(1:INH) = FILM(1:INH)
FILCHK(INH+1:INH+4) = TCHK(1:4)

FILEOUT(1:INH) = FILM(1:INH)
FILEOUT(INH+1:INH+4) = TOUT(1:4)

FILGEO(1:INH) = FILM(1:INH)
FILGEO(INH+1:INH+4) = TCEO(1:4)

FILPO1(1:INH) = FILM(1:INH)
FILPO1(INH+1:INH+4) = TPO1(1:4)
FILPO2(1:INH) = FILM(1:INH)
FILPO2(INH+1:INH+4) = TPO2(1:4)
FILPO3(1:INH) = FILM(1:INH)
FILPO3(INH+1:INH+4) = TPO3(1:4)

C
DATA TP04(1:INH) = FILM(1:INH)
FILPO4(INH+1:INH+4) = TPO4(1:4)
FILPO5(1:INH) = FILM(1:INH)
FILPO5(INH+1:INH+4) = TPO5(1:4)
FILPO6(1:INH) = FILM(1:INH)
FILPO6(INH+1:INH+4) = TPO6(1:4)
FILPO7(1:INH) = FILM(1:INH)
FILPO7(INH+1:INH+4) = TPO7(1:4)
FILPO8(1:INH) = FILM(1:INH)
FILPO8(INH+1:INH+4) = TPO8(1:4)
FILPO9(1:INH) = FILM(1:INH)
FILPO9(INH+1:INH+4) = TPO9(1:4)
FILP10(1:INH) = FILM(1:INH)
FILP10(INH+1:INH+4) = TP10(1:4)
FILP11(1:INH) = FILM(1:INH)
FILP11(INH+1:INH+4) = TP11(1:4)
FILP12(1:INH) = FILM(1:INH)
FILP12(INH+1:INH+4) = TP12(1:4)
FILP13(1:INH) = FILM(1:INH)
FILP13(INH+1:INH+4) = TP13(1:4)
FILP14(1:INH) = FILM(1:INH)
FILP14(INH+1:INH+4) = TP14(1:4)
FILP15(1:INH) = FILM(1:INH)
FILP15(INH+1:INH+4) = TP15(1:4)
FILP16(1:INH) = FILM(1:INH)
FILP16(INH+1:INH+4) = TP16(1:4)
FILP17(1:INH) = FILM(1:INH)
FILP17(INH+1:INH+4) = TP17(1:4)
FILP18(1:INH) = FILM(1:INH)
FILP18(INH+1:INH+4) = TP18(1:4)
FILP19(1:INH) = FILM(1:INH)
FILP19(INH+1:INH+4) = TP19(1:4)

C
OPEN(UNIT = 10,FILE = FILIMP,STATUS = 'OLD',ERR=10)
GO TO 20
PRINT*,',',
PRINT*,',',
PRINT*,',',Unable to open file : ',FILIMP
PRINT*,',',
PRINT*,',',
PRINT 1000,' Do you want to try again? [y]',
READ (*,2000)INUTIL, RESP
IF (RESP.EQ.'N'.OR.RESP.EQ.'n') STOP
PRINT 1000,' Choose another Job_name ',
READ (*,2000) INH,FILE

```

```

FILP09(1:1:INH) = FILM(1:1:INH)
FILP09(INH+1:INH+4) = TP09(1:4)
FILP09(INH+5:25) = ' ,
FILP10(1:1:INH) = FILM(1:1:INH)
FILP10(INH+1:INH+4) = TP10(1:4)
FILP10(INH+5:25) = ' ,
FILP11(1:1:INH) = FILM(1:1:INH)
FILP11(INH+1:INH+4) = TP11(1:4)
FILP11(INH+5:25) = ' ,
FILP12(1:1:INH) = FILM(1:1:INH)
FILP12(INH+1:INH+4) = TP12(1:4)
FILP12(INH+5:25) = ' ,
FILP13(1:1:INH) = FILM(1:1:INH)
FILP13(INH+1:INH+4) = TP13(1:4)
FILP13(INH+5:25) = ' ,
FILP14(1:1:INH) = FILM(1:1:INH)
FILP14(INH+1:INH+4) = TP14(1:4)
FILP14(INH+5:25) = ' ,
FILP15(1:1:INH) = FILM(1:1:INH)
FILP15(INH+1:INH+4) = TP15(1:4)
FILP15(INH+5:25) = ' ,
FILP16(1:1:INH) = FILM(1:1:INH)
FILP16(INH+1:INH+4) = TP16(1:4)
FILP16(INH+5:25) = ' ,
FILP17(1:1:INH) = FILM(1:1:INH)
FILP17(INH+1:INH+4) = TP17(1:4)
FILP17(INH+5:25) = ' ,
FILP18(1:1:INH) = FILM(1:1:INH)
FILP18(INH+1:INH+4) = TP18(1:4)
FILP18(INH+5:25) = ' ,
FILP19(1:1:INH) = FILM(1:1:INH)
FILP19(INH+1:INH+4) = TP19(1:4)
FILP19(INH+5:25) = ' ,
OPEN(UNIT = 10, FILE = FILIMP, STATUS = 'OLD', ERR=10)
C
20
CONTINUE
C
OPEN(UNIT = 13, FILE = FILCHK)
OPEN(UNIT = 14, FILE = FILOUT)
OPEN(UNIT = 15, FILE = FILGEO)
OPEN(UNIT = 16, FILE = FILP01)
OPEN(UNIT = 17, FILE = FILP02)
OPEN(UNIT = 18, FILE = FILP03)
OPEN(UNIT = 19, FILE = FILP04)

```

```

FILIMP(1:1:INH) = FILM(1:1:INH)
FILIMP(INH+1:INH+4) = TIMP(1:4)
FILIMP(INH+5:25) = ' ,
FILE_NAME(1:1:INH) = FILM(1:1:INH)
FILE_NAME(INH+1:INH+4) = TABQ(1:4)
FILE_NAME(INH+5:25) = ' ,
FILCHK(1:1:INH) = FILM(1:1:INH)
FILCHK(INH+1:INH+4) = TCHK(1:4)
FILCHK(INH+5:25) = ' ,
FILOUT(1:1:INH) = FILM(1:1:INH)
FILOUT(INH+1:INH+4) = TOUT(1:4)
FILOUT(INH+5:25) = ' ,
FILGEO(1:1:INH) = FILM(1:1:INH)
FILGEO(INH+1:INH+4) = TGED(1:4)
FILGEO(INH+5:25) = ' ,
FILP01(1:1:INH) = FILM(1:1:INH)
FILP01(INH+1:INH+4) = TP01(1:4)
FILP01(INH+5:25) = ' ,
FILP02(1:1:INH) = FILM(1:1:INH)
FILP02(INH+1:INH+4) = TP02(1:4)
FILP02(INH+5:25) = ' ,
FILP03(1:1:INH) = FILM(1:1:INH)
FILP03(INH+1:INH+4) = TP03(1:4)
FILP03(INH+5:25) = ' ,
FILP04(1:1:INH) = FILM(1:1:INH)
FILP04(INH+1:INH+4) = TP04(1:4)
FILP04(INH+5:25) = ' ,
FILP05(1:1:INH) = FILM(1:1:INH)
FILP05(INH+1:INH+4) = TP05(1:4)
FILP05(INH+5:25) = ' ,
FILP06(1:1:INH) = FILM(1:1:INH)
FILP06(INH+1:INH+4) = TP06(1:4)
FILP06(INH+5:25) = ' ,
FILP07(1:1:INH) = FILM(1:1:INH)
FILP07(INH+1:INH+4) = TP07(1:4)
FILP07(INH+5:25) = ' ,
FILP08(1:1:INH) = FILM(1:1:INH)
FILP08(INH+1:INH+4) = TP08(1:4)
FILP08(INH+5:25) = ' ,

```

```

OPEN(UNIT = 20,FILE = FILP05)
OPEN(UNIT = 21,FILE = FILP06)
OPEN(UNIT = 22,FILE = FILP07)
OPEN(UNIT = 23,FILE = FILP08)
OPEN(UNIT = 24,FILE = FILP09)
OPEN(UNIT = 25,FILE = FILP10)
OPEN(UNIT = 26,FILE = FILP11)
OPEN(UNIT = 27,FILE = FILP12)
OPEN(UNIT = 28,FILE = FILP13)
OPEN(UNIT = 29,FILE = FILP14)
OPEN(UNIT = 30,FILE = FILP15)
OPEN(UNIT = 31,FILE = FILP16)
OPEN(UNIT = 32,FILE = FILP17)
OPEN(UNIT = 33,FILE = FILP18)
OPEN(UNIT = 34,FILE = FILP19)

```

```

MORI = 10
MOWC = 13
MOWO = 14
MOWG = 15

```

```

MOWP(1) = 16
MOWP(2) = 17
MOWP(3) = 18
MOWP(4) = 19
MOWP(5) = 20
MOWP(6) = 21
MOWP(7) = 22
MOWP(8) = 23
MOWP(9) = 24
MOWP(10) = 25
MOWP(11) = 26
MOWP(12) = 27
MOWP(13) = 28
MOWP(14) = 29
MOWP(15) = 30
MOWP(16) = 31
MOWP(17) = 32
MOWP(18) = 33
MOWP(19) = 34

```

```
KERROR = 0
```

```
Accessing file 8
```

```

MNU = 1
LRUNIT(1,1) = 8
LRUNIT(2,1) = 2
CALL INITPF(MRU,LRUNIT,LOUTF)
JUNIT = 8
CALL DBRMU(JUNIT)
C
C Geometry input. Connectivity matrices
C
C CALL GEDIMP
C
C IF(KERROR.GT.0) GO TO 200
C
C Interface geometry. Curv. coordinate and normal to the interface.
C
C CALL GEDITF
C
C IF(KERROR.GT.0) GO TO 200
C
C Shape function matrices
C
C CALL PRESFM
C
C IF(KERROR.GT.0) GO TO 200
C
C Setting up the coefficient matrix
C
C CALL MATRIX
C
C IF(KERROR.GT.0) GO TO 200
C
C Input the control variables of the procedure
C
C CALL CTRIMP
C
C IF(KERROR.GT.0) GO TO 200
C
C IF(KPSTOP.EQ.1) GO TO 300
C
C Evaluate the normal force for all the step/increment required by user
C
C

```



```

C C
C C
C C *****
C C *
C C *
C C * F U N C T I O N   A L C A L 1
C C *
C C *
C C *****
C C
C C FUNCTION ALCAL1(A,B,C)
C C
C C INCLUDE 'domain_common'
C C
C C Evaluate the integral for -1<X<0 of DSQRT(C*X**2 + B*X + A)
C C
C C IF ( C ) 100,200,300
C C
C C
C C Negative C
C C
C C 100 CONTINUE
C C
C C TERM1 = B*(DSQRT(A))-(B-2*C)*DSQRT(A-B+C)
C C DELTA = B**2 - 4*A*C
C C TERM2 = (DELTA/(2*DSQRT(-C)))*(DSIN(B/(DSQRT(DELTA))))-
C C *          DSIN((B-2*C)/(DSQRT(DELTA))))
C C *
C C
C C *****
C C *
C C * F U N C T I O N   A L C A L 2
C C *
C C *
C C *****
C C
C C FUNCTION ALCAL2(A,B,C)
C C
C C INCLUDE 'domain_common'
C C
C C Evaluate the integral for 0<X<1 of DSQRT(C*X**2 + B*X + A)
C C
C C IF ( C ) 100,200,300
C C
C C
C C Negative C
C C
C C 100 CONTINUE
C C
C C TERM1 = (B+2*C)*DSQRT(A+B+C)-B*(DSQRT(A))

```

```

C C
C C Positive C
C C
C C 300 CONTINUE
C C
C C TERM1 = B*(DSQRT(A))-(B-2*C)*DSQRT(A-B+C)
C C TERM2 = ((4*A*C-B**2)/(2*DSQRT(C)))*DLOG((2*DSQRT(C*A)+B);
C C *          (2*DSQRT(C*(A-B+C))-2*C*B))
C C *

```

```

C C
C C ALCAL1 = (TERM1+TERM2) / (4*C)
C C
C C 400 CONTINUE
C C
C C RETURN
C C END

```

```

C
C      DELTA = B**2 - 4*A*C
C      TERM2 = (DELTA/(2*DSQRT(-C)))*(DSIN((B+2*C)/(DSQRT(DELTA))))-
C      *      DSIN(B/(DSQRT(DELTA)))
C
C      ALCAL2 = (TERM1 +TERM2) / (4*C)
C
C      GO TO 400
C
C      Zero C
C
C      200 CONTINUE
C      IF(B.EQ.0) ALCAL2 = DSQRT(A)
C      IF(B.NE.0) ALCAL2 = (2*((A+B)**1.5-A**1.5))/(3*B)
C
C      GO TO 400
C
C      Positive C
C
C      300 CONTINUE
C      TERM1 = (B+2*C)*DSQRT(A+B+C)-B*(DSQRT(A))
C      TERM2 = ((4*A*C-B**2)/(2*DSQRT(C)))*
C      *      DLOG((2*DSQRT(C*(A+B+C))+2*C+B)/(2*DSQRT(C*A)+B))
C
C      ALCAL2 = (TERM1+TERM2) / (4*C)
C
C      400 CONTINUE
C      RETURN
C      END

```

```

*****
*
*      S U B R O U T I N E   B Q C A L C
*
*****

```

SUBROUTINE BQCALC(IT)

Evaluates the quadratic form BQUAD(3,3,3).

BQUAD(i,j,k) = Integr[-1 +1] (Mi*j+dMk/dr *dr)

Parameters

I/ IT: Element type

8 : 2D - 8 nodes isop. element

NOTE!!! ONLY FOR 2nd ORDER - 8 NODES - ISOPARAMETRIC 2D ELEMENTS

INCLUDE 'domain_common'

IF (IT.EQ.8) GO TO 100

KERROR = KERROR + 1

WRITE(MWC,1000) IT

GO TO 200

CONTINUE

BQUAD(1,1,1) = 1./3.

BQUAD(1,1,2) = -2./5.

BQUAD(1,1,3) = 1./15.

BQUAD(2,2,1) = 8./15.

BQUAD(2,2,2) = -0.

BQUAD(2,2,3) = -8./15.

BQUAD(3,3,1) = -1./15.

BQUAD(3,3,2) = 2./5.

BQUAD(3,3,3) = -1./3.

BQUAD(1,2,1) = 1./5.

BQUAD(2,1,1) = 1./5.

BQUAD(1,2,2) = -4./15.

BQUAD(2,1,2) = -4./15.

BQUAD(1,2,3) = 1./15.

```

C          BQUAD(2,1,3) = 1./15.
C          BQUAD(1,3,1) = -1./30
C          BQUAD(3,1,1) = -1./30
C          BQUAD(1,3,2) = 0.
C          BQUAD(3,1,2) = 0.
C          BQUAD(1,3,3) = 1./30
C          BQUAD(3,1,3) = 1./30
C          BQUAD(2,3,1) = -1./15.
C          BQUAD(3,2,1) = -1./15.
C          BQUAD(2,3,2) = 4./15.
C          BQUAD(3,2,2) = 4./15.
C          BQUAD(2,3,3) = -1./5.
C          BQUAD(3,2,3) = -1./5.
C
C 200 CONTINUE
C
C 1000 FORMAT(1H1,///,20X,'** * ERROR IN SER.BQCALC * * *',//,
& 10X,'ONLY ELEMENT-TYPE 8 IS IMPLEMENTED',//,
& 10X,'ELEMENT-TYPE = ',I4)
C
C      RETURN
C      END
C
C          BQUAD(2,1,3) = 1./15.
C          BQUAD(1,3,1) = -1./30
C          BQUAD(3,1,1) = -1./30
C          BQUAD(1,3,2) = 0.
C          BQUAD(3,1,2) = 0.
C          BQUAD(1,3,3) = 1./30
C          BQUAD(3,1,3) = 1./30
C          BQUAD(2,3,1) = -1./15.
C          BQUAD(3,2,1) = -1./15.
C          BQUAD(2,3,2) = 4./15.
C          BQUAD(3,2,2) = 4./15.
C          BQUAD(2,3,3) = -1./5.
C          BQUAD(3,2,3) = -1./5.
C
C *****
C *
C *           S U B R O U T I N E   C C I N C 2
C *
C *****
C
SUBROUTINE CCINC2(X,AL)
C
C Evaluates the arclength AL(2) between three side-nodes of a second
order 2D isoparametric element.
C
Parameters
I/    X(2,3) : cartesian coordinates of the three nodes
O/    AL(2) : arclength
      AL(1) = node1-node2
      AL(2) = node2-node3
C
INCLUDE 'domain_common'
DIMENSION X(2,3),AL(2),IX(2,3,3)
DO 100 M = 1,2
DO 100 I = 1,3
DO 100 J = 1,3
C      IX(M,I,J) = X(M,I)*X(M,J)
C
Evaluating the constants A,B,C
A = 0.
B = 0.
C = 0.
DO 200 I = 1,2
A = A + 0.25*IX(I,1,1) + 0.25*IX(I,3,3) - 0.5*IX(I,1,3)
B = B - IX(I,1,1) + IX(I,3,3) + 2*IX(I,1,2)
& - 2*IX(I,2,3)
C

```

```

C
      C = C +      XX(I,1,1) +      4*XX(I,2,2) +      XX(I,3,3)      C
      *      -      4*XX(I,1,2) +      2*XX(I,1,3) -      4*XX(I,2,3)
200 CONTINUE
C
C
C
      Check the values of A,B,C (MUST BE C**2+B**2+A > 0 FOR -1<X<1)
C
      RLAG = 0.
      RSMAL = 0.
C
      DELTA = B**2 - 4*A*C
      IF(DELTA.LE.0.OR.C.LE.0) GO TO 220
      RLAG = (B+DSQRT(DELTA))/(2*C)
      RSMAL = (B-DSQRT(DELTA))/(2*C)
C
220 CONTINUE
C
      IF( (A.LT.0) .OR.
      * ((-C-B).GT.A) .OR.
      * (C.GT.0.AND.DELTA.GT.0.AND.B.GT.0.AND.RSMAL.LT.1) .OR.
      * (C.GT.0.AND.DELTA.GT.0.AND.B.LT.0.AND.RLAG.GT.-1)) GO TO 250
      GO TO 300
C
250 CONTINUE
      WRITE (NWC,1000) A,B,C,X
      KERRR = KERRR +1
      GO TO 400
C
300 CONTINUE
C
      AL(1) = ALCAL1(A,B,C)
      AL(2) = ALCAL2(A,B,C)
C
400 CONTINUE
C
1000 FORMAT(1H1,///,20X,'** ERROR IN SBR. CCINC2 * * *',/,
      * 20X,' BAD VALUES FOR CONSTANTS A,B,C',/,
      * 20X,' A = ',E12.5,' B = ',E12.5,' C = ',E12.5,/,
      * 20X,' NODE COORDINATES ARE :',/
      * 20X,'          X1          X2 ',
      * /,20X,' NODE1',2(6X,F10.5),/,
      * 20X,' NODE2',2(6X,F10.5),/,
      * 20X,' NODE3',2(6X,F10.5),/
)
      RETURN
      END

```

```

C
C
C *****
C *
C * SUBROUTINE CHKINTF
C *
C *
C *****
C
C SUBROUTINE CHKINTF
C
C Check for the double nodes on the interf. if the coords are the same
C
C INCLUDE 'domain_common'
C
C SMALL = 1.D-20
C
C DO 100 NNIS = 1, NTOTIS
C   NMLC1 = MCONH(2,1,NNIS)
C   NMLC2 = MCONH(2,2,NNIS)
C   ABSDIF = DABS(COORDS(MD,NMLC1) - COORDS(MD,NMLC2))
C   IF(ABSDIF.LT.SMALL) GO TO 100
C   KERROR = KERROR +1
C   WRITE(MOWC,1000)NNIS,MD,MCONH(1,1,NNIS),MCONH(1,2,NNIS)
C   100 CONTINUE
C
C 1000 FORMAT(1H1,/,/,20X,'* * WARNING OF SBR. CHKINTF * * *,/,/,
C   & 10X,'THE ', I3,'th NODES OF THE INTERFACE DO NOT HAVE THE SAME',
C   & 1X,I3,' COORDINATE ',/,/,10X,'ABAQUS NODE # ',I5,' AND ',I5)
C
C RETURN
C END
C

C
C *****
C *
C * SUBROUTINE CHKSET
C *
C *
C *****
C
C SUBROUTINE CHKSET(ISET,MAB,MLC)
C
C Find the local identity number
C
C Parameters
C   I/   ISET : Set flag
C          ISET = 0 : Element set
C          ISET = 1 : Node input set
C          ISET = 2 : Node set
C   I/   MAB : Abaqus number
C   0/   MLC : Local number: MLC =
C          IELC (ISET = 0)
C          +/- NNIS (ISET = 1)
C          NMLC (ISET = 2)
C          MLC = 0 if the node/elt doesn't
C             belong to the set
C
C INCLUDE 'domain_common'
C
C MLC = 0
C
C GO TO (100,200) ISET
C
C Element set
C
C DO 50 IE = 1, NTELT
C   IF (IELTOP(1,IE).NE.MAB)GO TO 50
C   MLC = IE
C   GO TO 300
C
C CONTINUE
C GO TO 300
C
C
C

```

```

C   Mode input set
C
C   100 CONTINUE
C
C   DO 150 NNIS = 1,NTOTIS
C   DO 150 ISIDE = 1,IDOUBL
C     IF(MCORN(1,ISIDE,NNIS).NE.NAB) GO TO 150
C     MLC = NNIS
C     IF(ISIDE.EQ.1) MLC = -NNIS
C     GO TO 300
C   150 CONTINUE
C     GO TO 300
C
C   Mode set
C
C   200 CONTINUE
C
C   DO 250 IM = 1,IMTHOD
C     IF(MABAQ(IM).NE.NAB) GO TO 250
C     MLC = IM
C     GO TO 300
C   250 CONTINUE
C
C   300 CONTINUE
C     RETURN
C     END
C
C
C   Mode input set
C
C   *****
C   *
C   * SUBROUTINE CKPERM
C   *
C   *****
C
C   SUBROUTINE CKPERM(ID,IMOVE,INEW,B,Z)
C
C   Check if in the matrix AM rows have been permuted. If yes(IMOVE=1)
C   it permutes the Right Hand Side B according to the order given by
C   vector INEW
C
C   INCLUDE 'domain_common'
C
C   DIMENSION INEW(ID),B(ID),X(ID)
C
C   IF(IMOVE.NE.1) GO TO 500
C
C     DO 100 NR = 1,ID
C       X(NR) = B(INEW(NR))
C     DO 200 NR = 1,ID
C       B(NR) = X(NR)
C
C   500 CONTINUE
C
C   RETURN
C   END
C

```



```

      MCONB(KP, ISIDE, NNIS) = IEAB
      MCONB(KP+1, ISIDE, NNIS) = ITEL
      MCONB(KP+2, ISIDE, NNIS) = II
    C
    100 CONTINUE
    C
      IA = 2+(NN-1)*2
      IELTOP(IA, ITEL) = IIAB
      IELTOP(IA+1, ITEL) = IDOME(IIAB)
    200 CONTINUE
      ITEL = ITEL + 1
    C
    C Check max number of elt's (1000) and nodes (3200)
    C
    C IF(I TELT.LT.1000.AND.MTHOD.LT.3200) GO TO 500
      WRITE(MONG, 2000) ITEL, MTHOD
      GO TO 600
    C
    500 CONTINUE
    600 CONTINUE
    C ITEL = ITEL - 1
    C
    700 CONTINUE
    C IF (IDOUTG.EQ.0) GO TO 900
    C
    800 ISIDE = 1, IDOUBL
      WRITE(MONG, 3000) ISIDE
    C
    900 NNIS = 1, NTOTIS
      IMAX = MCONB(3, ISIDE, NNIS)*3+3
      WRITE(MONG, 4000) NNIS, (MCONB(I, ISIDE, NNIS), I=1, IMAX)
    750 CONTINUE
    C
      WRITE(MONG, 5000)
    C
    800 IELC = 1, ITEL
      IMAX = IELT+2 + 1
      WRITE(MONG, 6000) IELC, (IELTOP(I, IELC), I = 1, IMAX)
    C
      WRITE(MONG, 7000)
    C

```

```

      MAPPO = (MTHOD-1)/8+1
      DO 850 NROW = 1, MAPPO
      NF = (NROW-1)*8
    850 WRITE(MONG, 8000) (NF+K, MABAQ(NF+K), K = 1, 8)
    C
    900 CONTINUE
    C
    1000 FORMAT(1H1, ///, 20X, ' * * ERROR IN SBR. CONNEC * * * ', //,
      & 10X, 'MAX NUMBER OF ELEMENTS CONNECTED TO ONE NODE EXCEEDED', //,
      & 10X, 'MORE THAN 6 ELEMENTS ARE CONNECTED TO NODE ', I4,
      & 10X, 'MAX NUMBER OF ELEMENTS and/or NODES EXCEEDED', //,
      & 10X, 'TOTAL NUMBER OF READ ELEMENTS = ', I4, ' (MAX: 1000)', //,
      & 10X, 'TOTAL NUMBER OF READ NODES = ', I4, ' (MAX: 3200)', //,
      & 40X, ' * * * I S I D E = ', I2, ' * * * ', //,
      & 1X, 'NNIS NNAB NNLC NBE IAB1 LC1 P1 IAB2 LC2 P2 IAB3 LC3 P3 ',
      & 1AB4 LC4 P4 IAB5 LC5 P5 IAB6 LC6 P6', /)
    4000 FORMAT(1X, I3, 2X, I4, 1X, I3, 1X, I3, 6(1X, I4, 1X, I3, 1X, I2))
    5000 FORMAT(1H1, ///, 40X, ' * * * I E L T O P * * * ', //,
      & 1X, 'IELC IEAB IAB1 ILC1 IAB2 ILC2 IAB3 ILC3 IAB4 ILC4 IAB5 ',
      & 1X, 'IELC IAB6 ILC6 IAB7 ILC7 IAB8 ILC8', /)
    6000 FORMAT(18(1X, I4))
    7000 FORMAT(1H1, ///, 40X, ' * * * N A B A Q * * * ', //,
      & 1X, 8('NNLC NNAB '), /)
    8000 FORMAT(8(2(1X, I4), 1X))
    C
    C RETURN
    C END

```

```

C
C
C *****
C *
C * SUBROUTINE CTRIMP
C *
C *
C *****
C
C SUBROUTINE CTRIMP
C
C Reads the control variables of the procedure
C
C INCLUDE 'domain_common'
C
C READ(NORI,3000) NCNTOU
C
C DO 100 ISIDE = 1,2
C
C 100 READ(NORI,4000) (MLAYER(ISIDE,NCOUNT),NCOUNT = 1,10)
C
C Check the maximum number of contour and layers
C
C IF(NCNTOU.LE.10) GO TO 200
C   KERROR = KERROR +1
C   WRITE(NOWC,1000) NCNTOU
C   GO TO 400
C 200 CONTINUE
C
C DO 300 J = 1,NCNTOU
C DO 300 I = 1,2
C   IF(MLAYER(I,J).LE.15) GO TO 300
C   KERROR = KERROR +1
C   WRITE(NOWC,2000) J,I,MLAYER(I,J)
C 300 CONTINUE
C
C READ(NORI,5000) NTOUT,ICREEP
C
C DO 350 MOUT = 1,NTOUT
C 350 READ(NORI,5000) NKSTEP(MOUT),MAXMCR(MOUT)
C
C 400 CONTINUE
C
1000 FORMAT(1H1,///,20X,'* * * ERROR IN SBR. CTRIMP * * *',//,
* 10X,'MAXIMUM NUMBER OF CONTOUR EXCEEDED (MAX = 10)',//,
* 10X,'REQUIRED NUMBER OF CONTOUR = ',I4)
2000 FORMAT(1H1,///,20X,'* * * ERROR IN SBR. CTRIMP * * *',//,
* 10X,'MAXIMUM NMB. OF LAY. PER CONTOUR EXCEEDED (MAX = 15)',//,
* 10X,'LAYER',I4,' ISIDE',I4,' REQUIRED NUMBER OF LAYERS = ',I4)
3000 FORMAT(15)
4000 FORMAT(10(I5))
5000 FORMAT(2(I5))
C
RETURN
END

```

```

C
C
C *****
C *
C *
C * F U N C T I O N   D L I S C O
C *
C *
C *****
C
C
C FUNCTION DLISCO(L,K,J,I,IR)
C
C Evaluates the dimensionless isoparametric coordinates of the nodes
C and of the integration points
C
C Parameters
C   L : identity flag: 0-> node 1-> int.pt.
C   K : node/int.pt number
C   J : required coordinate
C       1 : G
C       2 : H
C       3 : R
C
C   I : Element type
C       8 : 2D - 8 nodes isop. element
C
C   IR: Reduced integration flag
C       0 : full integration (9 i.p.)
C       1 : reduced integration (4 i.p.)
C
C NOTE!!! ONLY FOR 2nd ORDER - 8 NODES - ISOPARAMETRIC 2D ELEMENTS
C =====
C
C INCLUDE 'domain_common'
C
C DLISCO = 0.
C FIV = .577350269189626
C SEV = .774596669241483
C
C IF ( I.EQ.8) GO TO 100
C   KERROR = KERROR + 1
C   WRITE(MWC,1000) I
C   GO TO 900
C
C 100 CONTINUE
C
C IF (L.EQ.1) GO TO 400
C
C   node coords
C
C   GO TO (200,300) J
C   KERROR = KERROR + 1
C   WRITE(MWC,2000) J
C   GO TO 900
C
C   First coordinate : G
C
C 200 CONTINUE
C
C   GO TO (210,220,230,240,250,260,270,280) K
C
C   KERROR = KERROR + 1
C   WRITE(MWC,3000) K
C   GO TO 900
C
C 210 CONTINUE
C   DLISCO = -1.
C   GO TO 900
C
C 220 CONTINUE
C   DLISCO = 1.
C   GO TO 900
C
C 230 CONTINUE
C   DLISCO = 1.
C   GO TO 900
C
C 240 CONTINUE
C   DLISCO = -1.
C   GO TO 900
C
C 250 CONTINUE
C   DLISCO = 0.
C   GO TO 900
C
C 260 CONTINUE
C   DLISCO = 1.
C   GO TO 900
C
C 270 CONTINUE
C   DLISCO = 0.

```

```

C          GO TO 900
C 280 CONTINUE
C       DLISCO = -1.
C       GO TO 900
C
C       Second coordinate : H
C 300 CONTINUE
C       GO TO (310,320,330,340,350,360,370,380) K
C
C       ERROR = KERROR + 1
C       WRITE(MWC,3000) K
C       GO TO 900
C
C 310 CONTINUE
C       DLISCO = -1.
C       GO TO 900
C
C 320 CONTINUE
C       DLISCO = -1.
C       GO TO 900
C
C 330 CONTINUE
C       DLISCO = 1.
C       GO TO 900
C
C 340 CONTINUE
C       DLISCO = 1.
C       GO TO 900
C
C 350 CONTINUE
C       DLISCO = -1.
C       GO TO 900
C
C 360 CONTINUE
C       DLISCO = 0.
C       GO TO 900
C
C 370 CONTINUE
C       DLISCO = 1.
C       GO TO 900
C
C 380 CONTINUE

```

```

DLISCO = 0.
GO TO 900
C 400 CONTINUE
C       integration points coords
C       IF(IR.EQ.1) GO TO 700
C       Full integration
C       GO TO (500,600) J
C       KERROR = KERROR + 1
C       WRITE(MWC,2000) J
C       GO TO 900
C
C       First coordinate : G
C 500 CONTINUE
C       GO TO (510,520,530,540,550,560,570,580,590) K
C
C       KERROR = KERROR + 1
C       WRITE(MWC,4000) K
C       GO TO 900
C
C 510 CONTINUE
C       DLISCO = -SEV
C       GO TO 900
C
C 520 CONTINUE
C       DLISCO = 0.
C       GO TO 900
C
C 530 CONTINUE
C       DLISCO = SEV
C       GO TO 900
C
C 540 CONTINUE
C       DLISCO = -SEV
C       GO TO 900
C
C 550 CONTINUE
C       DLISCO = 0.
C       GO TO 900

```

```

C 560 CONTINUE
      DLISCO = SEV
      GO TO 900
C
C 570 CONTINUE
      DLISCO = -SEV
      GO TO 900
C
C 580 CONTINUE
      DLISCO = 0.
      GO TO 900
C
C 590 CONTINUE
      DLISCO = SEV
      GO TO 900
C
C      Second coordinate : H
C 600 CONTINUE
      GO TO (610,620,630,640,650,660,670,680,690) K
C
      KERROR = KERROR + 1
      WRITE(NWC,4000) K
      GO TO 900
C
C 610 CONTINUE
      DLISCO = -SEV
      GO TO 900
C
C 620 CONTINUE
      DLISCO = -SEV
      GO TO 900
C
C 630 CONTINUE
      DLISCO = -SEV
      GO TO 900
C
C 640 CONTINUE
      DLISCO = 0.
      GO TO 900
C
C 650 CONTINUE
      DLISCO = 0.
      GO TO 900
C
      GO TO 900
C
C 660 CONTINUE
      DLISCO = 0.
      GO TO 900
C
C 670 CONTINUE
      DLISCO = SEV
      GO TO 900
C
C 680 CONTINUE
      DLISCO = SEV
      GO TO 900
C
C 690 CONTINUE
      DLISCO = SEV
      GO TO 900
C
C 700 CONTINUE
      Reduced integration
      GO TO (800,850) J
      KERROR = KERROR + 1
      WRITE(NWC,2000) J
      GO TO 900
C
C      First coordinate : G
C 800 CONTINUE
      GO TO (810,820,830,840) K
C
      KERROR = KERROR + 1
      WRITE(NWC,5000) K
      GO TO 900
C
C 810 CONTINUE
      DLISCO = -FIV
      GO TO 900
C
C 820 CONTINUE
      DLISCO = FIV
      GO TO 900
C

```

```

830 CONTINUE
DLISCO = -FIV
GO TO 900
C
840 CONTINUE
DLISCO = FIV
GO TO 900
CC
C Second coordinate : H
C
850 CONTINUE
C GO TO (860,870,880,890) K
C
      KERROR = KERROR + 1
      WRITE(MOWC,5000) K
      GO TO 900
C
860 CONTINUE
DLISCO = -FIV
GO TO 900
C
870 CONTINUE
DLISCO = -FIV
GO TO 900
C
880 CONTINUE
DLISCO = FIV
GO TO 900
C
890 CONTINUE
DLISCO = FIV
GO TO 900
C
900 CONTINUE
C
1000 FORMAT(1H1,///,20X,'*** ERROR IN FWC.DLISCO ***',//,
& 10X,'ONLY ELEMENT-TYPE 8 IS IMPLEMENTED',//,
& 10X,'ELEMENT-TYPE = ',I4)
2000 FORMAT(1H1,///,20X,'*** ERROR IN FWC.DLISCO ***',//,
& 10X,'THE REQUIRED-COORDINATE-CODE MUST BE 1 (G) OR 2(H)',//,
& 10X,'REQUIRED COORDINATE CODE = ',I4)
3000 FORMAT(1H1,///,20X,'*** ERROR IN FWC.DLISCO ***',//,
& 10X,'FOR THIS EL-TYPE THE MODE NUMBER MUST BE BETW. 1 AND 8',//,
& 10X,'MODE NUMBER = ',I4)
4000 FORMAT(1H1,///,20X,'*** ERROR IN FWC.DLISCO ***',//,
& 10X,'FOR THIS EL-TYPE THE IT.P NUMBER MUST BE BETW. 1 AND 9',//,
& 10X,'IT.P NUMBER = ',I4)
5000 FORMAT(1H1,///,20X,'*** ERROR IN FWC.DLISCO ***',//,
& 10X,'FOR THIS EL-TYPE THE IT.P NUMBER MUST BE BETW. 1 AND 4',//,
& 10X,'IT.P NUMBER = ',I4)
C RETURN
C END
C

```



```

C *****
C *
C *
C *      S U B R O U T I N E  F 8 I P I N
C *
C *
C *****
C SUBROUTINE F8IPIIN(MOUT,KREQ,VARELT)
C
C Read variable data from Abaqus-file 8 at element integration points
C
C Parameters
C I/ MOUT : Serial number of the required step/increment
C I/ KREQ : Abaqus file 8-read-key for the required variable
C O/ VARELT: Variable values at integration points
C
C VARELT(I,J,K) = value of the Ith component
C               at int. pt. J
C               of element K
C
C the components of the variable are stored as :
C
C          scalar      vector      tensor
C ROW 1          a          v(1)          t(1,1)
C ROW 2          /          v(2)          t(2,2)
C ROW 3          /          v(3)          t(3,3)
C ROW 4          /          /          t(1,2)
C ROW 5          /          /          t(1,3)
C ROW 6          /          /          t(2,3)
C ROW 7          /          /          t(2,1)
C ROW 8          /          /          t(3,1)
C ROW 9          /          /          t(3,2)
C
C INCLUDE 'domain_common'
C
C DOUBLE PRECISION ARRAY
C DIMENSION JV(9,1000),JRRAY(2,513)
C DIMENSION JV(9,1000),VECT(9),VARELT(9,9,1000)
C EQUIVALENCE (ARRAY(4),JRRAY(1,1))
C
C DO 10 K=1,1000
C DO 10 J= 1,9
C     JV(J,K) = 0
10

```

```

C Revind file 8

```

```

C CALL DBFILE(2,ARRAY,JRCD)

```

```

C Scanning file 8

```

```

C DO 300 K = 1,999999

```

```

C CALL DBFILE(O,ARRAY,JRCD)

```

```

C IF(JRCD.ME.O) GO TO 350

```

```

C LR = JRRAY(1,1)

```

```

C KEY = JRRAY(1,2)

```

```

C Finding the right step/increment

```

```

C IF (KEY.ME.2000) GO TO 330

```

```

C MST = JRRAY(1,8)

```

```

C MIM = JRRAY(1,9)

```

```

C IF(MKSTEP(MOUT).ME.MST.OR.MKINCR(MOUT).ME.MIM) GO TO 330

```

```

C JF = 1

```

```

C DO 300 KK = 1,999999

```

```

C CALL DBFILE(O,ARRAY,JRCD)

```

```

C IF(JRCD.ME.O) GO TO 350

```

```

C LR = JRRAY(1,1)

```

```

C KEY = JRRAY(1,2)

```

```

C IF(KEY.EQ.2001) GO TO 350

```

```

C IEAB = JRRAY(1,3)

```

```

C IP = JRRAY(1,4)

```

```

C ILOC = JRRAY(1,6)

```

```

C IF(KEY.ME.1.OR.ILOC.ME.O) GO TO 300

```

```

C The subsequent record of file 8 contains
C values at integration points of elt IEAB

```

```

C CALL DBFILE(O,ARRAY,JRCD)

```

```

C LR = JRRAY(1,1)

```

```

C KEY = JRRAY(1,2)

```

```

C IF(KEY.ME.KREQ) GO TO 300

```

```

C Fill VARELT

```

```

C CALL FILLIN(KREQ,LR,ARRAY,VECT)

```



```

150      CALL CHKSET(O,I EAB,I ELC)
160      IF (I ELC.GT.O) GO TO 150
170      WRITE(MWC,2000) I EAB
180      GO TO 300
190      CONTINUE
200      DO 200 I = 1,9
210      VARELT(I,IP,I ELC) = VECT(I)
220      JV(IP,I ELC) = 1
230
240
250      CONTINUE
260      CONTINUE
270      CONTINUE
280      CONTINUE
290
300      Check if the required step/incr has been found
310
320
330      IF(JF.EQ.1) GO TO 400
340      KERRR = KERRR +1
350      WRITE(MWC,3000) MKNCR(MOUT),MNSTP(MOUT)
360      CONTINUE
370
380      Check if all int.pts. have been found
390
400
410      DO 500 K = 1,MELT
420      DO 500 J = 1,MINTP
430      IF(JV(J,K).EQ.1) GO TO 500
440      KERRR = KERRR +1
450      WRITE(MWC,1000) J,IELTOP(1,K),AREQ
460      CONTINUE
470
480      CONTINUE
490
500      FORMAT(1H1,///,20X,'** ERROR IN SBR. FSIPII **',//,
510      & 10X,'INT. PT. ',I4,' OF ELT',I4,' HAS NOT BEEN FOUND',
520      & ' FOR KEY = ',I4)
530      FORMAT(1H1,///,20X,'** *WARNING OF SBR. FSIPII * *',//,
540      & 10X,'LOCAL NUMBER OF THE ELEMENT',I4,' HAS NOT BEEN FOUND')
550      FORMAT(1H1,///,20X,'** ERROR IN SBR. FSIPII * *',//,
560      & 10X,'INCREMENT ',I4,' OF STEP',I4,' HAS NOT BEEN FOUND')
570
580      RETURN
590      END
600
610
620
630
640
650
660
670
680
690
700
710
720
730
740
750
760
770
780
790
800
810
820
830
840
850
860
870
880
890
900
910
920
930
940
950
960
970
980
990

```

```

*****
*
*          S U B R O U T I N E   F 8 M O I H
*
*****
SUBROUTINE F8MOIH(MOUT,AREQ,VARMGD)
Read variable data at nodes from Abaqus-file 8
Parameters
I/ MOUT : Serial number of the required step/increment
I/ AREQ : Abaqus file 8-read-key for the required variable
O/ VARMOD: Variable values at all nodes
VARMOD(I,J) = value of the Ith component
             at node J
the components of the variable are stored as :

```

ROW	scalar	vector	tensor
ROW 1	a	v(1)	t(1,1)
ROW 2	/	v(2)	t(2,2)
ROW 3	/	v(3)	t(3,3)
ROW 4	/	/	t(1,2)
ROW 5	/	/	t(1,3)
ROW 6	/	/	t(2,3)
ROW 7	/	/	t(2,1)
ROW 8	/	/	t(3,1)
ROW 9	/	/	t(3,2)

```

INCLUDE 'domain_common'
DOUBLE PRECISION ARRAY
DIMENSION ARRAY(513),JRRAY(2,513)
DIMENSION JV(3200),VARMOD(9,3200),VECT(9)
EQUIVALENCE (ARRAY(1),JRRAY(1,1))
DO 10 K=1,3200
JV(K) = 0

```

```

C      start from here if nodal variable is required
C
C      50
C      CONTINUE
C      IF(KEY.NE.KREQ) GO TO 300
C
C      Fill VARNOD
C      CALL FILLIN(KREQ,LR,ARRAY,VECT)
C      CALL CHKSET(2,MMAB,NNLC)
C      IF (NNLC.GT.0) GO TO 100
C      WRITE(MOWC,1000) MMAB
C      GO TO 300
C      CONTINUE
C      DO 200 I = 1,9
C      VARNOD(I,NNLC) = VECT(I)
C      JV(NNLC) = 1
C
C      100
C      CONTINUE
C      200
C      CONTINUE
C      300
C      CONTINUE
C      330
C      CONTINUE
C      350
C      CONTINUE
C      Check if the required step/incr has been found
C      IF(JF.EQ.1) GO TO 400
C      KERRCR = KERROR + 1
C      WRITE(MOWC,3000) MKINCR(MOUT),MKSTEP(MOUT)
C      400
C      CONTINUE
C
C      Check if all nodes have been found
C      DO 500 K = 1,NTNOD
C      IF(JV(K).EQ.1) GO TO 500
C      KERROR = KERROR + 1
C      WRITE( MOWC,2000 ) K,KREQ
C      500
C      CONTINUE
C      600
C      CONTINUE
C      1000
C      FORMAT(1H1,///,20X,'* * * WARNING OF SBR. F800IN * * *',//,
C      & 10X,'LOCAL NUMBER FOR MODE ',I4,' HAS NOT BEEN FOUND',)
C      2000
C      FORMAT(1H1,///,20X,'* * * ERROR IN SBR. F800IN * * *',//,
C      & 10X,'MODE NUMBER',I4,'OF THE MODE SET HAS NOT BEEN FOUND',
C      & , FOR KEY = ',I4)

```

```

C      Rewind file 8
C      CALL DBFILE(2,ARRAY,JRCD)
C      Scanning file 8
C      DO 330 K = 1,999999
C      CALL DBFILE(0,ARRAY,JRCD)
C      IF(JRCD.NE.0) GO TO 350
C      LR = JRRAY(1,1)
C      KEY = JRRAY(1,2)
C      Finding the right step/increment
C      IF (KEY.NE.2000) GO TO 330
C      NST = JRRAY(1,8)
C      NIW = JRRAY(1,9)
C      IF(MKSTEP(MOUT).NE.NST.OR.MKINCR(MOUT).NE.NIW) GO TO 330
C      JF = 1
C      DO 300 KK = 1,999999
C      CALL DBFILE(0,ARRAY,JRCD)
C      IF(JRCD.NE.0) GO TO 350
C      LR = JRRAY(1,1)
C      KEY = JRRAY(1,2)
C      IF(KEY.EQ.2001) GO TO 350
C      MMAB = JRRAY(1,3)
C      Check if a node or an element variable is required
C      IF(KREQ.GE.100) GO TO 50
C      Element variable is required
C      ILOC = JRRAY(1,6)
C      IF(KEY.NE.1.OR.ILOC.NE.4) GO TO 300
C      The subsequent record of file 8 contains nodal averaged
C      values at node MMAB
C      CALL DBFILE(0,ARRAY,JRCD)
C      LR = JRRAY(1,1)
C      KEY = JRRAY(1,2)

```

```

C      3000 FORMAT(1H1,///,20X,'** * ERROR IN SBR. F8H01M * * *',//,
C      & 10X,'INCREMENT ',I4,' OF STEP',I4,' HAS NOT BEEN FOUND')
C
C      RETURN
C      END
C
C      SUBROUTINE FILLM(KEY,LR,ARRAY,VECT)
C
C      Fills VECT with the values given by ARRAY according to rules
C      defined by KEY
C
C      Parameters
C      I/   KEY : Abaqus file-8-reading key
C      I/   LR  : Record length of ARRAY
C      I/   ARRAY: Input record read from file 8
C      0    VECT : internal variable input array
C
C      INCLUDE 'domain_common'
C      DOUBLE PRECISION ARRAY
C      DIMENSION ARRAY(513),VECT(9)
C
C      DO 10 I = 1,9
C      VECT(I) = 0.
C
C      IF(KEY.GE.100) GO TO 400
C
C      Element variable
C
C      IF(KEY.EQ.2.OR.KEY.EQ.14) GO TO 100
C      IF(KEY.EQ.11) GO TO 200
C      IF(KEY.GE.21.AND .KEY.LE.25) GO TO 300
C
C      KERROR = KERROR + 1
C      WRITE (NWC,1000) KEY
C      GO TO 700
C
C      1 component-variable
C
C      100 CONTINUE
C
C      VECT(1) = ARRAY(3)

```

```

C      GO TO 700
C      Stress tensor
C      200 CONTINUE
C      VECT(1) = ARRAY(3)
C      VECT(2) = ARRAY(4)
C      VECT(3) = ARRAY(5)
C      VECT(4) = ARRAY(6)
C      VECT(7) = ARRAY(6)
C      IF(MDIM.LT.3) GO TO 700
C      VECT(5) = ARRAY(7)
C      VECT(8) = ARRAY(7)
C      VECT(6) = ARRAY(8)
C      VECT(9) = ARRAY(8)
C      GO TO 700
C      Strain tensor
C      300 CONTINUE
C      VECT(1) = ARRAY(3)
C      VECT(2) = ARRAY(4)
C      VECT(3) = ARRAY(5)
C      VECT(4) = ARRAY(6)*0.5
C      VECT(7) = ARRAY(6)*0.5
C      IF(MDIM.LT.3) GO TO 700
C      VECT(5) = ARRAY(7)*0.5
C      VECT(8) = ARRAY(7)*0.5
C      VECT(6) = ARRAY(8)*0.5
C      VECT(9) = ARRAY(8)*0.5
C      GO TO 700
C      Mode variable
C      400 CONTINUE
C      DO 500 J = 4,LR
C      IC = J-3
C      IF(IC.LT.9) GO TO 500
C      KERROR = KERROR + 1
C      WRITE(MOVC,2000)
C      GO TO 700
C      500 VECT(IC) = ARRAY(J)
C
C
C      700 CONTINUE
C
C      1000 FORMAT(1H1,///,20X,'** * ERROR IN SBR. FILLIN * * *',//,
C      & 10X,'ONLY KEY = 2,11,14,21,22,23,24,25 OR KEY GT. 100',
C      & ' ARE IMPLEMENTED OPTIONS',///,10X,'KEY = ',I4)
C      2000 FORMAT(1H1,///,20X,'** * ERROR IN SBR. FILLIN * * *',//,
C      & 10X,'FOR MODE VARIABLES ONLY 9 COMMENTS CAN BE READ ')
C      RETURN
C      END
C

```

```

C C
C C
C C *****
C C *
C C *
C C *
C C *
C C *
C C *
C C *****
C C SUBROUTINE FINDIE(NNLC1, NNLC2, NNLC3, NBEL, IELOC, NSID)
C C Find the elements to which nodes nnlc belong and on what side
C C
C C Parameters
C C I/ NNLC1 NNLC2 NNLC3 : local numbers for 3 nodes
C C O/ NBEL : number of elements to which all the three
C C nodes belong (max 2)
C C O/ IELOC(2): local numb. for the elts to which nnlc belong
C C O/ NSID(2) : side of IELOC to which nnlc belong (must be
C C consec. nodes on a side - otherwise nsid=0)
C C it is NSID = +/- 1 <-> +/- 4
C C
C C INCLUDE 'domain_common'
C C DIMENSION NSLC(3), IELOC(2), NSID(2), NP(3)
C C
C C NBEL = 0
C C DO 10 I = 1,2
C C IELOC(I) = 0
C C NSID(I) = 0
C C NSLC(1) = NNLC1
C C NSLC(2) = NNLC2
C C NSLC(3) = NNLC3
C C
C C DO 200 IELOC = 1, NTELT
C C
C C NN = 0
C C DO 50 N = 1,3
C C NP(N) = 0
C C DO 100 IP = 1, NTELT
C C DO 100 NN = 1,3
C C
C C KP = (IP-1) *2 +3
C C IF (IELTOP(KP, IELOC.EQ. NSLC(NN))) THEN
C C NP(NN) = IP

```

```

      NTH = NTH +1
    ENDIF
    CONTINUE
  100 CONTINUE
  C
  IF (NTH.EQ.3) THEN
    NBEL = NBEL+1
    IELOC(NBEL) = IELOC
    NP1 = NP(1)
    NP2 = NP(2)
    NP3 = NP(3)
    CALL SIDMOD(1, NP1, NP2, NP3, NSIDE)
    NSID(NBEL) = NSIDE
  ENDIF
  200 CONTINUE
  C
  RETURN
  END
  C

```

```

C
C
C *****
C *
C *
C *
C *
C *
C *
C *****
C
C
C SUBROUTINE FINDPM(NSIDE,IPONE,IPHALF,IPZERO)
C
C Find the nodes IPHALF,IPZERO to be perturbed by the q field
C
C Parameters
C I/ NSIDE : side (-1/-4 +1/+4) to which IPONE belongs
C I/ IPONE : node with perturbation = 1
C O/ IPHALF: node with perturbation = 1/2
C O/ IPZERO: node with perturbation = 0
C
C NOTE!!! ONLY FOR 2nd ORDER - 8 NODES - ISOPARAMETRIC 2D ELEMENTS
C =====
C
C INCLUDE 'domain_common'
C
C GO TO (100,200,300,400,500,600,700,800)IPONE
C
C
C ERROR = KERROR + 1
C WRITE(MWC,1000) IPONE
C GO TO 900
C
C 100 CONTINUE
C IF(ABS(NSIDE).EQ.1) GO TO 130
C IF(ABS(NSIDE).EQ.4) GO TO 160
C
C ERROR = KERROR + 1
C WRITE(MWC,2000) IPONE,NSIDE
C GO TO 900
C
C 130 CONTINUE
C IPHALF = 8
C IPZERO = 4
C GO TO 900
C
C 160 CONTINUE
C IPHALF = 5
C IPZERO = 2
C GO TO 900
C
C 200 CONTINUE
C IF(ABS(NSIDE).EQ.2) GO TO 230
C IF(ABS(NSIDE).EQ.1) GO TO 260
C
C ERROR = KERROR + 1
C WRITE(MWC,2000) IPONE,NSIDE
C GO TO 900
C
C 230 CONTINUE
C IPHALF = 5
C IPZERO = 1
C GO TO 900
C
C 260 CONTINUE
C IPEALF = 6
C IPZERO = 3
C GO TO 900
C
C 300 CONTINUE
C IF(ABS(NSIDE).EQ.3) GO TO 330
C IF(ABS(NSIDE).EQ.2) GO TO 360
C
C ERROR = KERROR + 1
C WRITE(MWC,2000) IPONE,NSIDE
C GO TO 900
C
C 330 CONTINUE
C IPHALF = 6
C IPZERO = 2
C GO TO 900
C
C 360 CONTINUE
C IPHALF = 7
C IPZERO = 4
C GO TO 900
C
C 400 CONTINUE
C IF(ABS(NSIDE).EQ.4) GO TO 430
C IF(ABS(NSIDE).EQ.3) GO TO 460
C
C

```

```

C      ERROR = ERROR + 1
      WRITE(MOVC,2000) IPONE,MSIDE
      GO TO 900
C
430  CONTINUE
      IPHALF = 7
      IPZERO = 3
      GO TO 900
C
460  CONTINUE
      IPHALF = 8
      IPZERO = 1
      GO TO 900
C
500  CONTINUE
      IF(ABS(MSIDE).EQ.1) GO TO 550
C
      ERROR = ERROR + 1
      WRITE(MOVC,2000) IPONE,MSIDE
      GO TO 900
C
550  CONTINUE
      IPHALF = 0
      IPZERO = 7
      GO TO 900
C
600  CONTINUE
      IF(ABS(MSIDE).EQ.2) GO TO 650
C
      ERROR = ERROR + 1
      WRITE(MOVC,2000) IPONE,MSIDE
      GO TO 900
C
650  CONTINUE
      IPHALF = 0
      IPZERO = 8
      GO TO 900
C
700  CONTINUE
      IF(ABS(MSIDE).EQ.3) GO TO 750
C
      ERROR = ERROR + 1
      WRITE(MOVC,2000) IPONE,MSIDE
      GO TO 900
C
      ERROR = ERROR + 1
      WRITE(MOVC,2000) IPONE,MSIDE
      GO TO 900
C
800  CONTINUE
      IF(ABS(MSIDE).EQ.4) GO TO 850
C
      ERROR = ERROR + 1
      WRITE(MOVC,2000) IPONE,MSIDE
      GO TO 900
C
850  CONTINUE
      IPHALF = 0
      IPZERO = 6
C
900  CONTINUE
C
1000 FORMAT(1H1,///,20X,'* * * ERROR IN SBR. FINDPM * * *',//,
& 10X,'THE MODE NUMBER MUST BE BETW.1 AND 8',//,
& 10X,'MODE NUMBER = ',I4)
2000 FORMAT(1H1,///,20X,'* * * ERROR IN SBR. FINDPM * * *',//,
& 10X,'MODE ',I4,' DOES NOT BELONG TO SIDE ',I4)
C
      RETURN
      END

```

```

C C
C C *****
C C *
C C *
C C *
C C *
C C *
C C *
C C *
C C *
C C *
C C *****
C C SUBROUTINE GEOIMP
C C
C C Manages the geometric input
C C
C C INCLUDE 'domain_common'
C C
C C DIMENSION IFIS(0),IDOME(10000)
C C
C C READ(MORI,1000) ITYPE,IRDINT,KPSTOP,IOUTG,IDOUBL
C C
C C IF(ITYPE.EQ.8) GO TO 10
C C KERROR = KERROR +1
C C WRITE(MOWC,2000)ITYPE
C C GO TO 100
C C CONTINUE
C C
C C NIELT = 8
C C NLELT = 3
C C NDIM = 2
C C NINTP = 9
C C IF (IRDINT.EQ.1) NINTP = 4
C C
C C Interface definition
C C
C C CALL IFDEF(IFIS(0))
C C
C C IF (KERROR.GT.0) GO TO 100
C C
C C Connectivity matrices
C C
C C CALL CONNSEC(IFIS(0),IDOME)
C C
C C IF (KERROR.GT.0) GO TO 100
C C

```

```

C C CALL IIFCOM
C C
C C IF (KERROR.GT.0) GO TO 100
C C
C C Mode cartesian components
C C
C C CALL MCARGO(IDOME)
C C
C C If the nodes on the iterface are double, check if coords coincide
C C
C C IF (IDOUBL.EQ.2) CALL CHKITF
C C
C C 100 CONTINUE
C C
C C 1000 FORMAT(5(1S))
C C 2000 FORMAT(1H1,///,20X,',' * * * ERROR IN SBR.GEOIMP * * *',//,
C C * 10X,'ONLY ELEMENT-TYPE 8 IS IMPLEMENTED',//,
C C * 10X,'ELEMENT-TYPE = ',I4)
C C RETURN
C C END
C C

```



```

C C
C *****
C *
C *
C *
C *
C *
C *
C *
C *
C *
C *
C *****
C SUBROUTINE GEOTIF
C
C Evaluates curvilinear coordinate , normal and tangent vector to
C the interface
C
C NOTE!!! ONLY FOR 2nd ORDER - 8 NODES - ISOPARAMETRIC 2D ELEMENTS
C =====
C INCLUDE 'domain_common'
C
C DIMENSION N(3), X(2,3), T(2,3), AL(2), TOLD(2)
C
C TOLD(1) = 0.
C TOLD(2) = 0.
C SCURV(1) = 0.
C
C Following the interface
C
C DO 500 NE = 1, NTOTL
C   DO 100 I = 1, 3
C     N(I) = (NE-1)*2 + I
C     N(I) = NCONN(2,I,N(I))
C     DO 100 J = 1, NDI
C       X(J,I) = COORDS(J,N(I))
C
C     Evaluating the cart. comp. of the tang. at the three nodes
C     CALL TANG2D(X,T)
C
C     Average value of the tangent vector at node 1
C     IF(NE.EQ.1) GO TO 200
C     T(1,1) = (T(1,1)+TOLD(1))/2.
C     T(2,1) = (T(2,1)+TOLD(2))/2.
C
C *****
C *
C *
C *
C *
C *
C *
C *
C *
C *
C *
C *****
C SUBROUTINE GEOTIF
C
C Cartesian component of the normal at nodes 1,2,3
C
C DO 300 I = 1, 3
C   N(I) = (NE-1)*2 + I
C   PATANG(1,N(I)) = T(1,I)
C   PATANG(2,N(I)) = T(2,I)
C   PATANG(3,N(I)) = 0.
C   PATOR(1,N(I)) = -T(2,I)
C   PATOR(2,N(I)) = T(1,I)
C   PATOR(3,N(I)) = 0.
C
C CONTINUE
C
C Evaluating the arclength (1-2) and (2-3) : AL(2)
C
C CALL CCINC2(X,AL)
C
C IF (KERROR.GT.0) GO TO 600
C
C Curvilinear coordinate
C
C DO 400 I = 2, 3
C   N(I) = (NE-1)*2 + I
C   SCURV(N(I)) = SCURV(N(I)-1) + AL(I-1)
C
C CONTINUE
C
C CONTINUE
C
C CONTINUE
C
C IF (IOUTG.EQ.0) GO TO 800
C
C WRITE(NOWG,1000)
C
C DO 700 N(I) = 1, NTOTIS
C   WRITE(NOWG,2000) N(I), SCURV(N(I)), (PATANG(I,N(I)), I = 1, 3),
C     & (PATOR(I,N(I)), I = 1, 3)
C
C CONTINUE
C
C 1000 Format(1h1, //, 40x, ' * * I N T E R F. G E O M E T R Y * * *', //
C  & 1x, N(I), SCURV, COOR, T(1), T(2), T(3), N(1), N(2), N(3), //)
C 2000 FORMAT(1x, I4, 1x, F10.5, 6(1x, F6.3))

```

```

C
C
C      RETURN
C      END
C
C
C *****
C *
C *
C *      SUBROUTINE GRADCR
C *
C *
C *****
C
C SUBROUTINE GRADCR(IELC)
C
C Evaluates the gradient of the creep strain field CRESTR at
C the integration points of the element IELC
C CRGRAD(MC,I,J,IELC)= dCRESTR(nc)/dxi at i.p. J of elt IELC
C
C Parameters
C I/   IELC : Local elt number
C
C INCLUDE 'domain_common'
C
C DIMENSION F(3,8),OU(9,9)
C
C DO 10 N = 1,3
C DO 10 I = 1,8
C   10 F(N,I) = 0.
C
C DO 350 MLEV = 1,3
C
C   MSTART = (MLEV-1)*3
C
C DO 200 NN = 1,NELT
C
C   NLCP = (NN-1)*2+3
C   NMLC = IELTOP(NLCP,IELC)
C   DO 100 ND = 1,NDIM
C     F(ND,NN) = CRESTR(ND+MSTART,NMLC)
C
C   100 CONTINUE
C
C   200 CALL GRADIE(IELC,1,F,OU)
C     IF (KERROR.NE.0) GO TO 400
C
C   DO 300 J = 1,9
C     CRGRAD(MSTART+1,1,J,IELC) = OU(1,J)

```

```

CRGRAD(MSTART+2,2,J,IELC) = OU(2,J)
CRGRAD(MSTART+3,3,J,IELC) = OU(3,J)
CRGRAD(MSTART+1,2,J,IELC) = OU(4,J)
CRGRAD(MSTART+1,3,J,IELC) = OU(5,J)
CRGRAD(MSTART+2,3,J,IELC) = OU(6,J)
CRGRAD(MSTART+2,1,J,IELC) = OU(7,J)
CRGRAD(MSTART+3,1,J,IELC) = OU(8,J)
CRGRAD(MSTART+3,2,J,IELC) = OU(9,J)
300 CONTINUE
350 CONTINUE
C
ICGRAD(IELC) = 1
C
400 CONTINUE
C
RETURN
END
C

.....
*
*           S U B R O U T I N E   G R A D I E
*
* .....
SUBROUTINE GRADIE(IELC, IDIM, F, OU)
C
C Evaluates the gradient of a scalar field or of a vector field F at
C the integration points of the element IELC
C
C Parameters
C   I/   IDIM : Dimension flag of the input field
C             0 : scalar field
C             1 : vector field
C   I/   F   : Input field at all nodes of the elt
C   O/   OU  : Output gradient field at the int.points
C             OU(I,J) = comp.I at int.pt. J
C
C   INCLUDE 'domain_common'
C
C DIMENSION F(3,8),OU(9,9),GR(3,3)
C DIMENSION AM(3,3),AU(3,3),AL(3,3),B(3),I(3),IENV(3)
C
C Local array :
C   AM : coeff. matrix -> AM(I,J) = [d H(k)/d c(I)] * X(k)(J)
C   AL,AU : Triang. fact. matr. AM = AL*AU
C   B : RHS -> Bj(I) = [d H(k)/d c(I)] * Fj(k)
C   X : Unknown vect -> Xj(I) = d Fj/d x(I)
C
C GR : Gradient at the int. point ->
C           GR(J,I) = d Fj/ d x(I)
C           C
C           H(k) : Kth shape function
C           c(I) : Ith isop. coord.
C           X(k)(J) : Jth cart coord of the Kth node
C           x(I) : Ith cartesian coordinate
C           Fj(k) :Jth comp. of input field at node k

```



```

C C
C C
C *****
C *
C *
C *
C *
C *
C *
C *****
C SUBROUTINE GRADIQ(IFLAG,NNIS,IELC,IPONE,IPHALF,IPZERO,QGRAD)
C
C Evaluates the gradient of the perturbation field Q at
C the integration points of the element IELC
C
C Parameters
C I/ IFLAG : perturbation flag
C I/ IPONE
C I/ IPHALF : nodes to be perturbed
C IPZERO
C
C IFLAG = 0 ->partial perturbation Q =1 on IPONE
C =1/2 on IPHALF
C =0 on IPZERO
C IFLAG = 1 ->Total perturbation Q =1 on IPONE
C =1 on IPHALF
C =-1 on IPZERO
C
C I/ NNIS : ref. intf. node : Q = unit normal to intf at NNIS
C I/ IELC : Local elt number
C O/ QGRAD: Gradient of Q at the integration points
C
C QGRAD(1,J) : dU1/dX1 at integration point J
C QGRAD(2,J) : dU2/dX2 at integration point J
C QGRAD(3,J) : dU3/dX3 at integration point J
C QGRAD(4,J) : dU1/dX2 at integration point J
C QGRAD(5,J) : dU1/dX3 at integration point J
C QGRAD(6,J) : dU2/dX3 at integration point J
C QGRAD(7,J) : dU2/dX1 at integration point J
C QGRAD(8,J) : dU3/dX1 at integration point J
C QGRAD(9,J) : dU3/dX2 at integration point J
C
C
C INCLUDE 'domain_common'
C
C DIMENSION F(3,8),QGRAD(9,9)

```

```

C
C DO 10 M = 1,3
C DO 10 I = 1,8
C F(M,I) = 0.
C
C DO 100 MD = 1,NDIM
C F(MD,IPONE) = PATWOR(MD,NNIS)
C
C IF (IFLAG.EQ.1) F(MD,IPZERO) =PATWOR(MD,NNIS)
C IF (IPHALF.EQ.0) GO TO 100
C F(MD,IPHALF) = 0.5 * PATWOR(MD,NNIS)
C IF (IFLAG.EQ.1) F(MD,IPHALF) =PATWOR(MD,NNIS)
C 100 CONTINUE
C
C CALL GRADIE(IELC,1,F,QGRAD)
C
C RETURN
C END
C

```

```

C
C
C *****
C *
C *
C * SUBROUTINE GRADIU
C *
C *
C *
C *****
C
C SUBROUTINE GRADIU(IELC)
C
C Evaluates the gradient of the displacement field U at
C the integration points of the element IELC
C
C Parameters
C I/ IELC : Local elt number
C
C INCLUDE 'domain_common'
C
C DIMENSION F(3,8),OU(9,9)
C
C DO 10 N = 1,3
C DO 10 I = 1,8
10 F(N,I) = 0.
C
C DO 200 NN = 1,NELT
C
C   NLCP = (NN-1)*2+3
C   NELC = IELTOP(NLCP,IELC)
C   DO 100 ND = 1,NDIM
100 F(ND,NN) = UMODE(ND,NELC)
C
200 CONTINUE
C
C CALL GRADIE(IELC,1,F,OU)
C IF (KERROR.NE.0) GO TO 400
C
C DO 300 I = 1,9
C DO 300 J = 1,9
300 UGRAD(I,J,IELC) = OU(I,J)
C
C IUGRAD(IELC) = 1
C
400 CONTINUE
C
C RETURN
C END

```

```

C C
C C
C C *****
C C *
C C *
C C *
C C *
C C *
C C *
C C *****
C C
C C SUBROUTINE GRAMAT(IELC,IP,AM)
C C
C C Evaluate the coefficient matrix AM for integration point IP
C C of element IELC
C C
C C Parameters
C C I/ IELC : local elt id number
C C I/ IP : position of the integr.point in the elt
C C O/ AM : coeff. matrix ->
C C AM(I,J) = [d N(k)/d c(I)] * X(k)(J)
C C
C C N(k) : Kth shape function
C C c(I) : Ith isop. coord.
C C X(k)(J): Jth cart coord of the Kth integr.point
C C
C C INCLUDE 'domain_common'
C C DIMENSION AM(3,3)
C C
C C DO 20 NR = 1,NDIM
C C DO 10 NC = 1,3
C C AM(NR,NC) = 0.
C C AM(NR,NR) = 1.
C C
C C DO 200 NR = 1,NDIM
C C DO 200 NC = 1,NDIM
C C SUM = 0.
C C DO 100 K = 1, NEELT
C C IELC = 3 +(K-1)*2
C C NMLC = IELTOP(IELC,IELC)
C C SUM = SUM+ SFDITP(IP,K,NR) * COORDS(NC,NMLC)
C C AM(NR,NC) = SUM
C C
C C RETURN
C C END
C C
C C *****
C C *
C C *
C C *
C C *
C C *
C C *
C C *****
C C
C C SUBROUTINE GRAMHS(IELC,IP,F,ID,B)
C C
C C Evaluates the Right Hand Side of the system to be solved in order
C C to find the gradient of the IDth component of the field F
C C
C C Parameters
C C I/ IELC : local elt id number
C C I/ IP : position of the int. point in the elt
C C I/ F : input field at each node
C C I/ ID : component of F to be considered
C C O/ B : RHS -> B(I) = [d N(k)/d c(I)] * F(ID)(k)
C C
C C N(k) : Kth shape function
C C c(I) : Ith isop. coord.
C C F(ID)(k):IDth comp. of input field at int. point k
C C
C C INCLUDE 'domain_common'
C C DIMENSION F(3,8),B(3)
C C
C C DO 10 I = 1,3
C C B(I) = 0.
C C
C C DO 200 J = 1,NDIM
C C SUM = 0.
C C DO 100 K = 1,NEELT
C C SUM = SUM + SFDITP(IP,K,J) * F(ID,K)
C C B(J) = SUM
C C
C C RETURN
C C END
C C

```

```

C
C
C *****
C *
C *
C *      S U B R O U T I N E   I D T C A L
C *
C *
C *****
C
C SUBROUTINE IDTCAL(NNIS,ISIDE,LAYMAX,IDDOTOP)
C
C Evaluates the topology matrix IDDOTOP for the domain integral
C
C Parameters
C   I/ LAYMAX: farthest layer from the interface for which
C             IDDOTOP must be evaluated
C   I/ NNIS  : interface number for which IDDOTOP must be eval.
C   I/ ISIDE : side of the intf. for which IDDOTOP must be eval.
C   0/ IDDOTOP: Output topology matrix
C             IDDOTOP(I,J) = topology of layer J
C             the component of each row are:
C
C   I = 1  2  3  4  5  6  7  8  9
C
C WELLY,IELC1,IPONE1,IPHALF1,IPZERO1,IELC2,IPONE2,IPHALF2,IPZERO2
C
C
C INCLUDE 'domain_common'
C DIMENSION IDDOTOP(9,15),IELLOC(2),NSID(2)
C
C DO 10 M = 1,9
C DO 10 I = 1,15
C IDDOTOP(M,I) = 0
C
C WELT = LMOCOM(1,NNIS)
C
C DO 700 LE = 1,WELT
C
C   LEP = (LE-1)*2+2
C   IELT = LMOCOM(LEP,NNIS)
C   IPL  = LMOCOM(LEP+1,NNIS)
C
C   WELC = LELCOM(IPL,ISIDE,LELT)
C   IELC = LELCOM( I  ,ISIDE,LELT)
C   WSIDE= LELCOM( 5 ,ISIDE,LELT)
C
C *****
C *
C *
C *      S U B R O U T I N E   I P O N E
C *
C *
C *****
C
C CALL FINDPH(NSIDE,IPONE,IPHALF,IPZERO)
C IF (ERROR.GT.0) GO TO 900
C
C IDDOTOP(1,1) = IDDOTOP(1,1) +1
C   KP = (IDDOTOP(1,1)-1)*4 +2
C IDDOTOP(KP,1) = IELC
C IDDOTOP(KP+1,1) = IPONE
C IDDOTOP(KP+2,1) = IPHALF
C IDDOTOP(KP+3,1) = IPZERO
C
C DO 600 MLAY = 2, LAYMAX
C
C   WLCZP = (IPZERO-1)*2 +3
C   WMLCZ = IELTOP(WLCZP,IELC)
C   WSOP = NSIDOP(NSIDE)
C   IF (ERROR.GT.0) GO TO 900
C
C CALL SIDMOD(O,IP1,IP2,IP3,NSOP)
C IF (ERROR.GT.0) GO TO 900
C
C   WIP = (IP1-1)*2+3
C   WMLC1 = IELTOP(WIP,IELC)
C   WIP2 = (IP2-1)*2+3
C   WMLC2 = IELTOP(WIP2,IELC)
C   WIP3 = (IP3-1)*2+3
C   WMLC3 = IELTOP(WIP3,IELC)
C
C CALL FINDIE(WMLC1,WMLC2,WMLC3,WBEL,IELOC,NSID)
C IF (WBEL.GT.1) GO TO 200
C
C   KERROR = KERROR +1
C   WRITE(NONC,1000) WMLC1,WMLC2,WMLC3,IELC
C   GO TO 900
C
C CONTINUE
C
C DO 300 WB = 1, WBEL
C
C   IF (IELOC(WB).EQ.IELC) GO TO 300

```



```

C
WELLY = IDTOP(1,MLAY)
SUMP = 0.
SUMT = 0.
DO 200 ME = 1, WELLY
C
  KP = (ME-1)*4 + 2
  IELC = IDTOP(KP, MLAY)
  NONE = IDTOP(KP+1, MLAY)
  MHALF = IDTOP(KP+2, MLAY)
  NZERO = IDTOP(KP+3, MLAY)
C
  IF(IUGRAD(IELC).NE.1) CALL GRADIU(IELC)
  IF(KERROR.NE.0) GO TO 900
C
  CALL GRADIQ(1, NUIS, IELC, NONE, MHALF, NZERO, QGRAD)
  IF(KERROR.NE.0) GO TO 900
C
  IF (ICREEP.EQ.1) THEN
C
    CALL QVCALC(1, NUIS, IELC, NONE, MHALF, NZERO, QVEC)
    IF(KERROR.NE.0) GO TO 900
C
    IF(ICGRAD(IELC).NE.1) CALL GRADCR(IELC)
    IF(KERROR.NE.0) GO TO 900
C
    ENDIF
C
  CALL INTEGR(IELC, QGRAD, QVEC, TIMTG)
  IF(KERROR.NE.0) GO TO 900
C
  SUMT = SUMT + TIMTG
C
  IF (LAYREQ(MLAY).EQ.1) THEN
C
    CALL GRADIQ(0, NUIS, IELC, NONE, MHALF, NZERO, QGRAD)
    IF(KERROR.NE.0) GO TO 900
C
    IF (ICREEP.EQ.1) THEN
C
      CALL QVCALC(0, NUIS, IELC, NONE, MHALF, NZERO, QVEC)
      IF(KERROR.NE.0) GO TO 900
C
      ENDIF
C
  ENDIF
C
  CALL INTEGR(IELC, QGRAD, QVEC, PINTG)
  IF(KERROR.NE.0) GO TO 900
C
  SUMP = SUMP + PINTG
  ENDIF
  CONTINUE
C
  PARINT(MLAY) = SUMP
  TOTINT(MLAY) = SUMT
  CONTINUE
C
  RETURN
  END
C

```



```

C
C      CGR(3,2,J) = CGRAD(9,J,IP,IELC)
C
C      310
C      CONTINUE
C
C      SUM = 0.
C      DO 350 M=1,NDIM
C      DO 350 N=1,NDIM
C      DO 350 I=1,NDIM
C
C      SUM = SUM+SIG(K,M)*CGR(M,N,I)*QVEC(I,IP)
C      350
C      F(IP) = F(IP)-SUM
C
C      ENDIF
C
C      400 AINTG = AINTG + WEIGHT(IP)*F(IP)*AJACOB(IP)
C
C      RETURN
C      END
C
C
C      CGR(3,2,J) = CGRAD(9,J,IP,IELC)
C
C      310
C      CONTINUE
C
C      SUM = 0.
C      DO 350 M=1,NDIM
C      DO 350 N=1,NDIM
C      DO 350 I=1,NDIM
C
C      SUM = SUM+SIG(K,M)*CGR(M,N,I)*QVEC(I,IP)
C      350
C      F(IP) = F(IP)-SUM
C
C      ENDIF
C
C      400 AINTG = AINTG + WEIGHT(IP)*F(IP)*AJACOB(IP)
C
C      RETURN
C      END
C
C
C      INCLUDE 'domain_common'
C      DIMENSION IELC(2),NSIDE(2)
C
C      NLELT = (NTOIS-1)/2
C
C      DO 300 LEIT = 1, NLELT
C
C      DO 100 NN = 1, NLELT
C
C      NUIS = (LELT-1)*2+NN
C      LWOCN (1, NUIS)=LWOCN (1, NUIS)+1
C      K = (LWOCN(1, NUIS)-1)*2 +2
C      LWOCN (K, N) =LELT
C      LWOCN (K+1, NUIS)=NN
C
C      DO 100 IS = 1,2
C      ISIDE = IS
C      IF (IDOUBL.EQ.1) ISIDE = 1
C      100 LELCON (NN,IS,LELT) = NCONN (2,ISIDE, NUIS)
C
C      DO 200 IS = 1,2
C
C      CALL FINDIE(LELCON(1,IS,LELT),LELCON(2,IS,LELT),LELCON(3,IS,LELT),
C      * NBEI,IELC,NSIDE)
C      DO 200 NBE = 1, NBEI
C      IF((IS.EQ.1.AND.NSIDE(NBE).LT.0).OR.(IS.EQ.2.AND.NSIDE(NBE).GT.0))
C      * THEN
C      * LELCON (4,IS,LELT)=IELC(NBE)

```

```

C      LELCON (6,IS,LELT)=NSIDE(MBE)
C      ENDIF
C      200 CONTINUE
C      300 CONTINUE
C
C      IF (IOUTG.EQ.0) GO TO 600
C      WRITE(MOWG,1000)
C      DO 400 LEI = 1,MLELT
C      WRITE(MOWG,2000) ((LELCON(I,J,LELT),I=1,5),J=1,2)
C
C      WRITE(MOWG,3000)
C      DO 500 NUIS = 1, NUTIS
C      WRITE(MOWG,4000) (LMOCOM(I,NUIS),I = 1,5)
C
C      600 CONTINUE
C      1000 FORMAT(1H1,///,40X,'* * * L S L C O * * *',//,
C      & 14X,'ISIDE = 1',28X,'ISIDE = 2',//,
C      & 1X,'NMLC1 NMLC2 NMLC3 IELC NSIDE NMLC1 NMLC2 NMLC3',
C      & ', IELC NSIDE',//)
C      2000 FORMAT(5(1X,I5,1X),2X,5 (1X,I5,1X))
C      3000 FORMAT(1H1,///,40X,'* * * L M O C O * * *',//,
C      & 1X,'MELT LELT1 IP1 LELT2 IP2',//)
C      4000 FORMAT(5(1X,I5,1X))
C
C      RETURN
C      END
C
C      LELCON (6,IS,LELT)=NSIDE(MBE)
C      *****
C      *
C      * SUBROUTINE ITFDEF
C      *
C      *****
C      SUBROUTINE ITFDEF(IFISH0)
C
C      Reads input set nodes. Find total number of input set nodes
C      Fills MCONH(1,ISIDE,NUIS)
C
C      Parameters
C      0/ IFISH0(10000) :NUIS input-set-number for abaqus nodes
C                        if >0 -> node on outer interface
C                        if <0 -> node on the inner interface
C
C      INCLUDE 'domain_common'
C      DIMENSION IFISH0(10000),NIMP(15)
C
C      ISIGH = 1
C      DO 300 ISIDE = 1,IDOURL
C      ISIGN = -ISIGH
C      NUIS = 0
C      READ(MORI,1000) NSET
C      DO 100 NS = 1,NSET
C      READ(MORI,2000) IM,(NIMP(K),K=1,15)
C      IF(IM.NE.0)THEN
C      NF = NIMP(1)
C      NL = NIMP(2)
C      NT = 1+(NL-NF)/IM
C      DO 30 N = 1,NT
C      NUIS = NUIS+1
C      NNAB = NF + (N-1)*IM
C      MCONH(1,ISIDE,NUIS) = NNAB
C      IFISH0(NNAB) = NUIS*ISIGN
C      CONTINUE
C      ELSE
C      DO 60 NN=1,15
C      IF(NIMP(NN).EQ.0) GO TO 60
C      NNAB = NIMP(NN)
C      NUIS = NUIS + 1
C
C      30 CONTINUE
C
C      60 CONTINUE

```

```

C          NCON(1,ISIDE,NIIS) = NNAB
C          IFISO(MAB) = NIIS*ISIGN
C          CONTINUE
C          ENDIF
100      CONTINUE
C          MTOTIS = NIIS
C          Check the max number of nodes
C          IF (MTOTIS.LE.200) GO TO 200
C          KERROR = KERROR +1
C          WRITE(NONC,3000) ISIDE,MTOTIS
200      CONTINUE
300      CONTINUE
C          1000 FORMAT(15)
C          2000 FORMAT(16(15))
C          3000 FORMAT(14,///,20X,'* * * ERROR IN SBR. IFFDEF * * *',//,
C          & 10X,'MAX NUMBER OF INPUT SET NODES EXCEEDED ON SIDE ',I2,//,
C          & 10X,'TOTAL NUMBER OF I.S. NODES = ',I4,' (MAX: 200)')
C          RETURN
C          END
C
C          INCLUDE 'domain_common'
C          DIMENSION AJACOB(9)
C          DO 10 NC = 1,9
C          AJACOB(NC) = 0.
C          DO 200 IP = 1,NIITP
C          DIDG = 0.
C          DIDH = 0.
C          DYDG = 0.
C          DYDH = 0.
C          DO 100 K = 1,NEELT
C          IELC = 3 + (K-1)*2
C          IELC = IELTOP(IELC,IELC)
C          DIDG = DIDG +SFDITP(IP,K,1)*COORDS(1,IELC)
C          DIDH = DIDH +SFDITP(IP,K,2)*COORDS(1,IELC)
C          DYDG = DYDG +SFDITP(IP,K,1)*COORDS(2,IELC)
C          DYDH = DYDH +SFDITP(IP,K,2)*COORDS(2,IELC)
100      CONTINUE
C          AJACOB(IP) = DIDG*DYDH-DYDG*DIDH
200      CONTINUE

```

```

C
C      RETURN
C      END
C
C *****
C *
C *      S U B R O U T I N E   L U F A C T
C *
C *
C *
C *****
C
C SUBROUTINE LUFACT(KER, ID, IMOVE, INEW, AM, AU, AL)
C
C Factorize a square matrix AM(ID, ID) into a lower triang. matrix
C AL(ID, ID) and an upper triang. matrix AU(ID, ID) . AM = AL*AU
C If elements on the main diagonal of AM are equal to zero,
C rows of AM are permuted and a track is kept in array INEW.
C Then (AM)perm. is factorized.
C Parameters
C I/O      KER : error count.
C I/       ID : matrix dimension
C O/       IMOVE : row permutation code (=1 : row permuted)
C O/       INEW : perm. record : INEW(J)= old # of new row $J
C I/       AM : square input matrix
C O/       AL : lower triang matrix
C O/       AU : upper triang matrix
C
C INCLUDE 'domain_common'
C
C DIMENSION AM(ID, ID), AU(ID, ID), AL(ID, ID), INEW(ID)
C
C Check if matrix AM has zero elements on the main diagonal
C and permutation of rows if it is needed.
C
C CALL RPERM (ID, IMOVE, INEW, AM, AU, AL)
C
C Check if AM has any zero pivot
C
C IF(IMOVE.GE.C) GO TO 5
C   KER = KER+1
C   GO TO 200
C   CONTINUE
C
C PIVMIN = 1.D-10
C
C DO 20 IC = 1, ID

```

```

DO 10 NR = 1, ID
  AU(NR, NC) = AH(NR, NC)
  AL(NR, NC) = 0.
  AL(NC, NC) = 1.
C
DO 100 NFR = 1, ID-1
  PIVOT = AU(NFR, NFR)
  IF(DABS(PIVOT).GT.PIVMIN) GO TO 50
  KER = KER + 1
  WRITE (13,1000) NFR, PIVOT
  WRITE (13,*) AN
  IF(IMOVE.GT.0) WRITE(13,2000)
  IF(IMOVE.GT.0) WRITE(13,*) INEW
  GO TO 200
C
50 CONTINUE
DO 100 MSR = NFR+1, ID
  AL(MSR, NFR) = AU(MSR, NFR)/PIVOT
DO 100 MC = NFR, ID
  AU(MSR, MC) = AU(MSR, MC)-AU(NFR, MC)*AL(MSR, NFR)
C
200 CONTINUE
1000 FORMAT(1H1,///,20X,'** ERROR IN SBR. LUFAC T * * ',//,
& 10X,'ROW ',14,' PIVOT TOO SMALL!!!! PIVOT = ',E12.5,///,
& 10X,'INPUT MATRIX :',//)
2000 FORMAT(///,20X,'* * * * * 0 T E ! ! * * * *',//,
& 10X,'ROWS HAVE BEEN PERMUTED . PERMUTATION RECORD VECTOR ',
& 10X,'IN EW FOLLOWS: (IN EW(J) = OLD # OF ACTUAL ROW # J)',/)
C
RETURN
END
C

```

```

*****
*
* SUBROUTINE M A T R I X
*
*****
SUBROUTINE MATRIX
C
C Evaluate the coefficient matrix AMAT(200,200)
C
INCLUDE 'domain_common'
C
DO 50 I = 1,200
DO 50 J = 1,200
  AMAT(I,J) = 0.
C
DO 70 J=NTOTIS+1,200
  AMAT(J,J) = 1.
C
DO 400 NNIS = 1,NTOTIS
  NLELT = LHOCOM(1,NNIS)
  DO 300 LE = 1,NLELT
    LEP = (LE-1)*2 + 2
    LELE = LHOCOM(LEP,NNIS)
    IP = LHOCOM(LEP+1,NNIS)
    DO 200 NE=1,NLELELT
      NCOL = (LELT-1)*2+NE
      SURV = 0.
      DO 100 NS = 1,NLELELT
        NIS = (LELT-1)*2 + NS
        SC = SCURV(NNIS)
        SUM = SUM +BQUAD(IP,NS,NS)*SC
        AMAT(NNIS,NCOL) = AMAT(NNIS,NCOL)+SUM
      C
    C
  C
300 CONTINUE

```



```

C
C 400 CONTINUE
C
C RETURN
C END
C
C *****
C *
C * SUBROUTINE MCARCO
C *
C *
C *
C *****
C
C SUBROUTINE MCARCO(IDONE)
C
C Reads the cartesian coordinates of the nodes
C
C Parameters
C I/ IDONE (10000) :local number for abaqus nodes
C
C INCLUDE 'domain_common'
C
C DOUBLE PRECISION ARRAY
C DIMENSION ARRAY(513),JRRAY(2,513),IDONE (10000)
C EQUIVALENCE (ARRAY(1), JRRAY(1,1))
C
C Revind file 8
C
C CALL DBFILE(2,ARRAY,JRCD)
C
C Scanning file 8
C
MCHECK = 0
DO 200 K = 1,99999
  CALL DBFILE(0,ARRAY,JRCD)
  IF (JRCD.NE.0) GO TO 300
  LR = JRRAY(1,1)
  KEY = JRRAY(1,2)
  IF (KEY.NE.1901) GO TO 200
  NNAB = JRRAY(1,3)
  NNLC = IDONE(NNAB)
  IF (NNLC.EQ.0) GO TO 200
  MCHECK = MCHECK + 1
  DO 100 MD = 1, MDIM
    COORDS(MD,NNLC) = ARRAY(3+MD)
100 CONTINUE
200 CONTINUE
300 CONTINUE

```

```

C
C      Check if all the nodes have been found
C
C      IF(MCHECK.EQ.NTHOD) GO TO 400
C          ERROR = ERROR +1
C          WRITE(MOWC,1000) MCHECK,NTHOD
C      400 CONTINUE
C
C      IF(1OUTG.EQ.0) GO TO 600
C          WRITE(MOWG,2000)
C
C          DO 500 MLC = 1,NTHOD
C      500 WRITE(MOWG,3000) MLC,MABAQ(MLC),(COORDS(I,MLC),I =1,3)
C
C          600 CONTINUE
C
C      1000 FORMAT(1H1,///,20X,'** ERROR IN SBR. MARGO * * *',//,
C          & 10X,'TOTAL NUMBER OF READ NODES :',I4,'IS NOT CONSISTENT WITH ',
C          & 'THE TOTAL NUMBER OF NODES :',I4)
C
C      2000 FORMAT(1H1,///,40X,'** C O R D I M A T E S * * *',//
C          & 'MLC MAB I1 I2 I3',/)
C
C      3000 FORMAT (2(1X,I4),3(2X,F6.3,2X))
C
C          RETURN
C          END
C
C
C      Check if all the nodes have been found
C
C          *****
C          *
C          *          F U N C T I O N   M S I D O P
C          *
C          *****
C
C      FUNCTION MSIDOP(MSIDE)
C
C          Gives the identity of the element side opposite to mside
C
C          Parameters
C          MSIDE : input side of elt
C
C          NOTE!!! ONLY FOR 2nd ORDER - 8 NODES - ISOPARAMETRIC 2D ELEMENTS
C          -----
C          MSIDOP = 0
C          MS = MSIDE +5
C          GO TO (100,200,300,400,500,600,700,800,900) MS
C
C          ERROR = ERROR + 1
C          WRITE(MOWC,1000) MSIDE
C          GO TO 990
C
C          100 CONTINUE
C          MSIDOP = 2
C          GO TO 990
C          200 CONTINUE
C          MSIDOP = 1
C          GO TO 990
C          300 CONTINUE
C          MSIDOP = 4
C          GO TO 990
C          400 CONTINUE
C          MSIDOP = 3
C          GO TO 990
C          500 CONTINUE
C          ERROR = ERROR + 1

```

```

600 WRITE(NOWC,1000) NSIDE
C GO TO 990
C CONTINUE
C NSIDOP = -3
700 GO TO 990
C CONTINUE
C NSIDOP = -4
800 GO TO 990
C CONTINUE
C NSIDOP = -1
900 GO TO 990
C CONTINUE
C NSIDOP = -2
C CONTINUE
C CONTINUE
1000 FORMAT(1H1,///,20X,'* * ERROR IN FWC.NSIDOP * *',//,
& 10X,'THE SIDE NUMBER MUST BE BETW.-4 AND -1 OR 1 AND 4',//,
& 10X,'SIDE NUMBER = ',I4)
C
C RETURN
C END

C
C *****
C * SUBROUTINE OUTPUT *****
C *
C * SUBROUTINE OUTPUT *****
C *****
C SUBROUTINE OUTPUT(FILM)
C
C Parameter
C
C I/ NOUT : Serial number of the current step/increment
C I/ FILM : Job name
C
C Print the energy momentum tensor
C
C INCLUDE 'domain_common'
C CHARACTER*20 FILE
C WRITE(NOWD,1000)
C WRITE(NOWD,2000)(NC,NC=1,NCNTOU)
C
C DO 100 NNIS = 1,NTOTIS
C
C WRITE(NOWD,3000) SCURV(NNIS),(FFORM(K,NNIS),K=1,NCNTOU)
100 CONTINUE
C
C WRITE(NOWP(NOUT),4000) FILM,NKSTEP(NOUT),NKINCR(NOUT)
C
C DO 300 K = 1,NCNTOU
C IF (K.GT.1) WRITE(NOWP(NOUT),5000) K+1
C DO 200 NNIS = 1,NTOTIS
C
C WRITE(NOWP(NOUT),6000) SCURV(NNIS),FFORM(K,NNIS)
200 CONTINUE
300 CONTINUE
C
C *****

```

```

1000 FORMAT(1H4,////,20X,*** E N E R G Y M O M E N T U M',
& , T E M S O R ***,/)
2000 FORMAT(/,1X,'CURV.COOR',10('CONT.#',I2,' '))
3000 FORMAT(1X,F8.4,2X,10(1X,E11.4))
4000 FORMAT(1X,'curvilinear coordinate',/,1X,'normal force on the',
& , interface (MPa)',/, 'TYPE 3',/, 'LABEL 2',/, '.5 .1',/
& , 'A',/, '.5 .2 .1',/, 'NSTEP : ',I2,' MINCR : ',I3,/, 'END')
5000 FORMAT('1.0E32 30',I1)
6000 FORMAT(1X,F8.4,2X,E12.5)
RETURN
END
C
C *****
C *
C * F U N C T I O N P D S H F N
C *
C *****
C
C FUNCTION PDSHFN(G,H,R,K,J,I)
C
C Evaluate partial derivative of sh. function dN(k)/dc(j) at(G,H,R)
C
C Parameters
C G : 1st| isoparametric coordinate of the location at
C H : 2nd| which the partial derivative must be
C R : 3rd| evaluated
C
C K : number of the shape function
C J : isoparametric coordinate with respect to which
C the shape function must be differentiated
C I : Element type
C
C 8 : 2D - 8 nodes isop. element
C
C INCLUDE 'domain_common'
C
C PDSHFN = 0.
C
C IF(I.EQ.8) GO TO 10
C ERROR = KERROR+1
C WRITE (NWC,1000) I
C GO TO 900
10 CONTINUE
C
C IF(J.EQ.1.OR.J.EQ.2) GO TO 20
C ERROR = KERROR+1
C WRITE (NWC,2000) J
C GO TO 900
20 CONTINUE
C
C GO TO (100,200,300,400,500,600,700,800) K
C KERROR = KERROR +1
C WRITE (NWI,3000) K
C GO TO 900

```

```

C 100 CONTINUE
IF(J.EQ.1) PDSHFH = 0.25*(1-H)*(2*G+H)
IF(J.EQ.2) PDSHFH = 0.25*(1-G)*(2*H+G)
GO TO 900

C 200 CONTINUE
IF(J.EQ.1) PDSHFH = 0.25*(1-H)*(2*G-H)
IF(J.EQ.2) PDSHFH = 0.25*(1+G)*(2*H-G)
GO TO 900

C 300 CONTINUE
IF(J.EQ.1) PDSHFH = 0.25*(1+H)*(2*G+H)
IF(J.EQ.2) PDSHFH = 0.25*(1+G)*(2*H+G)
GO TO 900

C 400 CONTINUE
IF(J.EQ.1) PDSHFH = 0.25*(1+H)*(2*G-H)
IF(J.EQ.2) PDSHFH = 0.25*(1-G)*(2*H-G)
GO TO 900

C 500 CONTINUE
IF(J.EQ.1) PDSHFH = -(1-H)*G
IF(J.EQ.2) PDSHFH = -0.5*(1-G)*(1+G)
GO TO 900

C 600 CONTINUE
IF(J.EQ.1) PDSHFH = 0.5*(1-H)*(1+H)
IF(J.EQ.2) PDSHFH = -(1+G)*H
GO TO 900

C 700 CONTINUE
IF(J.EQ.1) PDSHFH = -(1+H)*G
IF(J.EQ.2) PDSHFH = 0.5*(1-G)*(1+G)
GO TO 900

C 800 CONTINUE
IF(J.EQ.1) PDSHFH = -0.5*(1-H)*(1+H)
IF(J.EQ.2) PDSHFH = -(1-G)*H
GO TO 900

C 900 CONTINUE

C 1000 FORMAT(1H1,///,20I,'* * * ERROR IN FHC.PDSHFH * * *',//,
& 10X,'ONLY ELEMENT-TYPE 8 IS IMPLEMENTED',//,
& 10X,'ELEMENT-TYPE = ',I4)
2000 FORMAT(1H1,///,20I,'* * * ERROR IN FHC.PDSHFH * * *',//,
& 10X,'THE REQUIRED-COORDINATE-CODE MUST BE 1 (G) OR 2(H)',//,
& 10X,'REQUIRED COORDINATE CODE = ',I4)
3000 FORMAT(1H1,///,20I,'* * * ERROR IN FHC.PDSHFH * * *',//,
& 10X,'FOR THIS EL-TYPE THE MODE NUMBER MUST BE BETW. 1 AND 8',//,
& 10X,'MODE NUMBER = ',I4)
RETURN
END

```

```

C C *****
C C *
C C *
C C *
C C *
C C *
C C *
C C *****
C C FUNCTION PDSHFH(G,H,R,K,J,I)
C C
C C Evaluate partial derivative of sh. function dH(k)/dc(j) at(G,H,R)
C C
C C Parameters
C C G : 1st| isoparametric coordinate of the location at
C C H : 2nd| which the partial derivative must be
C C R : 3rd| evaluated
C C
C C K : number of the shape function
C C J : isoparametric coordinate with respect to which
C C the shape function must be differentiated
C C I : Element type
C C 8 : 2D - 8 nodes isop. element
C C
C C INCLUDE 'domain_common'
C C
C C PDSHFH = 0.
C C
C C IF(I.EQ.8) GO TO 10
C C     KERROR = KERROR+1
C C     WRITE (NOWC,1000) I
C C     GO TO 900
C C CONTINUE
C C
C C IF(J.EQ.1.OR.J.EQ.2) GO TO 20
C C     KERROR = KERROR+1
C C     WRITE (NOWC,2000) J
C C     GO TO 900
C C CONTINUE
C C
C C GO TO (100,200,300,400,500,600,700,800) K
C C     KERROR = KERROR +1
C C     WRITE (NOWI,3000) K
C C     GO TO 900
C C
C C *****
C C *
C C *
C C *
C C *
C C *
C C *
C C *****
C C 100 CONTINUE
C C IF(J.EQ.1) PDSHFH = 0.25*(1-H)*(2*G+H)
C C IF(J.EQ.2) PDSHFH = 0.25*(1-G)*(2*H+G)
C C GO TO 900
C C
C C 200 CONTINUE
C C IF(J.EQ.1) PDSHFH = 0.25*(1-H)*(2*G-H)
C C IF(J.EQ.2) PDSHFH = 0.25*(1+G)*(2*H-G)
C C GO TO 900
C C
C C 300 CONTINUE
C C IF(J.EQ.1) PDSHFH = 0.25*(1+H)*(2*G+H)
C C IF(J.EQ.2) PDSHFH = 0.25*(1+G)*(2*H+G)
C C GO TO 900
C C
C C 400 CONTINUE
C C IF(J.EQ.1) PDSHFH = 0.25*(1+H)*(2*G-H)
C C IF(J.EQ.2) PDSHFH = 0.25*(1-G)*(2*H-G)
C C GO TO 900
C C
C C 500 CONTINUE
C C IF(J.EQ.1) PDSHFH = -(1-H)*G
C C IF(J.EQ.2) PDSHFH = -0.5*(1-G)*(1+G)
C C GO TO 900
C C
C C 600 CONTINUE
C C IF(J.EQ.1) PDSHFH = 0.5*(1-H)*(1+H)
C C IF(J.EQ.2) PDSHFH = -(1+G)*H
C C GO TO 900
C C
C C 700 CONTINUE
C C IF(J.EQ.1) PDSHFH = -(1+H)*G
C C IF(J.EQ.2) PDSHFH = 0.5*(1-G)*(1+G)
C C GO TO 900
C C
C C 800 CONTINUE
C C IF(J.EQ.1) PDSHFH = -0.5*(1-H)*(1+H)
C C IF(J.EQ.2) PDSHFH = -(1-G)*H
C C
C C 900 CONTINUE
C C
C C 1000 FORMAT(1H1,///,20X,'* * ERROR IN FIG.PDSHFH * *',//,
C C & 10X,'ONLY ELEMENT-TYPE 8 IS IMPLEMENTED',//,

```

```

& 10X,'ELEMENT-TYPE = ',I4)
2000 FORMAT(IH1,///,20X,'* * * ERROR IN FWC.PDSHF * * *',//,
& 10X,'THE REQUIRED COORDINATE-CODE MUST BE 1 (G) OR 2(H)',//,
& 10X,'REQUIRED COORDINATE CODE = ',I4)
3000 FORMAT(IH1,///,20X,'* * * ERROR IN FWC.PDSHF * * *',//,
& 10X,'FOR THIS EL-TYPE THE NODE NUMBER MUST BE BETW. 1 AND 8',//,
& 10X,'NODE NUMBER = ',I4)
C
      RETURN
      END
C
& 10X,'ELEMENT-TYPE = ',I4)
2000 FORMAT(IH1,///,20X,'* * * ERROR IN FWC.PDSHF * * *',//,
& 10X,'THE REQUIRED COORDINATE-CODE MUST BE 1 (G) OR 2(H)',//,
& 10X,'REQUIRED COORDINATE CODE = ',I4)
3000 FORMAT(IH1,///,20X,'* * * ERROR IN FWC.PDSHF * * *',//,
& 10X,'FOR THIS EL-TYPE THE NODE NUMBER MUST BE BETW. 1 AND 8',//,
& 10X,'NODE NUMBER = ',I4)
C
      RETURN
      END
C
      SUBROUTINE PRESF
      DIMENSION C(3)
      INCLUDE 'domain_common'
      DO 50 I = 1,3
      C(I) = 0.
      IR = IRDINT
      IT = ITYPE
      CALL BQCALC(IT)
      CALL WEIGAL(IT,IR)
      Derivatives of the shape functions at the nodes
      DO 200 I = 1,NEELT
      DO 100 M = 1,NDIM
      C(M) = DLISCO(0,I,M,IT,IR)
      DO 200 K = 1,NEELT
      DO 200 J = 1,NDIM
      SFDNOD(I,K,J) = PDSHF(C(1),C(2),C(3),K,J,IT)
      200 CONTINUE
      Derivatives of the shape functions and shape functions
      at the integration points
      DO 400 I = 1,NIINTP
      DO 300 M = 1,NDIM
      C(M) = DLISCO(1,I,M,IT,IR)
      300

```

```

C      DO 400 K = 1, NNELT
C      SFDITP(I,K)=SHFMC(C(1),C(2),C(3),K,IT)
C      DO 400 J = 1, NDIM
C      SFDITP(I,K,J) = PDSHF(C(1),C(2),C(3),K,J,IT)
C      400 CONTINUE
C
C      IF (IOUTG.EQ.0) GO TO 700
C      WRITE(NWNG,1000)
C      DO 500 I = 1, NNELT
C      DO 500 K = 1, NNELT
C      DO 500 J = 1, NDIM
C      WRITE(NWNG,2000) I,K,J,SFDMOD(I,K,J)
C      500 CONTINUE
C      WRITE(NWNG,3000)
C      DO 600 I = 1, NINTP
C      DO 600 K = 1, NNELT
C      DO 600 J = 1, NDIM
C      WRITE(NWNG,2000) I,K,J,SFDITP(I,K,J)
C      600 CONTINUE
C      700 CONTINUE
C
C      1000 FORMAT(1H,////,40X,'** * SHAPE FUNCTION DERIVATIVE * * *',//,
C      & 1X,'MODE SH.FN J D(SH.FN)/D(COORD.J)',//)
C      2000 FORMAT(1X,I4,3X,I2,4X,I1,4X,F10.5)
C      3000 FORMAT(1H,////,40X,'** * SHAPE FUNCTION DERIVATIVE * * *',//,
C      & 1X,'IT.P SH.FN J D(SH.FN)/D(COORD.J)',//)
C
C      RETURN
C      END
C
C
C      *****
C      *
C      * SUBROUTINE QV CALC
C      *
C      *****
C      SUBROUTINE QV CALC(IFLAG, NNIS, IELC, IPONE, IPHALF, IPZERO, QVEC)
C      C
C      C Evaluates the perturbation field Q at
C      C the integration points of the element IELC
C
C      C Parameters
C      C I/ IFLAG : perturbation flag
C      C I/ IPONE
C      C I/ IPHALF : nodes to be perturbed
C      C IPZERO
C
C      C IFLAG = 0 ->partial perturbation Q =1 on IPONE
C      C =1/2 on IPHALF
C      C =0 on IPZERO
C      C IFLAG = 1 ->Total perturbation Q =1 on IPONE
C      C =1 on IPHALF
C      C =1 on IPZERO
C
C      C NNIS : ref. intf. node : Q = unit normal to intf at NNIS
C      C I/ IELC : Local elt number
C      C O/ QVEC: Q at the integration points
C
C      C QVEC(1,J) : Q1 at integration point J
C      C QVEC(2,J) : Q2 at integration point J
C      C QVEC(3,J) : Q3 at integration point J
C
C      INCLUDE 'domain_common'
C
C      DIMENSION F(3,8),QVEC(3,9)
C
C      DO 10 M = 1,3
C      DO 10 I = 1,8
C      F(M,I) = 0.
C
C      DO 300 ND = 1,NDIM
C      F(ND,IPONE) = PAYTOR(ND,NNIS)

```



```

C
C IF (IFLAG.EQ.1) F(ND,IPZERO) =PATHOR(ND,NNIS)
C IF (IPHALF.EQ.0) GO TO 50
C F(ND,IPHALF) = 0.5 * PATHOR(ND,NNIS)
C IF (IFLAG.EQ.1) F(ND,IPHALF) =PATHOR(ND,NNIS)
C
C 50 CONTINUE
C
C DO 200 IP = 1,NIINTP
C
C SUM = 0.
C DO 100 NN=1,NEBELT
C SUM = SUM+SFNITP(IP,NN)*F(ND,NN)
C QVEC(ND,IP) = SUM
C 200 CONTINUE
C
C 300 CONTINUE
C
C RETURN
C END
C

C
C *****
C *
C * SUBROUTINE RESETV
C *
C *****
C
C SUBROUTINE RESETV
C
C Reset to zero the memory used in the loop over the step/increment
C
C INCLUDE 'domain_common'
C
C DO 300 N = 1,1000
C IUGRAD(N) = 0.
C ICGRAD(N) = 0.
C DO 200 J=1,9
C DO 200 K=1,9
C UGRAD(J,K,N) = 0.
C DO 100 I=1,3
C CRGRAD(J,I,K,N) = 0.
C
C 100 CONTINUE
C 200 CONTINUE
C 300 CONTINUE
C
C DO 600 N=1,200
C DO 400 I=1,10
C DELEN(I,N) = 0.
C DO 500 M=1,15
C DO 500 I=1,2
C DINTG(I,M,N) = 0.
C 600 CONTINUE
C
C RETURN
C END

```

```

C C *****
C C *
C C *
C C *
C C *
C C *
C C *****
C C
C C SUBROUTINE RWPERM(ID,IMOVE,INEW,AM,AP,AN)
C C
C C Change the order of the rows of AM if ZERO elements are on the
C C main diagonal.
C C
C C Parameters:
C C I/ ID : matrix dimension
C C O/ IMOVE : row permutation code (=1 : row permuted )
C C O/ INEW : perm. record :INEW(J)= old # of new row #J
C C I/O AM : square input/output matrix
C C / AP : matrix used locally to keep record of non-zero
C C / pivots
C C / AN : matrix used locally to store the new perm. matr.
C C
C C DIMENSION AM(ID,ID),AP(ID,ID),AN(ID,ID),INEW(ID)
C C INCLUDE 'domain_common'
C
C DO 10 NR = 1, ID
C INEW(NR) = 0
C DO 10 NC = 1, ID
C AP(NR,NC) = 0.
C AN(NR,NC) = 0.
C
C 10 CONTINUE
C
C IMOVE = 0
C PIVMIN = 0.00001
C
C Check if matrix AM has zero elements on the main diagonal
C
C DO 50 NR = 1, ID
C IF(DABS(AM(NR,NR)) .GE. PIVMIN) GO TO 50
C IMOVE = 1
C 50 CONTINUE
C
C IF(IMOVE.EQ.0) GO TO 900
C
C *****
C C
C C Permutation required
C C
C C Prepare matrix AP with the position of non-zero pivots and
C C vector INEW with the # of rows which have non-zero pivots
C C
C DO 100 NPIV = 1, IZ
C DO 100 NR = 1, ID
C IF(DABS(AM(NR,NPIV)).LT.PIVMIN) GO TO 100
C IPOS = INEW(NPIV)+1
C INEW(NPIV) = IPOS
C AP(NPIV,IPOS) = DFLOAT(NR)
C 100 CONTINUE
C
C Permutation
C
C MP = 0
C
C 200 CONTINUE
C
C DO 700 NPIV = 1, ID
C
C IF(INEW(NPIV).NE.MP) GO TO 700
C
C IF(MP.EQ.0) THEN
C IMOVE = -1
C WRITE(13,1000) NPIV
C
C DO 210 JJ = 1, ID
C WRITE(13,*) (AM(JJ,NR),NR=1,ID)
C GO TO 900
C
C ENDIF
C
C PIVMAX = PIVMIN
C
C DO 300 MCP = 1, MP
C NR = INT(AP(NPIV,MCP))
C PIVOT = DABS(AM(NR,NPIV))
C IF(PIVOT.GE.PIVMAX) THEN
C PIVMAX = PIVOT
C NRCH = NR
C ENDIF
C 300 CONTINUE
C
C INEW(NPIV) = -NRCH

```

```

350 DO 350 MC = 1, ID
C   AN(MPIV, MC) = AM(MRCH, MC)
C
C   Packing of AP
C
C   DO 600 MR = 1, ID
C   IF(IHEW(MR).LT.0) GO TO 600
C   DO 500 MC = 1, ID
C   IF(IINT(AP(MR, MC)).EQ.MRCH) THEN
C     IHEW(MR) = IHEW(MR) - 1
C     DO 400 MLC = MC, ID-1
C     AP(MR, MLC) = AP(MR, MLC+1)
C     AP(MR, ID) = 0.
C     GO TO 600
C   ENDIF
C   CONTINUE
C   CONTINUE
C
C   MP = MP-1
C   GO TO 200
C
C   CONTINUE
C
C   MP = MP+1
C
C   Check if all the pivot have been found
C
C   INEG = 1
C   DO 750 MR = 1, ID
C   IF(IHEW(MR).GT.0) INEG = 0
C
C   IF(INEG.EQ.1) GO TO 800
C
C   IF(MP.LE.ID) GO TO 200
C
C   IMOVE = -1
C   WRITE(13,2000)
C   WRITE(13,*) IHEW
C   WRITE(13,3000)
C   WRITE(13,*) AM
C   WRITE(13,4000)
C   WRITE(13,*) AP
C   WRITE(13,5000)
C   WRITE(13,*) AM
C
C   800 CONTINUE

```

```

C
C   DO 850 MR = 1, ID
C   IHEW(MR) = -IHEW(MR)
C   DO 850 MC = 1, ID
C   AM(MR, MC) = AM(MR, MC)
C   CONTINUE
C
C   900 CONTINUE
C
C   1000 FORMAT(1H1,///,20X,'** * ERROR IN SBR. RWPERM * * *',//,
C   & 20X,'NO PIVOT AVAILABLE FOR ROW #',I4,//,
C   & 20X,'INPUT MATRIX AM FOLLOWS',//)
C   2000 FORMAT(1H1,///,20X,'** * ERROR IN SBR. RWPERM * * *',//,
C   & 20X,'MP GREATER THAN ID. MP = ',I4,' ID = ',I4,//,
C   & 20X,'PERMUTATION RECORD VECTOR IHEW FOLLOWS',//)
C   3000 FORMAT(1X,///,20X,'INPUT MATRIX AM FOLLOWS',//)
C   4000 FORMAT(1X,///,20X,'PIVOT MATRIX AP FOLLOWS',//)
C   5000 FORMAT(1X,///,20X,'OUTPUT MATRIX AM FOLLOWS',//)
C   RETURN
C   END

```

```

C C
C C
C *****
C *
C *
C *
C *
C *
C *
C *
C *
C *
C *
C *****
C
C FUNCTION SHPFNC(G,H,R,K,I)
C
C Evaluate shape function I(k) at(G,H,R)
C
C Parameters
C G : 1st| isoparametric coordinate of the location at
C H : 2nd| which the shape function must be
C R : 3rd| evaluated
C
C K : number of the shape function
C I : Element type
C
C 8 : 2D - 8 nodes isop. element
C
C INCLUDE 'domain_common'
C
C SHPFNC= 0.
C
C IF(I.EQ.8) GO TO 10
C ERROR = KERROR+1
C WRITE (NOWC,1000) I
C GO TO 900
C
C 10 CONTINUE
C
C GO TO (100,200,300,400,500,600,700,800) K
C KERROR = KERROR +1
C WRITE (NOWI,3000) K
C GO TO 900
C
C
C 100 CONTINUE
C SHPFNC = -0.25*(1-G)*(1-H)*(1+G+H)
C GO TO 900
C
C 200 CONTINUE
C SHPFNC = -0.25*(1+G)*(1-H)*(1-G+H)
C GO TO 900
C
C 300 CONTINUE
C SHPFNC = -0.25*(1+G)*(1+H)*(1-G-H)
C GO TO 900
C
C 400 CONTINUE
C SHPFNC = -0.25*(1-G)*(1+H)*(1+G-H)
C GO TO 900
C
C 500 CONTINUE
C SHPFNC = 0.5*(1-G)*(1+G)*(1-H)
C GO TO 900
C
C 600 CONTINUE
C SHPFNC = 0.5*(1+G)*(1-H)*(1+H)
C GO TO 900
C
C 700 CONTINUE
C SHPFNC = 0.5*(1-G)*(1+G)*(1+H)
C GO TO 900
C
C 800 CONTINUE
C SHPFNC = 0.5*(1-G)*(1+H)*(1-H)
C
C 900 CONTINUE
C
C 1000 FORMAT(1H1,///,20X,'* * ERROR IN FNC.PDSHF * *',//,
C & 10X,'ONLY ELEMENT-TYPE 8 IS IMPLEMENTED',//,
C & 10X,'ELEMENT-TYPE = ',I4)
C 3000 FORMAT(1H1,///,20X,'* * ERROR IN FNC.PDSHF * *',//,
C & 10X,'FOR THIS EL-TYPE THE NODE NUMBER MUST BE BETW. 1 AND 8',//,
C & 10X,'NODE NUMBER = ',I4)
C
C RETURN
C END
C

```

```

C
C
C *****
C *
C *
C *     S U B R O U T I N E   S I D N O D
C *
C *
C *****
C
C
C SUBROUTINE SIDMOD(IFLAG,M1,M2,M3,MSIDE)
C
C Find the side to which M1,M2,M3 belong (if IFLAG = 1) or
C the nodes M1,M2,M3 that belong to MSIDE (if IFLAG = 0)
C
C Parameters
C I/ L : identity flag: 0-> find node 1-> find side
C I/0 M1,M2,M3 : node position (1-8)
C I/0 MSIDE : side (-1/-4 +1/+4)(nodes must be consecutive)
C
C NOTE!!! ONLY FOR 2nd ORDER - 8 NODES - ISOPARAMETRIC 2D ELEMENTS
C =====
C INCLUDE 'domain_common'
C
C IF(IFLAG.EQ.0) GO TO 500
C
C MSIDE has to be found
C
C MSIDE = 0
C GO TO (100,200,300,400)M1
C GO TO 600
C
C 100 CONTINUE
C IF(M2.EQ.5.AND.M3.EQ.2) MSIDE = 1
C IF(M2.EQ.8.AND.M3.EQ.4) MSIDE =-4
C GO TO 600
C
C 200 CONTINUE
C IF(M2.EQ.6.AND.M3.EQ.3) MSIDE = 2
C IF(M2.EQ.5.AND.M3.EQ.1) MSIDE =-1
C GO TO 600
C
C 300 CONTINUE
C IF(M2.EQ.7.AND.M3.EQ.4) MSIDE = 3
C IF(M2.EQ.6.AND.M3.EQ.2) MSIDE =-2
C GO TO 600
C
C 400 CONTINUE
C IF(M2.EQ.8.AND.M3.EQ.1) MSIDE = 4
C IF(M2.EQ.7.AND.M3.EQ.3) MSIDE =-3
C GO TO 600
C
C 500 CONTINUE
C M1,M2,M3 have to be found
C
C MS = MSIDE +5
C GO TO (510,520,530,540,550,560,570,580,590) MS
C
C KERROR = KERROR + 1
C WRITE(ROWC,1000) #SIDE
C GO TO 600
C
C 510 CONTINUE
C M1 = 1
C M2 = 8
C M3 = 4
C GO TO 600
C
C 520 CONTINUE
C M1 = 4
C M2 = 7
C M3 = 3
C GO TO 600
C
C 530 CONTINUE
C M1 = 3
C M2 = 6
C M3 = 2
C GO TO 600
C
C 540 CONTINUE
C M1 = 2
C M2 = 5
C M3 = 1
C GO TO 600
C
C 550 CONTINUE
C KERROR = KERROR+1
C WRITE(ROWC,1000) #SIDE
C GO TO 600

```

```

560 CONTINUE
    N1 = 1
    N2 = 5
    N3 = 2
    GO TO 600
570 CONTINUE
    N1 = 2
    N2 = 6
    N3 = 3
    GO TO 600
580 CONTINUE
    N1 = 3
    N2 = 7
    N3 = 4
    GO TO 600
590 CONTINUE
    N1 = 4
    N2 = 8
    N3 = 1
C
600 CONTINUE
1000 FORMAT(1H1,///,20X,'** ERROR IN SBR. SIDMOD **',//,
& 10X,'THE SIDE NUMBER MUST BE BETW.-4 AND -1 OR 1 AND 4',//,
& 10X,'SIDE NUMBER = ',I4)
C
      RETURN
      END

```

```

*****
*
*
*           S U B R O U T I N E   S O L V E R
*
*****
SUBROUTINE SOLVER(ID,IMOVE,INEV,AU,AL,B,X)
C
C Solve the systems AL*C = B and AU*X = C
C If matrix AM has been permuted, the RHS is permuted too
C
C Parameters
C   I/ ID : matrix/vector dimension
C   I/ IMOVE : row permutation code (=1 : row permuted)
C   I/ INEV : perm. record :INEV(J)= old # of new row #J
C   I/ AL : lower triang matrix AL(ID,ID)
C   I/ AU : upper triang.matrix AU(ID,ID)
C   I/ B : RHS of the system AL*AU * X = B
C   O/ X : unknown vector
C
C INCLUDE 'domain-common'
C DIMENSION AU(ID,ID), AL(ID,ID), B(ID), X(ID),INEV(ID)
C
C Check if rows of AM have been permuted. If YES, permute B
C
C CALL CPERM(ID,IMOVE,INEV,B,X)
C
C DO 10 NC = 1,ID
10 X(NC) = 0.
C
C Evaluate X -> AL*X = B
C
C DO 200 NR = 1,ID
    SUM = 0.
    IF(NR.EQ.1) GO TO 200
    DO 100 NC = 1,NR-1
      SUM = SUM + X(NC) * AL(NR,NC)
200 X(NR) = B(NR) -SUM
C
C Copy X in B
C

```

```

DO 250 I = 1, ID
B(I) = X(I)
250 X(I) = 0.
C
C Evaluate X -> AU*X = B
C
DO 400 NR = ID, 1, -1
SUM = 0.
IF (NR.EQ.ID) GO TO 400
DO 300 NC = NR+1, ID
SUM = SUM + X(NC) * AU(NR, NC)
400 X(NR) = (B(NR)-SUM)/AU(NR, NR)
C
C RETURN
C END
C

DO 250 I = 1, ID
B(I) = X(I)
250 X(I) = 0.
C
C SUBROUTINE SYSOLV
C
C Solve the system AHAT=F*DELEN and evaluates FFORM=force
on the interface
C
C INCLUDE 'domain_common'
C
C DIMENSION AH(200,200),AU(200,200),AL(200,200)
C DIMENSION B(200),X(200), INEW(200)
C
C Local array :
C AH : coeff. matrix =AHAT
C AL,AU : Triang. fact. matr. AH = AL*AU
C B : RHS -> B(j,I) = DELEN(j,I)
C X : Unknown vect -> X(j,I) = FFORM(j,I)
C
DO 10 I = 1,200
DO 10 J = 1,200
10 AH(I,J) = AHAT(I,J)
C
C LU factorization
C
KER = KERROR
CALL LUFAC(TKER,200,IMOVE,INEW,AH,AU,AL)
KERROR = KER
IF(KERROR.GT.0) GO TO 500
C
C Solving the system for all the components of DELEN
C
DO 300 NCOUNT = 1, NCONT00
C
C Evaluating the RHS
C
DO 100 I = 1,200
B(I) = DELEN(NCOUNT,I)
100

```

```

C
C      solving the system
C
C      CALL SOLVER (200,IMOVE,INER,AU,AL,B,X)
C
C      Storing the solution
C
C      DO 200 I=1,200
C      FFORM(FCOMT,I) = X(I)
C
C      300 CONTINUE
C
C      500 CONTINUE
C
C      RETURN
C      END
C
C
C
C      *****
C      *
C      *
C      *       S U B R O U T I N E   T A N G 2 D
C      *
C      *
C      *****
C
C      SUBROUTINE TANG2D(X,T)
C
C      Evaluates the components of the unit tangent vector at the three
C      subsequent nodes on a side of a 2nd ord. isop 2D elt
C
C      Parameters
C      I/   X : Cartesian coordinate of the nodes
C      O/   T : Cartesian components of the unit tangent vector
C           at the nodes
C
C      NOTE!!! ONLY FOR 2nd ORDER - 8 NODES - ISOPARAMETRIC 2D ELEMENTS
C      =====
C
C      INCLUDE 'domain_common'
C
C      DIMENSION X(2,3),T(2,3),DXDS(2,3),SQMOD(3)
C
C      First node
C
C      SQMOD(1) = 0.
C      DO 100 I = 1,2
C         DXDS(I,1) = -1.5 * X(I,1) + 2 * X(I,2) - 0.5 * X(I,3)
C      SQMOD(1) = SQMOD(1) + DXDS(I,1)**2
C
C      second node
C
C      SQMOD(2) = 0.
C      DO 200 I = 1,2
C         DXDS(I,2) = -0.5 * X(I,1) + 0.5 * X(I,3)
C      SQMOD(2) = SQMOD(2) + DXDS(I,2)**2
C
C      third node
C
C      SQMOD(3) = 0.
C      DO 300 I = 1,2

```



```

C
C      DXDS(I,3) = 0.5 * X(I,1) - 2 * X(I,2) + 1.5 * X(I,3)
300 SQMOD(3) = SQMOD(3) + DXDS(I,3)**2
C
C      DO 400 N = 1,3
C      DO 400 I = 1,2
400 T(I,N) = DXDS(I,N)/DSQRT(SQMOD(N))
C
C      RETURN
C      END
C

SUBROUTINE VARIMP(NOUT)
C
C      Parameter
C      I/ NOUT : Serial number of the required step/increment
C
C      Reads Elastic energy and Stres tensor at the integration points
C      Reads also the displacement field and the creep strains at the nodes
C
C      INCLUDE 'domain_common'
C      DIMENSION VARELT(9,1000),VAREMOD(9,3200)
C
C      Input the elastic energy
C      CALL F8IPIN(NOUT,14,VARELT)
C
C      DO 100 IE = 1, NIELT
C      DO 100 IP = 1, NINTP
100 VEMIP(IP,IE) = VARELT(1,IP,IE)
C
C      Input the stress tensor
C      CALL F8IPIN(NOUT,11,VARELT)
C
C      DO 200 IE = 1, NIELT
C      DO 200 IP = 1, NINTP
C      DO 200 IC = 1, 9
200 SIGHIP(IC,IP,IE) = VARELT(IC,IP,IE)
C
C      Input the displacement at the nodes
C      CALL F8N0IN(NOUT,101,VAREMOD)
C
C      DO 300 NMLC = 1, NTHOD

```

```

C          DO 300 ND = 1,NDIM
C          UNODE(ND,NELC) = VARNO(ND,NELC)
C          IF(ICREEP.EQ.1) THEN
C
C              Input the creep strain at the nodes
C              CALL F8FOIN(NOUT,23,VARNO)
C
C              DO 400 NMLC = 1,NTMOD
C              DO 400 NC = 1,9
C              CRESTR(NC,NMLC) = VARNO(NC,NMLC)
C          400
C          ENDIF
C          RETURN
C          END

```

```

*****
*
*          SUBROUTINE WEICALL
*
*
*****
SUBROUTINE WEICALL(IT,IR)
Evaluates the gauss weights at integration points WEIGHT(9)

Parameters
I/      I : Element type
        8 : 2D - 8 nodes  isop. element
        0 : full integration flag
        1 : reduced integration (4 i.p.)

C          NOTE!!! ONLY FOR 2nd ORDER - 8 NODES - ISOPARAMETRIC 2D ELEMENTS
C          =====
C          INCLUDE 'domain_common'
C          FIV = .5555555555555556
C          EIG = .888888888888889
C          IF ( IT.EQ.8) GO TO 100
C              ERROR = ERROR + 1
C              WRITE(NOWC,1000) IT
C              GO TO 900
C          100 CONTINUE
C          IF(IR.EQ.1) GO TO 200
C          Full integration
C          WEIGHT(1) = FIV*FIV
C          WEIGHT(2) = EIG*FIV
C          WEIGHT(3) = FIV*FIV
C          WEIGHT(4) = EIG*FIV

```

```

WEIGHT(5) = EIG*EIG
WEIGHT(6) = EIG*FIV
WEIGHT(7) = FIV*FIV
WEIGHT(8) = EIG*FIV
WEIGHT(9) = FIV*FIV

```

```

C
GO TO 900

```

```

CONTINUE

```

```

Reduced integration

```

```

WEIGHT(1) = 1.
WEIGHT(2) = 1.
WEIGHT(3) = 1.
WEIGHT(4) = 1.
WEIGHT(5) = 0.
WEIGHT(6) = 0.
WEIGHT(7) = 0.
WEIGHT(8) = 0.
WEIGHT(9) = 0.

```

```

CONTINUE

```

```

1000 FORMAT(1H1,///,20X,'** * ERROR IN SBR. WEICAL * * *',//,
& 10X,'ONLY ELEMENT-TYPE 8 IS IMPLEMENTED',//,
& 10X,'ELEMENT-TYPE = ',I4)

```

```

RETURN
END

```

```

*****
*
*
* COMMON B L O K S   O F   P R O G R A M   D O M A I N *
*
*****

```

```

Common variables, program DOMAIN

```

```

IMPLICIT REAL*8 (A-H,O-Z)

```

```

COMMON / COMN / NCOMN(21,2,200),IELTOP(17,1000),NABAQ(3200)
COMMON / COML / LELCOM(5,2,100),LWDCOM(5,200)
COMMON / COOR / COORDS(3,3200)
COMMON / CTRL / ITYPE,IRDINT,IOUTG,IPSTOP,IDOUBL,ICREEP
COMMON / CTRV / ECFTU,FLAYER(2,10)
COMMON / ELBS / DIETG(2,15,200),DELEN(10,200)
COMMON / ERRO / ERROR
COMMON / EVR1 / VEIP(9,1000),SIGHIP(9,9,1000)
COMMON / EVR2 / UGRAD(9,9,1000),UGRAD(1000)
COMMON / EVR3 / CRGRAD(9,3,9,1000),ICGRAD(1000)
COMMON / INTF / PATHOR(3,200),PATANG(3,200),SCURV(200)
COMMON / MATR / ANAT(200,200)
COMMON / NURB / NBELT,NLELT,NDIM,NINP,NUTIS,NTHOD,NTELT,NTELE
COMMON / NVAR / UNODE(3,3200),FNORM(10,200),CRESTR(9,3200)
COMMON / SHFV / SFDITP(9,8,2),SFDMOD(8,8,2),SFTIIP(9,8)
COMMON / STEP / EKSTEP(19),EKINCR(19),NTOUT
COMMON / UNIT / MORI,MONC,MONO,MONG,MONP(19)
COMMON / WEIG / BQUAD(3,3,3),WEIGHT(9)

```

**APPENDIX III: THE COMPUTER
PROGRAM GOODIER**

```

C *****
C *
C *
C *     P R O G R A M   G O O D I E R
C *
C *
C *****
C
C Evaluates the normal component of the force on the interface
C of a cylindrical misfitting inclusion in an infinite matrix
C (both isotropic media with the same poisson ratio).
C
C Values are given at N (number of nodes) locations along the
C interface.
C
C Only the upper-right quadrant of the inclusion is considered (for
C symmetry) the first node is at angle=0. with the direction of the
C applied stress .
C
C File Handling
C
C DIMENSION TAUM(100)
C CHARACTER*80 FILOUT
C
C PRINT *,'* * * * *           PROGRAM GOODIER          * * *'
C PRINT *,',',
C PRINT *,',',
C
C PRINT 1000,' Please enter the FILOUT name'
C READ(*,*) FILOUT
C
C OPEN(UNIT = 13,FILE = FILOUT,STATUS = 'NEW')
C
C NOW = 13
C SMALL = 1.E-32
C PI2 = ASINH(1.)
C RAD = 1./PI2
C
C PRINT 1000,' Please enter E matrix'
C READ(*,*) EMATRI
C WRITE(*,*) EMATRI
C PRINT 1000,' Please enter E inclusion'

```

```

C READ(*,*) EIMCLU
C WRITE(*,*) EIMCLU
C PRINT 1000,' Please enter Poisson ratio'
C READ(*,*) PFU
C WRITE(*,*) PFU
C
C AMUM = EMATRI/(2.*(1+PFU))
C AMUI = EIMCLU/(2.*(1+PFU))
C
C WRITE(*,*) AMUM , AMUM , AMUI , AMUI
C
C PRINT 1000,' Please enter Sigma inf.'
C READ(*,*) SINF
C WRITE(*,*) SINF
C PRINT 1000,' Please enter misfit'
C READ(*,*) DELTA
C WRITE(*,*) DELTA
C
C evaluate factor K (AK) , L (AL) , M (AM)
C
C AK =(AMUM-AMUI)/(AMUM+AMUI)/(1.-2.*PFU)
C AL =(AMUM-AMUI)/(AMUM+(3.-4.*PFU)*AMUI)
C AM = 1. + (1.-2.*PFU)*AMUM/AMUI
C
C WRITE(*,*) AK , AK , AL , AL , AM , AM
C
C PRINT 1000,' Please enter number of nodes'
C READ(*,*) NMOD
C WRITE(*,*) NMOD
C
C ASTEP = PI2/(NMOD-1)
C
C SUMLEF = 0.
C SUMRIG = 0.
C
C DO 200 M = 1,NMOD
C
C     ANG = (M-1)*ASTEP
C     SCURV = RAD*ANG
C
C Inside the inclusion.Jump if hole (AMUI = 0)
C
C IF(AMUI.LT.SMALL) GO TO 100

```

```

C
SRR = (1.-AK)*SINF/2.+ (1.-AL)*COS(2.*ANG)*SINF/2.+
& -2.*AMUH*DELTA/AM
SIT = (1.-AK)*SINF/2.- (1.-AL)*COS(2.*ANG)*SINF/2.+
& -2.*AMUH*DELTA/AM
SRT = - (1.-AL)*SIN(2.*ANG)*SINF/2.
C
DURDR= (SINF/(4.*AMUH))*((1.-2.*PHU)*(1.-AK)+
& (1.-AL)*COS(2.*ANG))+
& +DELTA*(1.-2.*PHU)*AMUH/(AM*AMUH)
DUTDR=- (SINF/(4.*AMUH))*((1.-AL)*SIN(2.*ANG)
C
V = (1./(4.*AMUH))*((1.-PHU)*(SRR**2+SIT**2)-
& 2.*PHU*SRR*SIT + 2.*SRT**2)
TDUDR = SRR*DURDR+SRT*DUTDR
C
ERTI = V-TDUDR
C
100 CONTINUE
C
in the matrix
C
SRR = (1.-AK)*SINF/2.+ (1.-AL)*COS(2.*ANG)*SINF/2.+
& -2.*AMUH*DELTA/AM
SIT = (1.-AK)*SINF/2.- (1.+3.*AL)*COS(2.*ANG)*SINF/2.+
& +2.*AMUH*DELTA, AM
SRT = - (1.-AL)*SIN(2.*ANG)*SINF/2.
C
DURDR= (SINF/(4.*AMUH))*((1.-2.*PHU)-AK+
& (1.-AL*(1.-4.*PHU))*COS(2.*ANG))+
& -DELTA/AM
DUTDR= (SINF/(4.*AMUH))*(AL*(5.-4.*PHU)-1)*SIN(2.*ANG)
C
V = (1./(4.*AMUH))*((1.-PHU)*(SRR**2+SIT**2)-
& 2.*PHU*SRR*SIT + 2.*SRT**2)
TDUDR = SRR*DURDR+SRT*DUTDR
C
ERTH = V-TDUDR
TAUH(##) = ERTH-ERTI
C
WRITE(NOV,*) SCURV,TAUH(##)
C
IF(##.LE.##OD/2) SUMLEF = SUMLEF +TAUH(##)
IF(##.GT.##OD/2) SUMRIG = SUMRIG +TAUH(##)

```

```

C
C
200 CONTINUE
YMLEF = SUMLEF*2/(##GD)
YMRIG = SUMRIG*2/(##OD)
C
WRITE(NOV,*)YMLEF,YMRIG
C
1000 FORMAT($,A,' : ')
C
STOP
END

```

**APPENDIX IV: ABAQUS INPUT FILE FOR
THE TEST CASE:
A CYLINDRICAL INCLUSION IN AN
INFINITE MATRIX**

```

**
** Abaqus 4.7 input file for cylindrical inclusion
** in an infinite matrix.
**
** HEADING
** INCLUSION 200/100
** NEUTRAL FILE GENERATED ON: 04-JUN-87
** NODE, INPUT=16, NSET=ALL
** ELEMENT, TYPE=CPE8, ELSET=FIBER
367 59 60 62 61 187 189 191 188
368 61 62 64 63 191 193 195 192
388 63 64 66 65 195 197 199 196
389 48 63 65 49 194 196 198 166
390 47 61 63 48 190 192 194 164
391 46 59 61 47 186 188 190 162
392 65 66 68 67 199 201 203 200
393 67 68 70 69 203 205 207 204
394 69 70 72 71 207 209 211 208
395 71 72 74 73 211 213 215 212
396 81 82 84 83 231 233 235 232
397 73 74 76 75 215 217 219 216
398 79 80 82 81 227 229 231 228
399 75 76 78 77 219 221 223 220
400 77 78 80 79 223 225 227 224
401 49 65 67 50 198 200 202 168
402 42 49 50 41 167 168 169 157
403 43 48 49 42 165 166 167 158
404 44 47 48 43 163 164 165 159
405 45 46 47 44 161 162 163 160
406 50 67 69 51 202 204 206 170
407 51 69 71 52 206 208 210 172
408 52 71 73 53 210 212 214 174
409 53 73 75 54 214 216 218 176
410 57 81 83 58 230 232 234 184
411 56 79 81 57 226 228 230 182
412 54 75 77 55 218 220 222 178
413 55 77 79 56 222 224 226 180
414 41 50 51 36 169 170 171 149
415 36 37 42 41 148 151 157 149
416 37 38 43 42 150 153 158 151
417 38 39 44 43 152 155 159 153
418 39 40 45 44 154 156 160 155
419 36 51 52 31 171 172 173 140
420 31 52 53 26 173 174 175 131
421 26 53 54 21 175 176 177 122
422 6 57 58 1 183 184 185 86
423 21 54 55 16 177 178 179 113
424 11 56 57 6 181 182 183 95
425 16 55 56 11 179 180 181 104
426 31 32 37 36 139 142 148 140
427 32 33 38 37 141 144 150 142
428 33 34 39 38 143 146 152 144
429 34 35 40 39 145 147 154 146
430 26 27 32 31 130 133 139 131
431 21 22 27 26 121 124 130 122
432 1 2 7 6 85 88 94 86
433 16 17 22 21 112 115 121 113
434 6 7 12 11 94 97 103 95
435 11 12 17 16 103 106 112 104
436 27 28 33 32 132 135 141 133
437 28 29 34 33 134 137 143 135
438 29 30 35 34 136 138 145 137
439 22 23 28 27 123 126 132 124
440 2 3 8 7 87 90 96 88
441 17 18 23 22 114 117 123 115
442 7 8 13 12 96 99 105 97
443 12 13 18 17 105 108 114 106
444 23 24 29 28 125 128 134 126
445 24 25 30 29 127 129 135 128
446 3 4 9 8 89 92 98 90
447 4 5 10 9 91 93 100 92
448 18 19 24 23 116 119 125 117
449 8 9 14 13 98 101 107 99
450 13 14 19 18 107 110 116 108
451 19 20 25 24 118 120 127 119
452 9 10 15 14 100 102 109 101
453 14 15 20 19 109 111 118 110
**ELEMENT, TYPE=CPE8, ELSET=BEAR
73 523 524 527 526 1179 1181 1185 1180
74 526 527 530 529 1185 1187 1191 1186
75 529 530 533 532 1191 1193 1196 1192
76 532 533 536 535 1196 1199 1203 1198
77 535 536 539 538 1203 1205 1209 1204
78 538 539 542 541 1209 1211 1214 1210
79 541 542 545 544 1214 1217 1221 1216
80 556 557 560 559 1245 1247 1250 1246
81 544 545 548 547 1221 1223 1227 1222
82 553 554 557 556 1239 1241 1245 1240
83 547 548 551 550 1227 1229 1232 1228
84 550 551 554 553 1232 1235 1239 1234
85 522 523 526 525 1177 1180 1183 1178

```


86 525 526 529 528 1183 1186 1189 1184
87 528 529 532 531 1189 1192 1195 1190
88 531 532 535 534 1195 1198 1201 1197
89 534 535 538 537 1201 1204 1207 1202
90 537 538 541 540 1207 1210 1213 1208
91 540 541 544 543 1213 1216 1219 1215
92 555 556 559 558 1243 1246 1249 1244
93 543 544 547 546 1219 1222 1225 1220
94 552 553 556 555 1237 1240 1243 1238
95 546 547 550 549 1225 1228 1231 1226
96 549 550 553 552 1231 1234 1237 1233
97 473 522 525 477 1176 1178 1182 1083
98 477 525 528 481 1182 1184 1188 1091
99 481 528 531 485 1188 1190 1194 1099
100 485 531 534 489 1194 1197 1200 1107
101 489 534 537 493 1200 1202 1206 1115
102 493 537 540 497 1206 1208 1212 1123
103 497 540 543 501 1212 1215 1218 1131
104 517 555 558 521 1242 1244 1248 1171
105 501 543 546 505 1218 1220 1224 1139
106 513 552 555 517 1236 1238 1242 1163
107 505 546 549 509 1224 1226 1230 1147
108 509 549 552 513 1230 1233 1236 1155
109 472 473 477 476 1081 1083 1089 1082
110 476 477 481 480 1089 1091 1097 1090
111 480 481 485 484 1097 1099 1105 1098
112 484 485 489 488 1105 1107 1111 1106
113 488 489 493 492 1111 1115 1121 1114
114 492 493 497 496 1121 1123 1129 1122
115 496 497 501 500 1129 1131 1137 1130
116 516 517 521 520 1169 1171 1175 1170
117 500 501 505 504 1137 1139 1143 1138
118 512 513 517 516 1161 1163 1169 1162
119 504 505 509 508 1143 1147 1153 1146
120 508 509 513 512 1153 1155 1161 1154
121 471 472 476 475 1079 1082 1087 1080
122 475 476 480 479 1087 1090 1095 1088
123 479 480 484 483 1095 1098 1103 1096
124 483 484 488 487 1103 1106 1110 1104
125 487 488 492 491 1110 1114 1119 1113
126 491 492 496 495 1119 1122 1127 1120
127 495 496 500 499 1127 1130 1135 1128
128 515 516 520 519 1167 1170 1174 1168
129 499 500 504 503 1135 1138 1142 1136
130 511 512 516 515 1159 1162 1167 1160
131 503 504 508 507 1142 1146 1151 1145
132 507 508 512 511 1151 1154 1159 1152
133 470 471 475 474 1077 1080 1085 1078
134 474 475 479 478 1085 1088 1093 1086
135 478 479 483 482 1093 1096 1101 1094
136 482 483 487 486 1101 1104 1109 1102
137 486 487 491 490 1109 1113 1117 1112
138 490 491 495 494 1117 1120 1125 1118
139 494 495 499 498 1125 1128 1133 1126
140 514 515 519 518 1165 1168 1173 1166
141 498 499 503 502 1133 1136 1141 1134
142 510 511 515 514 1157 1160 1165 1158
143 502 503 507 506 1141 1145 1149 1144
144 506 507 511 510 1149 1152 1157 1150
145 409 470 474 410 1076 1078 1084 960
146 410 474 478 411 1084 1086 1092 961
147 411 478 482 412 1092 1094 1100 962
148 412 482 486 413 1100 1102 1108 963
149 413 486 490 438 1108 1112 1116 1016
150 438 490 494 439 1116 1118 1124 1017
151 439 494 498 440 1124 1126 1132 1018
152 468 514 518 469 1164 1166 1172 1075
153 440 498 502 441 1132 1134 1140 1019
154 467 510 514 468 1156 1158 1164 1074
155 441 502 506 466 1140 1144 1148 1072
156 466 506 510 467 1148 1150 1156 1073
157 404 409 410 405 952 960 954 951
158 405 410 411 406 954 961 956 953
159 406 411 412 407 956 962 958 955
160 407 412 413 408 968 963 959 957
161 408 413 438 434 969 1016 1010 1008
162 434 438 439 435 1010 1017 1012 1009
163 435 439 440 436 1012 1018 1014 1011
164 464 468 469 465 1070 1075 1071 1069
165 436 440 441 437 1014 1019 1015 1013
166 463 467 468 464 1068 1074 1070 1067
167 437 441 466 462 1015 1072 1066 1064
168 462 466 467 463 1066 1073 1068 1065
169 399 404 405 400 943 951 945 942
170 400 405 406 401 945 953 947 944
171 401 406 407 402 947 955 949 946
172 402 407 408 403 949 957 950 948
173 403 408 434 430 950 1008 1002 1000
174 430 434 435 431 1002 1009 1004 1001
175 431 435 436 432 1004 1011 1006 1003

176 460 464 465 461 1062 1069 1063 1061
177 432 436 437 433 1006 1013 1007 1005
178 459 463 464 460 1060 1067 1062 1059
179 433 437 462 458 1007 1064 1058 1056
180 458 462 463 459 1058 1065 1060 1057
181 394 399 400 395 934 942 936 933
182 395 400 401 396 936 944 938 935
183 396 401 402 397 938 946 940 937
184 397 402 403 398 940 948 941 939
185 398 403 430 426 941 1000 994 992
186 426 430 431 427 994 1001 996 993
187 427 431 432 428 996 1003 998 995
188 456 460 461 457 1054 1061 1055 1053
189 428 432 433 429 998 1005 999 997
190 455 459 460 456 1052 1059 1054 1051
191 429 433 458 454 999 1056 1050 1048
192 454 458 459 455 1050 1057 1052 1049
193 389 394 395 390 925 933 927 924
194 390 395 396 391 927 935 929 926
195 391 396 397 392 929 937 931 928
196 392 397 398 393 931 939 932 930
197 393 398 426 422 932 992 986 984
198 422 426 427 423 986 993 988 985
199 423 427 428 424 988 995 990 987
200 452 456 457 453 1046 1053 1047 1045
201 424 428 429 425 990 997 991 989
202 451 455 456 452 1044 1051 1046 1043
203 425 429 454 450 991 1048 1042 1040
204 450 454 455 451 1042 1049 1044 1041
205 384 389 390 385 916 924 918 915
206 385 390 391 386 918 926 920 917
207 386 391 392 387 920 928 922 919
208 387 392 393 388 922 930 923 921
209 388 393 422 418 923 984 978 976
210 418 422 423 419 978 985 980 977
211 419 423 424 420 980 987 982 979
212 448 452 453 449 1038 1045 1039 1037
213 420 424 425 421 982 989 983 981
214 447 451 452 448 1036 1043 1038 1035
215 421 425 450 446 983 1040 1034 1032
216 446 450 451 447 1034 1041 1036 1033
217 379 384 385 380 907 915 909 906
218 380 385 386 381 909 917 911 908
219 381 386 387 382 911 919 913 910
220 382 387 388 383 913 921 914 912
221 383 388 418 414 914 976 970 968
222 414 418 419 415 970 977 972 969
223 415 419 420 416 972 979 974 971
224 444 448 449 445 1030 1037 1031 1029
225 416 420 421 417 974 981 975 973
226 443 447 448 444 1028 1035 1030 1027
227 417 421 446 442 975 1032 1026 1024
228 442 446 447 443 1026 1033 1028 1025
229 286 379 380 287 901 906 902 729
230 287 380 381 288 902 908 903 730
231 288 381 382 289 903 910 904 731
232 289 382 383 290 904 912 905 732
233 290 383 414 331 905 968 964 813
234 331 414 415 332 964 969 965 814
235 332 415 416 333 965 971 966 815
236 377 444 445 378 1022 1029 1023 900
237 333 416 417 334 966 973 967 816
238 376 443 444 377 1021 1027 1022 899
239 334 417 442 375 967 1024 1020 897
240 375 442 443 376 1020 1025 1021 898
241 281 286 287 282 721 729 723 720
242 282 287 288 283 723 730 725 722
243 283 288 289 284 725 731 727 724
244 284 289 290 285 727 732 728 726
245 285 290 331 327 728 813 807 805
246 327 331 332 328 807 814 809 806
247 328 332 333 329 809 815 811 808
248 373 377 378 374 895 900 896 894
249 329 333 334 330 811 816 812 810
250 372 376 377 373 893 899 895 892
251 330 334 375 371 812 897 891 889
252 371 375 376 372 891 898 893 890
253 276 281 282 277 712 720 714 711
254 277 282 283 278 714 722 716 713
255 278 283 284 279 716 724 718 715
256 279 284 285 280 718 726 719 717
257 280 285 327 323 719 805 799 797
258 323 327 328 324 799 806 801 798
259 324 328 329 325 801 808 803 800
260 369 373 374 370 887 894 888 886
261 325 329 330 326 803 810 804 802
262 368 372 373 369 885 892 887 884
263 326 330 371 367 804 889 883 881
264 367 371 372 368 883 890 885 882
265 271 276 277 272 703 711 705 702

266 272 277 278 278 273 705 713 707 704
267 273 278 279 274 707 715 709 706
268 274 279 280 275 709 717 710 708
269 275 280 323 319 710 797 791 789
270 319 323 324 320 791 798 793 790
271 320 324 325 321 793 800 795 792
272 365 369 370 366 879 886 880 878
273 321 325 326 322 795 802 796 794
274 364 368 369 365 877 884 879 876
275 322 326 367 363 796 881 875 873
276 363 367 368 364 875 882 877 874
277 266 271 272 267 694 702 696 693
278 267 272 273 268 696 704 698 695
279 268 273 274 269 698 706 700 697
280 269 274 275 270 700 708 701 699
281 270 275 319 315 701 789 783 781
282 315 319 320 316 783 790 785 782
283 316 320 321 317 785 792 787 784
284 361 365 366 362 871 878 872 870
285 317 321 322 318 787 794 788 786
286 360 364 365 361 869 876 871 868
287 318 322 363 359 788 873 867 865
288 359 363 364 360 867 874 869 866
289 261 266 267 262 685 693 687 684
290 262 267 268 263 687 695 689 686
291 263 268 269 264 689 697 691 688
292 264 269 270 265 691 699 692 690
293 265 270 315 311 692 781 775 773
294 311 315 316 312 775 782 777 774
295 312 316 317 313 777 784 779 776
296 357 361 362 358 863 870 864 862
297 313 317 318 314 779 786 780 778
298 356 360 361 357 861 868 863 860
299 314 318 359 355 780 865 859 857
300 355 359 360 356 859 866 861 858
301 256 261 262 257 676 684 678 675
302 257 262 263 258 678 686 680 677
303 258 263 264 259 680 688 682 679
304 259 264 265 260 682 690 683 681
305 260 265 311 307 683 773 767 765
306 307 311 312 308 767 774 769 766
307 308 312 313 309 769 776 771 768
308 353 357 358 354 855 862 856 854
309 309 313 314 310 771 778 772 770
310 352 356 357 353 853 860 855 852
311 310 314 355 351 772 857 851 849
312 351 355 356 352 851 858 853 850
313 251 256 257 252 667 675 669 666
314 252 257 258 253 669 677 671 668
315 253 258 259 254 671 679 673 670
316 254 259 260 255 673 681 674 672
317 255 260 307 303 674 765 759 757
318 303 307 308 304 759 766 761 758
319 304 308 309 305 761 768 763 760
320 349 353 354 350 847 854 848 846
321 305 309 310 306 763 770 764 762
322 348 352 353 349 845 852 847 844
323 306 310 351 347 764 849 843 841
324 347 351 352 348 843 850 845 842
325 246 251 252 247 658 666 660 657
326 247 252 253 248 660 668 662 659
327 248 253 254 249 662 670 664 661
328 249 254 255 250 664 672 665 663
329 250 255 303 299 665 757 751 749
330 299 303 304 300 751 758 753 750
331 300 304 305 301 753 760 755 752
332 345 349 350 346 839 846 840 838
333 301 305 306 302 755 762 756 754
334 344 348 349 345 837 844 839 836
335 302 306 347 343 756 841 835 833
336 343 347 348 344 835 842 837 834
337 241 246 247 242 649 657 651 648
338 236 241 242 237 640 648 642 639
339 242 247 248 243 651 659 653 650
340 243 248 249 244 653 661 655 652
341 244 249 250 245 655 663 656 654
342 245 250 299 295 656 749 743 741
343 295 299 300 296 743 750 745 742
344 296 300 301 297 745 752 747 744
345 341 345 346 342 831 838 832 830
346 297 301 302 298 747 754 748 746
347 340 344 345 341 829 836 831 828
348 298 302 343 339 748 833 827 825
349 339 343 344 340 827 834 829 826
350 237 242 243 238 642 650 644 641
355 238 243 244 239 644 652 646 643
356 239 244 245 240 646 654 647 645
357 240 245 295 291 647 741 735 733
358 291 295 296 292 735 742 737 734
359 292 296 297 293 737 744 739 736

360 337 341 342 338 823 823 830 824 822
361 293 297 298 294 739 746 740 738
362 336 340 341 337 821 828 823 820
363 294 298 339 335 740 825 819 817
364 335 339 340 336 819 826 821 818
*ELEMENT, TYPE=CPES, ELSET=FAE
1 577 581 582 578 1284 1290 1286 1283
2 578 582 583 579 1286 1291 1288 1285
3 579 583 584 580 1288 1292 1289 1287
4 580 584 600 597 1289 1326 1322 1320
5 597 600 601 598 1322 1327 1324 1321
6 598 601 602 599 1324 1328 1325 1323
7 599 602 618 615 1325 1362 1358 1356
8 634 637 638 635 1396 1400 1397 1395
9 615 618 619 616 1358 1363 1360 1357
10 633 636 637 634 1394 1399 1396 1393
11 616 619 620 617 1360 1364 1361 1359
12 617 620 636 633 1361 1398 1394 1392
13 574 577 578 574 1277 1283 1279 1276
14 574 578 579 575 1279 1285 1281 1278
15 575 579 580 576 1281 1287 1282 1280
16 576 580 597 594 1282 1320 1316 1314
17 594 597 598 595 1316 1321 1318 1315
18 595 598 599 596 1318 1323 1319 1317
19 596 599 615 612 1319 1356 1352 1350
20 631 634 635 632 1390 1395 1391 1389
21 612 615 616 613 1352 1357 1354 1351
22 630 633 634 631 1388 1393 1390 1387
23 613 616 617 614 1354 1359 1355 1353
24 614 617 633 630 1355 1392 1388 1386
25 569 573 574 570 1270 1276 1272 1269
26 570 574 575 571 1272 1278 1274 1271
27 571 575 576 572 1274 1280 1275 1273
28 572 576 594 591 1275 1314 1310 1308
29 591 594 595 592 1310 1315 1312 1309
30 592 595 596 593 1312 1317 1313 1311
31 593 596 612 609 1313 1350 1346 1344
32 628 631 632 629 1384 1389 1385 1383
33 609 612 613 610 1346 1351 1348 1345
34 627 630 631 628 1382 1387 1384 1381
35 610 613 614 611 1348 1353 1349 1347
36 611 614 630 627 1349 1386 1382 1380
37 565 569 570 566 1263 1269 1265 1262
38 566 570 571 567 1265 1271 1267 1264
39 567 571 572 568 1267 1273 1268 1266
40 568 572 591 588 1268 1308 1304 1302
41 588 591 592 589 1304 1309 1306 1303
42 589 592 593 590 1306 1311 1307 1305
43 590 593 609 606 1307 1344 1340 1338
44 625 628 629 626 1378 1383 1379 1377
45 606 609 610 607 1340 1345 1342 1339
46 624 627 628 625 1376 1381 1378 1375
47 607 610 611 608 1342 1347 1343 1341
48 608 611 627 624 1343 1380 1376 1374
49 561 565 566 562 1256 1262 1258 1255
50 562 566 567 563 1258 1264 1260 1257
51 563 567 568 564 1260 1266 1261 1259
52 564 568 588 585 1261 1302 1298 1296
53 585 588 589 586 1298 1303 1300 1297
54 586 589 590 587 1300 1306 1301 1299
55 587 590 606 603 1301 1338 1334 1332
56 622 625 626 623 1372 1377 1373 1371
57 603 606 607 604 1334 1339 1336 1333
58 621 624 625 622 1370 1375 1372 1369
59 604 607 608 605 1336 1341 1337 1335
60 605 608 624 621 1337 1374 1370 1368
61 524 561 562 527 1251 1255 1252 1181
62 527 562 563 530 1252 1257 1253 1187
63 530 563 564 533 1253 1259 1254 1193
64 533 564 585 536 1254 1296 1293 1199
65 536 585 586 539 1293 1297 1294 1205
66 539 586 587 542 1294 1299 1295 1211
67 542 587 603 545 1295 1332 1329 1217
68 557 622 623 560 1366 1371 1367 1247
69 545 603 604 548 1329 1333 1330 1223
70 554 621 622 557 1365 1369 1366 1241
71 548 604 605 551 1330 1335 1331 1229
72 551 605 621 554 1331 1368 1365 1235
*MPC
9 193 641
9 62 237
9 189 639
9 60 236
9 64 238
9 197 643
9 66 239
9 201 645
9 68 240
9 205 733
9 70 281

```

9 209 734
9 72 292
9 213 736
9 233 822
5 84 338
9 74 293
9 217 738
9 82 337
9 229 820
9 76 294
9 221 817
9 80 336
9 78 335
9 225 818
*HSET,HSET=INTBOUN
193,62,189,60,64,197,66,201,68,206,70,209,72,213,
233,84,74,217,82,229,76,221,80,78,225
*HSET,HSET=EXTBOUN
641,237,639,236,238,643,239,645,240,733,291,734,292,
736,822,338,293,738,337,820,294,817,336,335,818
*ELSET,ELSET=CLOSE,GENERATE
241,364,1
*HSET,HSET=LEFT
1 2 3 4 5 58 83 84 85 87 89
91 185 234 235 338
342 346 350 354 358 362 366 370 374 378 445
449 453 457 461 465
469 518 519 520 521 558 559 560 623 626 629
632 635 638 824 832
840 848 856 864 872 880 888 896 1023 1031 1039
1047 1055 1063 1071 1172
1173 1174 1175 1248 1249 1250 1367 1373 1379 1385 1391
1397
*HSET,HSET=BOTTOM
5 10 15 20 25 30 35 40 45 46 59
60 93 102 111 120
129 138 147 156 161 186 187 236 241 246 251
256 261 266 271 276
281 286 379 384 389 394 399 404 409 470 471
472 473 522 523 524
561 565 569 573 577 581 640 649 658 667 676
685 694 703 712 721
901 907 916 925 934 943 952 1076 1077 1079 1081
1176 1177 1179 1251 1256
1263 1270 1277 1284
*HSET,HSET=TOP
638,637,636,620,619,618,602,1400,1399,1398,1364,1363,1362
*HSET,HSET=RIGHT
561,582,583,584,600,601,602,1290,1291,1292,1326,1327,1328
*ELSET,ELSET=INNER
HEAR,FIBER
*ELSET,ELSET=MATRIX
HEAR,FAR
*EQUATION
2
1400,2,1,638,2,-1
2
637,2,1,638,2,-1
2
1399,2,1,638,2,-1
2
636,2,1,638,2,-1
2
1398,2,1,638,2,-1
2
620,2,1,638,2,-1
2
1364,2,1,638,2,-1
2
619,2,1,638,2,-1
2
1363,2,1,638,2,-1
2
618,2,1,638,2,-1
2
1362,2,1,638,2,-1
2
602,2,1,638,2,-1
2
1328,1,1,602,1,-1
2
601,1,1,602,1,-1
2
1327,1,1,602,1,-1
2
600,1,1,602,1,-1
2
1326,1,1,602,1,-1
2
584,1,1,602,1,-1

```

```

2
1292,1,1,602,1,-1
2
583,1,1,602,1,-1
2
1291,1,1,602,1,-1
2
582,1,1,602,1,-1
2
1290,1,1,602,1,-1
2
581,1,1,602,1,-1
*BOUNDARY
LEFT,1,0.
BOTTOM,2,0.
*SOLID SECTION,ELSET=MATRIX,MATERIAL=MMATRIX
*SOLID SECTION,ELSET=FIBER,MATERIAL=HFIBER
*MATERIAL,NAME=MMATRIX
*ELASTIC,TYPE=ISO
200.0E3,0.3
*EXPANSION,ZERO=0.
0.0,0.
*MATERIAL,NAME=HFIBER
*ELASTIC,TYPE=ISO
100.0E3,0.3
*EXPANSION,TYPE=ORTHO,ZERO=0.
1.E-6,1.E-6,0.,0.
*INITIAL CONDITIONS,TYPE=TEMPERATURE
ALL,0.
*STEP,LINER
*STATIC
*TEMPERATURE
ALL,-1000.
*LOAD
638,2,100.
S
*EL PRINT,ELSET=FIBER,POSITION=AVERAGED AT NODES
S
EMER
EE
*EL PRINT,ELSET=CLOSE,POSITION=AVERAGED AT NODES
S
EMER
EE
*MODE PRINT,MODE=ALL
U

```

```

*PLOT
def.conf. Em/Ef = 2 Misfit -1.e-3 Load = 100MPa
*DETAIL,ELSET=INNER
*DISPLACED
U
*PLOT
def.conf. Em/Ef = 2 Misfit -1.e-3 Load = 100MPa
*DETAIL,ELSET=FAR
*DISPLACED
U
*PLOT
stress Em/Ef = 2 Misfit -1.e-3 Load = 100MPa
*DETAIL,ELSET=INNER
*CONTOUR
S11
S22
S12
S33
*DETAIL,ELSET=FAR
*CONTOUR
S11
S22
S12
S33
*MODE FILE,MODE=ALL
U
*EL FILE
S
EMER
EE
*END STEP

```

**APPENDIX V: TYPICAL ABAQUS INPUT
FILE FOR THE ELASTIC
ANALYSIS OF A $\gamma - \gamma'$ UNIT CELL**

```

**
**      Abaqus 4.7 Input file for elastic analysis
**      of gamma-gamma' unit cell.
**
**
**HEADING
Miyazaki, Kakamura, Mori alloy /tension.
*NODE,INPUT=16
*NODE,INPUT=17
*SET,ASET=ALL,GENERATE
1,5002
*SET,ASET=BOTTOM1,GENERATE
1,41,1
*SET,ASET=BOTTOM2,GENERATE
1843,4597,81
*SET,ASET=BOTTOM
BOTTOM1,BOTTOM2
*SET,ASET=LEFT1,GENERATE
1,1641,41
*SET,ASET=LEFT2,GENERATE
1763,4517,81
*SET,ASET=LEFT
LEFT1,LEFT2
*SET,ASET=INTBOUN,GENERATE
2978,3058
*SET,ASET=EXTBOUN,GENERATE
3059,3139
*ELEMENT,TYPE=CGPE10R
1,1,3,85,83,2,44,84,42,5001,5002
1,20,2,1,20,82,20
*ELEMENT,TYPE=CGPE10R
401,1641,1643,1846,1844,1642,1765,1845,1763,5001,5002
*ELGEM,ELSET=FLAYL
401,20,2
*ELEMENT,TYPE=CGPE10R,ELSET=FLAYR
421,1681,1599,1886,1884,1640,1805,1885,1703,5001,5002
422,1599,1517,1888,1886,1558,1807,1887,1805,5001,5002
423,1517,1435,1890,1888,1476,1809,1889,1807,5001,5002
424,1435,1353,1892,1890,1394,1811,1891,1809,5001,5002
425,1353,1271,1894,1892,1312,1813,1893,1811,5001,5002
426,1271,1189,1896,1894,1230,1815,1895,1813,5001,5002
427,1189,1107,1898,1896,1148,1817,1897,1815,5001,5002
428,1107,1025,1900,1898,1066,1819,1899,1817,5001,5002
429,1025,943,1902,1900,984,1821,1901,1819,5001,5002
430,943,861,1904,1902,902,1823,1903,1821,5001,5002

431,861,779,1906,1904,820,1825,1905,1823,5001,5002
432,779,697,1908,1906,738,1827,1907,1825,5001,5002
433,697,615,1910,1908,656,1829,1909,1827,5001,5002
434,615,533,1912,1910,574,1831,1911,1829,5001,5002
435,533,451,1914,1912,492,1833,1913,1831,5001,5002
436,451,369,1916,1914,410,1835,1915,1833,5001,5002
437,369,287,1918,1916,328,1837,1917,1835,5001,5002
438,287,205,1920,1918,246,1839,1919,1837,5001,5002
439,205,123,1922,1920,164,1841,1921,1839,5001,5002
440,123,41,1924,1922,82,1843,1923,1841,5001,5002
*ELSET,ELSET=FLAYR
FLAYL,FLAYR
*ELEMENT,TYPE=CGPE10R
441,1844,1846,2008,2006,1845,1927,2007,1925,5001,5002
*ELGEM,ELSET=SLAYER
441,40,2,1,7,162,40
*ELEMENT,TYPE=CGPE10R
721,3059,3061,3223,3221,3060,3142,3222,3140,5001,5002
*ELGEM,ELSET=TLAYER
721,40,2,1,9,162,40
*ELSET,ELSET = ELEXBD,GENERATE
721,761
*ELSET,ELSET = ELIIBD,GENERATE
681,720
*ELSET,ELSET = GAMMA,GENERATE
721,1080
*ELSET,ELSET = GAMMAP,GENERATE
1,720
*SOLID SECTION,ELSET=GAMMA,MATERIAL=MGAMMA
*SOLID SECTION,ELSET=GAMMAP,MATERIAL=MGAMMAP
*MATERIAL,NAME=MGAMMA
*ELASTIC,TYPE=ORTHO
112400.,62700.,112400.,62700.,62700.,112400.,56900.,56900.,25.
*EXPANSION,ZERO=25.
0.0E-5,850.
*MATERIAL,NAME=MGAMMAP
*ELASTIC,TYPE=ORTHO
166600.,106500.,166600.,106500.,106500.,166600.,99200.,99200.,25.
*EXPANSION,ZERO=25.
1.E-6,850.
*BOUNDARY
BOTTOM,2,,0,0
LEFT,1,,0,0

```


5002,1,2,0,0
*EQUATION
2
4518,2,1,4517,2,-1
2
4519,2,1,4517,2,-1
2
4520,2,1,4517,2,-1
2
4521,2,1,4517,2,-1
2
4522,2,1,4517,2,-1
2
4523,2,1,4517,2,-1
2
4524,2,1,4517,2,-1
2
4525,2,1,4517,2,-1
2
4526,2,1,4517,2,-1
2
4527,2,1,4517,2,-1
2
4528,2,1,4517,2,-1
2
4529,2,1,4517,2,-1
2
4530,2,1,4517,2,-1
2
4531,2,1,4517,2,-1
2
4532,2,1,4517,2,-1
2
4533,2,1,4517,2,-1
2
4534,2,1,4517,2,-1
2
4535,2,1,4517,2,-1
2
4536,2,1,4517,2,-1
2
4537,2,1,4517,2,-1
2
4538,2,1,4517,2,-1
2
4539,2,1,4517,2,-1
2
4540,2,1,4517,2,-1
2
4541,2,1,4517,2,-1
2
4542,2,1,4517,2,-1
2
4543,2,1,4517,2,-1
2
4544,2,1,4517,2,-1
2
4545,2,1,4517,2,-1
2
4546,2,1,4517,2,-1
2
4547,2,1,4517,2,-1
2
4548,2,1,4517,2,-1
2
4549,2,1,4517,2,-1
2
4550,2,1,4517,2,-1
2
4551,2,1,4517,2,-1
2
4552,2,1,4517,2,-1
2
4553,2,1,4517,2,-1
2
4554,2,1,4517,2,-1
2
4555,2,1,4517,2,-1
2
4556,2,1,4517,2,-1
2
4557,2,1,4517,2,-1
2
4557,1,1,4597,1,-1
2
4558,1,1,4597,1,-1
2
4559,1,1,4597,1,-1
2
4560,1,1,4597,1,-1
2

2
 4561,1,1,4597,1,-1
 2
 4562,1,1,4597,1,-1
 2
 4563,1,1,4597,1,-1
 2
 4564,1,1,4597,1,-1
 2
 4565,1,1,4597,1,-1
 2
 4566,1,1,4597,1,-1
 2
 4567,1,1,4597,1,-1
 2
 4568,1,1,4597,1,-1
 2
 4569,1,1,4597,1,-1
 2
 4570,1,1,4597,1,-1
 2
 4571,1,1,4597,1,-1
 2
 4572,1,1,4597,1,-1
 2
 4573,1,1,4597,1,-1
 2
 4574,1,1,4597,1,-1
 2
 4575,1,1,4597,1,-1
 2
 4576,1,1,4597,1,-1
 2
 4577,1,1,4597,1,-1
 2
 4578,1,1,4597,1,-1
 2
 4579,1,1,4597,1,-1
 2
 4580,1,1,4597,1,-1
 2
 4581,1,1,4597,1,-1
 2
 4582,1,1,4597,1,-1
 2

4583,1,1,4597,1,-1
 2
 4584,1,1,4597,1,-1
 2
 4585,1,1,4597,1,-1
 2
 4586,1,1,4597,1,-1
 2
 4587,1,1,4597,1,-1
 2
 4588,1,1,4597,1,-1
 2
 4589,1,1,4597,1,-1
 2
 4590,1,1,4597,1,-1
 2
 4591,1,1,4597,1,-1
 2
 4592,1,1,4597,1,-1
 2
 4593,1,1,4597,1,-1
 2
 4594,1,1,4597,1,-1
 2
 4595,1,1,4597,1,-1
 2
 4596,1,1,4597,1,-1
 *EQUATION
 2
 INTBOUN,2,1,EXTBOUN,2,-1
 2
 INTBOUN,1,1,EXTBOUN,1,-1
 *INITIAL CONDITIONS,TYPE=TEMPERATURE
 ALL,0.0
 *STEP,LINEAR
 *STATIC
 *TEMPERATURE
 ALL,5000.
 *CLOAD
 4517,2,147.
 *EL PRINT,ELSET=FLAYR
 S
 *NODE PRINT, #SET=INTBOUN
 U
 *PLOT

MEM TENSION
*DISPLACED
U
*PLOT
N/M/M misfit and load
*CONTOUR
S11
S22
S33
S12
MISES
PRESS
*NODE FILE
U
*EL FILE
S
EMER
*END STEP

**APPENDIX VI: TYPICAL ABAQUS INPUT
FILE FOR THE
ANALYSIS OF A STRESS-ANNEALING
TRANSIENT FOR A $\gamma - \gamma'$ UNIT CELL**

```

**
** Abaqus 4.7 input file for analysis of stress annealing
** transient for a gamma-gamma' unit cell.
**
** HEADING
Miyazaki,Makemura,Mori
**NODE,INPUT=16
**NODE,INPUT=17
**NSET,NSET=ALL,GENERATE
1,5002
**NSET,NSET=BOTTOM1,GENERATE
1,41,1
**NSET,NSET=BOTTOM2,GENERATE
1843,4597,81
**NSET,NSET=BOTTOM
BOTTOM1,BOTTOM2
**NSET,NSET=LEFT1,GENERATE
1,1641,41
**NSET,NSET=LEFT2,GENERATE
1763,4517,81
**NSET,NSET=LEFT
LEFT1,LEFT2
**NSET,NSET=INTROUM,GENERATE
2978,3058
**NSET,NSET=EXTROUM,GENERATE
3059,3139
**ELEMENT,TYPE=CGPELOR
1,1,3,85,83,2,44,84,42,5001,5002
**ELGEN,ELSET=CARTES
1,20,2,1,20,82,20
**ELEMENT,TYPE=CGPELOR
401,1641,1643,1846,1844,1642,1765,1845,1763,5001,5002
**ELGEN,ELSET=FLAYL
401,20,2
**ELEMENT,TYPE=CGPELOR,ELSET=FLAYR
421,1681,1599,1886,1884,1640,1805,1885,1803,5001,5002
422,1599,1517,1888,1886,1558,1807,1887,1805,5001,5002
423,1517,1435,1890,1888,1476,1809,1889,1807,5001,5002
424,1435,1353,1892,1890,1394,1811,1891,1809,5001,5002
425,1353,1271,1894,1892,1312,1813,1893,1811,5001,5002
426,1271,1189,1896,1894,1230,1815,1895,1813,5001,5002
427,1189,1107,1898,1896,1148,1817,1897,1815,5001,5002
428,1107,1025,1900,1898,1066,1819,1899,1817,5001,5002
429,1025,943,1902,1900,984,1821,1901,1819,5001,5002
430,943,861,1904,1902,902,1823,1903,1821,5001,5002
431,861,779,1906,1904,820,1825,1905,1825,5001,5002
432,779,697,1908,1906,738,1827,1907,1825,5001,5002
433,697,615,1910,1908,656,1829,1909,1827,5001,5002
434,615,533,1912,1910,574,1831,1911,1829,5001,5002
435,533,451,1914,1912,492,1833,1913,1831,5001,5002
436,451,369,1916,1914,410,1835,1915,1833,5001,5002
437,369,287,1918,1916,328,1837,1917,1835,5001,5002
438,287,205,1920,1918,246,1839,1919,1837,5001,5002
439,205,123,1922,1920,164,1841,1921,1839,5001,5002
440,123,41,1924,1922,82,1843,1923,1841,5001,5002
**ELSET,ELSET=FLAYER
FLAYL,FLAYR
**ELEMENT,TYPE=CGPELOR
441,1844,1846,2008,2006,1845,1927,2007,1925,5001,5002
**ELGEN,ELSET=SLAYER
441,40,2,1,7,162,40
**ELEMENT,TYPE=CGPELOR
721,3059,3061,3223,3221,3060,3142,3222,3140,5001,5002
**ELGEN,ELSET=TLAYER
721,40,2,1,9,162,40
**ELSET,ELSET = ELEXBD,GENERATE
721,761
**ELSET,ELSET = ELINBD,GENERATE
681,720
**ELSET,ELSET = GAMMA,GENERATE
721,1080
**ELSET,ELSET = GAMMAP,GENERATE
1,720
**SOLID SECTION,ELSET=GAMMA,MATERIAL=HGAMMA
**SOLID SECTION,ELSET=GAMMAP,MATERIAL=HGAMMAP
**MATERIAL,NAME=HGAMMA
112400,62700,112400,62700,62700,112400,56900,56900,25,
56900,25,
**EXPANSION,ZERO=25.
0.0E-5,850.
**CREEP,LAW=STRAIN
S,4E-15,4.8,0,850.
**MATERIAL,NAME=HGAMMAP
**ELASTIC,TYPE=ORTHO
166600,106500,166600,106500,106500,166600,99200,99200,25,
99200,25,
**EXPANSION,ZERO=25.
1.E-6,850.
**BOUNDARY
BOTTOM,2,,0.0

```

```

LEFT,1,,0.0
5002,1,2,0.0
*EQUATION
2
4518,2,1,4517,2,-1
2
4519,2,1,4517,2,-1
2
4520,2,1,4517,2,-1
2
4521,2,1,4517,2,-1
2
4522,2,1,4517,2,-1
2
4523,2,1,4517,2,-1
2
4524,2,1,4517,2,-1
2
4525,2,1,4517,2,-1
2
4526,2,1,4517,2,-1
2
4527,2,1,4517,2,-1
2
4528,2,1,4517,2,-1
2
4529,2,1,4517,2,-1
2
4530,2,1,4517,2,-1
2
4531,2,1,4517,2,-1
2
4532,2,1,4517,2,-1
2
4533,2,1,4517,2,-1
2
4534,2,1,4517,2,-1
2
4535,2,1,4517,2,-1
2
4536,2,1,4517,2,-1
2
4537,2,1,4517,2,-1
2
4538,2,1,4517,2,-1
2
4539,2,1,4517,2,-1
2
4540,2,1,4517,2,-1
2
4541,2,1,4517,2,-1
2
4542,2,1,4517,2,-1
2
4543,2,1,4517,2,-1
2
4544,2,1,4517,2,-1
2
4545,2,1,4517,2,-1
2
4546,2,1,4517,2,-1
2
4547,2,1,4517,2,-1
2
4548,2,1,4517,2,-1
2
4549,2,1,4517,2,-1
2
4550,2,1,4517,2,-1
2
4551,2,1,4517,2,-1
2
4552,2,1,4517,2,-1
2
4553,2,1,4517,2,-1
2
4554,2,1,4517,2,-1
2
4555,2,1,4517,2,-1
2
4556,2,1,4517,2,-1
2
4557,2,1,4517,2,-1
2
4557,1,1,4597,1,-1
2
4558,1,1,4597,1,-1
2
4559,1,1,4597,1,-1
2

```

```

4560,1,1,4597,1,-1
2
4561,1,1,4597,1,-1
2
4562,1,1,4597,1,-1
2
4563,1,1,4597,1,-1
2
4564,1,1,4597,1,-1
2
4565,1,1,4597,1,-1
2
4566,1,1,4597,1,-1
2
4567,1,1,4597,1,-1
2
4568,1,1,4597,1,-1
2
4569,1,1,4597,1,-1
2
4570,1,1,4597,1,-1
2
4571,1,1,4597,1,-1
2
4572,1,1,4597,1,-1
2
4573,1,1,4597,1,-1
2
4574,1,1,4597,1,-1
2
4575,1,1,4597,1,-1
2
4576,1,1,4597,1,-1
2
4577,1,1,4597,1,-1
2
4578,1,1,4597,1,-1
2
4579,1,1,4597,1,-1
2
4580,1,1,4597,1,-1
2
4581,1,1,4597,1,-1
2
4582,1,1,4597,1,-1
2
4583,1,1,4597,1,-1
2
4584,1,1,4597,1,-1
2
4585,1,1,4597,1,-1
2
4586,1,1,4597,1,-1
2
4587,1,1,4597,1,-1
2
4588,1,1,4597,1,-1
2
4589,1,1,4597,1,-1
2
4590,1,1,4597,1,-1
2
4591,1,1,4597,1,-1
2
4592,1,1,4597,1,-1
2
4593,1,1,4597,1,-1
2
4594,1,1,4597,1,-1
2
4595,1,1,4597,1,-1
2
4596,1,1,4597,1,-1
*EQUATION
2
INTBOUN,2,1,EXTBOUN,2,-1
2
INTBOUN,1,1,EXTBOUN,1,-1
*AMPLITUDE,TIME=V,NAME=LOWER
0,0,0,1,0,1,0
*INITIAL CONDITIONS,TYPE=TEMPERATURE
ALL,0,0
*STEP
*STATIC,PTOL=1.
*TEMPERATURE
ALL,5000.
*EL PRINT,ELSET=FLAYR
S
*MODE PRINT,MSET=INTBOUN
U

```

```

*PLOT
deformed conf. temperature
*DISPLACED
U
*PLOT
M/M/M misfit only
*CONTOUR
S11
S22
S33
S12
MISES
PRESS
*MODE FILE
U
*CL FILE
S
ENER
*END STEP
*STEP,INC=60
*VISCD,PTOL=0.005,CETOL=7.0E-4
0.0001,5.0E4
*CLOAD,AMP=LOWER
4517,2,147.
*EL PRINT,ELSET=FLAVR,FREQ=60
S
*MODE PRINT,_MSET=INTBOUN,FREQ=60
U
*PLOT,FREQ=5
M/M/M tension
*CONTOUR
MISES
S11
S22
CEEQ
*MODE FILE,FREQUENCY = 5
U
*EL FILE,FREQUENCY=5
S
ENER
*EL FILE,FREQUENCY=5,POSITION=AVERAGED AT MODES
CE
*END STEP

```